DOCUMENTATION OF THE SAPRC-99 CHEMICAL MECHANISM FOR VOC REACTIVITY ASSESSMENT

Report to California Air Resources Board
Contract 92-329
Contract 95-308

By

William P. L. Carter

May 8, 2000

Air Pollution Research Center and
College of Engineering
Center for Environmental Research and Technology
University of California
Riverside, California 92521

00-AP-RT4P-001-FR

ABSTRACT

A detailed mechanism for the gas-phase atmospheric reactions of volatile organic compounds (VOCs) and oxides of nitrogen (NO_x) in urban and regional atmospheres is comprehensively documented in this report. This can be used in airshed models to determine absolute and relative ozone impacts (reactivities) of the many types of VOCs that can be emitted into the atmosphere, and for other control strategy and research applications. This mechanism, designated SAPRC-99, represents a complete update of the SAPRC-90 mechanism of Carter (1990), and incorporates recent reactivity data from a wide variety of VOCs. The mechanism has assignments for ~400 types of VOCs, and can be used to estimate reactivities for ~550 VOC categories. A condensed version was developed for use in regional models. A unique feature of this mechanism is the use of a computerized system to estimate and generate complete reaction schemes for most non-aromatic hydrocarbons and oxygenates in the presence of NO_x, from which condensed mechanisms for the model can be derived. The mechanism was evaluated against the results of approximately 1700 environmental chamber experiments carried out at the University of California at Riverside, including experiments to test ozone reactivity predictions for over 80 types of VOCs. The mechanism was used to update the various ozone reactivity scales developed by Carter (1994a), including the widely used Maximum Incremental Reactivity (MIR) scale. However, the reactivity estimates for many VOC classes are uncertain, which must be taken into account when using these data for regulatory applications. For this reason, uncertainty classifications have been assigned to all VOCs, and upper limit MIRs for VOCs with uncertain mechanisms are presented.

ACKNOWLEDGEMENTS

The Author wishes to acknowledge and thank Dr. Roger Atkinson of the Air Pollution Research Center at the University of California at Riverside for many valuable discussions, help with the mechanism, the estimation methods, and the atmospheric chemistry literature, and making data available prior to publication. Dr. William Stockwell of Desert Research Institute provided a comprehensive review of the base mechanism that resulted in significant improvements. Members of the California Air Resources Reactivity (CARB) Research Advisory Committee, and Dr. Jonathan Kurland of Union Carbide Co. in particular, provided helpful input concerning assignments for individual VOCs. The author also wishes to thank Mr. Bart Croes, Dr. Randy Pasek, and Dr. Eileen McCauley of the CARB not only for their input, support, and especially their patience during the long period of this project. The author also thanks Dr. Eileen McCauley for helpful editorial comments on the draft version of this report.

This work was funded primarily through CARB Contract 92-329 and in part through Contract 95-308. The development of the mechanism for airshed models was funded by the U.S. Environmental Protection Agency through a consulting contract. The development of the capability to explicitly represent reactions of major VOC products when estimating their reactivities was funded by a contract from the Chemical Manufacturers association Glycol Ethers Panel. This work uses results of previously unreported environmental chamber experiments funded by the CARB through contract 95-308, by Safety-Kleen Corporation, by the Aluminum Association, and by other sources. However, this report has not been reviewed by any of these agencies or corporations, and no official endorsement should be inferred.

The opinions and conclusions in this report are entirely those of the author. Mention of trade names and commercial products does not constitute endorsement or recommendation for use.

TABLE OF CONTENTS

LIST OF TABLES

LIST OF FIGURES

I. INTRODUCTION

A. Background

Airshed models are essential for the development of effective control strategies for reducing photochemical air pollution because they provide the only available scientific basis for making quantitative estimates of changes in air quality resulting from changes in emissions. The chemical mechanism is the portion of the model that represents the processes by which emitted primary pollutants, such as volatile organic compounds (VOCs) and oxides of nitrogen (NO_x), interact in the gas phase to form secondary pollutants such as ozone (O_3) and other oxidants. This is an important component of airshed models because if the mechanism is incorrect or incomplete in significant respects, then the model's predictions of secondary pollutant formation may also be incorrect, and its use might result in implementation of inappropriate or even counter-productive air pollution control strategies.

One airshed model application where the accuracy of the chemical mechanism is particularly important is the assessment or implementation of control strategies to encourage use of VOCs that have lower impacts on ozone or other secondary pollutant formation than VOCs that are currently emitted. Such strategies require a means to quantify the impacts, or "reactivities" of the VOCs with respect to O_3 or other measures of air quality. There are several examples of control strategies where accurate O_3 reactivity estimates are important. In the California Air Resources Board (CARB)'s "Low Emissions Vehicle/Clean Fuels" regulations, "reactivity adjustment factors" are used to place exhaust emissions standards for alternatively-fueled vehicles on an equal ozone impact basis as those for vehicles using conventional gasoline (CARB, 1993). These are calculated using the Maximum Incremental Reactivity (MIR) scale (Carter, 1994a), which is a measure of effect of a VOC on O_3 formation in a set of standard airshed scenarios that represent NO_x conditions where ozone formation is most sensitive to VOCs (Carter, 1994a; CARB, 1993). The CARB is now considering using an updated MIR scale for reactivity adjustments in its proposed consumer products regulations (CARB, 1999). In addition, the EPA has used O_3 impacts of VOCs calculated for various environments among the factors they consider when evaluating proposals to exempt various compounds from controls as ozone precursors (Dimitriades, 1999).

The MIR scale adopted in the CARB vehicle regulation was calculated using the SAPRC-90 chemical mechanism (Carter, 1990), which had assigned or estimated mechanisms for over 100 types of VOCs. Although other state-of-the art mechanisms were available for airshed model applications (e.g., Gery et al, 1998, Stockwell et al, 1990), SAPRC-90 used for this purpose because it was the only mechanism that that represented a large number of VOCs that was evaluated against environmental chamber data. However, although this mechanism represented the state of the art at the time it was developed, since then there has been continued progress in basic atmospheric chemistry, and new information has become available concerning the reactions and O_3 impacts of many individual VOCs.

This mechanism has been updated several times to incorporate some of the new information that has become available, with the major documented updates being the "SAPRC-93" (Carter et al, 1993a; Carter, 1995) and the "SAPRC-97" (Carter et al, 1997a) versions. However, the reactions and rate constants for most of the inorganic species and common organic products have not been updated, and the latest documented update (SAPRC-97) does not incorporate important new information concerning mechanisms and reactivities of many classes of VOCs (e.g., Carter et al, 2000a, see also references cited below). This includes particularly improved estimation methods and new reactivity data on many types of

oxygenated VOCs that have not previously been studied but that are or may be important in stationary source emissions, and updated mechanisms for components of mineral spirits and other high molecular weight alkanes.

Because of this, an updated mechanism that represents the current state of the art is needed to calculate an reactivity scale that is appropriate for the CARB's proposed reactivity-based consumer products regulations (CARB, 1999). In addition, the CARB vehicle regulations requires that the MIR scale it uses be updated approximately every three years, and therefore an update of that scale, using an updated and fully documented mechanism, is overdue. To address this need, the CARB contracted the author to develop an updated version of the SAPRC mechanism that represents the state of the art, that can appropriately represent the classes of compounds that need to be considered in VOC regulations, and that is comprehensively documented so that it can undergo peer review. This report documents the updated version of the mechanism, designated SAPRC-99, that represents the results of this effort.

B. Mechanism Overview

The major components of the SAPRC mechanisms are the base mechanism, the assignments and/or estimation procedures used to estimate the reactions of the represented VOCs that are not in the base mechanism, and the lumping procedures used to represent complex mixtures or VOCs for which assignments or estimates are not available. The base mechanism is the portion of the mechanism that represents the reactions of the inorganic species, the common organic products, the intermediate radicals leading to these products, including those formed from the initial reactions of the represented VOCs not in the base mechanism. Most of the VOCs that can be separately represented are not in the base mechanism, but can be added to the mechanism, either as explicit reactions for individual VOCs or as lumped model species whose parameters are derived from the mixture of detailed model species they represent, as needed in the model application. The updates to these various components are briefly summarized below, and are discussed in more detail in the remainder of this report. The remaining areas of uncertainty, and aspects of the mechanism additional work is needed, are also briefly summarized in this section.

1. Updates to the Base Mechanism

This version of the mechanism incorporates the first complete update of the base mechanism since SAPRC-90 was developed. The IUPAC (Atkinson et al, 1997, 1999) and NASA (1997) evaluations, the various reviews by Atkinson (1989, 1991, 1994, 1997a), and other available information were used to update all the applicable rate constants, absorption cross sections, quantum yields, and reaction mechanisms where appropriate. Although many small changes were made, most are not considered to have obviously important impacts on reactivity predictions. The one possible exception is the ~30% reduction in important OH + NO_2 rate constant based on the new evaluation by NASA (1997)[1]. However, a complete analysis of the effects of all the changes has not been carried out, so the possibility that other changes to the base mechanism may be important cannot be ruled out.

The base mechanism was also modified to improve somewhat the accuracy and level of detail in the mechanism in representing no-NO_x or low-NO_x conditions. The methyl peroxy and acetyl peroxy radical model species are now represented explicitly, without using "operator" approximations or the steady-state approximation that was incorporated in previous mechanisms. This should give somewhat

[1] The high rate constant in the current IUPAC (Atkinson et al, 1997) evaluation is probably inappropriate (Golden, personal communication, 1998).

more accurate predictions of radical fates and C_4 product formation yields under low NO_x or nighttime conditions when peroxy + peroxy reactions become nonnegligible. The explicit treatment of methyl peroxy is based on the approach used in the RADM-2 mechanism (Stockwell et al, 1990), which was shown to give a good approximation to a version of the mechanism with explicit representation of all peroxy + peroxy reactions (Carter and Lurmann, 1990). However, "operator" and steady state approximation methods are still employed to represent the higher peroxy radicals, and the current mechanism, like the previous versions, is still not capable of predicting how the C_{2+} organic products may differ under conditions where peroxy + peroxy reactions compete with peroxy + NO reactions. But these approximations have little or no effect on predictions of O_3 formation or O_3 reactivities, especially for the relatively high NO_x scenarios used for calculating the MIR scale (Carter, 1994a), and significantly reduce the number of active species that need to be included in the mechanism.

Although the base mechanism for SAPRC-99 employs a larger number of species than that for SAPRC-90 and as such is more detailed in most respects, a few condensations were employed, relative to the level of detail in the earlier mechanism. The separate model species used to predict formation of low-reactivity C_1-C_3 organic nitrates in the reactions of peroxy radicals with NO was lumped with the model species used to predict the formation of higher nitrates in these reactions because of the low total yield of the low reactivity nitrates. The PAN analogue formed from glyoxal, GPAN, is now lumped with the rest of the higher PAN analogues because of the relatively low amounts of GPAN predicted to be formed in atmospheric simulations. The effects of these approximations, which resulted in fewer species and significantly fewer reactions in the base mechanism, was shown to be small even in simulations of VOCs where these model species are predicted to be formed.

Because of the importance of isoprene emissions in many regional model applications, the base mechanism was expanded to include the isoprene photooxidation products used in the "four-product" condensed isoprene mechanism of Carter (1996). Thus, the base mechanism now includes explicit representation of methacrolein, methyl vinyl ketone, lumped C_5 unsaturated aldehyde products (ISOPROD), and the methacrolein PAN analogue (MPAN) formed when they react. Although the more condensed "one product" mechanism gives reasonably good approximations to predictions of effects of isoprene on ozone (Carter, 1996), the four product mechanism is considered to be more accurate, and allows prediction and appropriate representation of the major oxidation products of this important biogenic compound in ambient simulations.

2. Mechanism Generation and Estimation System

Probably the most important single advance in this version of the mechanism is the use of a new mechanism generation and estimation software system to derive fully detailed mechanisms for the atmospheric reactions of many classes of VOCs in the presence of NO_x, which can be used as the basis for deriving an appropriate representation of the VOC in the model. The automated procedure for generated alkane reaction mechanisms for SAPRC-90 (Carter, 1990) was updated based on the results of the evaluation of Atkinson (1997a) and an independent evaluation of alkoxy and peroxy radical reactions, as discussed in this report. More significantly, the software was completely revised and the capabilities of the system were extended to include not only alkanes, but also alkenes (with no more than one double bond), and many classes of oxygenates including alcohols, ethers, glycols, esters, aldehydes, ketones, glycol ethers, carbonates, etc. Although many of the estimated rate constants and rate constant ratios are highly uncertain, this procedure provides a consistent basis for deriving "best estimate" mechanisms for chemical systems which are too complex to be examined in detail in a reasonable amount of time. The system allows for assigning or adjusting rate constants or branching ratios in cases where data are available, or where adjustments are necessary for model simulations to fit chamber data. Therefore, it could be used for deriving

fully detailed mechanisms for VOCs that fully incorporate whatever relevant data are available, relying on various estimation methods only when information is not otherwise available. The program also outputs documentation for the generated mechanism, indicating the source of the estimates or assumptions or explicit assignments that were used.

A major effort in developing this system involved incorporating results of various mechanistic, product, and environmental chamber studies that have been carried out in recent years to reduce uncertainties in mechanisms and reactivity predictions for various classes of oxygenated compounds. The branching ratios derived from experimental product studies or adjusted to fit environmental chamber reactivity experiments were used not only as a basis to derive explicit assignments for maximum accuracy of representation and reactivity predictions of the applicable compounds, but also to improve the reliability and scope of the estimation methods when applied to compounds for which data are not available. An important source of the environmental chamber data used for this purpose came from the CARB-funded study of the reactivity of selected consumer products VOCs (Carter et al, 2000a), as well as other recent studies of individual compounds of interest to various private sector groups (see references cited elsewhere in this report)[2].

This mechanism generation system is used as the primary means of deriving SAPRC-99 mechanistic parameters for all the classes of VOCs that it can handle, including alkanes, alkenes, and the variety of oxygenated species as indicated above. Although the program outputs mechanisms that can (for larger molecules) involve hundreds or even thousands of reactions or products, various "lumping rules" are used to convert the detailed generated mechanisms and product distributions into the lumped reactions incorporating the appropriate model species used in the base mechanism. The use of this program has permitted estimation of detailed mechanisms for a much larger number of compounds than otherwise would be possible without incorporating approximations that might significantly compromise the accuracy of reactivity predictions.

The mechanism generation system was also used to generate the reactions of the major reactive oxidation products of the non-aromatic hydrocarbon and oxygenated VOCs. These are used for deriving more accurate representations of the reactions of these products that can be used when assessing the reactivities of the individual VOCs. However, the present version of the software cannot derive adjusted mechanisms for products formed by reactions of VOCs in complex mixtures that are represented by lumped model species.

Although the mechanism generation system currently cannot be used to derive mechanisms for dialkenes and unsaturated aldehydes and ketones, the estimates in the detailed mechanism of Carter and Atkinson (1996) for isoprene and its major products were incorporated explicitly in the mechanism generation system, allowing full mechanisms for these species to be generated. The results are therefore are consistent with the detailed mechanism of Carter and Atkinson (1996) and the condensed mechanisms of Carter (1996) for these compounds. A similar approach was used so the system could be used to generate reactions of 1,3-butadiene acrolein, and various alkynes.

3. Assigned or Parameterized Mechanisms

Despite progress in recent years, there are still too many uncertainties concerning the details of the photooxidation mechanisms of aromatics and the reactive products they form to allow for explicit mechanisms to be derived or estimated. Therefore, simplified and parameterized mechanisms, with

[2] Reports on recent environmental chamber studies of various VOCs can be downloaded from http: //cert.ucr.edu/~carter/bycarter.htm

uncertain parameters adjusted to fit environmental chamber data, are still employed. However, the representation of the uncharacterized aromatic ring fragmentation products was revised somewhat based new data obtained for unsaturated dicarbonyls (e.g., Bierback et al, 1994), and to allow for explicit representation of the α-dicarbonyl products formed from the methylbenzenes. As with SAPRC-97, this version of the mechanisms appropriately represents reactivity differences among various xylene and trimethylbenzene isomers, and is able to correctly simulate how aromatic reactivities vary with differing light sources. In addition, this version of the mechanism has parameterized mechanisms for the naphthalenes and tetralin optimized to simulate environmental chamber experiments employing those compounds.

Because the mechanism generation system cannot derive mechanisms for bicyclic compounds, simplified mechanisms for these compounds were derived, based on environmental chamber data for several representative terpenes. Some parameters, such as overall organic nitrate yields and numbers of NO to NO_2 conversions in the OH reaction, were adjusted based on the chamber data, and the mechanism generation system for compounds for compounds with similar structures was employed to derive estimated mechanisms for their reactions with ozone. The mechanism correctly predicts observed reactivity differences among various terpene isomers, though some experiments, particularly with β-pinene, are not well simulated in some respects.

Assigned mechanisms were also derived for styrene, N-methyl-2-pyrroladone, toluene diisocyanate, and diphenylene diisocyanate, based on available kinetic and mechanistic data, estimated or parameterized mechanisms, and results of environmental chamber experiments employing those or related compounds.

Although ClO_x or BrO_x chemistries have been incorporated as extensions to the SAPRC-97 mechanism (Carter et al, 1996d, 1997d, 1997h), this is not yet incorporated in the current version of this updated mechanism. With the exception of chloropicrin, which appears to have relatively simple and unique chemistry (Carter et al, 1997h), the few halogenated compounds we have studied [trichloroethylene (Carter et al, 1996d) and alkyl bromides (Carter et al, 1997d)] indicate that we cannot account for the reactivities of those compounds with explicit mechanisms. Therefore, the current version of the mechanisms uses a highly simplified and parameterized "placeholder" mechanism to provide very rough estimates of the approximate range of reactivities of halogenated compounds under MIR conditions, given their OH radical rate constants. The predictions of these mechanisms must be considered to be highly uncertain, and the available chamber data indicate they are almost certainly not valid under low NO_x conditions.

A parameterized "placeholder" mechanism is also used to estimate the approximate reactivity ranges of amines, given their measured or estimated OH radical rate constants. The predictions of this mechanism for those compounds must also be considered to be highly uncertain, especially since they have not been evaluated using environmental chamber data. However, use of this mechanism allows at least approximate estimates to be made.

4. Mechanism Evaluation

The performance of the mechanism in simulating O_3 formation, rates of NO oxidation, and other measures of reactivity was evaluated by conducting model simulations of over 1600 environmental chamber experiments carried out the Statewide Air Pollution Research Center (SAPRC) and the College of Engineering Center for Environmental Research and Technology (CE-CERT) at the University of California at Riverside (UCR). These include 481 single VOC - NO_x experiments, 447 incremental reactivity experiments, and 673 experiments with mixtures, though approximately 560 of the mixture runs

were replicate base case reactivity experiments of various types. These include not only experiments in the UCR database through 1993 (Carter et al, 1995d), but also experiments carried out at CE-CERT through mid 1999 for the purpose of developing and evaluating mechanisms for various types of VOCs[3].

The results of the evaluation indicated that this version of the mechanism performed approximately as well or better than the previous versions (Carter and Lurmann, 1991; Carter, 1995; Carter et al, 1997a) in simulating experiments with the major hydrocarbon classes found in ambient air and complex or surrogate mixtures. In addition, this version of the mechanism generally gave satisfactory fits to the reactivity data for most of the experiments using the various compounds that were studied more recently, which were either not represented or poorly represented in the previous versions. However, as with previous evaluations of this (Carter and Lurmann, 1991; Carter, 1995; Carter et al, 1997a) and other (Carter and Lurmann, 1990, Gery et al, 1988) mechanisms, there were cases where satisfactory simulations were not obtained. Many of these cases of poor performance in simulating the data can be attributed to problems with the mechanism, but this is probably not true in all cases.

For example, the mechanism did not perform particularly well in simulating the experiments with benzene, despite the fact that it generally performed satisfactorily in simulating experiments with most of the alkylbenzenes that were studied. The experiments with the 1-alkenes could only be simulated if it was assumed that the OH yields in the reaction of O_3 with those compounds were lower than indicated by laboratory data. The effects of varying reaction conditions on reactivities of some of the individual VOCs that were studied were not always successfully simulated, despite adjusting uncertain parameters in the mechanisms. These cases are noted in the summaries of the evaluation results for the various compounds. However, reactivities of most VOCs were reasonably well simulated, though in many cases adjustments to uncertain portions were made to achieve the fits. These cases are also noted in the summary of the evaluation results.

C. Updated Reactivity Estimates

The updated mechanism was used to calculate updated MIR and other ozone reactivity scales, using the scenarios and methodology developed previously for this purpose (Carter, 1994a,b). Reactivity estimates are given for approximately 560 VOC's, including many that were not in previous tabulations, or whose estimates were based on much more uncertain or approximate mechanisms. The reactivity tabulations include footnotes indicating the type of mechanism or representation employed when calculating the reactivities, the extent to which the reactivity predictions were evaluated against experimental data, and an uncertainty ranking. Upper limit reactivity estimates are also included.

The updated reactivity scale given in this report supercedes those of Carter (1994a) and other interim updates that have been distributed previously. It is therefore recommended that these be used in any application that calls for use of the MIR scale or any of the other scales given by Carter (1994a). Although the estimates for many of the VOCs remain highly uncertain, the present scale provides the best estimates that are currently available. The uncertainty classification given with the scale and the other associated footnotes can be used to indicate the qualitative level of uncertainty for any given VOC. It is recommended that any regulatory application that employs any of the scales given in this report appropriately take uncertainty into account for those VOCs whose reactivities are indicated as having a high level of uncertainty.

[3] The experiments used for mechanism evaluation include most of those described in the various reports on CE-CERT chamber studies that can be downloaded from http://cert.ucr.edu/~carter/bycarter.htm.

II. BASE MECHANISM

The base mechanism is the portion of the mechanism which must be incorporated when representing the reactions of any generic VOC, and includes the inorganic reactions, the reactions of the common organic products and the reactions of the common radicals formed from these products or any generic VOC. A complete listing of the base mechanism is given in Appendix A on Table A-1 through Table A-5. The species used in the base mechanism listed on Table A-1, their reactions and rate constants listed on Table A-2, the rate constant and mechanism documentation notes referred to there are given in Table A-4, and the absorption cross sections and quantum yields for the photolysis reactions listed on Table A-5. The major features of the mechanisms, and the changes made relative to the previous version (Carter et al, 1997a) are discussed in the following sections.

A. Inorganic Reactions

The inorganic reactions in the mechanism are essentially the same as in the previous versions, except all the rate constants have been updated based on the results of the most recent evaluations (Atkinson et al, 1997, 1999; Atkinson, 1997a; NASA, 1997). This resulted in changes to most of the rate constants, though in most cases the changes were small and probably not of significance to model predictions. In addition, a few reactions that were previously judged to be negligible were added to extend the range of validity of the mechanism. The changes that may not be negligible, and the aspects of the inorganic mechanism that are still considered to be uncertain, are briefly summarized below, in the order that the reactions appear on Table A-2.

- Reactions of O^3P with O_3 and NO, which were omitted from the previous mechanism, are now included. These are believed to be negligible under most atmospheric conditions, but may not be in some high concentration experiments.
- The rate constant used for the "homogeneous" portion of the N_2O_5 hydrolysis reaction was decreased from 1×10^{-21} cm^3 $molec^{-1}$ s^{-1} to 2.6×10^{-22} cm^3 $molec^{-1}$ s^{-1}, based on the data of Mentel et al (1996). Note that this reaction may be primarily heterogeneous in nature, and the appropriate rate constant to use in atmospheric simulations is uncertain. However, the rate constant we use is not inconsistent with the IUPAC (Atkinson et al, 1997) recommendation that the gas-phase rate constant is less than 2×10^{-21} cm^3 $molec^{-1}$ s^{-1}.
- The rate constant for OH + NO for 1 atmosphere and 300K increased by over a factor of 1.5, based on the NASA (1997) recommendation for the high pressure rate constant. The IUPAC (Atkinson et al, 1997) recommendations is to use an even higher high pressure rate constant, but that recommendation is not used because the NASA value is more consistent with measurements made under near-atmospheric conditions.
- There is a significant discrepancy between the NASA (1997) and IUPAC (Atkinson et al, 1997) recommendation concerning the important OH + NO_2 reaction. Again, the NASA recommendation is preferred because it is more consistent with measurements made under near-atmospheric conditions. [The rate parameters actually used are those that will be in the update to the NASA (1977) evaluation (Golden, private communication, 1999).] The high k_∞ recommended by IUPAC is based on very high pressure data in helium, and there may be artifacts due to the contribution of a second reaction channel, involving HOONO formation, becoming important at higher pressures (Golden, personal communication, 1998). The value used in the current mechanism is about 20% lower than that used in the previous version. Given the importance of

this reaction as a radical termination and NO_x removal process, this change may have a non-negligible effect on model simulations.

- The reaction of OH with HONO, which was omitted in the previous mechanism because of its low importance in ambient simulations, is now included. This reaction can be important in simulations of experiments with HONO added as a radical source, which may be useful for assessing some aspects of VOC reactivity (unpublished results from this laboratory).
- A second photolysis channel for HONO, forming H. + NO_2, was added based on the IUPAC (Atkinson et al, 1997) recommendations. This channel is calculated to occur ~10% of the time under atmospheric conditions.
- The reaction of OH with NO_3, omitted from the previous mechanism, is now included. The possibility that it may be non-negligible under some nighttime conditions or in some dark experiments has not been ruled out.
- The rate constant for the reaction of HO_2 with NO_3 was increased based on recent laboratory data of Mellouki et al (1993).
- The reaction of NO_3 with itself, which may be non-negligible under some nighttime conditions, (Stockwell et al, 1997) is now included.
- The reaction of OH with hydrogen was added because it may be a non-negligible sink for OH radicals in cleaner or remote atmospheres. The reaction is of negligible importance in urban or environmental chamber simulations, but may be needed in regional models.

The effects of these changes on model simulations have not been evaluated. It is expected the ~20% change in the OH + NO_2 may be the most important in terms of predictions of ozone formation, and in the model simulations of the environmental chamber experiments used to evaluate the mechanism, as discussed in Section V. However some of the changes concerning NO_3 reactions may have non-negligible effects on nighttime simulations. As indicated above, a number of changes were added that are not expected to influence ambient simulations, but which may be important in simulations of experiments that may be useful for evaluating other aspects of the mechanism. Since including these reactions did not add new species to the model, the impact of these reactions in terms of computational burden in airshed models should be minor.

B. Representation of Radical Species

The approaches used to represent the various types of radical species formed in the atmosphere are discussed in this section. As with the previous mechanism, most of the inorganic and a few of the organic radicals are represented explicitly, but most of the organic radicals are either lumped or not explicitly represented in the model. In particular, rapidly-reacting organic radicals which either react in only one way or whose reactions do not depend on other reacting species are replaced by the set of products they form, and most other radicals are either lumped or represented using a limited number of chemical "operators". The various approaches employed are discussed in this section.

With regard to computational impacts of radical species incorporated in the model, a distinction is made between *active* species and species where the *steady state* approximation can be employed. Active species are model species whose concentrations need to be calculated by the solver software by integrating their rates of change, and which must be transported in multi-cell model simulations. Steady state species are model species (usually representing rapidly reacting radical or chemical operators representing radicals) for which the steady state approximation can be employed. In that approximation,

the concentration of the species is calculated at each time step assuming that the instantaneous rate of formation is equal to the rate of destruction. This means that the species does not need to be transported or integrated by the model software, saving computer time and memory in multi-cell simulations. This approximation can appropriately be used by species such as alkyl and alkoxy radicals that always react rapidly with O_2 or have rapid unimolecular reactions, and is implicitly used when a radical is removed in the model by replacing it with the compound(s) it forms. However, experience has shown that it cannot be used for peroxy or NO_3 radicals, since their loss processes can become slow compared to their rates of change under low NO_x conditions or at nighttime. In addition because of limitations in the mechanism compiling software used in this work [and also implemented in the FCM version of the UAM (Kumar et al, 1995) and the CALGRID model], the steady state approximation cannot be used for species that react with themselves or other steady state species, or whose instantaneous concentrations cannot be calculated from the active species concentrations in a stepwise manner (Carter, 1988). Because of the latter restriction, the steady state approximation cannot be used for OH radicals when the mechanism is implemented with this software, though probably it is not a bad approximation for this species.

1. Inorganic Radicals

Most of the inorganic radicals in the mechanism are represented explicitly, as shown on Table A-1. The two exceptions are H atoms and $HOSO_2$ radicals, where the latter is formed in the reaction of OH with SO_2. H atoms are assumed to react exclusively and rapidly with O_2 to form HO_2, so any reaction that forms H atoms is represented as forming HO_2 instead. Likewise, $HOSO_2$ are assumed to react primarily with O_2 to form HO_2 and SO_3, so it is replaced by the HO_2 and sulfate (SULF) model species in the OH + SO_2 reaction. Table A-1 indicates those radicals for which the steady state approximation can be used. Note that this approximation should not be used for HO_2 or NO_3 radicals because they may build up significantly in concentration at nighttime or in the absence of NO_x. It probably could be used for OH radicals, but is not because of limitations of software used to implement the mechanism, as indicated above.

2. Rapidly Reacting Radicals.

As with the previous versions of the mechanism, many rapidly reacting radicals are removed from the mechanism by replacing them by the species they are assumed to rapidly form. Note that this can only be done for radicals where (1) the steady state approximation is appropriate, (2) the product(s) they ultimately form do not depend on any other reactants, and (3) the products they form also do not depend on reaction conditions (e.g., temperature) or the variation can be assumed to be insignificant for the conditions of the model application. The specific types of rapidly reacting radical substitution reactions used in this mechanism are as follows. Except as indicated, the substitution is due to an expected rapid reaction of the radical with O_2.

- HCO is replaced by HO_2 + CO.
- Based on product data for reactions of OH radicals with alcohols and other species, α-Hydroxy alkyl radicals are assumed to react with O_2 primarily by abstraction from the α-hydroxy rather than by addition. Therefore, such radicals are replaced by HO_2 + the corresponding carbonyl compound formed when it reacts with O_2. For example, $CH_3CH(\cdot)OH$ is replaced by CCHO + HO_2, where CCHO is the model species for acetaldehyde.
- α-Nitrato alkyl radicals are assumed to decompose unimolecularly to NO_2 + the corresponding carbonyl compound sufficiently rapidly that the decomposition will dominate over reaction with O_2. Therefore, such radicals are replaced by NO_2 + the corresponding carbonyl compound formed in the decomposition. For example, $CH_3CH(\cdot)NO_2$ is replaced by CCHO + NO_2.

- All other carbon-centered radicals, including acyl ($RCO\cdot$) and alkyl ($R\cdot$) are assumed to react entirely by O_2 addition. Therefore, these are replaced by the corresponding peroxy radical whenever they are formed.
- With the exception of t-butoxy (model species TBU-O·) and phenoxy (model species BZ-O·) radicals, which are represented explicitly in the mechanism, all alkoxy radicals are replaced by the set of products they are assumed to form when they react under atmospheric conditions. This would include reactions with O_2 and/or unimolecular reactions, as applicable. If the alkoxy radical has more than one reaction pathway that is assumed to be non-negligible, then non-integer stoichiometric coefficients are used for the products, as appropriate. The reactions of alkoxy radicals are discussed in Section III.J.
- The Crigiee biradicals formed in the reactions of O_3 with alkenes are replaced by the set of products they are assumed to form when they react in the atmosphere, which includes stabilization as well as the various decomposition pathways. These reactions are probably temperature and pressure dependent, but since insufficient information is available to estimate these dependences, this is ignored. The reactions of Crigiee biradicals are discussed in the Section III.K.
- Stabilized Crigiee biradicals with α hydrogens are replaced by the corresponding organic acid, on the assumption that their major fate under atmospheric conditions is reaction with H_2O to form the acid. The assumption that reaction with H_2O is the major fate of the biradicals is consistent with the rate constant ratios cited by Atkinson (1997a) for the reactions of $HCHO_2$ with H_2O, HCHO, CO, and NO_2. The mechanism for the reactions of stabilized $HCHO_2$ with water appear to be complex and may involve some formation of H_2O_2 or other peroxides, but based on the discussion of Atkinson (2000) we assume that acid formation is the major fate of the stabilized Crigiee biradicals where this reaction route is possible.

Note that branching ratios for some of the alkoxy radicals and the Crigiee biradicals may be temperature and pressure dependent, and this treatment ignores these dependencies. As discussed in Section III.J, the alkoxy radical branching ratios are estimated for 300°C and 1 atmosphere total pressure, and thus they may not be optimum for simulations of high altitude or extreme temperature conditions. However, it should be pointed out that no other current mechanism represents these temperature and pressure dependences of product branching ratios, and doing so would require a significant increase in the complexity of the mechanism, or would require the model software to support temperature and pressure-varying parameters. Since no information is available concerning the temperature and pressure dependences of Crigiee biradical reactions, any representation of this in the model would be entirely speculative.

3. Explicitly Represented Organic Radicals

Most of the organic radical species are represented either by replacing them with the radicals or products they are expected to exclusively form, or by using the lumped peroxy radical species or "operators" as discussed in the following two sections. However, a few organic radical species are represented explicitly, either because their reactions are sufficiently different that they are not appropriately represented using the other approaches, or because it is believed representing them explicitly will improve the accuracy of the model sufficiently to make the added model species worthwhile. These are briefly discussed below.

Methyl Peroxy Radicals. In the previous mechanism, all peroxy radicals, including methyl peroxy, were represented using the general peroxy radical operators + the products they were expected to

form, as discussed below. In this approach, the same organic products are assumed to be ultimately formed regardless of whether the radical reacts with NO, HO_2, or another peroxy radical. Although, as discussed below, this approach is still used for most of the higher peroxy radicals in this mechanism, in this mechanism methyl peroxy radicals ($CH_3OO\cdot$) are represented explicitly, using the model species C-O2·. Thus, the appropriate C_1 products are formed when it reacts with HO_2, itself, or other peroxy radicals, which are different than the formaldehyde formed when it reacts with NO. This allows for a more accurate representation of the reactions of at least this peroxy radical and gives this mechanism a level of detail approaching that of the RADM2 (Stockwell et al, 1990) or RACM (Stockwell et al, 1997) mechanisms in the way peroxy radical reactions are treated. As discussed by Carter and Lurmann (1990), the peroxy radical lumping approach used in the RADM2 mechanism appears to be somewhat less approximate than the lumping approach used in the previous SAPRC mechanisms.

Note that the reactions of peroxy radicals with NO_3 were not in the previous version of the mechanism. This reaction, which may be non-negligible at nighttime, was added based on the recommendations of the current evaluations (Atkinson et al, 1997).

Acyl Peroxy Radicals. The previous mechanism used separate steady-state model species to represent acyl peroxy radicals (CCO-O2·), general lumped higher acyl peroxy radicals (C2CO-O2·), and the higher peroxy radicals formed from glyoxal (HCOCO-O2·) and benzaldehyde (BZCO-O2·). In addition, the model species (RCO3·) was used to compute the total concentration without using the steady state approximation, for the purpose of computing peroxy + peroxy reaction rates. The PAN analogues for these radicals (PAN, PPN, GPAN, and BZ-PAN) were also included in the mechanism as active species. In this mechanism, the acyl peroxy radical formed from glyoxal (and its PAN analogue) are removed by lumping them with the other higher general lumped peroxy radicals (or PAN analogues), the acyl peroxy radical (and PAN analogue) formed from methacrolein and other isoprene products are added, and the total acyl peroxy radical model species (RCO3·) is removed. The need for RCO3· is eliminated by treating all the acyl peroxy radical model species as active, and including all their cross reactions. Although this requires more reactions and active species in the mechanism than the approach used previously, it gives a somewhat more accurate representation of the peroxy + peroxy reactions of these species, which can be important at nighttime, and eliminates the need to include a separate total peroxy radical operator as a co-product in every reaction forming such radicals.

t-Butoxy Radicals. As indicated above, most alkoxy radicals are not represented explicitly in the mechanism, but are replaced by the set of species they are assumed to form when they react. In the previous mechanism this was the case for all organic alkoxy radicals except for phenoxy (see below), and in particular t-butoxy radicals were assumed to react exclusively by decomposition to acetone and methyl radicals. However, the decomposition of t-butoxy is believed to be relatively slow (see Table A-2), and if NO_2 levels are sufficiently high then reaction with NO_2 may be non-negligible in high-NO_x scenarios or chamber experiments. The reaction of t-butoxy with NO_2 had to be included for the model to appropriately simulate results of incremental reactivity chamber experiments with isobutane (Carter et al, 1993a). Because the competition between decomposition and NO_2 depends on the NO_2 concentration, this requires that t-butoxy radicals be represented explicitly in the model. This is not necessary for most other alkoxy radicals, which can either react sufficiently rapidly with O_2, or have sufficiently rapid decomposition or isomerization pathways, that reaction with NO_2 can be neglected.

Phenoxy Radicals. Phenoxy radicals are represented explicitly in this and the previous mechanism because they are not expected to react with O_2 and have no known rapid decomposition pathway. In the presence of NO_x, the major fate of phenoxy radicals is believed to be reaction with NO_2, since it has no obvious unimolecular reaction route or mechanism for reaction with O_2. (Reaction with

NO would be expected to form a nitrite that would rapidly photolyze to re-form NO and phenoxy.) Nitrophenol formation has generally been assumed in this reaction (e.g., see Atkinson, 1990; Carter, 1990), presumably via some rearrangement of an initially formed unstable adduct. However, based on lower than expected yields of Nitrophenol in NO_3 + cresol and OH + benzaldehyde systems (Atkinson, 1994), this may be an oversimplification. In the absence of NO_x, the major fate of phenoxy is assumed to be reaction with HO_2, though the model also includes a slow unimolecular loss to account for situations where NO_2 or HO_2 may be low. Note that the phenoxy radical model species is used as a surrogate for substituted phenoxy radicals as well, except for lumped nitro-substituted phenoxy radicals, discussed below.

Nitro-Phenoxy Radicals. Although their reaction mechanisms are assumed to be the same as phenoxy radicals, the NO_2-substituted phenoxy radicals assumed to be formed from the reactions of NO_3 with phenols are represented separately. This is done to account for nitrogen balance, and because the dinitroaromatics expected to be formed in the reaction with NO_2 are expected to be either non-volatile or non-reactive, and are thus represented in the model as "lost nitrogen". This is the same representation as used in the previous mechanisms.

Formaldehyde + HO_2 Intermediate. The radical believed to be formed when HO_2 reacts with formaldehyde has to be represented explicitly because its subsequent fate is believed to be affected by NO levels, as shown on Table A-2. The mechanism used is based on the IUPAC (Atkinson et al, 1999) recommendation, and is essentially the same as used in the previous mechanism.

4. Peroxy Radical Operators

Representation of peroxy radical reactions in mechanisms is complicated by the fact that a relatively large number of such radicals are formed even in condensed mechanisms, and they can react to a non-negligible extent with themselves and other peroxy radicals under some conditions. The approach employed in the Carter (1990) mechanism is to represent organic peroxy radicals with the set of products they would ultimately form if they reacted fully in the presence of NO_x and sunlight, together with a set of chemical "operators" that represent their other effects on the system. A total peroxy radical operator (RO2·) is used to compute the total peroxy radical concentrations for the purpose of computing peroxy + peroxy radical reaction rates; this allows the steady-state approximation to be used for the other peroxy radical operators.

The approach used in this mechanism is similar, except that as indicated above it is not used for methyl peroxy which is now represented explicitly, and also the total peroxy radical species (RO2·) is eliminated. Instead of the latter, all the peroxy radical operators are treated as active species, and the cross-reactions between the operators are included. The elimination of RO2· simplifies the representation of peroxy radical chemistry and reduces the total number of species in the mechanism, though at the expense of having a somewhat larger number of active species and peroxy + peroxy radical cross reactions. The number of peroxy radical operators used to represent organic nitrate formation was reduced to reduce the number of species and cross-reactions. The peroxy radical operators employed in this mechanism are summarized below.

RO2-R·. This operator represents the effect of peroxy radical reactions that ultimately cause one NO to NO2 conversion and formation of HO_2 when they react with NO. It is representing as having zero carbons. When this operator reacts with HO_2, it is represented as forming ROOH, the lumped higher hydroperoxide species. Unlike the previous mechanism (Carter, 1990), which used a zero-carbon lumped hydroperoxide operator (-OOH) to represent the effect of hydroperoxide photolysis to form radicals, in this mechanism the higher hydroperoxides are represented by a model species whose reactions are based

on those estimated for n-propyl hydroperoxide. In other words, a lumped molecule[4] approach is used rather than the lumped structure approach. Since the organic portion of the radicals is already represented by the products formed if the radical reacted with NO (which is why the RO2-R· operators are zero carbon species), formation of the ROOH in the HO_2 reaction does not conserve carbon. To account for this, loss of three "lost carbon" (XC) species are included in this reaction to maintain carbon balance. Although this may appear to be a worse approximation than using a zero-carbon lumped structure species such as the -OOH in the previous mechanism, for most radicals, carbon is lost in the model when the peroxy reacts with NO (because of the use of relatively small products to represent most of the lumped products), so this tends to work towards compensating for that effect. Tracing the "lost carbon" (XC) levels in the model can be used to track the extent to which carbon is lost due to the way the product species are represented.

When this operator reacts with explicitly the represented radical species [i.e., NO_3, methyl peroxy, or any of the acyl peroxy species] the products formed are the same as would be formed if ethyl peroxy (CH_3CH_2OO·) reacted with those species, except that any C_2 organic products (acetaldehyde or ethanol) are removed, and if ethoxy radicals are formed, they are replaced by HO_2 (based on the fact that ethoxy can be represented as rapidly forming acetaldehyde + HO_2, with acetaldehyde removed). In other words, since the since RO2-R· does not represent the organic portions of the peroxy radicals, the organic products formed in its reactions are ignored. Note that it is assumed that in RO_2· + RO_2· reactions that formation of 2 RO· + O_2 and disproportionation to an alcohol + a carbonyl + O_2 occur with equal probability, based on available data for higher peroxy radicals (Atkinson et al, 1999). In the case of reaction of methyl peroxy, it is assumed that the disproportionation forming methanol and that forming formaldehyde occur with equal probability.

R2O2·. This represents the effects of extra NO to NO_2 conversions caused by multi-step reaction mechanisms, as would occur, for example, in mechanisms involving alkoxy radical decompositions or isomerizations. Again, R2O2· is used so the model can account for the formation of RO_2, and [R2O2] is used for the actual reactions of the operator. Unlike the RO2-R· and the other peroxy operators, this is not strictly speaking a radical species, and it is not represented as having any effect on the system except when it reacts with NO. This is because it does not react to form radical or radical sink species, and is only appropriately used in conjunction with RO2-R.

RO2-N·. This represents the reactions of peroxy radicals with NO to form organic nitrates of various types, which are all represented in the model by the 6-carbon lumped alkyl nitrate model species RNO3 (see Section C.2). Note that in previous versions of the mechanisms two additional operators were used to represent these processes. RO2-XN· was used to represent peroxy radicals that reacted with NO to form relatively unreactive C_{3-} nitrates, and RO2-XN· was used to represent aromatic peroxy radicals that reacted with NO to form aromatic nitrates. In this mechanism RO2-XN· was removed because the amount of C_{3-} nitrate formation tends to be extremely small, and RO2-NP· was removed nitrate formation is assumed to be relatively minor for most aromatics. In addition, the reactions of the aromatic nitrates formed are so uncertain that representing them separately may not necessarily be any more accurate than lumping them with RNO3.

Since the RO2-N· operator is used to represent the organic nitrates formed when the peroxy radicals react with NO, it is represented as having the number of carbons of the nitrate it forms when it reacts with NO, and its reactions with species other than NO are based on this representation. The

[4] The "lumped molecule" approach refers to representing a compound in the model by another compound, on a mole for mole basis. See Section VI.A.1.

products are derived based on what is considered to be appropriate for a C_{6+} alkyl peroxy radical, since those tend to be the radicals that are the largest precursors to alkyl nitrates in atmospheric simulations. In addition, since primary radicals tend to be formed in lower relative yields from such higher molecular weight compounds than secondary or tertiary radicals (whose C-H bonds tend to be more labile), the carbonyl products are represented by ketone model species (MEK or PROD2), rather than by aldehydes. The specific products used are indicated in the footnotes to Table A-2 for the various reactions.

RO_2 + RO_2 Reactions. Because the rate constants for peroxy + peroxy radical reactions can vary by orders of magnitude depending on the type of radical (e.g., Atkinson, 1997), the rate constant used for the peroxy + peroxy reactions of the peroxy radical operators must necessarily be very approximate. The value used for all these operators is based roughly on the range of rate constants for secondary peroxy radicals given by Atkinson (1997a) and Atkinson et al (1997), and is 30 times higher than the 1×10^{-15} cm^3 $molec^{-1}$ s^{-1} value used in the previous mechanism (Carter 1990).

C. Reactions of Common Products

A total of 24 model species are used in this mechanism to represent the reactive organic product species, 11 of which are used for organic compounds that are represented explicitly, and 13 of which are used to represent groups of similar products using the "lumped molecule" approach. In most cases, the model species and mechanisms are not significantly different than in previous versions of the mechanisms, except that some of the rate constants were updated as indicated in footnotes to Table A-2. Most of the updates for the C_{3-} products are based on IUPAC (Atkinson et al, 1997, 1999) recommendations. The species used are summarized below.

1. Explicitly Represented and Lumped Molecule Products

Formaldehyde (HCHO) and Acetaldehyde (CCHO). The mechanisms for these two compounds are essentially the same as in the previous mechanism, except that some of the rate constants and absorption cross sections have been updated as recommended by IUPAC (Atkinson et al, 1997, 1999). Note that this mechanism differs from most condensed mechanisms in that acetaldehyde is represented explicitly, with most higher aldehydes lumped with propionaldehyde, as discussed below. The one exception is glycolaldehyde ($HOCH_2CHO$), which is expected to have a reactivity closer to acetaldehyde than propionaldehyde, and therefore is represented by acetaldehyde in this mechanism.

Propionaldehyde and Lumped Higher Aldehydes (RCHO). The reactions of the model species RCHO, which represents all C_{3+} aldehydes except α-dicarbonyls, aromatic aldehydes, and acroleins, is based on the expected mechanism for propionaldehyde. Note that, based on structure-reactivity methods of Kwok and Atkinson (1995), as updated by Kwok et al (1996), approximately 4% of the reaction with OH radicals is estimated to occur by abstraction from the CH_2 group and ~1% at the methyl. The reactions of the radicals subsequently formed are derived using the general mechanism estimation methods, as discussed below. However, most of the OH reaction is analogous to the reaction of OH with acetaldehyde, forming RCO-O2·, the lumped higher acyl peroxy radical. The NO_3 and photolysis reactions are also assumed to be analogous to those for acetaldehyde, though a slightly higher NO_3 radical rate constant is assumed (based on the somewhat higher OH rate constant), and absorption cross sections and quantum yields specific to propionaldehyde are used.

Acetone (ACET). Acetone is represented explicitly because its reactivity is significantly lower than that for other ketones, yet is sufficiently reactive that its reactions are probably not negligible in long-range transport scenarios. Its mechanism is based on that discussed by Carter et al (1993b). Based on

the data of Jenkin et al (1993), the $CH_3COCH_2O\cdot$ radical is believed to primarily decompose to formaldehyde and $CH_3CO\cdot$. The absorption cross sections and quantum yields are based on the IUPAC (Atkinson et al, 1997), except that the reported quantum yields at 230 and 330 nm are believed to be high, and were corrected as discussed by Carter et al (1993b) and the footnotes to the acetone photolysis reaction on Table A-2.

Methyl Ethyl Ketone and Lumped Lower Reactivity Ketones (MEK). This model species is used to represent ketones and other reactive oxygenated product species whose OH radical rate constant is between 5 x 10^{-13} and 5 x 10^{-12} cm^3 $molec^{-1}$ s^{-1}. Note that this is different from previous versions of the SAPRC mechanism, where MEK was used for all higher non-aldehyde, non-aromatic oxygenated products that were more reactive than acetone. The MEK mechanism is based on that derived for methyl ethyl ketone using the general mechanism estimation methods discussed below, the IUPAC recommended OH rate constant (Atkinson et al, 1999) and absorption cross sections provided by Moortgat (private communication, 1996). The overall photolysis quantum yield of 15% was derived by fits to MEK - NO_x and MEK incremental reactivity environmental chamber experiments carried out in our laboratories (see Section V and Carter et al, 2000a), and is somewhat higher than the ~10% overall quantum yield derived previously based on fits to a few UNC outdoor chamber experiments (Carter, 1990; Carter and Lurmann, 1991).

Methanol (MEOH). In previous SAPRC mechanisms methanol in emissions was represented as an assigned parameter detailed model species, which permitted it to be represented explicitly or lumped with other compounds, depending on the model application. However, this approach does not permit representing formation of methanol as a reaction product. In this mechanism methanol is assigned an explicit model species in order to permit its formation of a product in no-NO_x reactions of methyl peroxy reaction. These reactions, and the subsequent reactions of methanol so formed, may be non-negligible in some long-range transport scenarios. Since methanol is potentially important in emissions, many model applications would probably use a separate model species for it in any case. Indeed, methanol is now represented explicitly even in some condensed models such as expanded Carbon Bond IV (e.g., Carter, 1994b and references therein). The mechanism is based on IUPAC (Atkinson et al, 1997, 1999) recommendations.

Methyl Hydroperoxide (COOH) and Lumped Higher Peroxides (ROOH). In previous SAPRC mechanisms, the hydroperoxide species formed in peroxy + HO_2 reactions were represented by a single "lumped structure" model species "-OOH", combined with the organic products formed in the peroxy + NO reactions. In this mechanism, for more accurate representation of low-NO_x chemistry, for regional or long-range transport simulations, methyl hydroperoxide is represented explicitly, and the other hydroperoxides are represented using a separate model species (ROOH) using the "lumped molecule" approach. In the case of methyl hydroperoxide, the OH reaction is assumed to occur at both the methyl and OOH positions as recommended by IUPAC (Atkinson et al, 1997, 1999), with the $\cdot CH_2OOH$ radical formed in the former reaction being assumed to rapidly decompose to formaldehyde + OH. The absorption cross sections are also based on IUPAC recommendations, with unit quantum yields assumed, and with the reaction assuming to proceed entirely by breaking the weak O-O bond.

The reactions of the lumped higher hydroperoxide (ROOH) are based on the estimated mechanism for n-propyl hydroperoxide. As discussed in footnotes to Table A-2 in Table A-4, the OH reaction is estimated to occur at the OOH group ~2/3 of the time, based on assuming the same rate constant as the same reaction of methyl hydroperoxide. Most of the remainder of the reaction is assumed to occur at the 1-position, yielding an α-hydroperoxy radical which is assumed to rapidly decompose to

propionaldehyde (RCHO) and OH. The photolysis is assumed to have the same rate and an analogous mechanism as methyl hydroperoxide.

Glyoxal (GLY). Glyoxal, which is formed in the reactions of most aromatics, acetylene, and some other species [including some isoprene oxidation products (Carter and Atkinson, 1996)], continues to be represented explicitly in this mechanism. Since it is less reactive than some other aromatic products it is often not represented in condensed mechanisms, but it is known to make an important contribution to the reactivity of acetylene (Carter et al, 1997c) and benzene (see Section IV.A.1) and its reactivity is not well approximated by other model species. On the hand, this mechanism is somewhat more condensed than previous detailed SAPRC mechanisms in that the acyl peroxy radical and PAN analogue predicted to be formed from the OH + glyoxal reaction [HCO(CO)OO· and HCO(CO)OONO_2)] are not represented explicitly, but are lumped with RCO-O2· and PAN2 (see below). The mechanism for the OH reaction is based on the data of Niki et al (1985) as discussed by IUPAC (Atkinson et al, 1997).

The glyoxal absorption cross sections were the same as used previously (Plum et al, 1983), as recommended by the IUPAC evaluation (Atkinson et al, 1997). However, the quantum yields were significantly revised based modeling of acetylene - NO_x and acetylene reactivity environmental chamber data (Carter et al, 1997c), as discussed in the footnotes to Table A-2 in Table A-4. The model simulations of those chamber experiments were found to be highly sensitive to glyoxal absorption cross sections used in the mechanism, and no other reasonable adjustments to the mechanism would yield acceptable fits to the data (Carter et al, 1997c). Note that to fit the data quantum yields which are ~1.4 times higher than overall quantum yield reported by Plum et al (1983) for conditions of those experiments must be used. Although use of acetylene reactivity data is a highly indirect way to obtain glyoxal quantum yields, we consider it to be a less uncertain way to estimate radical quantum yields then the data of Plum et al (1993), which uses a UV-poor light source, and only measures rates of glyoxal decay. Clearly this is uncertain and direct measurements of glyoxal quantum yields as a function of wavelength are needed.

Methyl Glyoxal (MGLY) and Other Higher α-dicarbonyl aldehydes. Methyl glyoxal is formed in the reactions of methylbenzenes and from some carbonyl compounds. Because of its high reactivity, its formation can significantly affect the reactivity of compounds that form it. The MGLY model species is also used to represent other α-dicarbonyl aldehydes, such as ethylglyoxal, etc. However, unlike the SAPRC-97 mechanism of Carter et al (1997a), but like earlier versions of the mechanism (Carter, 1990, 1995; Carter et al, 1993b), it is not used in this version of the mechanism to represent any of the uncharacterized aromatic ring fragmentation products (see discussion of unknown aromatic fragmentation products, below). The mechanism for the OH and NO_3 reactions are similar to those in the previous mechanism, with the latter reaction assumed to have the same rate constant and analogous mechanism as for acetaldehyde.

The IUPAC recommended (Atkinson et al, 1997, 1999) absorption cross sections for methyl glyoxal are approximately a factor of 2 higher than the Plum et al (1983) values used in the previous mechanism. The current mechanism uses cross sections obtained from Moortgat (personal communication, 1996), which are consistent with the IUPAC recommendations but have higher resolution. Unit quantum yields were assumed in the low wavelength band ($\lambda \leq 340$ nm) and zero quantum yields were assumed for wavelengths above the cutoff of 421 nm, as determined by the thermochemistry. For the rest of the high wavelength regime, the quantum yield was assumed to decline linearly from unity at 344 nm to zero at a wavelength (407 nm) that was adjusted such that the calculated overall photolysis rates under the conditions of the experiments of Plum et al (1983) agreed with the experimentally measured values. (An analogous treatment was used in when deriving the quantum yields for glyoxal and biacetyl, though in the glyoxal case the adjustment was to fit the acetylene chamber data,

as indicated above.) Note that this gives a different wavelength dependence than assumed in the previous mechanism, where a wavelength-dependent overall quantum yield was assumed for the entire high-wavelength band, including wavelengths above the high wavelength cutoff.

Biacetyl (BACL) and Other α-Dicarbonyl Ketones. Biacetyl or other α-dicarbonyl ketones are formed in significant yields from p-xylene, 1,2,4-trimethylbenzene and other o-dimethyl aromatics, and might be formed from the reactions of some carbonyl compounds. Biacetyl was not represented in previous versions of the mechanism, being in effect represented by methyl glyoxal. However, because its chemistry is in some ways quite different from methyl glyoxal (it reacts only slowly with OH, and its photolysis forms only PAN precursors), it was decided to represent it explicitly in this mechanism. The BACL model species is also used for other α-dicarbonyl ketones.

The reaction of biacetyl with OH radicals is ignored because the OH + biacetyl rate constant is probably not much different than that for acetone, making it a negligible loss process compared to photolysis. The photolysis is assumed to proceed via breaking the weak CO-CO bond, as shown on Table A-2. The absorption cross sections used were those from Plum et al (1983), and the wavelength-dependence of the quantum yields were derived from the data of Plum et al (1983) in a manner exactly analogous to that discussed above for methyl glyoxal (see footnotes to Table A-2 in Table A-4).

Phenol (PHEN) and Cresols (CRES). Cresols are formed in the reactions of the substituted aromatics, and phenol is formed from the reactions of benzene. In addition, phenol is represented as being formed in the subsequent reactions of aromatic ring-retaining products such as cresols or benzaldehydes. Cresol is used to represent phenolic products formed from all alkyl-substituted benzenes, while phenol is used to represent such products formed from benzene and naphthalene, as well as phenolic products formed in secondary reactions of cresols. The relatively rapid reactions of these compounds with NO_3 represents a NO_x sink in the aromatic mechanisms that largely explains their predicted tendency to inhibit O_3 under low NO_x conditions. Therefore, it is important that these model species be in the mechanism. They are kept as separate model species because the reactions of cresols are assumed to involve some PAN (or PAN analogue) formation, while this is assumed not to be the case for phenol.

There are still inadequate data concerning the atmospheric reactions of these compounds and the products they form, and the highly parameterized mechanisms used in the previous versions of the SAPRC mechanisms are essentially unchanged in this version. The main consumption reactions are with OH and NO_3, and the rate constants used are those recommended by Atkinson (1994). The OH + cresol mechanism is based on the highly parameterized mechanism derived by Carter (1990), but the version for this mechanism was reoptimized to fit the data from the single o-cresol - NO_x chamber experiment EC281 (Pitts et al, 1979; Carter et al, 1995d). The OH + phenol mechanism was derived by analogy with the resulting cresol mechanism. The NO_3 reactions are assumed to proceed via the formation of phenoxy radicals + HNO_3, with the BZ-O· model species used for substituted as well as unsubstituted radicals, The BZ-O· then reacts as discussed above in Section B.3. Note that although the mechanism for the NO_3 reaction (like that for the reaction with OH) is highly uncertain, it clearly must involve some sort of NO_x sink process in order for model simulations to fit chamber data for aromatics.

Nitrophenols (NPHE). The “nitrophenol” model species is used to represent whatever products are formed when phenoxy reacts with NO_2, which as indicated above is uncertain. It is assumed that the NO_2-substitution slows down the rate of reaction with OH radicals, and that its only significant consumption process is reaction with NO_3, for which it is assumed to have the same rate constant as phenol. This representation is unchanged from previous versions of the mechanism. Obviously this aspect of the mechanism is uncertain, but this representation appears to perform reasonably well in simulating

effects of aromatics on peak O_3 yields, which are determined by NO_x-sink processes that are represented by the formation and reactions of NPHE.

Benzaldehyde (BALD) and Other Aromatic Aldehydes. Benzaldehyde, tolualdehydes and other aromatic aldehydes that are formed in a minor but non-negligible route in the reactions of OH with methylbenzenes are represented by the benzaldehyde (BALD) model species. Its OH and NO_3 reactions are assumed to be analogous to other aldehydes, except that separate model species (BZCO-O2· and BZ-PAN) are used to represent the acyl peroxy radical and PAN analogue formed. This is necessary because the reaction of the benzoyl peroxy radical with NO forms phenoxy radicals, and the subsequent reactions of phenoxy radicals are not believed to regenerate radicals, unlike the subsequent reactions of the radicals formed when the other acyl peroxy radicals react with NO.

The absorption cross sections for benzaldehyde (Majer et al, 1969) indicate that its photolysis can be significant if the quantum yield is sufficiently high. The quantum yields are unknown, but chamber data indicates that it is probably consumed to a non-negligible by photolysis, though the overall quantum yield is relatively low and the photolysis apparently does not involve significant radical formation, The overall quantum yield derived by Carter (1990) to fit SAPRC evacuable chamber data (Pitts et al, 1979) is retained in this mechanism. It was found to give reasonably good model simulations of benzaldehyde - NO_x experiments carried out in the CE-CERT Xenon Teflon Chamber (Carter et al, 1998a).

Methacrolein (METHACRO) and Methyl Vinyl Ketone (MVK). This version of the mechanism incorporates the "four product" isoprene mechanism (Carter, 1996) as part of the base mechanism, so it includes model species for methacrolein, MVK, and the lumped other isoprene products (ISOPROD). The mechanisms used for methacrolein and MVK are essentially the same as derived by Carter and Atkinson (1996), with some minor updates as indicated in footnotes to Table A-2 in Table A-4. The mechanisms were generated using the mechanism generation system discussed in Section III, which incorporated most of the estimates and assignments of Carter and Atkinson (1996) for the reactions specific to the isoprene and isoprene product system. The use of the mechanism generation system resulted in some minor changes to yields of minor product in some reactions. In addition, because of these changes and changes to the overall base mechanism, the overall quantum yields for the methacrolein MVK photolysis were reoptimized, using the same procedures and data as discussed by Carter and Atkinson (1996). This resulted the overall quantum yield for methacrolein being increased by ~14%, while that for MVK was reduced by over a factor of ~5. The reason for this large change in the optimized MVK quantum yield is not clear, but it may be due to a relatively low sensitivity of model simulation results to large changes in this parameter. (See Section V and Appendix B for results of model simulations of the methacrolein and MVK experiments.)

Methacrolein is also used to represent acrolein in reactions where acrolein is predicted to be formed as a product. This is to avoid adding a new model species to represent a relatively minor product in most ambient mixtures. However, as discussed later and shown on Table A-6, acrolein can be represented explicitly for the purpose of assessing the reactivities of acrolein or VOCs that form acrolein as a major product.

Lumped Isoprene Products (ISOPROD). The ISOPROD model species is used to represent reactive isoprene products other than methacrolein and MVK, and also to represent other unsaturated ketones or aldehydes (other than acrolein itself, which is represented by methacrolein) when formed in reactions of other VOCs. Its mechanism is based on the ISOPROD model species in the "four product" isoprene mechanism of Carter (1996), with some minor modifications as indicated in footnotes to Table A-2 in Table A-4. Its mechanism is derived from weighted averages of rate constants and parameters for a

mixture of 30% hydroxymethacrolein and 23α% each cis-$HCOC(CH_3)$-$CHCH_2OH$, trans-$HCOC(CH_3)$-$CHCH_2OH$, and $HCOCH=C(CH_3)CH_2OH$. As with methacrolein and MVK, the mechanisms for these species were derived using the mechanism generation system discussed in Section III, incorporating estimates and assignments of Carter and Atkinson (1996) where applicable.

2. Lumped Parameter Products

"Lumped parameter" species refer to model species whose mechanisms are derived by averaging rate constants and product yield parameters from a representative mixture of compounds that they are designed to represent. Although the previous versions of the SAPRC mechanism used this approach only for model species representing emitted VOCs, this mechanism also uses this approach for two of the lumped organic product species, as discussed below.

Lumped Higher Reactivity Non-Aldehyde Oxygenates (PROD2). This model species, which is new to this version of the mechanism, is used to represent ketones, alcohols, and other reactive non-aromatic and non-double-bond-containing oxygenated products whose rate constants are greater than 5 x 10^{-12} cm^3 $molec^{-1}$ s^{-1}. This was added because it was judged that many of the bi- or polyfunctional product species that were previously represented by MEK when they were formed as products are in fact much more reactive than MEK, at least in terms of their reaction rate with OH radicals. The reaction mechanism of PROD2 is based on averaging mechanisms derived for a representative set of product species as discussed below.

Lumped Organic Nitrate Products (RNO3). This model species is used to represent various organic nitrates (other than PAN or PAN analogues), primarily those formed in the reactions of peroxy radicals from NO. This is consumed primarily by reaction with OH radicals, but a slow photolysis, which may be non-negligible in long-range transport simulations, is also included in the mechanism. Unlike previous SAPRC mechanisms, RNO3 is also used to represent those species formed from aromatic peroxy radicals with NO; previously the nitrophenol (NPHE) model species was used for this purpose. As indicated above, this change was made to avoid having to add the separate peroxy radical "operator" needed to support separate representation of aromatic nitrates, which are formed in relatively low yields and for which the appropriateness of the NPHE vs the RNO3 representation is unknown. The reaction mechanism of RNO3 is based on averaging mechanisms derived for a representative set of product species as discussed below.

Derivation of PROD2 and RNO3 Mechanisms. Although in principle the mechanisms for the lumped parameter product species can be derived for each emissions inventory in the manner used for the lumped parameter model species used for emitted VOCs (see Section III.A), the necessary software to do this has not yet been developed. Instead, in this version of the mechanism the parameters are derived from sets of representative species representing products predicted to be formed from the reactions of the mixture of VOCs used as the "Base ROG" mixture in the atmospheric reactivity calculations (Carter, 1994a; see also Section VII.A.1), and are held fixed in the model simulations. The Base ROG mixture is used to represent reactive VOCs from all sources, and is derived from the "all city average" mixture derived by Jeffries et al (1989) from analysis of air quality data, with minor modifications as discussed by Carter (1994a,b)[5]. For the purpose of determining the contributions of the reactions of the compounds in the mixture to the formation of a lumped product, the contribution of each emitted VOC is weighed by the amount of each VOC that is estimated to react in a one-day scenario, multiplied by the yield of the

[5] The complete mixture, indicating the specific detailed model species used to represent it in the model, is given in Table 50. See also Carter (1994b).

lumped product used in the model for the reactions of the VOC. The amount reacted is obtained from the amount emitted multiplied by the "mechanistic reactivity" (Carter and Atkinson, 1989a; Carter, 1994a), which is the fraction of the VOC estimated to react. The latter is obtained from mechanistic reactivities in the "averaged conditions" scenario where the NO_x inputs are adjusted to yield maximum peak ozone concentrations (the "MOIR" scenario)[6] (Carter, 1994a). Table 1 and Table 2 show the contributions of the reactions of various types of VOCs in the base ROG mixture to the formation of the RNO3 and PROD2 model species.

The set of compound that are represented by various model species can be calculated for those model species whose mechanisms can be derived using the mechanism generation/estimation system that is discussed in Section III. For each of these compounds, the system generates the set of products that are predicted to be formed using a fully explicit mechanism for the reactions in the presence of NO_x, which are then used, together with the "lumping rules" discussed in Section III.K.5, to determine the lumped product yields for the model. From this, the distribution of individual product VOCs represented by each lumped product model species can be determined, at least for the reactions of the VOCs whose mechanisms can be generated using this system. Although this system cannot generate mechanisms for aromatic compounds and terpenes, for which parameterized mechanisms must still be used, Table 1 and Table 2 show that their contributions to PROD2 or RNO3 formation from the base ROG mixture are minor. In particular, reactions of aromatics and terpenes account for less than 6% of the PROD2 formation, and for less than 5% of the formation of RNO3 in one-day scenarios.

Table 3 and Table 4 show the 35 most important products predicted to be formed from the reactions of the VOCs in the base ROG mixture that are represented by PROD2 (Table 3) or RNO3 (Table 4). The tables also show the contribution of each product to the total of all products represented by PROD2 or RNO3, their OH radical rate constant and carbon numbers, and the average OH rate constant and carbon number for all the products, weighed by their molar contribution to the total. Note that no single compound dominates the lists, and in the case of the organic nitrates the top 35 compounds account for less than half of the products formed that are represented by RNO3. Therefore, in both cases there is no obvious choice of a single "representative" or "typical" compound to use for lumped molecule representations.

In the case of PROD2, the average OH radical rate constant is 1.5×10^{-11} cm^3 $molec^{-1}$ s^{-1}, and the average carbon number is slightly over 7. For the purpose of deriving a PROD2 mechanism in the model, five individual compounds, indicated by being underlined on Table 3, were chosen as being representative of the entire set. The choice was largely subjective, but was made such that the average OH rate constant and the average number of carbons was approximately the same as the average, and so they included examples of different types of compounds on the list. For each of these five compounds the reaction mechanism with OH and photolysis was generated using the mechanism estimation/generation procedure discussed in Section III, and the PROD2 parameters were derived by averaging the values obtained, weighing each of the five compounds equally[7]. Since most of these compounds are ketones, the ketone absorption cross sections and the quantum yields assumed to be appropriate for ketones with 7 carbons

[6] The MOIR mechanistic reactivities are used because they are typical mechanistic reactivities in a wide range of scenarios. MIR mechanistic reactivities tend to be lower than in other scenarios because the relatively high NO_x levels tend to suppress radical levels.

[7] The mechanisms derived for these representative individual compounds are included with the mechanism listings for the detailed model species, given in Section VI. The detailed model species names assigned to them are indicated on Table 3 or Table 4.

(see Section III.G.1) were used for the photolysis reactions. The mechanisms derived for these representative individual compounds are included with the mechanism listings for the detailed model

Table 1. Contributions of various types of model species in the base ROG mixture to the formation of the PROD2 lumped product species.

VOC	Cont'n	VOC	Cont'n	VOC	Cont'n	VOC	Cont'n
N-C5	14.5%	4-ME-C7	2.9%	1-C9E	1.0%	3-ME-C11	0.3%
N-C10	8.1%	1-HEPTEN	2.7%	24-DM-C5	0.9%	26DM-C9	0.2%
N-C6	6.2%	24-DM-C7	2.5%	3-ME-C6	0.9%	ME-CYCC6	0.2%
N-C7	5.8%	3-ME-C6	2.2%	1-HEXENE	0.8%	1-C10E	0.2%
Aromatics	5.2%	2-ME-C6	1.9%	N-C11	0.7%	4-ME-C10	0.2%
1-HEXENE	5.0%	4-ME-C8	1.9%	3-ME-C5	0.6%	3-ME-C10	0.2%
24-DM-C6	4.5%	2-ME-C8	1.8%	36DM-C10	0.6%	1-PENTEN	0.1%
2-ME-C7	4.2%	26DM-C8	1.7%	24-DM-C5	0.5%	23-DM-C5	0.1%
2-ME-C5	3.6%	4-ME-C9	1.6%	1-OCTENE	0.5%	1-PENTEN	0.1%
N-C8	3.5%	2-ME-C9	1.6%	ET-CYCC6	0.4%	N-C13	0.1%
N-C9	3.4%	N-C12	1.4%	1-C11E	0.3%	2-ME-C5	0.1%
CYCC6	3.0%	ME-CYCC6	1.1%	5-ME-C11	0.3%	3M-1-BUT	0.0%

Table 2. Contributions of various types of model species in the base ROG mixture to the formation of the RNO3 lumped product species.

VOC	Cont'n	VOC	Cont'n	VOC	Cont'n	VOC	Cont'n
2-ME-C4	7.7%	23-DM-C5	1.6%	N-C11	0.6%	C-2-BUTE	0.2%
N-C4	5.9%	Terpenes	1.4%	1-C11E	0.5%	1-PENTEN	0.2%
N-C10	5.8%	24-DM-C5	1.3%	ET-CYCC6	0.5%	1-C10E	0.2%
24-DM-C6	4.9%	2-ME-C3	1.3%	2M-1-BUT	0.5%	1-BUTENE	0.2%
N-C5	4.9%	2-ME-C9	1.3%	1-OCTENE	0.5%	1C6RCHO	0.2%
2-ME-C5	4.0%	2-ME-C8	1.3%	T-3-C7E	0.5%	T-2-C7E	0.2%
ME-CYCC5	3.1%	4-ME-C9	1.2%	1-PENTEN	0.4%	13-BUTDE	0.2%
Aromatics	2.7%	4-ME-C8	1.2%	PROPENE	0.4%	3M-1-BUT	0.2%
24-DM-C7	2.5%	1-C9E	1.2%	T-4-C9E	0.4%	T-4-C10E	0.2%
26DM-C8	2.5%	PROPANE	1.2%	T-2-C6E	0.4%	3-ME-C10	0.1%
3-ME-C5	2.4%	N-C12	1.1%	C-2-C6E	0.4%	1C5RCHO	0.1%
2-ME-C7	2.4%	CYCC5	1.0%	T-5-C11E	0.4%	4-ME-C10	0.1%
N-C7	2.4%	2-ME-C6	0.9%	22-DM-C4	0.3%	CYC-HEXE	0.1%
4-ME-C7	2.3%	CYCC6	0.9%	T-2-BUTE	0.3%	MEK	0.1%
3-ME-C6	2.1%	ISOBUTEN	0.9%	ME-CYCC6	0.3%	23-DM-C4	0.1%
N-C9	2.1%	3-ME-C6	0.9%	3-ME-C11	0.3%	2-ME-C5	0.1%
N-C8	1.9%	23-DM-C4	0.9%	5-ME-C11	0.3%	3-ME-C5	0.1%
N-C6	1.8%	C-2-PENT	0.8%	26DM-C9	0.3%	N-C13	0.1%
1-HEPTEN	1.8%	T-2-PENT	0.8%	T-4-C8E	0.3%	36DM-C11	0.0%
ME-CYCC6	1.7%	24-DM-C5	0.7%	2M-2-BUT	0.3%		
1-HEXENE	1.7%	36DM-C10	0.6%	1-HEXENE	0.2%		

Table 3. Product compounds predicted to be formed in the atmospheric reactions of compounds in the base ROG mixture that are represented by the PROD2 model species.

Cont'n [a]	kOH [b]	nC [c]	Model Species [d]	Product Structure [e]
	1.5e-11	7.19		Average of all Products
16.4%	9.6e-12	5	PROD2-1	CH3-CO-CH2-CH2-CH2-OH
6.1%	1.7e-11	6		CH3-CH(OH)-CH2-CH2-CO-CH2-OH
3.8%	1.5e-11	6	PROD2-2	CH3-CO-CH2-CH(CH3)-CH2-OH
3.4%	6.4e-12	6		*CH2-CH2-CH2-CH2-CH2-CO-*
3.1%	1.4e-11	6		CH3-CH(OH)-CH2-CH2-CO-CH3
2.9%	1.1e-11	6		CH3-CH2-CO-CH2-CH2-CH2-OH
2.9%	2.0e-11	7		CH3-CH2-CH(OH)-CH2-CH2-CO-CH2-OH
2.7%	5.5e-12	6		CH3-CO-CH2-C(CH3)(OH)-CH2-OH
2.7%	1.5e-11	7	PROD2-3	CH3-CH(OH)-CH2-CH2-CO-CH2-CH3
2.3%	2.7e-11	5		CH3-CH(OH)-CH2-CO-CH3
2.2%	1.7e-11	7		CH3-CH2-CH(OH)-CH2-CH2-CO-CH3
2.2%	2.3e-11	10		CH3-CH2-CH2-CH(OH)-CH2-CH2-CO-CH2-CH2-CH3
2.1%	2.1e-11	10		CH3-CH2-CH2-CH2-CH(OH)-CH2-CH2-CO-CH2-CH3
2.0%	7.1e-12	8		CH3-C(CH3)(OH)-CH2-CH2-CO-CH2-CH3
1.7%	2.1e-11	10		CH3-CH2-CH2-CH2-CH2-CH(OH)-CH2-CH2-CO-CH3
1.5%	1.9e-11	7		CH3-CH(OH)-CH(CH3)-CH2-CO-CH3
1.3%	2.2e-11	8		CH3-CH2-CH(OH)-CH(CH3)-CH2-CO-CH3
1.3%	1.8e-11	8	PROD2-4	CH3-CH2-CH(OH)-CH2-CH2-CO-CH2-CH3
1.3%	6.0e-12	7		CH3-C(CH3)(OH)-CH2-CH2-CO-CH3
1.3%	2.4e-11	10		CH3-CH2-CH(OH)-CH2-CH2-CO-CH2-CH2-CH2-CH3
1.3%	1.9e-11	8		CH3-CH(OH)-CH2-CH2-CO-CH2-CH2-CH3
1.2%	7.4e-12	8		CH3-C(CH3)(OH)-CH2-CH(CH3)-CO-CH3
1.2%	1.7e-11	8		CH3-CH(OH)-CH2-CH(CH3)-CO-CH2-CH3
1.2%	1.4e-11	7		CH3-CH2-CH2-CO-CH2-CH2-CH2-OH
1.1%	1.6e-11	7		CH3-CH(OH)-CH2-CH(CH3)-CO-CH3
1.1%	1.9e-11	8		CH3-CH2-CH2-CH(OH)-CH2-CH2-CO-CH3
1.1%	2.0e-11	9	PROD2-5	CH3-CH2-CH2-CH(OH)-CH2-CH2-CO-CH2-CH3
1.1%	2.2e-11	9		CH3-CH2-CH(OH)-CH2-CH2-CO-CH2-CH2-CH3
1.0%	1.4e-11	6		CH3-CH(CH3)-CH2-CO-CH3
1.0%	2.3e-11	9		CH3-CH2-CH2-CH2-CH(OH)-CH2-CH2-CO-CH2-OH
1.0%	2.2e-11	10		CH3-CH(OH)-CH2-CH2-CO-CH2-CH2-CH2-CH2-CH3
0.8%	2.0e-11	9		CH3-CH2-CH2-CH2-CH(OH)-CH2-CH2-CO-CH3
0.8%	1.9e-11	8		CH3-CH(CH3)-CH(OH)-CH2-CH2-CO-CH3
0.8%	1.7e-11	7		*CH(CH3)-CH2-CH2-CH2-CO-CH2-*
0.8%	1.7e-11	8		CH3-CH(OH)-CH2-CH2-CO-CH(CH3)-CH3
21.6%				All Others

[a] Amount of formation of this compound relative to all products represented as PROD2, on a molar basis.

[b] OH radical rate constant estimated using structure-reactivity methods of Kwok and Atkinson (1995), as updated by Kwok et al (1996), in units of cm^3 $molec^{-1}$ sec^{-1}.

[c] Number of carbons.

[d] Detailed model species name used when computing mechanism for compound that was used for deriving PROD2 mechanism for the model.

[e] Product structure as used in the mechanism generation system. The "*" symbol is used to indicate groups that are bonded in cyclic compounds. Underlined structures are those used to derive the PROD2 mechanism.

Table 4. Product compounds predicted to be formed in the atmospheric reactions of compounds in the base ROG mixture that are represented by the RNO3 model species.

Cont'n [a]	kOH [b]	nC [c]	Model Species [d]	Product Structure [e]
	7.8e-12	6.58		Average of all Products
6.5%	1.6e-12	4	RNO3-1	CH3-CH(ONO2)-CH2-CH3
3.6%	3.0e-12	5		CH3-CH(CH3)-CH(ONO2)-CH3
2.8%	4.2e-13	3		CH3-CH(ONO2)-CH3
2.6%	1.7e-12	5		CH3-C(CH3)(ONO2)-CH2-CH3
2.5%	3.0e-12	5		CH3-CH(ONO2)-CH2-CH2-CH3
1.4%	2.8e-12	5		CH3-CH2-CH(ONO2)-CH2-CH3
1.0%	4.7e-12	6	RNO3-3	CH3-CH(ONO2)-CH(CH3)-CH2-CH3
1.0%	1.2e-11	5	RNO3-2	CH3-CH(OH)-CH2-CH2-CH2-ONO2
1.0%	5.1e-13	4		CH3-C(CH3)(ONO2)-CH3
1.0%	3.1e-12	6		CH3-C(CH3)(ONO2)-CH2-CH2-CH3
0.9%	4.5e-12	4		CH3-C(CH3)(ONO2)-CH2-OH
0.9%	4.2e-12	6		CH3-CH(CH3)-CH(ONO2)-CH2-CH3
0.9%	9.9e-12	10	RNO3-6	CH3-CH2-CH(ONO2)-CH2-CH2-CH2-CH2-CH2-CH2-CH3
0.9%	9.9e-12	10		CH3-CH2-CH2-CH(ONO2)-CH2-CH2-CH2-CH2-CH2-CH3
0.9%	9.9e-12	10		CH3-CH2-CH2-CH2-CH(ONO2)-CH2-CH2-CH2-CH2-CH3
0.9%	5.6e-12	8	RNO3-5	CH3-CH(CH3)-CH2-C(CH3)(ONO2)-CH2-CH3
0.8%	9.9e-12	7	RNO3-4	CH3-CH2-CH2-CH2-CH2-CH(ONO2)-CH2-OH
0.8%	2.8e-12	6		CH3-CH2-C(CH3)(ONO2)-CH2-CH3
0.8%	1.0e-11	5		CH3-CH(OH)-CH(ONO2)-CH2-CH3
0.8%	1.2e-11	5		CH3-CH(ONO2)-CH(OH)-CH2-CH3
0.8%	4.4e-12	6		CH3-CH(CH3)-CH2-CH(ONO2)-CH3
0.8%	7.2e-12	6		*CH(ONO2)-CH2-CH2-CH2-CH2-CH2-*
0.7%	1.0e-11	10		CH3-CH(ONO2)-CH2-CH2-CH2-CH2-CH2-CH2-CH2-CH3
0.7%	6.2e-12	8		CH3-C(CH3)(ONO2)-CH2-CH(CH3)-CH2-CH3
0.7%	4.2e-12	7		CH3-CH2-C(CH3)(ONO2)-CH2-CH2-CH3
0.7%	4.2e-12	6		CH3-CH2-CH(ONO2)-CH2-CH2-CH3
0.7%	5.6e-12	7		CH3-CH2-CH(ONO2)-CH2-CH2-CH2-CH3
0.7%	8.5e-12	6		CH3-CH2-CH2-CH2-CH(ONO2)-CH2-OH
0.6%	8.9e-12	4		CH3-CH(OH)-CH(ONO2)-CH3
0.6%	1.9e-11	10		CH3-CH2-CH(OH)-CH2-CH2-CH(ONO2)-CH2-CH2-CH2-CH3
0.6%	1.9e-11	10		CH3-CH2-CH2-CH(OH)-CH2-CH2-CH(ONO2)-CH2-CH2-CH3
0.6%	3.1e-12	6		CH3-C(CH3)(ONO2)-CH(CH3)-CH3
0.6%	1.8e-11	6		CH3-CH(ONO2)-CH2-CH2-CH(OH)-CH2-OH
0.6%	3.4e-12	6		CH3-C(CH3)(OH)-CH2-CH2-CH2-ONO2
0.6%	4.4e-12	6		CH3-CH(ONO2)-CH2-CH2-CH2-CH3
58.0%				All Others

[a] Amount of formation of this compound relative to all products represented as RNO3, on a molar basis.

[b] OH radical rate constant estimated using structure-reactivity methods of Kwok and Atkinson (1995), as updated by Kwok et al (1996), in units of cm^3 $molec^{-1}$ sec^{-1}.

[c] Number of carbons.

[d] Detailed model species name used when computing mechanism for compound that was used for deriving the RNO3 mechanism for the model.

[e] Product structure as used in the mechanism generation system. See Section III.B. The "*" symbol is used to indicate groups that are bonded in cyclic compounds. Underlined structures are those used to derive the RNO3 mechanism.

species, given in Table A-6. Note that although the PROD2 mechanism is derived based on a set of model species with average carbon numbers of 7, this is represented as having 6 carbons in the mechanism for the purpose of computing carbon balance.

In the case of RNO3, the average OH radical rate constant is 7.8 x 10^{-12} cm^3 $molec^{-1}$ s^{-1}, and the average carbon number is around 6.5. The RNO3 mechanism in the model is derived by choosing one representative compound each for carbon numbers of 4-8 and 10, such that the average OH rate constant is close to the average for the mixture. These six compounds are indicated by being underlined on Table 4. The mechanisms for these compounds were generated and the product yield parameters obtained[7] were averaged (weighing each equally) to obtain the product yields for the reactions of RNO3. The rate of photolysis is estimated by using the absorption cross sections given by IUPAC (Atkinson et al, 1997, 1999) for isopropyl nitrate, assuming unit quantum yield for production for NO_2.

3. Uncharacterized Aromatic Ring Fragmentation Products

Despite considerable progress in recent years towards understanding aromatic reaction mechanism (e.g., see Atkinson, 2000, and references therein), there is still insufficient information about the ring-opening products formed when OH radicals react with aromatic compounds to determine the appropriate mechanism for atmospheric modeling. In particular, the observed α-dicarbonyl and ring-retaining products from the aromatics are insufficient to account for the observed reactivity of aromatics in environmental chamber experiments, and it is necessary to assume formation of products that photolyze relatively rapidly to form radicals for model simulations to fit the environmental chamber data (e.g. Carter, 1990). To fit the data, the Carter (1990) mechanism included model species AFG1 and AFG2 to represent the contribution to reactivity of these uncharacterized ring-fragmentation products, with their yields and approximate photolysis rates adjusted to fit chamber data. Their mechanisms were based roughly on those for glyoxal and methyl glyoxal, respectively, although their action spectrum had a greater short wavelength contribution [eventually being based on that for acrolein (Carter et al, 1993b; Carter, 1995)] in order to fit reactivity data using differing types of light sources. More recently, to fit new aromatics environmental chamber data obtained using Teflon chambers with a xenon arc light source, it was found that it was also necessary to represent at least portion of the uncharacterized ring-opening products by model species with α-dicarbonyl action spectra (Carter et al, 1997a). These were represented in the model by methyl glyoxal – i.e., by increasing the methyl glyoxal yield by an adjustable amount in order to fit the chamber data (Carter et al, 1997a).

In this version of the mechanism, the general approach of using photoreactive model species with yields adjusted to fit the chamber data to represent the effects of unknown reactive aromatic ring fragmentation products is retained. However, the number of model species used for this purpose was increased to three, and their mechanisms were derived to be somewhat more consistent with the actual types of species expected to be involved. Their mechanisms were changed to be more consistent with the actual types of unsaturated dicarbonyl species expected to be involved, and their names were changed from AFGn to DCBn. A third model species (DCB3) was added to allow for separate representation of products with action spectra like α-dicarbonyls, and thus end the use the methyl glyoxal model species (MGLY) for this purpose. This was done so that the mechanism used may be more appropriate for an unsaturated carbonyl, and so model predictions of MGLY will actually represent methyl glyoxal and similar species. These are discussed in more detail below[8].

[8] See also Section IV.A for a discussion of the derivations of the yields and photolysis rates of these species based on model simulations of the aromatic - NO_x chamber experiments.

DCB1 is used to represent the uncharacterized ring-opening products that do not undergo significant photodecomposition to form radicals. This includes not only the ring fragmentation formed from benzene and naphthalene, but also unsaturated diketones such as 3-hexene-2,5-dione, which the data of Bierbach et al (1994) and Tuazon et al (1985) show do not undergo significant radical-forming photodecomposition. This non-photoreactive model species replaces the AFG1 used in the previous versions of the mechanism to represent the uncharacterized ring-fragmentation products from benzene because fits to the benzene - NO_x chamber data are not significantly improved if it is assumed that there are other photoreactive ring-opening products besides glyoxal. This is in contrast with the previous version of the mechanism, where significant photolysis of AFG1 to radicals had to be assumed to fit these data. This change is because benzene also forms glyoxal, whose photolysis to radicals was increased significantly in this version of the mechanism in order to be consistent with new chamber data on the reactivity of acetylene (Carter et al, 1997c). Also, the reaction of this species with O_3 is an additional radical source that was not in the previous mechanism.

This species is also used in the mechanisms of the alkylbenzenes because at least some of the ring-opening products are expected to have low photoreactivity, yet are expected to react rapidly by other means, particularly with OH. In particular, o-substituted aromatics such as o-xylene and 1,2,4-trimethylbenzene are expected to form higher yields of unsaturated diketones, which as indicated above do not seem to be highly photoreactive (Bierbach et al, 1994; Tuazon et al, (1985). The fact that these o-substituted aromatics have relatively low reactivity in environmental chamber experiments, and that lower yields of photoreactive products give the best fits to these data (Carter et al, 1997a), is consistent with the expected lower photoreactivity of these compounds. As discussed in Section IV.A, the yield of DCB1 is determined by assuming that the sum of all the DCBs (DCB1 + DCB2 + DCB3) is equal to the total ring fragmentation route, where the yields of the photoreactive DCB1 and DCB2 being determined by optimization. Note that this means the DCBs are used represent co-products formed with the measured α-dicarbonyls, as well as products formed in non-α-dicarbonyl-forming fragmentation routes.

The DCB1 reactions are based roughly on those estimated for HCOCH=CHCHO, with OH and O_3 rate constants based on the data of Bierbach et al (1994), and the mechanisms derived as discussed in Footnotes to Table A-2 in Table A-4. Although an OH reaction mechanism for an unsaturated diketone product such as might be formed from o-substituted aromatics may be somewhat different than that expected for 2-butene 1,4-dial, best fits to the p-xylene and 1,2,4-trimethylbenzene chamber data are obtained if the present DCB1 + OH mechanism is used.

DCB2 and DCB3 are used to represent the highly photoreactive ring-opening products formed from alkylbenzenes. As discussed by Carter et al (1997a), to fit chamber data using various light sources, it is necessary to assume two separate model species for this purpose, one with an action spectrum like acrolein, and the other with an action spectrum like an α-dicarbonyl. DCB2 is used to represent those compounds with action spectra like α-dicarbonyls, and thus uses absorption cross sections of methyl glyoxal, with a wavelength-independent overall quantum yield adjusted to give best fits to the chamber data as discussed in Section IV.A. Likewise, DCB3 uses the absorption cross sections of acrolein, with the overall quantum yield adjusted to fit the same chamber data. Note that the overall "quantum yield" used in the model for DCB3 is greater than unity, indicating that the absorption cross sections of the actual compounds being represented must be significantly greater than those for acrolein. However, in view of lack of information concerning the nature of these compounds and their photolysis reactions, it is assumed that the wavelength dependences of the action spectra are approximately the same as that for acrolein.

Other than the photolysis rates, the reactions of DCB2 and DCB3 are the same. They are based roughly on estimated mechanisms for $CH_3C(O)CH=CHCHO$. The rate constant for the OH reaction was assumed to be the same as that used for DCB1, with the mechanism estimated as indicated in footnotes to Table A-2 in Table A-4. Because of the rapid photolysis, it is assumed that consumption of these species by reaction with O_3 is negligible. The photolysis mechanisms are unknown, and are probably highly variable depending on the individual species involved. In this mechanism, these are very approximately represented by an estimated set of products which gives reasonably good performance in model simulations of available chamber data (see Section IV.A).

4. Unreactive Product Species

The mechanism has several model species whose subsequent reactions are ignored, either because they are unreactive or because the effects of their gas-phase reactions are expected to be small. These also include "counter species" for the purpose of tracking carbon and nitrogen balance. Since their computed concentrations do not effect transformations of any of the other gas-phase species, they could be eliminated from the model if their concentrations, or tracking carbon or nitrogen balance, are not of interest.

Formic Acid (HCOOH), Acetic Acid (CCO-OH), Lumped Higher Organic Acids (RCO-OH), Peroxy Acetic Acid (CCO-OOH), and Lumped Higher Organic Peroxy Acids (RCO-OOH). Formic acid is predicted to be formed in the reactions of formaldehyde with HO_2, acetic and higher organic acids are predicted to be formed from the reactions of acyl peroxy radicals with other peroxy radicals, and peroxy acetic and higher peroxy acids are predicted to be formed when acyl peroxy radicals react with HO_2. In addition, formation of formic and higher organic acids are assumed to be the major fate of stabilized Crigiee biradicals (Atkinson, 1997a, 2000). Their subsequent reactions with OH radicals is assumed to be negligible compared to other loss processes such as deposition, though the reaction with OH may in fact be non-negligible for the higher acids or peroxy acids. Formation of these acids is included in the model because of their potential involvement in acid deposition. Depending on the model application, it may be appropriate to remove them from the model or lump them into a single organic acid species.

Carbon Dioxide (CO2). Since CO_2 does not undergo gas-phase reactions and its formation is not expected to have any other effects on the environment (since background CO_2 concentrations are much higher), the only reason for having this species in the model is carbon balance.

Unreactive Carbon (NROG). This model species is used to represent emitted VOCs whose subsequent reactions are assumed to be negligible, and which are not otherwise represented in the model. It can be removed from the model if carbon balance is not of interest. It is represented as having one carbon, with the other carbons in the unreactive VOC or product being represented by the "lost carbon" species.

Lost Carbon (XC). The lost carbon model species is used to account for carbons that are lost (or gained) if the model species has a different number of carbons than the VOC or VOC products being represented. Note that this is different from the "unreactive carbon" (NROG) model species in that the former is used to represent *molecules* that are treated as unreactive, while the latter represents *parts of molecules* that are not being represented (i.e., that are "lost") as a result of the mechanism condensation processes. This model species can be removed in model applications where carbon balance is not of interest.

Lost Nitrogen (XN). This model species is analogous to the lost carbon (XC) species except that in this case it is used for nitrogen balance. It is not recommended that this be removed from the

mechanism, so that nitrogen balance can always be verified in any model simulation. Because of the importance of nitrogen species in affecting not only O_3 formation but also radical cycles and chain lengths, any modeling system that does not maintain proper nitrogen balance must be considered to be unreliable.

Sulfates (SULF). The SULF model species is used to represent the formation of SO_3 from the reactions of SO_2 with OH. It is assumed that the fate of SO_3 in the atmosphere would be formation of sulfate aerosol. This model species would be important in models for secondary aerosol formation in scenarios where SO_2 is emitted, but could be removed if aerosols are not represented in the model application.

III. GENERATED AND ESTIMATED MECHANISMS

The atmospheric reaction mechanisms for most of the organic compounds that are represented by this mechanism are complex, can involve a large number of reactive intermediates (particularly for larger molecules), and in almost all cases involve reactions whose rate constants are unknown and have to be estimated. Because of the complexity, for practical reasons it is necessary either to greatly simplify the mechanisms for most VOCs, use extensive lumping or condensations in VOC representations, or use an automated procedure to generate the mechanisms. In the previous versions of the SAPRC mechanism, an automated procedure was used to derive mechanisms for the alkanes, but molecule-by-molecule assignments or various lumping or condensation approaches were used for all the other VOCs. In this version, an automated procedure is now used to derive the mechanisms for a much wider variety of compounds, which includes almost all compounds for which mechanistic assignments have been made except for the aromatics and terpenes. This procedure, and the estimation methods and assignments that it employs, are discussed in this section.

A. Mechanism Generation Procedure Overview

The mechanism generation is carried out using a set of object-oriented computer programs that derives explicit mechanisms for the major atmospherically-relevant reactions of a VOC in the presence of NO_x, given the structure of the VOC. The results are then used to determine the representation of these reactions in terms of the model species in the base mechanism. The current system can generate the atmospherically-relevant reactions of alkanes, monoalkenes, a variety of oxygenates, and selected dialkenes and alkynes with OH, reactions of monoalkenes and selected dialkenes with O_3, NO_3, and O^3P, and photolysis reactions of carbonyls and organic nitrates. The overall operation of the system involves the following steps:

- The user inputs the structure of the compound. The structure is specified in terms of "groups" such as $–CH_2$-, -CO-, -OH, etc., which are similar to those used in the group additivity thermochemical estimation methods of Benson (1976) or the structure-reactivity kinetic estimate methods of Atkinson (1987). The specific groups used are summarized in Section III.B.
- The initial reactions of the compound with OH, O_3, NO_3, O^3P or photolysis are processed as shown schematically on Figure 1. The rates of reactions at competing positions are estimated as discussed in Sections III.C through III.G, and the products and radicals formed, together with their yields, are logged. Documentation text is generated and logged, as appropriate.
- For each reactive organic radical formed, either in the initial reaction with OH, etc., or through the reactions of a previously formed radical, the system generates all the reactions that are believed to be potentially important for the radical in the presence of NO_x in air. The radicals and products formed, and their yields (obtained by multiplying the yield of the starting radical times the branching ratios for the reactions forming them) are logged for further processing. Documentation text is also generated and logged for those reactions where estimates are involved. The types of radicals involved, and the reactions the system considers, are as follows:

Figure 1. Flow diagram for the initial reactions of a VOC in the mechanism generation process.

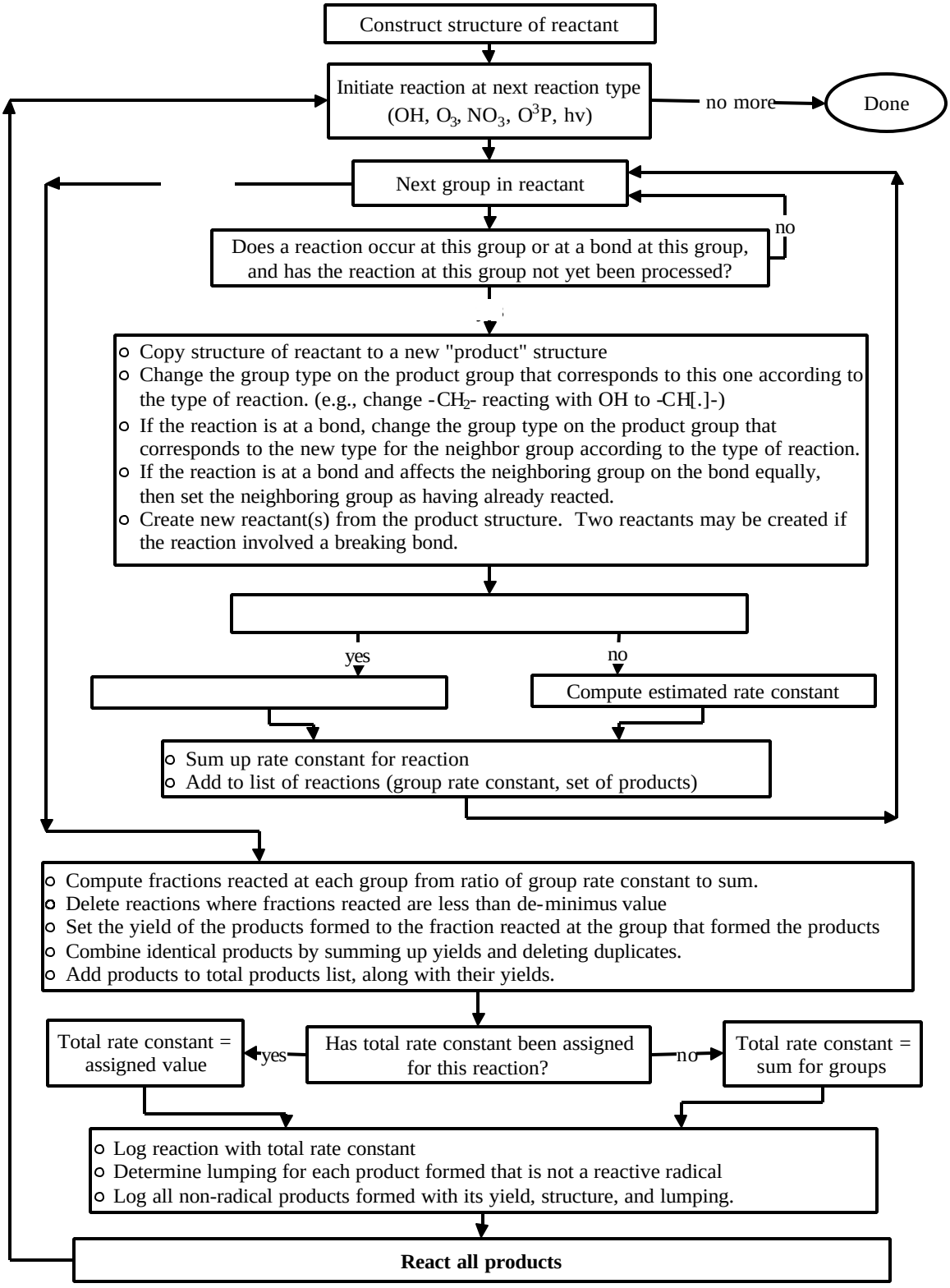

- Carbon centered (e.g, alkyl) radicals: Reaction with O_2. In most cases this involves formation of the corresponding peroxy radical, but in a few cases (e.g, α-hydroxy alkyl radicals) other reactions can occur. In all cases, only a single reaction pathway is assumed, so the yield of the product(s) are assigned the yield of the starting radical. These reactions are discussed in Section III.H.

- Peroxy radicals (other than acetyl peroxy): Reaction with NO. This can involve formation of the corresponding alkyl nitrate ($RONO_2$) or formation of NO_2 and the corresponding alkoxy ($RO\cdot$) radical. The conversion of NO to NO_2 in the latter reaction is logged as the formation of the "NO to NO_2 conversion product". Nitrate yield estimates, discussed in Section III.I, are used to determine the yields of the nitrate, alkoxy radical, and NO to NO_2 conversion products relative to the starting radical.

- Alkoxy radicals: Reaction with O_2; ß-scission decomposition; 1,4-H shift isomerization; or α-ester rearrangement (Tuazon et al, 1998b), when possible. The O_2 reaction involves the formation of HO_2 and a stable product, while the other reactions can involve formation of various carbon-centered radicals, in some cases with stable co-products. Various estimation methods or assignments, discussed in Section III.J are used to derive the relevant rate constants or branching ratios.

Note that acetyl peroxy radicals (e.g. $RC(O)O_2\cdot$) are treated as product species and their reactions are not generated. This is because they are lumped with generic acyl peroxy radical species in the model (e.g., CCO-O2· or RCO-O2·), so the information obtained by generating their reactions is not used. Note that their ultimate products they form (PAN or RC(O)O· decomposition products) depend on environmental conditions and thus cannot be uniquely determined.

- For each "product" species formed, which includes acetyl peroxy radicals, HO_2 and the NO to NO_2 conversion product as well as stable organic products, the yield, structure, and generation (number of NO to NO_2 conversions involved before it is formed) is logged. The lumping assignment for the product (the way it is represented in the base mechanism) is also determined and logged. Lumping assignments are discussed in Section III.K.5.

- Processing is completed once all the reactive radicals have been converted to stable products or radicals whose reactions are not generated (e.g., HO_2 or acyl peroxy radicals). The generated reaction list, product log (list of all products giving yields, structure and lumping), is saved for output or processing.

- Once all the relevant reactions for a VOC have been generated, the overall reactions or mechanistic parameters for the species can be derived for use in model simulations. The sum of the yields of HO_2 and the NO to NO_2 conversion product in the product log are used to derive the corresponding HO2, RO2-R· and/or R2O2· yields. The yields of the lumped species representing the various organic products are summed to determine their total yields in the overall reaction. Loss or gain of carbon and nitrogens are tracked, and if necessary yields of "lost carbon" or "lost nitrogen" model species are determined to maintain balance.

- The system can also be used to generate mechanisms for the major reactive products formed from the reactions of the VOC, for more accurate representation of these products when calculating reactivities of the individual VOCs. The system uses the procedures discussed above to generate mechanisms for each of the VOC's reaction products that are formed in yields greater than 2.5% and that would otherwise be represented by relatively reactive organic product species (such as PROD2 or RCHO). These VOC product mechanisms are then used to derive lumped mechanisms for the major type of product species tailored to represent the specific set of product species the VOC is predicted to form.

This procedure is discussed in more detail in Section III.M. Note that these "explicit product" mechanisms with VOC-specific product model species can only be used when representing the VOCs explicitly, not when they are lumped with other VOCs in complex mixtures. Therefore, both explicit product and standard lumped product mechanisms are derived for each VOC where such mechanisms can be generated.

Note that the system does not generate complete mechanisms for the VOCs, since peroxy + peroxy and peroxy + NO_2 reactions are ignored, and as indicated above acetyl peroxy radical reactions are not generated. However, even if the system generated all the peroxy + peroxy reactions, the current mechanism is not set up to use this information, because of the way the reactions of peroxy radicals are represented (see Section II.B.4). The present mechanism neglects the formation and decompositions of most peroxynitrates because their rapid decompositions at ambient temperatures result in no net reaction, so information on the formation and generation of these species would also be ignored. The current mechanism is also not set up to take advantage of any detailed product information concerning the reactions of individual acyl peroxy radicals and their corresponding PAN analogues. Therefore the present system is sufficient to provide all the information that the current version of the mechanism can use. Expanded capabilities can be added in the future as mechanisms and models that can use them are developed.

B. Specification of Reactants and Summary of Groups

In this section, the method used to specify structures of reactions, and the types of structures that can be represented, are discussed. A knowledge of this is necessary not only for those who wish to use the system, but also because some of the tables given in this report use this method to identify reactants and radicals.

The structure of a reactant VOC or radical is specified by giving the "groups" in the molecule, and indicating which groups they are bonded to. Groups are parts of the molecule that are treated as a unit by the system, and as indicated above are generally the same as the groups used in the structure-reactivity kinetic estimation method of Atkinson and co-workers (Atkinson, 1987; Kwok and Atkinson, 1995; Atkinson, 1997a). The list of groups that can be supported by the present system is given in Table 5 and Table 6. Table 5 shows the groups that can be used for constructing VOC structures to be reacted with OH, etc, and Table 6 shows the groups that can appear in reactive radical and product species that are formed.

If the molecule or radical contains atoms not shown on Table 5 or Table 6, then the reactions of that species cannot be generated by the current system. In addition, there are some groups for which there are insufficient thermochemical group additivity data in the system's thermochemical database to support the data requirements of the estimation methods, which means that reactions of molecules containing those groups usually cannot be generated. Those cases are indicated on. Table 5.

The structures of the molecules are specified as follows. Straight chain structures are given by groups separated by "-" or "=". For example:

Propane:	CH3-CH2-CH3
Propene:	CH3-CH=CH2
Propionic acid:	CH3-CH2-CO-OH
Ethyl acetate:	CH3-CH2-O-CO-CH3
ethoxyethanol:	HO-CH2-CH2-O-CH2-CH2-O-CH2-CH2-OH

Table 5. Listing of groups for stable molecules that can be supported by the present mechanism generation system.

Group	Reactions at Group
Groups for which mechanisms can usually be generated	
-CH3	OH (H- Abstraction)
-CH2-	OH (H- Abstraction)
>CH-	OH (H- Abstraction)
>C<	none
-O-	none
-OH	OH (H- Abstraction)
-CHO	OH, NO_3 (H- Abstaction), hν (HCO..- Bond Scission)
-CO-	hν (CO..- Bond scission)
=CH2	OH, O_3, O^3P, NO_3 (Double Bond Addition)
=CH	OH, O_3, O^3P, NO_3 (Double Bond Addition)
=C<	OH, O_3, O^3P, NO_3 (Double Bond Addition)
Groups for which mechanisms can be generated in some cases	
-ONO2	hν (-O. + NO_2 formation)
Groups for which mechanisms usually cannot be generated	
-F	none
-Cl	none
-Br	none
-I	none
-NO2	none

Branched structures are indicated by using ()'s to show groups off to the side. For example:

Isobutane: CH3-CH(CH3)-CH3
3,3-diethyl pentan-2-ol: CH3-CH(OH)-C(CH2-CH3)(CH2-CH3)-CH2-CH3
4-isopropyl heptane: CH3-CH2-CH2-CH(CH(CH3)-CH3)-CH2-CH2-CH3

Cyclic structures are indicated by using a "*" character to mark the group which is used to close the ring. Note that the present system does not support specification of compounds with more than one ring, since no way of indicating such structures is presently defined.

3-methyl furan: *O-CH2-CH(CH3)-CH2-CH2-*

The system presently supports structures with single double bonds between carbon-centered groups only, and may not successfully generate reactions for non-hydrocarbon species with double bonds because of insufficient thermochemical group data in the present database. Double bonds are indicated using a "=" symbol in place of a "-", and *cis* and *trans* configurations are indicated using parentheses, as follows:

cis-2-butene: CH3-CH=CH-CH3
trans-2-Hexene: CH3-CH=CH(CH2-CH2-CH3)

Although one can often enter structures in more than one way (for example, both CH3-CH(CH3)-CH2-CH3 and CH3-CH2-CH(CH3)-CH3 are acceptable ways to enter 2-methyl butane), the system uses an algorithm to generate a (usually) unique structure definition string for each structure. This is done so that the structure definition string can be used to determine if two products or intermediate species generated by the system are the same compound. Therefore, the structure specification generated by the

Table 6. Listing of radical center groups and non-reactive product groups that can be supported by the present mechanism generation system.

Group	Reactions at Group
Carbon-Centered Radical centers	
CH3.	O2 -> CH3OO.
-CH2.	O2 -> -CH2OO.
-CH[.]-	O2 -> -CH[OO.]-
>C[.]-	O2 -> >C[OO.]-
HCO.	O2 -> HO2. + CO
-CO.	O2 -> -CO[OO.]
Vinylic Radical centers	
=CH.	X=CH2 + O2 -> X=O + HCO., where X is =CH2, =CH-, or =C<
=C[.]	X=CH[.]- + O2 -> X=O + -C[OO.], where X is =CH2, =CH-, or =C<
Peroxy Radical Centers	
CH3OO.	NO -> CH3O.
-CH2OO.	NO -> -CH2O. + [NO conv NO2], NO -> -CH2-ONO2
-CH[OO.]-	NO -> -CH[O.]- + [NO conv NO2], NO -> -CH(ONO2)-
>C[OO.]-	NO -> >C[O.]- + [NO conv NO2], NO -> >C(ONO2)-
Acyl Peroxy Radical Centers	
-CO[OO.]	Not reacted
Alkoxy radical Centers	
CH3O.	O2 -> HO2 + HCHO
-CH2O.	O2 -> HO2 + -CHO, Decomposition, 1,4-H-shift isom, Ester rearrangement
-CH[O.]-	O2 -> HO2 + -CO-, Decomposition, 1,4-H shift isom, Ester rearrangement
>C[O.]-	Decomposition, 1,4-H shift isom.
HCO2.	O2 -> HO2 + CO2
-CO2.	Decomposition to R. + CO2
Carbene Radical Centers	
CH2:	O2 -> CH2OO[excited]
-CH:	O2 -> -CHOO[excited]
-C[:]-	O2 -> COO[excited]
Excited Crigiee Biradical Centers	
CH2OO[excited]	Various unimolecular reactions -- see text
-CHOO[excited]	Various unimolecular reactions -- see text
-COO[excited]-	Various unimolecular reactions -- see text
Stabilized Crigiee Biradical Centers	
CH2OO[stab]	-> HCO-OH + H2O
-CHOO[stab]	-> -CO-OH + H2O
-COO[stab]-	No reaction (usually not formed -- see text)
Elementary Product Groups	
CH4	Not reacted (elementary product)
HCHO	Not reacted (elementary product)
CO	Not reacted (elementary product)
CO2	Not reacted (elementary product)
NO2	Not reacted (elementary product)
[NO conv NO2]	Used for Mechanism Processing

system when a new molecule is specified may be slightly different than the one input by the user, though they would refer to the same compound. Note that the current version of the software is not completely finished in this regard, since unique structure definition strings are not always produced for some cyclic compounds. However, this only causes inefficiency in the mechanism generation algorithm, not errors in the generation of the overall mechanisms.

In order for the system to be useful for generating mechanisms for a wider variety of compounds, it is also possible to specify *special reactants* whose structures cannot be specified explicitly. Although the system cannot automatically generate reactions for these special reactants, it will accept assignments for their reactions. If the these assigned reactions form products that can be specified with known groups, the system then automatically generate the reactions of these products, thus generating the overall reaction mechanism of the special reactant. The special reactants that are supported in the present system are listed in Table 7

Table 7. Special reactants that are presently supported as reactants or products in the mechanism generation system

Reactant	Designation	Reactions Supported
1,3-Butadiene	CH2=CH-CH=CH2	OH, O_3, O^3P, NO_3 (Double Bond Addition)
Isoprene	CH2=CH-C(CH3)=CH2	OH, O_3, O^3P, NO_3 (Double Bond Addition)
Acetylene	HC::CH	OH, O_3
Methyl Acetylene	HC::C-CH3	OH, O_3
1-Butyne	HC::C-CH2-CH3	OH, O_3
2-Butyne	CH3-C::C-CH3	OH, O_3
3-Methyl Furan	*O-CH=C(CH3)-CH=CH-*	Product only (formed from isoprene)

C. Reactions with OH Radicals

Reactions with OH radicals can occur by two mechanisms, depending on whether the group has a double bond or an abstractable hydrogen. If the group has an abstractable hydrogen, the reaction is

$$XH + OH \rightarrow X\cdot + H2O \qquad \text{(abstraction)}$$

where XH is any H-containing group and X· is the corresponding radical formed when the H atom is removed. If the compound has a double bond, the reaction is

$$>C=C< + OH \rightarrow >C(OH)-C[\cdot]- \qquad \text{(addition)}$$

Note that two reactions are generated for each double bond, one where the OH adds to each side of the bond. (If the reactions are equivalent, as would be the case for symmetrical molecules, they are combined after they are generated – the system uses the products formed to determine equivalency.) For each molecule that reacts with OH, one reaction is generated for each group in the molecule that can react in this way. The fractions reacted at the various group are determined from the ratio of the estimated rate

constant at each group, divided by the total of the estimated rate constants for all groups. The group rate constants are estimated as discussed below.

1. Assigned Total OH Radical Rate Constants

Total OH radical rate constants have been measured for many (indeed most) of the VOCs in the current mechanism, and in those cases assigned rate constants are used when generating the mechanisms rather than estimated values Table 8 gives the OH radical rate constants assigned to all VOCs in the current mechanism, along with references and notes indicating the basis for the assignment. Most of the rate constants are based on recommendations by Atkinson (1989, 1994, 1997a). For completeness, this table has the rate constants for all VOCs in the current mechanism for which such assignments have been made, including those (e.g., aromatics and terpenes) whose mechanisms cannot be generated by the current system. For VOCs whose OH reactions can be automatically generated by the system, the table also shows the estimated T=300K rate constants, which were derived as discussed in the following section. The percentage differences between the assigned and estimated values are also shown (unless the differences are greater than 100%).

2. Estimation of OH Abstraction Rate Constants

Group rate constants for OH abstraction reactions are estimated using the group additivity method developed by Atkinson (1987), as updated by Kwok and Atkinson (1995), Kwok et al (1996) and in this work. The rate constant for the reaction of OH at any group is a function of the group and the groups bonded to it (the "neighbor groups"), and is derived from the equation

$$k(OH + group) = k(group) \prod^{neighbor\ groups} F(neighbor\ \ group) \qquad (I)$$

where "k(group)" is the rate constant for OH reaction at the group if it were only bonded to methyl radicals, and "F(neighbor group)" is the substituent correction factor for a neighbor group. The group rate constants as currently implemented in the mechanism estimation system are given in Table 9. As indicated in the footnotes to the table, most of the group rate constants and correction factors were obtained from Kwok and Atkinson (1995), with one updated value from Kwok et al (1996) and with a few gaps filled in this work. Note that in some cases, the correction factor depends not only on the neighbor group but also the next nearest neighbor; these modified groups are referred to as "subgroups" on the table. Note also that formate -CHO groups are treated as separate groups than aldehyde -CHO groups for the purpose of OH rate constant estimates. This is because OH abstraction reaction appears to be essentially negligible for the former, but very rapid for the latter.

If the compound has a C=C double bond anywhere in the molecule, at present the system assumes the abstraction reactions from any H-containing group are all negligible compared to the addition to the C=C double bond, and the abstraction rate constant is set at zero. Although methods exist for estimating these abstraction rate constants (Kwok and Atkinson, 1997), it is currently necessary to make this approximation because general methods for generating and estimating the rates of all the possible reactions of the unsaturated radicals formed in these reactions have not yet been developed. Ignoring these abstraction reactions from unsaturated compounds is not a bad approximation for smaller molecules such as propene and the butenes, and all known mechanisms currently used in atmospheric models incorporate this approximation. However, abstraction at groups away from the double bonds can become non-negligible for the larger alkenes (see Atkinson, 1997a and references therein), so this approximation

Table 8. Rate constant and temperature dependence parameter assignments used for reactions of VOCs with OH radicals in the present mechanism.

Compound	Model Name	k(300) (cm^3 $molec^{-1}$ s^{-1})	A	B	Ea kcal/mole	Refs	Est'd k(300) k	(diff)
Alkanes								
Ethane	ETHANE	2.60e-13	1.37e-12	2.0	0.990	1	2.78e-13	7%
Propane	PROPANE	1.14e-12	1.40e-12	2.0	0.121	1	1.28e-12	12%
n-Butane	N-C4	2.47e-12	1.52e-12	2.0	-0.288	1	2.65e-12	7%
n-Pentane	N-C5	4.04e-12	2.20e-12	2.0	-0.364	1	4.07e-12	1%
n-Hexane	N-C6	5.47e-12	1.38e-12	2.0	-0.823	1	5.49e-12	0%
n-Heptane	N-C7	7.04e-12	1.43e-12	2.0	-0.950	1	6.91e-12	-2%
n-Octane	N-C8	8.76e-12	2.48e-12	2.0	-0.751	1	8.33e-12	-5%
n-Nonane	N-C9	1.00e-11	2.26e-12	2.0	-0.888	1	9.75e-12	-3%
n-Decane	N-C10	1.13e-11	2.82e-12	2.0	-0.827	1	1.12e-11	-1%
n-Undecane	N-C11	1.29e-11				1	1.26e-11	-2%
n-Dodecane	N-C12	1.39e-11				1	1.40e-11	1%
n-Tridecane	N-C13	1.60e-11				1	1.54e-11	-4%
n-Tetradecane	N-C14	1.80e-11				1	1.69e-11	-6%
n-Pentadecane	N-C15	2.10e-11				1	1.83e-11	-13%
n-C16	N-C16	2.30e-11				1	1.97e-11	-14%
Isobutane	2-ME-C3	2.21e-12	1.04e-12	2.0	-0.447	1	2.45e-12	11%
Neopentane	22-DM-C3	8.63e-13	1.62e-12	2.0	0.376	1	6.83e-13	-21%
Iso-Pentane	2-ME-C4	3.70e-12				1	4.05e-12	9%
2,2-Dimethyl Butane	22-DM-C4	2.38e-12	3.22e-11		1.552	1	1.84e-12	-23%
2,3-Dimethyl Butane	23-DM-C4	5.79e-12	1.12e-12	2.0	-0.982	1	5.45e-12	-6%
2-Methyl Pentane	2-ME-C5	5.30e-12				1	5.47e-12	3%
3-Methylpentane	3-ME-C5	5.40e-12				1	5.75e-12	6%
2,2,3-Trimethyl Butane	223TM-C4	4.25e-12	7.61e-13	2.0	-1.025	1	3.24e-12	-24%
2,2-Dimethyl Pentane	22-DM-C5	3.40e-12				1	3.26e-12	-4%
2,4-Dimethyl Pentane	24-DM-C5	5.00e-12				1	6.87e-12	37%
2,2,3,3-Tetrame. Butane	2233M-C4	1.06e-12	1.72e-12	2.0	0.286	1	1.02e-12	-4%
2,2,4-Trimethyl Pentane	224TM-C5	3.60e-12	1.87e-12	2.0	-0.389	1	4.66e-12	30%
2,2-Dimethyl Hexane	22-DM-C6	4.80e-12				1	4.68e-12	-2%
2,3,4-Trimethyl Pentane	234TM-C5	7.10e-12				1	8.55e-12	20%
2,3,5-Trimethyl Hexane	235TM-C6	7.90e-12				1	9.97e-12	26%
2-Methyl Octane	2-ME-C8	1.01e-11				1	9.73e-12	-4%
3,3-Diethyl Pentane	33-DE-C5	4.90e-12				1	5.31e-12	8%
4-Methyl Octane	4-ME-C8	9.70e-12				1	1.00e-11	3%
2,6-Dimethyl Octane	26DM-C8	1.29e-11				2	1.14e-11	-12%
2-Methyl Nonane	2-ME-C9	1.28e-11				2	1.12e-11	-12%
3,4-Diethyl Hexane	34-DE-C6	7.40e-12				3	1.25e-11	69%
Cyclopropane	CYCC3	8.40e-14				1	8.52e-14	1%
Cyclobutane	CYCC4	1.50e-12				1	1.59e-12	6%
Cyclopentane	CYCC5	5.06e-12	2.31e-12	2.0	-0.467	1	4.54e-12	-10%
Cyclohexane	CYCC6	7.26e-12	2.59e-12	2.0	-0.614	1	8.52e-12	17%
Isopropyl Cyclopropane	IPR-CC3	2.70e-12				1	2.86e-12	6%
Cycloheptane	CYCC7	1.30e-11				1	9.94e-12	-24%
Methylcyclohexane	ME-CYCC6	1.00e-11				1	1.02e-11	2%
Cyclooctane	CYCC8	1.40e-11				1	1.14e-11	-19%
1,1,3-Trimethyl Cyclohex.	113MCYC6	8.70e-12				1	9.12e-12	5%
Hexyl Cyclohexane	C6-CYCC6	1.78e-11				4	1.77e-11	-1%

Table 8 (Continued)

Compound	Model Name	k(300) (cm^3 $molec^{-1}$ s^{-1})	A	B	Ea kcal/mole	Refs	Est'd k(300) k	(diff)
Alkenes								
Ethene	ETHENE	8.43e-12	1.96e-12		-0.870	1	8.44e-12	0%
Propene	PROPENE	2.60e-11	4.85e-12		-1.002	1	3.16e-11	21%
1-Butene	1-BUTENE	3.11e-11	6.55e-12		-0.928	1	3.16e-11	2%
1-Pentene	1-PENTEN	3.11e-11	5.86e-12		-0.994	5	3.16e-11	2%
3-Methyl-1-Butene	3M-1-BUT	3.14e-11	5.32e-12		-1.059	1	3.16e-11	1%
1-Hexene	1-HEXENE	3.66e-11	6.91e-12		-0.994	5	3.16e-11	-14%
3,3-Dimethyl-1-Butene	33M1-BUT	2.77e-11	5.23e-12		-0.994	5	3.16e-11	14%
1-Heptene	1-HEPTEN	3.96e-11	7.47e-12		-0.994	5	3.16e-11	-20%
Isobutene	ISOBUTEN	5.09e-11	9.47e-12		-1.002	1	5.79e-11	14%
2-Methyl-1-Butene	2M-1-BUT	6.04e-11	1.14e-11		-0.994	5	5.79e-11	-4%
2-Methyl-1-Pentene	2M1-C5E	6.23e-11	1.18e-11		-0.994	5	5.79e-11	-7%
cis-2-Butene	C-2-BUTE	5.58e-11	1.10e-11		-0.968	1	6.34e-11	14%
trans-2-Butene	T-2-BUTE	6.32e-11	1.01e-11		-1.093	1	6.34e-11	0%
2-Methyl-2-Butene	2M-2-BUT	8.60e-11	1.92e-11		-0.894	1	8.71e-11	1%
cis-2-Pentene	C-2-PENT	6.43e-11	1.21e-11		-0.994	5	6.34e-11	-1%
trans-2-Pentene	T-2-PENT	6.63e-11	1.25e-11		-0.994	5	6.34e-11	-4%
2,3-Dimethyl-2-Butene	23M2-BUT	1.09e-10	2.05e-11		-0.994	5	1.05e-10	-4%
2-Methyl-2-Pentene	2M-2-C5E	8.81e-11	1.66e-11		-0.994	5	8.71e-11	-1%
Trans 4-Methyl-2-Hexene	T4M2-C5E	6.04e-11	1.14e-11		-0.994	5	6.34e-11	5%
2,3-Dimethyl-2-Hexene	23M2-C5E	1.02e-10	1.92e-11		-0.994	5	1.05e-10	3%
Trans-2-Heptene	T-2-C7E	6.73e-11	1.27e-11		-0.994	5	6.34e-11	-6%
Trans 4,4-dimethyl-2-Hexene	T44M2C5E	5.44e-11	1.03e-11		-0.994	5	6.34e-11	16%
Trans-4-Octene	T-4-C8E	6.83e-11	1.29e-11		-0.994	5	6.34e-11	-7%
Cyclopentene	CYC-PNTE	6.63e-11	1.25e-11		-0.994	5	6.34e-11	-4%
Cyclohexene	CYC-HEXE	6.70e-11	1.26e-11		-0.994	5	6.34e-11	-5%
1,3-Butadiene	13-BUTDE	6.59e-11	1.48e-11		-0.890	1		
Isoprene	ISOPRENE	1.00e-10	2.55e-11		-0.815	1		
3-Carene	3-CARENE	8.71e-11	1.64e-11		-0.994	5		
a-Pinene	A-PINENE	5.31e-11	1.21e-11		-0.882	1		
b-Pinene	B-PINENE	7.82e-11	2.38e-11		-0.709	1		
d-Limonene	D-LIMONE	1.69e-10	3.19e-11		-0.994	5		
Sabinene	SABINENE	1.16e-10	2.19e-11		-0.994	5		
Styrene	STYRENE	5.80e-11				1		
2-(Cl-methyl)-3-Cl-Propene	CL2IBUTE	3.16e-11				1	5.79e-11	83%
Aromatics								
Benzene	BENZENE	1.24e-12	2.47e-12		0.411	6		
Toluene	TOLUENE	5.91e-12	1.81e-12		-0.705	6		
Ethyl Benzene	C2-BENZ	7.10e-12				6		
Isopropyl Benzene (cumene)	I-C3-BEN	6.50e-12				6		
n-Propyl Benzene	N-C3-BEN	6.00e-12				6		
s-Butyl Benzene	S-C4-BEN	6.00e-12				7		
m-Xylene	M-XYLENE	2.36e-11	2.36e-11		0.000	6		
o-Xylene	O-XYLENE	1.37e-11	1.37e-11		0.000	6		
p-Xylene	P-XYLENE	1.43e-11	1.43e-11		0.000	6		
1,2,3-Trimethyl Benzene	123-TMB	3.27e-11	3.27e-11		0.000	6		
1,2,4-Trimethyl Benzene	124-TMB	3.25e-11	3.25e-11		0.000	6		
1,3,5-Trimethyl Benzene	135-TMB	5.75e-11	5.75e-11		0.000	6		
Indan	INDAN	9.20e-12				8		

Table 8 (Continued)

Compound	Model Name	k(300) (cm^3 $molec^{-1}$ s^{-1})	A	B	Ea kcal/mole	Refs	Est'd k(300) k	(diff)
Naphthalene	NAPHTHAL	2.12e-11	1.07e-12		-1.779	6		
Tetralin	TETRALIN	3.43e-11				9		
1-Methyl Naphthalene	1ME-NAPH	5.30e-11				10		
2-Methyl Naphthalene	2ME-NAPH	5.23e-11				11		
Methyl Naphthalenes	ME-NAPH	5.20e-11				12		
2,3-Dimethyl Naphth.	23-DMN	7.68e-11				11		
Phenol	PHENOL	2.63e-11				6		
m-Cresol	M-CRESOL	6.40e-11				6		
o-Cresol	O-CRESOL	4.20e-11				6		
p-Cresol	P-CRESOL	4.70e-11				6		
Nitrobenzene	NO2-BENZ	1.50e-13				13		
Monochlorobenzene	CL-BEN	7.70e-13				6		
Benzotrifluoride	CF3-BEN	4.60e-13				14		
p-Dichlorobenzene	CL2-BEN	5.55e-13				15		
p-Trifluoromethyl-Cl-Benzene	PCBTF	2.40e-13				14		
Alkynes								
Acetylene	ACETYLEN	9.12e-13	9.40e-12		1.391	16		
Methyl Acetylene	ME-ACTYL	5.90e-12				16		
2-Butyne	2-BUTYNE	2.72e-11	1.00e-11		-0.596	16		
Ethyl Acetylene	ET-ACTYL	8.00e-12				16		
Alcohols and Glycols								
Methanol	MEOH	9.34e-13	3.10e-12		0.715	17	6.25e-13	-33%
Ethanol	ETOH	3.28e-12	5.56e-13		-1.057	17	3.61e-12	10%
Isopropyl Alcohol	I-C3-OH	5.32e-12	6.49e-13		-1.254	16	7.26e-12	37%
n-Propyl Alcohol	N-C3-OH	5.53e-12				16	5.51e-12	0%
n-Butyl Alcohol	N-C4-OH	8.57e-12				16	6.93e-12	-19%
t-Butyl Alcohol	T-C4-OH	1.13e-12	3.86e-13		-0.640	18	6.87e-13	-39%
Cyclopentanol	CC5-OH	1.07e-11				19	1.03e-11	-4%
2-Pentanol	2-C5OH	1.18e-11				19	1.14e-11	-3%
3-Pentanol	3-C5OH	1.22e-11				19	1.30e-11	7%
Pentyl Alcohol	C5OH	1.11e-11				16	8.35e-12	-25%
1-Hexanol	1-C6OH	1.25e-11				16	9.78e-12	-22%
2-Hexanol	2-C6OH	1.21e-11				19	1.28e-11	6%
1-Heptanol	1-C7OH	1.37e-11				16	1.12e-11	-18%
1-Octanol	1-C8-OH	2.02e-11				20	1.26e-11	-38%
2-Octanol	2-C8-OH	2.52e-11				20	1.56e-11	-38%
3-Octanol	3-C8-OH	3.14e-11				20	1.73e-11	-45%
4-Octanol	4-C8-OH	2.87e-11				20	1.73e-11	-40%
Ethylene Glycol	ET-GLYCL	1.47e-11				21	8.38e-12	-43%
Propylene Glycol	PR-GLYCL	2.15e-11				21	1.28e-11	-40%
Ethers and Glycol Ethers								
Dimethyl Ether	ME-O-ME	3.01e-12	1.04e-11		0.739	16	2.30e-12	-24%
Trimethylene Oxide	TME-OX	1.03e-11				22	5.76e-12	-44%
Tetrahydrofuran	THF	1.61e-11				16	1.41e-11	-12%
Dimethoxy methane	METHYLAL	4.90e-12				23	6.69e-11	>100%
Diethyl Ether	ET-O-ET	1.31e-11	8.02e-13		-1.663	16	1.59e-11	22%
Alpha-Methyltetrahydrofuran	AM-THF	2.20e-11	2.52e-12		-1.292	24	2.08e-11	-5%
Tetrahydropyran	THP	1.38e-11				22	2.34e-11	70%

Table 8 (Continued)

Compound	Model Name	k(300) (cm^3 $molec^{-1}$ s^{-1})	A	B	Ea kcal/mole	Refs	Est'd k(300) k	(diff)
Methyl n-Butyl Ether	MNBE	1.48e-11				16	1.35e-11	-9%
Methyl t-Butyl Ether	MTBE	2.94e-12	5.89e-13	2.0	-0.960	16	1.66e-12	-44%
Ethyl n-Butyl Ether	ENBE	2.13e-11				16	2.03e-11	-5%
Ethyl t-Butyl Ether	ETBE	8.84e-12				16	8.48e-12	-4%
Methyl t-Amyl Ether	MTAE	7.91e-12				19	2.82e-12	-64%
Di n-Propyl Ether	PR-O-PR	1.84e-11	1.18e-12		-1.639	16	2.18e-11	18%
Di-n-butyl Ether	BU-O-BU	2.88e-11				16	2.46e-11	-15%
Di-Isobutyl Ether	IBU2-O	2.60e-11				25	2.46e-11	-5%
Di-n-Pentyl Ether	C5-O-C5	3.47e-11				26	2.75e-11	-21%
2-Methoxy-Ethanol	MEO-ETOH	1.33e-11	4.50e-12		-0.646	22	1.49e-11	12%
2-Ethoxy-Ethanol	ETO-ETOH	1.87e-11				27	2.17e-11	16%
1-Methoxy-2-Propanol	MEOC3OH	2.00e-11				28	1.93e-11	-3%
3-Ethoxy-1-Propanol	3ETOC3OH	2.20e-11				22	2.31e-11	5%
3-Methoxy-1-Butanol	3MEOC4OH	2.36e-11				22	2.67e-11	13%
2-Butoxy-Ethanol	BUO-ETOH	2.57e-11				29	2.61e-11	2%
2-(2-Ethoxyethoxy) EtOH	CARBITOL	5.08e-11				30	4.09e-11	-19%
Esters								
Methyl Formate	ME-FORM	2.27e-13				31	1.25e-13	-45%
Ethyl Formate	ET-FORM	1.02e-12				31	1.02e-12	0%
Methyl Acetate	ME-ACET	3.49e-13	8.30e-13		0.517	31	2.65e-13	-24%
n-Propyl Formate	C3-FORM	2.38e-12				31	2.37e-12	0%
Ethyl Acetate	ET-ACET	1.60e-12				6	1.72e-12	7%
Methyl Propionate	ME-PRAT	1.03e-12				31	6.87e-13	-33%
n-Butyl Formate	C4-FORM	3.12e-12				31	3.79e-12	21%
Ethyl Propionate	ET-PRAT	2.14e-12				31	2.14e-12	0%
Isopropyl Acetate	IPR-ACET	3.40e-12				6	3.48e-12	2%
Methyl Butyrate	ME-BUAT	3.04e-12				31	1.91e-12	-37%
Methyl Isobutyrate	ME-IBUAT	1.73e-12				32	1.17e-12	-32%
Propyl Acetate	PR-ACET	3.40e-12				6	3.21e-12	-6%
n-Butyl Acetate	BU-ACET	4.20e-12				6	4.63e-12	10%
Ethyl Butyrate	ET-BUAT	4.94e-12				31	3.36e-12	-32%
Methyl Pivalate	ME-PVAT	1.27e-12				33	7.34e-13	-42%
n-Propyl Propionate	PR-PRAT	4.02e-12				31	3.64e-12	-9%
s-Butyl Acetate	SBU-ACET	5.50e-12				6	5.34e-12	-3%
t-Butyl Acetate	TBU-ACET	4.25e-13				34	5.56e-13	31%
n-Propyl Butyrate	PR-BUAT	7.41e-12				31	4.86e-12	-34%
n-Butyl Butyrate	BU-BUAT	1.06e-11				31	6.28e-12	-41%
Dimethyl Carbonate	DMC	3.30e-13				23	4.44e-13	35%
Propylene Carbonate	PC	6.90e-13				35	3.79e-12	>100%
Methyl Lactate	ME-LACT	2.76e-12				36	2.67e-12	-3%
Ethyl Lactate	ET-LACT	3.91e-12				36	4.12e-12	5%
Methyl Isopropyl Carbonate	MIPR-CB	2.55e-12				37	3.66e-12	44%
Pr. Glycol Methyl Ether Acetate	PGME-ACT	1.44e-11				20	1.47e-11	2%
Dimethyl Succinate	DBE-4	1.50e-12				38	1.17e-12	-22%
Dimethyl Glutarate	DBE-5	3.50e-12				38	2.59e-12	-26%
Dimethyl Adipate	DBE-6	8.80e-12				38	4.01e-12	-54%
Oxides								
Ethylene Oxide	ETOX	7.60e-14				6	3.83e-13	>100%

Table 8 (Continued)

Compound	Model Name	k(300) (cm^3 $molec^{-1}$ s^{-1})	A	B	Ea kcal/mole	Refs	Est'd k(300) k	(diff)
Propylene Oxide	PROX	5.20e-13				6	7.57e-13	46%
1,2-Epoxybutane	12BUOX	1.91e-12				39	2.00e-12	5%
Acids								
Formic Acid	FORMACID	4.50e-13	4.50e-13		0.000	6	5.44e-11	>100%
Acetic Acid	ACETACID	8.00e-13				16	2.10e-13	-74%
Propionic Acid	PROPACID	1.16e-12				16	1.34e-12	16%
Misc. Unsaturated Oxygenates								
2-Methyl-2-Butene-3-ol	MBUTENOL	6.26e-11	8.20e-12		-1.212	40	3.16e-11	-50%
Aldehydes								
Acetaldehyde	ACETALD	1.57e-11	5.60e-12		-0.616	41	1.58e-11	0%
Propionaldehyde	PROPALD	2.00e-11				41	2.01e-11	1%
Butanal	1C4RCHO	2.33e-11	5.26e-12		-0.886	6	2.14e-11	-8%
2-Methylpropanal	2MEC3AL	2.60e-11	6.61e-12		-0.817	6	2.10e-11	-19%
Pentanal	1C5RCHO	2.82e-11	6.34e-12		-0.890	6	2.28e-11	-19%
2,2-Dimethylpropanal (pivaldehyde)	22DMC3AL	2.63e-11	6.82e-12		-0.805	6	1.97e-11	-25%
3-Methylbutanal	3MC4RCHO	2.74e-11				6	2.28e-11	-17%
Acrolein	ACROLEIN	1.99e-11				6	1.07e-11	-46%
Crotonaldehyde	CROTALD	3.64e-11				42	2.16e-11	-41%
Methacrolein	METHACRO	3.33e-11	1.86e-11		-0.348	43	1.97e-11	-41%
Hydroxy Methacrolein	HOMACR	4.30e-11				44	1.97e-11	-54%
Isoprene Product #1	IP-MHY1	7.00e-11				44	2.96e-11	-58%
Isoprene Product #2	IP-MHY2	7.00e-11				44	2.96e-11	-58%
Isoprene Product #3	IP-HMY	7.00e-11				44	2.96e-11	-58%
Ketones								
Acetone	ACETONE	2.22e-13	2.80e-12		1.510	41	2.09e-13	-6%
Cyclobutanone	CC4-KET	8.70e-13				45	4.42e-12	>100%
Methyl Ethyl Ketone	MEK	1.20e-12	1.30e-12		0.050	17	1.35e-12	13%
Cyclopentanone	CC5-KET	2.94e-12				45	6.83e-12	>100%
3-Pentanone	DEK	2.00e-12				6	2.49e-12	25%
2-Pentanone	MPK	4.56e-12				46	4.78e-12	5%
Cyclohexanone	CC6-KET	6.39e-12				45	1.21e-11	89%
4-Methyl-2-Pentanone	MIBK	1.41e-11				6	8.82e-12	-37%
Methyl n-Butyl Ketone	MNBK	9.10e-12				6	6.77e-12	-26%
Methyl t-Butyl Ketone	MTBK	1.21e-12				47	1.72e-12	42%
2-Heptanone	C7-KET-2	1.17e-11				46	8.19e-12	-30%
Di-Isopropyl Ketone	DIPK	5.38e-12				48	5.07e-12	-6%
2-Octanone	C8-KET-2	1.10e-11				47	9.61e-12	-13%
2-Nonanone	C9-KET-2	1.22e-11				47	1.10e-11	-10%
Di-isobutyl ketone (2,6-dimethyl-4-heptanone	DIBK	2.75e-11				6	1.74e-11	-37%
2-Decanone	C10-K-2	1.32e-11				47	1.24e-11	-6%
Methylvinyl ketone	MVK	1.87e-11	4.14e-12		-0.900	6	2.84e-11	52%
Hydroxy Acetone	HOACET	3.02e-12				22	3.11e-12	3%
Methoxy Acetone	MEOACET	6.77e-12				22	7.11e-12	5%
Nitrogen-Containing Compounds								
Para Toluene Isocyanate	P-TI	5.90e-12				49		
Toluene Diisocyanate	TDI	7.40e-12				50		

Table 8 (Continued)

Compound	Model Name	k(300) (cm^3 $molec^{-1}$ s^{-1})	A	B	Ea kcal/mole	Refs	Est'd k(300) k (diff)
Methylene Diphenylene Diisocyanate	MDI	1.18e-11				51	
Dimethyl Amine	DM-AMINE	6.58e-11	2.89e-11		-0.491	6	
Ethyl Amine	ET-AMINE	2.76e-11	1.47e-11		-0.376	6	
Trimethyl Amine	TM-AMINE	6.07e-11	2.62e-11		-0.501	6	
Methyl Nitrite	ME-NITRT	2.20e-13				16	
Ethanolamine	ETOH-NH2	3.15e-11				52	
Dimethylaminoethanol	DMAE	9.00e-11	9.00e-11		0.000	53	
Diethanol Amine	ETOH2-NH	9.37e-11				54	
Triethanolamine	ETOH3-N	1.16e-10				55	
N-Methyl-2-Pyrrolidone	NMP	2.15e-11				35	
Halogen-Containing Compounds							
Methyl Chloride	CH3-CL	4.48e-14	3.15e-13	2.0	1.163	16	
Vinyl Chloride	CL-ETHE	6.90e-12	1.69e-12		-0.839	16	
Ethyl Chloride	C2-CL	4.18e-13	6.94e-13	2.0	0.302	16	
Dichloromethane	CL2-ME	1.45e-13	7.69e-13	2.0	0.994	6	
Methyl Bromide	ME-BR	4.12e-14	2.34e-13	2.0	1.035	6	
1,1-Dichloroethane	11CL2-C2	2.60e-13				6	
Ethylene Dichloride	12CL2-C2	2.53e-13	9.90e-13	2.0	0.813	16	
Ethyl Bromide	C2-BR	3.08e-13	2.72e-11		2.671	6	
Chloroform	CHCL3	1.06e-13	5.67e-13	2.0	1.002	6	
n-Propyl Bromide	C3-BR	1.18e-12				56	
1,1,1-Trichloroethane	111-TCE	1.24e-14	5.33e-13	2.0	2.244	6	
1,1,2-Trichloroethane	112CL3C2	2.00e-13	4.00e-13	2.0	0.413	16	
n-Butyl Bromide	C4-BR	2.46e-12				56	
Ethylene Dibromide	11BR2-C2	2.27e-13	9.27e-13	2.0	0.839	16	
Trans-1,2-Dichloroethene	T-12-DCE	2.32e-12	1.01e-12		-0.497	16	
Trichloroethylene	CL3-ETHE	2.34e-12	5.63e-13		-0.849	16	
Perchloroethylene	CL4-ETHE	1.71e-13	9.64e-12		2.403	16	
Sulfur-Containing Compounds							
Dimethyl Sulfide	DMS	4.85e-12	1.13e-11		0.505	16	
Dimethyl Sulfoxide	DMSO	6.20e-11				6	
Silicon-Containing Compounds							
Hexamethyldisiloxane	SI2OME6	1.38e-12				6	
Hydroxymethyldisiloxane'	SI2OMEOH	1.89e-12				6	
D4 Cyclosiloxane	(SIOME)4	1.00e-12				6	
D5 Cyclosiloxane	(SIOME)5	1.55e-12				6	

References

1 Rate constant expression recommended by Atkinson (1997a)

2 Carter et al (2000b)

3 Atkinson et al. (2000a)

4 Room temperature rate constant from Carter et al (2000c).

5 T=298K rate constant recommended by Atkinson (1997a). Temperature dependence estimated based on data for similar alkenes.

6 Rate constant expression recommended by Atkinson (1989). Recommendation not changed in evaluation update by Atkinson (1994).

Table 8 (Continued)

7 Assumed to have same rate constant as n-propyl benzene

8 Rate constant from Baulch et al (1989).

9 Rate constant from Atkinson and Aschmann (1988a)

10 Rate constant from Atkinson and Aschmann (1987).

11 Rate constant from Atkinson and Aschmann (1986).

12 Rate constant based on average of values for 1- and 2- isomers tabulated by Atkinson (1989).

13 Rate constant based on data tabulated by Atkinson (1989) and consistent with more recent measurement given by Atkinson (1994).

14 Rate constant from Atkinson et al (1985).

15 Rate constant from average of values for o-, m- and p- isomers tabulated by Atkinson (1989).

16 Rate constant expression recommended by Atkinson (1994)

17 Rate expression recommended by IUPAC panel (Atkinson et al, 1999).

18 Rate constant used is Atkinson (1989) recommendation. k=8.1e-13 from Saunders et al (1994) not used because problems reported. k=1.43e-12 from Tuazon and co-workers (Carter et al, 1986c) does not fit chamber results (Carter et al, 1986c).

19 Rate constant from Wallington et al (1988a).

20 Rate constant from Carter et al (2000a).

21 Rate constant from Aschmann and Atkinson (1998).

22 Rate constant from Daguat et al (1988a).

23 Rate constant used is average of various measurements tabulated by Sidebottom et al (1997).

24 Rate constant from Wallington et al (1990).

25 Rate constant from Bennett and Kerr (1989).

26 Rate constant from Wallington et al (1988b).

27 Rate constant of Dagaut et al (1988a) used. Value of Hartmann et al (1986) not consistent with chamber data (Carter et al, 1993a)

28 Average of values of Porter et al (1995) and Aschmann and Atkinson (1998)

29 Average of values of Dagaut et al (1988a), Stemmler et al (1996) and Aschmann and Atkinson (1998), as tabulated by Aschmann and Atkinson (1997).

30 Rate constant from Carter et al (1993a).

31 Rate constant from Wallington et al (1988d).

32 Rate constant from Wells et al. (1999).

33 Absolute rate constant determined by Orkin (NIST unpublished results, 1999) is used. This value is in good agreement with a more imprecise relative determination of Carter et al (2000d)

34 Rate constant from Smith et al (1992). Average of values relative to propane and n-butane

35 Rate constant from Carter et al (1996c).

36 Rate constant from Atkinson and Carter (1995).

37 Carter et al (unpublished results, 2000d)

38 Rate constant from Carter et al (1997e).

39 Rate constant from Wallington et al (1988c).

40 Rudich et al (1995), as recommended by Atkinson (personal communication, 2000). Good agreement with data of Ferronato et al (1998).

41 Rate expression recommended by IUPAC panel (Atkinson et al, 1997a).

42 Rate constant from Atkinson et al (1983).

43 See Carter and Atkinson (1996) and references therein.

44 Rate constant estimated by Carter and Atkinson (1996).

Table 8 (Continued)

45 Rate constant from Daguat et al (1988b).

46 Atkinson et al, (2000b)

47 Rate constant from Wallington and Kurylo (1987).

48 Rate constant from Atkinson et al (1982).

49 Carter et al (1999a)

50 Becker et al (1988)

51 Estimated to have a rate constant that it twice that of pare-toluene isocyanate, based on the structure of the molecule (Carter et al, 1999a).

52 Rate constant estimated from the 298K rate constant for ethylamine and the difference between estimated rates of reaction at -CH3 or -CH2OH derived using the group-additivity methods of Kwok and Atkinson (1995).

53 Anderson and Stephens (1988), as recommended by Atkinson (1989)

54 Rate constant estimated by adding 2 times the difference between the rate constant for ethylene glycol and ethanol to the rate constant for dimethylamine.

55 Rate constant estimated by adding 3 times the difference between the rate constant for ethylene glycol and ethanol to the rate constant for trimethylamine.

56 Donaghy et al. (1993)

should be removed once methods to generate and estimate reactions of unsaturated radicals are developed.

3. Estimation of OH Addition Rate Constants

Rate constant estimates for additions to double bonds are made by estimating total rate constants for reaction at a double bond with a given number and configuration of substituents, and then, for unsymmetrical molecules, estimating the fraction that reacts at the each end. These estimates are shown in Table 10, along with an indication of the derivation of the values used. The total rate constant estimates are based on measured rate constants for representative molecules, but only limited information is available upon which to base the branching ratio estimates, which are therefore more uncertain. These estimates are then used to derive a group rate constant for each of the two groups around the double bond. Note that since the present system does not support generating mechanisms with more than one C=C double bond (except for "special reactants", as discussed later), the estimates on this table are only applicable to monoalkenes.

The group rate constant estimates on Table 10 are somewhat different than those given by Kwok and Atkinson (1997) for several reasons. Propene is not used when deriving the group rate constants for monosubstituted alkenes because its OH rate constant is known and kinetic data for the higher 1-alkenes, which are expected to be more similar to the types of compounds for which estimates may be needed, are better fit by slightly higher values. The estimates of Kwok and Atkinson (1997) also take into account the possibility that some of the reaction may be occurring by abstraction from other groups, which is ignored in our estimates (see below). Kwok and Atkinson (1997) give correction factors for oxygenated substituents, but these are also not fully implemented in the present system because in this work estimates are mainly needed only for hydrocarbon species. The few unsaturated oxygenated species that are handled by the system (primarily acrolein and isoprene products) already have measured or assigned total OH rate constants (e.g., see Carter and Atkinson, 1996). However, correction factors from Kwok and Atkinson

Table 9. Group rate constants and substituent factors used to estimate OH radical abstraction rate constants.

	k(group) = A T^B $e^{-D/T}$ (cm^3 $molec^{-1}$ s^{-1})					F(group)		F(subgroup)		
Group	k(298)	A	B	D	Ref	F	Ref	Subgroup	F	Ref
-CH3	1.36e-13	4.49e-18	2	320	a	1.00	a			
-CH2-	9.34e-13	4.50e-18	2	-253	a	1.23	a	-CH2(CO-)	3.90	a
								-CH2(CO-O-)	1.23	a
								-CH2(F)	0.61	a
								-CH2(Cl)	0.36	a
								-CH2(Br)	0.46	a
>CH-	1.95e-12	2.12e-18	2	-696	a	1.23	a	-CH(CO-)-	3.90	a
								-CH(CO-O-)-	1.23	a
								-CH(F)-	0.21	a
								-CH(Cl)-	0.36	a
								-CH(Br)-	0.46	a
>C<						1.23		>C(CO-)-	3.90	a
								>C(CO-O-)-	1.23	a
								>C(F)-	0.21	a
								>C(Cl)-	0.36	a
								>C(Br)-	0.46	a
-O-						8.40	a	-O(CO-)	1.60	a
								-O(CHO)-	0.90	e
								-O(NO2)-	0.04	a
-OH	1.40e-13	2.10e-18	2	85	a	3.50	a			
-CHO	1.58e-11	5.55e-12	0	-311	b	0.75	a			
HCO(O)-	0.00e+00				c	-				
-CO-						0.75	a	-CO(O-)	0.31	d
-ONO2						0.04	a			
-F						0.09	a			
-Cl						0.38	a			
-Br						0.28	a			
-I						0.53	a			
-NO2						0.00	a			

References

a Kwok and Atkinson (1995)

b Based on kOH for acetaldehyde (Atkinson et al, 1997a, 1999)

c Reaction at formate group assumed to be negligible based on low OH + formate rate constants (Atkinson, 1989)

d Updated value from Kwok et al (1996)

e Adjusted to fit experimental kOH's for ethyl and methyl formate. (Does not work well for methyl formate, but assigned kOH is used for that compound.)

Table 10. Group rate constants used for estimating rates of OH addition reactions.

Group	Estimated Total Rate Constant (300K) (cm^3 $molec^{-1}$ s^{-1})		Fraction reacting at least substituted end	
CH2=CH-	3.16e-11	Total rate constant based on average for 300K rate constants for 1-butene, 3-methyl-1-butene, 1-pentene, 1-hexene and 3-3-dimethyl-1-butene (Atkinson, 1997a).	0.65	Terminal bond addition fraction from Cvetanovic (1976).
CH2=C<	5.79e-11	Total rate constant based on average for 300K rate constants for isobutene, 2-methyl-1-butene and 2-methyl-1-pentene (Atkinson, 1997a).	1.00	100% addition at termal end assumed.
-CH=CH-	6.33e-11	Total rate constant based on average for 300K rate constants for the 2-butenes, the 2-pentenes, trans-4-methyl-2-pentene, trans-4,4-dimethyl-2-pentene, trans-2-heptene, trans-4-octene, cyclopentene, and cyclohexene (Atkinson, 1997a).	0.50	Equal addition at each position assumed.
-CH=C<	8.70e-11	Total rate constant based on average for 300K rate constants for 2-methyl-2-butene and 2-methyl-2-pentene (Atkinson, 1997a).	0.75	No information available concerning relative addition rates at the different positions. Roughly estimate 75% addition at the least substituted position.
>C=C<	1.05e-10	Total rate constant based on average for 300K rate constants for 2,3-dimethyl-2-butene and 2,3-dimethyl-2-pentene (Atkinson, 1997a).	0.50	Equal addition at each position assumed.

Table 11. Summary of average biases and errors in estimates of OH radical rate constants from data given on Table 8.

Class	Count	Average	
		Bias	Error
Alkanes	46	2%	11%
Alkenes	26	4%	10%
Alcohols and Glycols	41	-11%	22%
Esters	27	-9%	21%
Saturated Aldehydes	7	-13%	13%
Acyclic Ketones	16	9%	9%

Notes:

Bias is average of percentage differences between experimental and estimated values

Error is average of absolute value of percentage differences.

(1997) for -CHO and -CO- substituents, of 0.35 and 0.9, respectively, have been incorporated on a preliminary basis.

4. Comparison of Estimated and Assigned Rate Constants

Table 8, above, shows a comparison of the estimated and assigned OH radical rate constants, from which one can obtain an indication of the overall performance of the estimation methods for the various types of VOCs. Table 11shows a summary of average percentage errors (biases) and average absolute percentage errors (errors) for OH radical rate constant estimates for various classes of VOCs. It can be seen that the estimation method performs reasonably well for alkanes and alkenes, having biases of less than 5% and an average error of less than 12%. The estimates do not perform as well for the oxygenated compounds, with average errors on the order of 15-25%. Refinements to the estimation method may improve the performance for these oxygenates, but updating the work of Kwok and Atkinson (1995) was beyond the scope of this report.

5. Assigned Mechanisms for Initial OH Reactions

Because estimation methods for the branching ratios for the reactions of OH radicals at different positions of the molecule have some uncertainty, branching ratios are explicitly assigned for those compounds where experimental data are available, and indicate that the estimates may not be appropriate. In addition, as indicated in Table 7, several alkynes and dialkenes have also been incorporated into the mechanism generation system as “special reactants”, whose reactions cannot be estimated and therefore need to be specified explicitly. The explicitly assigned branching ratios for initial OH radical reactions that are currently incorporated in the system are summarized on Table 12, along with the basis for the various assignments that are used.

Table 12. Assigned mechanisms for the initial reactions of OH radicals with compounds for which estimates could not be made, or where experimental data indicate that the estimates may not be appropriate.

Reactant and Products [a]	Factor	Documentation
1,3-Butadiene [CH2=CH-CH=CH2]		
CH2=CH-CH[.]-CH2-OH	100.0%	Terminal addition assumed to dominate because of formation of resonance-stabilized radical.
Isoprene [CH2=CH-C(CH3)=CH2]		
CH2=CH-C[.](CH3)-CH2-OH	52.4%	Mechanism assumed to be as discussed by Carter and Atkinson (1996).
CH2=C(CH3)-CH[.]-CH2-OH	42.6%	See above.
CH2=CH-C(OH)(CH2.)-CH3	2.5%	Based on observed 3-methyl furan yields as discussed by Carter and Atkinson (1996).
CH2=C(CH3)-CH(CH2.)-OH	2.5%	See above.
Acetylene [HC::CH]		
HO-CH=CH.	90.0%	Estimated mechanism is based on the data of Hatakeyama et al (1986) and modeling acetylene environmental chamber runs Carter et al (1997c).
HCO-CH2.	10.0%	See above. Adjusted to fit chamber data.
Methyl Acetylene [HC::C-CH3]		
CH3-C[.]=CH-OH	100.0%	Estimated to be the major reaction pathway.
Ethyl Acetylene [HC::C-CH2-CH3]		
CH3-CH2-C[.]=CH-OH	100.0%	Estimated to be the major reaction pathway.
2-Butyne [CH3-C::C-CH3]		
CH3-C(OH)=C[.]-CH3	100.0%	Estimated to be the major reaction pathway.
Methanol [CH3-OH]		
HO-CH2.	85.0%	Branching ratios recommended by IUPAC (Atkinson et al, 1997, 1999).
CH3O.	15.0%	See above.
Ethanol [CH3-CH2-OH]		
CH3-CH[.]-OH	90.0%	Branching ratios recommended by IUPAC (Atkinson et al, 1997, 1999).
CH3-CH2O.	5.0%	See above
HO-CH2-CH2.	5.0%	See Above
1-Octanol [CH3-CH2-CH2-CH2-CH2-CH2-CH2-CH2-OH]		
CH3-CH2-CH2-CH2-CH2-CH2-CH2-CH[.]-OH	19.2%	Based on yields of octanal from 1-octanol (Carter et al, 2000a).
HO-CH2-CH2-CH2-CH2-CH2-CH2-CH2-CH2.	1.5%	Relative branching ratios of other routes estimated using method of Kwok and Atkinson (1995).
CH3-CH[.]-CH2-CH2-CH2-CH2-CH2-CH2-OH	10.8%	See above.
CH3-CH2-CH[.]-CH2-CH2-CH2-CH2-CH2-OH	13.3%	See above.
CH3-CH2-CH2-CH[.]-CH2-CH2-CH2-CH2-OH	13.3%	See above.
CH3-CH2-CH2-CH2-CH[.]-CH2-CH2-CH2-OH	13.3%	See above.

Table 12 (continued)

Reactant and Products [a]	Factor	Documentation
CH3-CH2-CH2-CH2-CH2-CH[.]-CH2-CH2-OH	13.3%	See above.
CH3-CH2-CH2-CH2-CH2-CH2-CH[.]-CH2-OH	13.3%	See above.
CH3-CH2-CH2-CH2-CH2-CH2-CH2-CH2O.	1.7%	See above.
2-Octanol [CH3-CH(OH)-CH2-CH2-CH2-CH2-CH2-CH3]		
CH3-C[.](OH)-CH2-CH2-CH2-CH2-CH2-CH3	36.5%	Based on yield of 2-octanone from 2-octanol (Carter et al, 2000a)
CH3-CH2-CH2-CH2-CH2-CH2-CH(CH2.)-OH	1.5%	Relative branching ratios of other routes estimated using method of Kwok and Atkinson (1995).
CH3-CH2-CH2-CH2-CH2-CH2-CH[O.]-CH3	1.5%	See above.
CH3-CH(OH)-CH[.]-CH2-CH2-CH2-CH2-CH3	12.3%	See above.
CH3-CH(OH)-CH2-CH[.]-CH2-CH2-CH2-CH3	12.3%	See above.
CH3-CH(OH)-CH2-CH2-CH[.]-CH2-CH2-CH3	12.3%	See above.
CH3-CH(OH)-CH2-CH2-CH2-CH[.]-CH2-CH3	12.3%	See above.
CH3-CH(OH)-CH2-CH2-CH2-CH2-CH[.]-CH3	9.9%	See above.
CH3-CH(OH)-CH2-CH2-CH2-CH2-CH2-CH2.	1.5%	See above.
3-Octanol [CH3-CH2-CH(OH)-CH2-CH2-CH2-CH2-CH3]		
CH3-CH2-C[.](OH)-CH2-CH2-CH2-CH2-CH3	42.4%	Based on yield of 3-octanone from 3-octanol (Carter et al, 2000a)
CH3-CH2-CH2-CH2-CH2-CH(OH)-CH2-CH2.	1.4%	Relative branching ratios of other routes estimated using method of Kwok and Atkinson (1995).
CH3-CH2-CH2-CH2-CH2-CH(OH)-CH[.]-CH3	9.4%	See above.
CH3-CH2-CH2-CH2-CH2-CH[O.]-CH2-CH3	1.4%	See above.
CH3-CH2-CH(OH)-CH[.]-CH2-CH2-CH2-CH3	11.5%	See above.
CH3-CH2-CH(OH)-CH2-CH[.]-CH2-CH2-CH3	11.5%	See above.
CH3-CH2-CH(OH)-CH2-CH2-CH[.]-CH2-CH3	11.5%	See above.
CH3-CH2-CH(OH)-CH2-CH2-CH2-CH[.]-CH3	9.4%	See above.
CH3-CH2-CH(OH)-CH2-CH2-CH2-CH2-CH2.	1.4%	See above.
4-Octanol [CH3-CH2-CH2-CH(OH)-CH2-CH2-CH2-CH3]		
CH3-CH2-CH2-C[.](OH)-CH2-CH2-CH2-CH3	36.6%	Based on yield of 4-octanone from 4-octanol (Carter et al, 2000a)
CH3-CH2-CH2-CH2-CH(OH)-CH2-CH2-CH2.	1.6%	Relative branching ratios of other routes estimated using method of Kwok and Atkinson (1995).
CH3-CH2-CH2-CH2-CH(OH)-CH2-CH[.]-CH3	10.3%	See above.

Table 12 (continued)

Reactant and Products [a]	Factor	Documentation
CH3-CH2-CH2-CH2-CH(OH)-CH[.]-CH2-CH3	12.7%	See above.
CH3-CH2-CH2-CH2-CH[O.]-CH2-CH2-CH3	1.6%	See above.
CH3-CH2-CH2-CH(OH)-CH[.]-CH2-CH2-CH3	12.7%	See above.
CH3-CH2-CH2-CH(OH)-CH2-CH[.]-CH2-CH3	12.7%	See above.
CH3-CH2-CH2-CH(OH)-CH2-CH2-CH[.]-CH3	10.3%	See above.
CH3-CH2-CH2-CH(OH)-CH2-CH2-CH2-CH2.	1.6%	See above.
Methyl t-Butyl Ether [CH3-C(CH3)(CH3)-O-CH3]		
CH3-C(CH3)(CH3)-O-CH2.	80.0%	Branching ratios based on product studies of Tuazon et al, (1991b); and Smith et al (1991), with overall yields increased to account for 100% reaction.
CH3-C(CH3)(CH2.)-O-CH3	20.0%	See Above
1-Methoxy-2-Propanol [CH3-CH(OH)-CH2-O-CH3]		
CH3-O-CH2-CH(CH2.)-OH	0.0%	Estimated to be minor
CH3-C[.](OH)-CH2-O-CH3	39.0%	Based on observed methoxyacetone yields (Tuazon et al, 1998a).
CH3-O-CH2-CH[O.]-CH3	0.0%	Estimated to be minor
CH3-CH(OH)-CH[.]-O-CH3	58.0%	Based on observed methyl formate and acetaldehyde yields, the expected products from this route (Tuazon et al, 1998a)
CH3-CH(OH)-CH2-O-CH2.	3.0%	Estimated to occur ~6% of the time. 3% yield assumed to account for 100% reaction.
2-Butoxy-Ethanol [CH3-CH2-CH2-CH2-O-CH2-CH2-OH]		
CH3-CH2-CH2-CH2-O-CH[.]-CH2-OH	57.0%	Branching ratio based on observed yield of n-butyl formate, which is the expected major product from this route (Tuazon et al, 1998a).
CH3-CH2-CH2-CH[.]-O-CH2-CH2-OH	22.0%	Branching ratio based on observed yields of 2-hydroxyetlyo formate and propanal, the expected major products from this route (Tuazon et al, 1998a).
HO-CH2-CH2-O-CH2-CH2-CH2-CH2.	0.5%	Relative branching ratios for this and the other routes estimated using method of Kwok and Atkinson (1996).
CH3-CH[.]-CH2-CH2-O-CH2-CH2-OH	3.5%	See above.
CH3-CH2-CH[.]-CH2-O-CH2-CH2-OH	4.3%	See above.
CH3-CH2-CH2-CH2-O-CH2-CH[.]-OH	12.2%	See above.
CH3-CH2-CH2-CH2-O-CH2-CH2O.	0.6%	See above.
Methyl Acetate [CH3-O-CO-CH3]		
CH3-CO-O-CH2.	100.0%	Environmental chamber reactivity data fit somewhat better if reaction at the CH3-CO end is assumed to be negligible.
CH3-O-CO-CH2.	0.0%	See above

Table 12 (continued)

Reactant and Products [a]	Factor	Documentation
Propylene Carbonate [*CH(CH3)-CH2-O-CO-O-*]		
CH(CH2.)-CH2-O-CO-O-	25.0%	Branching ratio estimated from ratio of estimate for reaction at this position using method of Kwok and Atkinson (1996) to measured total rate constant Carter et al, 1996c).
C[.](CH3)-CH2-O-CO-O-	37.5%	Model simulations are somewhat more consistent with environmental chamber reactivity data if the other two reaction routes are assumed to occur with approximately equal probability.
CH(CH3)-O-CO-O-CH[.]-	37.5%	See above
Methyl Isobutyrate [CH3-CH(CH3)-CO-O-CH3]		
CH3-C[.](CH3)-CO-O-CH3	67.0%	Branching ratio derived from total rate constant and estimated rate constants for the competing reaction routes. This results in higher predicted yields for acetone, which is more consistent with the product data of Wells et al (1999).
CH3-CH(CH2.)-CO-O-CH3	20.0%	Branching ratio derived from ratio of rate constant for this route estimated using the method of Kwok and Atkinson (1995), relative to the total rate constant.
CH3-CH(CH3)-CO-O-CH2.	13.0%	See above.
Propylene Glycol Methyl Ether Acetate [CH3-O-CH(CH3)-CH2-O-CO-CH3]		
CH3-CO-O-CH2-CH(CH3)-O-CH2.	7.9%	Group rate constant estimated using method of Kwok and Atkinson (1995)
CH3-O-C[.](CH3)-CH2-O-CO-CH3	45.3%	Group rate constant adjusted to fit environmental chamber reactivity data, and to be consistent with measured total rate constant.
CH3-O-CH(CH2.)-CH2-O-CO-CH3	1.2%	Group rate constant estimated using method of Kwok and Atkinson (1995)
CH3-O-CH(CH3)-CH[.]-O-CO-CH3	45.3%	Group rate constant adjusted to fit environmental chamber reactivity data, and to be consistent with measured total rate constant.
CH3-O-CH(CH3)-CH2-O-CO-CH2.	0.3%	Group rate constant estimated using method of Kwok and Atkinson (1995)
Dimethyl Succinate (DBE-4) [CH3-O-CO-CH2-CH2-CO-O-CH3]		
CH3-O-CO-CH2-CH2-CO-O-CH3 + OH -> H2O + CH3-O-CO-CH2-CH2-CO-O-CH2.	90.0%	Branching ratio derived from the ratio of the rate constant for the analogous reaction for dimethyl adipate (DBE-5) to the total rate constant. The former was derived from the DBE-5 yield data of Tuazon et al (1999) and total DBE-5 rate constant of Carter et al (1997e). Assuming that this reaction dominates also gives better results of model simulations of DBE-4 reactivity environmental chamber experiments.
CH3-O-CO-CH2-CH2-CO-O-CH3 + OH -> H2O + CH3-O-CO-CH2-CH[.]-CO-O-CH3	10.0%	Branching ratio derived from branching ratio estimated for competing reaction.
Dimethyl Adipate (DBE-5) [CH3-O-CO-CH2-CH2-CH2-CO-O-CH3]		
CH3-O-CO-CH2-CH2-CH2-CO-O-CH2.	39.0%	Based on yield of CH3-O-CO-CH2-CH2-CH2-CO-OH observed by Tuazon et al (1999)

Table 12 (continued)

Reactant and Products [a]	Factor	Documentation
CH3-O-CO-CH2-CH[.]-CH2-CO-O-CH3	41.0%	Yield of CH3-O-CO-CH2-CO-CH2-CO-O-CH3 observed by Tuazon et al (1999) corresponds to this route occurring 33% of the time. However, model simulations fit chamber data somewhat better if this route is assumed to be relatively more important; so the fraction reacted at in this position is estimated from the ratio of the rate constant derived using estimates of Kwok and Atkinson (1985) as updated by Kwok et al (1996) to the measured total rate constant. This is within the uncertainty of the yield measurement.
CH3-O-CO-CH2-CH2-CH[.]-CO-O-CH3	20.0%	See above
Dimethoxy Methane [CH3-O-CH2-O-CH3]		
CH3-O-CH2-O-CH2.	67.0%	Based on ratio of yields of CH3-O-CH2-O-CHO relative to CH3-O-CO-O-CH3 + CH3-O-CHO given by Sidebottom et al (1997), which is consistent with product data of Wallington et al (1997).
CH3-O-CH[.]-O-CH3	33.0%	See above.
2-Methyl-3-Buten-2-oh [CH2=CH-C(CH3)(OH)-CH3]		
CH3-C(CH3)(OH)-CH[.]-CH2-OH	66.7%	Based on product data reported by Alvarado et al (1999). The correspondig alkoxy radical is estimated to decompose form glycolaldehyde and the precursor to acetone, both observed products.
CH3-C(CH3)(OH)-CH(OH)-CH2.	33.3%	See above. Reaction at this position is assumed to be the only source of the observed formation of formaldehyde and 2-hydroxy-2-methylpropanal.
Acrolein [CH2=CH-CHO]		
CH2=CH-CO.	75.0%	Estimated rate constant for reaction at this position is intermediate between the estimate based on the analogous reaction of methacrolein and estimation using method of Atkinson (1987).
HCO-CH[.]-CH2-OH	17.0%	Addition to double bond assumed to occur 25% of the time, based on total rate constant and estimate for reaction at the CHO position. Terminal/internal ratio based on the ratio determined for OH + propene.
HCO-CH(CH2.)-OH	8.0%	See above.
Crotonaldehyde [CH3-CH=CH(CHO)]		
CH3-CH=CH(CO.)	45.0%	Assumed to occur with the same rate constant as the analogous reaction for methacrolein.
CH3-CH[.]-CH(OH)-CHO	27.5%	Fraction reacted based on total rate constant, estimated rate for abstraction from -CHO, and assumption that addition at each side of the double bond is equal.
CH3-CH(OH)-CH[.]-CHO	27.5%	See above.
Methacrolein [CH2=C(CHO)-CH3]		
CH3-C[.](CHO)-CH2-OH	44.0%	Adjusted to give same product distribution as used by Carter and Atkinson (1996), and to be consistent with available product data.
CH3-C(OH)(CH2.)-CHO	6.0%	See above.
CH2=C(CO.)-CH3	50.0%	See above.

Table 12 (continued)

Reactant and Products [a]	Factor	Documentation
Hydroxy Methacrolein [CH2=C(CHO)-CH2-OH]		
CH2=C(CO.)-CH2-OH	38.0%	Mechanism of Carter and Atkinson (1996) is assumed.
HO-CH2-C[.](CHO)-CH2-OH	52.0%	See above.
HCO-C(OH)(CH2.)-CH2-OH	10.0%	See above.
Isoprene Product #1 [CH3-C(CHO)=CH(CH2-OH)]		
CH3-C(CO.)=CH(CH2-OH)	25.0%	Mechanism of Carter and Atkinson (1996) is assumed.
CH3-C[.](CHO)-CH(OH)-CH2-OH	50.0%	See above.
CH3-C(CHO)(OH)-CH[.]-CH2-OH	25.0%	See above.
Isoprene Product #2 [CH3-C(CHO)=CH-CH2-OH]		
CH3-C(CO.)=CH-CH2-OH	25.0%	Mechanism of Carter and Atkinson (1996) is assumed.
CH3-C[.](CHO)-CH(OH)-CH2-OH	50.0%	See above.
CH3-C(CHO)(OH)-CH[.]-CH2-OH	25.0%	See above.
Isoprene Product #3 [HCO-CH=C(CH3)-CH2-OH]		
HO-CH2-C(CH3)=CH-CO.	25.0%	Mechanism of Carter and Atkinson (1996) is assumed.
HCO-CH(OH)-C[.](CH3)-CH2-OH	50.0%	See above.
HCO-CH[.]-C(CH3)(OH)-CH2-OH	25.0%	See above.
Cyclohexanone [*CH2-CH2-CH2-CH2-CH2-CO-*]		
CH2-CH2-CH2-CH2-CO-CH[.]-	44.0%	Better fits of model simulations to results of environmental chamber reactivity experiments are obtained if equal probability of reaction at alpha and beta positions (Carter et al, 2000a).
CH2-CH2-CH2-CO-CH2-CH[.]-	44.0%	See above.
CH2-CH2-CO-CH2-CH2-CH[.]-	12.0%	Approximately the fraction reacted at this position estimated by method of Kwok and Atkinson (1995)
Methylvinyl ketone [CH2=CH-CO-CH3]		
CH3-CO-CH[.]-CH2-OH	70.0%	Based on product distribution of Tuazon and Atkinson (1989), as discussed by Carter and Atkinson (1996)
CH3-CO-CH(CH2.)-OH	30.0%	See above.
Formic Acid [HCO-OH]		
HCO2.	100.0%	Believed to be the major reaction route.

[a] Formation of H_2O, where applicable, is not shown.

D. Reactions with NO_3 Radicals

Reactions with NO_3 radicals can be a non-negligible fate for alkenes and aldehydes under some conditions, and therefore are included in the mechanism. These reactions are considered in essentially the same way as reaction with OH radicals, except that HNO_3 or ONO_2-substituted products are formed. Thus, if the group has an abstractable hydrogen, the reaction is

$$XH + NO_3 \rightarrow X\cdot + HNO_3 \qquad \text{(abstraction)}$$

And if the molecule has a double bond, the reaction is

$$>C=C< + NO_3 \rightarrow >C(ONO_2)-C[\cdot]- \qquad \text{(addition)}$$

However, the current system assumes that rate constants for all abstraction reactions are negligible except for reaction at aldehyde -CHO groups. Therefore, only H abstraction reactions of NO_3 with aldehydes or additions to alkenes are considered in the current mechanism.

1. Assigned NO_3 Radical Rate Constants

NO_3 radical rate constants have been measured for a number of VOCs in the current mechanism, though the coverage is nowhere near as complete as is the case for the OH radical reaction. Table 13 gives the NO_3 radical rate constants assigned to all VOCs in the current mechanism for which the reaction with NO_3 radicals is represented. Note that the table does not include measured NO_3 radical rate constants for alkanes and other species that the current mechanism neglects as being of negligible importance. Footnotes indicate the basis for the rate parameter assignments, most of which are based on Atkinson (1991, 1994, 1997a) recommendations.

2. Estimated NO_3 Radical Rate Constants

Reaction of NO_3 with aldehyde groups are based on the measured rate constant for the reaction of NO_3 with acetaldehyde, which is (Atkinson et al, 1997, 1999),

$$k(NO_3 + X\text{-}CHO) = 1.40 \times 10^{-12}\, e^{-3.696/RT} \cdot F(X)\ cm^3\ molec^{-1}\ s^{-1}.$$

where F(X) is the substituent factor for groups other than $-CH_3$ bonded to the -CHO. The correlation between NO_3 and OH radical abstraction rate constants given by Atkinson (1991)[9] is used to estimate these group substituent correction factors, F(X), which are as follows:

- $F(-CH_2-) = F(-CH-) = F(>C<) = 1.34$ is derived from the correlation of Atkinson (1991) and the the rate constant for OH abstraction from -CHO groups derived by the group-additivity method of Kwok and Atkinson (1995).
- F(-CHO) = 0.18 is derived from the correlation and the OH rate constant for glyoxal.
- F(-CO-) = 0.89 is derived from the correlation and the OH rate constant for methyl glyoxal.

Note that rate constants for NO_3 abstraction from -CHO groups bonded to an oxygen (e.g., formates) are estimated to be zero, so such reactions are not generated.

The group rate constants used for estimating NO_3 addition rate constants is given on Table 14, along with the documentation for the rate constant assignments. Note that in the case of NO_3 reactions we assume that addition always occurs to the least substituted position around the bond, based on the assumption that since NO_3 addition rate constants are lower than those for OH addition, they will tend to be more selective. Rate constant data are available for only a few compounds of each type, so the estimates are necessarily more uncertain than those for OH radical reactions. As with the OH addition estimates, the rate constant for propene is not used for making the estimates for general 1-alkenes because 1-butene is considered to be more representative of the types of the higher monoalkenes for which rate constant estimates would be needed.

---

[9] Atkinson (1993) noted a good correlation between OH and NO_3 abstraction rate constants per abstractable hydrogen, with the data being fit by $\ln k_{NO3} = 6.498 + 1.611\ \ln k_{OH}$.

Table 13. Rate constant and temperature dependence parameter assignments used for reactions of VOCs with NO_3 radicals in the present mechanism.

Compound	Model Name	k(300)	A	B	Ea	Ref	Est'd k(300)	
		(cm^3 $molec^{-1}$ s^{-1})			kcal/mole		k	(diff)
Propene	PROPENE	9.73e-15	4.59e-13		2.297	1	1.38e-14	42%
1-Butene	1-BUTENE	1.38e-14	3.14e-13		1.864	1	1.38e-14	0%
Isobutene	ISOBUTEN	3.32e-13	3.32e-13		0.000	2	3.32e-13	0%
cis-2-Butene	C-2-BUTE	3.47e-13	1.10e-13		-0.687	3	3.70e-13	7%
trans-2-Butene	T-2-BUTE	3.92e-13	1.10e-13	2.0	-0.759	1	3.70e-13	-6%
2-Methyl-2-Butene	2M-2-BUT	9.37e-12	9.37e-12		0.000	2	9.37e-12	0%
2,3-Dimethyl-2-Butene	23M2-BUT	5.72e-11	5.72e-11		0.000	2	5.72e-11	0%
Cyclopentene	CYC-PNTE	5.30e-13	5.30e-13		0.000	2	3.70e-13	-30%
Cyclohexene	CYC-HEXE	5.88e-13	1.05e-12		0.346	1	3.70e-13	-37%
1,3-Butadiene	13-BUTDE	1.00e-13	1.00e-13		0.000	2		
Isoprene	ISOPRENE	6.85e-13	3.03e-12		0.886	1		
a-Pinene	A-PINENE	6.09e-12	1.19e-12		-0.974	1		
3-Carene	3-CARENE	9.10e-12	9.10e-12		0.000	2		
b-Pinene	B-PINENE	2.51e-12	2.51e-12		0.000	2		
Sabinene	SABINENE	1.00e-11	1.00e-11		0.000	2		
d-Limonene	D-LIMONE	1.22e-11	1.22e-11		0.000	2		
2-Methyl-2-Butene-3-ol	MBUTENOL	1.21e-14	4.60e-14		0.795	13	1.38e-14	14%
2-(Cl-methyl)-3-Cl-Propene	CL2IBUTE	1.00e-15				4		
Styrene	STYRENE	1.51e-13				5		
Acetaldehyde	ACETALD	2.84e-15	1.40e-12		3.696	6	2.84e-15	0%
Methylvinyl ketone	MVK	0.00e+00				7	2.76e-18	
Methacrolein	METHACRO	4.76e-15	1.50e-12		3.430	8		
Isoprene Product #1	IP-MHY1	1.00e-13				9		
Isoprene Product #2	IP-MHY2	1.00e-13				9		
Isoprene Product #3	IP-HMY	1.00e-13				9		
Hydroxy Methacrolein	HOMACR	4.76e-15	1.50e-12		3.430	10		
Crotonaldehyde	CROTALD	5.12e-15				11		

References

1 Rate constant expression recommended by Atkinson (1997a)

2 Rate constant from Atkinson (1997a). Temperature dependence is assumed to be small.

3 T=298K rate constant recommended by Atkinson (1997a). Temperature dependence estimated by assuming the A factor is the same as for trans-2-butene.

4 This rate constant estimated by Atkinson (private communication, 1997) based on the rate constant for NO3 + Allyl chloride (Atkinson, 1991)

5 Rate constant from Atkinson and Aschmann (1988a).

6 Rate constant expression recommended by IUPAC, Supplement V (Atkinson et al, 1997).

7 Data of Kwok et al (1997) indicate that the total rate constant is less than 6e-18 cm3 molec-1 s-1, which make it unimportant under atmospheric conditions.

8 Total rate constant from Kwok et al (1996). Temperature dependence estimated by Carter and Atkinson (1996)

9 Rate constant estimated by Carter and Atkinson (1996).

10 Rate constant assumed to be the same as for methacrolein (Carter and Atkinson, 1996)

11 Atkinson et al (1987)

12 Rate constant from Carter et al (1996c).

Table 14. Group rate constants and group substituent correction factors used for estimating rates of NO_3 addition reactions.

Groups	Estimated Total Rate Constant (300K) (cm3 molec-1 s-1)		Fraction reacting at least substituted end	
CH2=CH-	1.38e-14	Total rate constant based on 300K value for 1-butene (Atkinson, 1997a).	1.0	100% addition at terminal end assumed.
CH2=C<	3.32e-13	Total rate constant based on 300K value for isobutene (Atkinson, 1997a)	1.0	100% addition at terminal end assumed.
-CH=CH-	1.85e-13	Total rate constant based on averaging the 300K values for cis and trans 2-butene (Atkinson, 1997a).	0.5	Equal addition at each position assumed.
-CH=C<	3.32e-13	Total rate constant based on 300K value for 2-methyl-2-butene (Atkinson, 1997a).	1.0	100% addition at the least substituted end is assumed.
>C=C<	2.86e-11	Total rate constant based on the 300K value for 2,3-dimethyl-2-butene (Atkinson, 1997a).	0.5	Equal addition at each position assumed.

The group rate constants shown on Table 14 are strictly speaking applicable only for estimating rate constants for unsaturated hydrocarbons. Group correction factors, which are multiplied by the group rate constants shown on Table 14, are used for estimating rate constants for NO_3 to double bonds in unsaturated carbonyls. These are as follows:

- A factor of 0.007 is used if the double bond has a -CHO substituent, based on the ratio of the estimated rate constant for NO_3 addition to methacrolein (Carter and Atkinson, 1996) to the group rate constant for CH2=C<.
- A factor of 2×10^{-4} is used if the double bond has a -CO- substituent, based on the upper limit rate constant for the reaction of NO_3 with methyl vinyl ketone (Carter and Atkinson, 1996). The actual upper limit rate constant of 6×10^{-18} cm^3 $molec^{-1}$ s^{-1} corresponds to a factor of $\sim 4 \times 10^{-4}$, but we arbitrarily use a factor which is half that. This is sufficiently small to make reactions of NO_3 with such compounds to be of negligible importance.

The performance of the estimation method in predicting the measured NO_3 radical rate constants is indicated on Table 13. Except for propene (for which estimates are not needed) and the halogenated alkene on the list (whose subsequent reactions are not currently supported by the system), the estimates generally perform reasonably well. Of course, in most cases this is because the estimates are based on these data. There does seem to be a bias towards underpredicting the rate constants for the cycloalkenes, and it may be appropriate to add a ring correction term for such compounds.

3. Assigned Mechanisms for Initial NO_3 Reactions

As with OH reactions discussed above, explicit assignments are used for the initial reactions for those VOCs where estimates cannot be made, where available experimental data indicate the estimates are inappropriate, or where alternative estimates are used. The explicitly assigned branching ratios for the

initial NO_3 radical reactions that are currently incorporated in the system are summarized on Table 15, along with the basis for the various assignments that are used.

E. Reactions with O_3

Reactions with O_3 are assumed to occur only at carbon-carbon double bonds[10], and the reactions are assumed to involve ultimately breaking the bond and forming a carbonyl and an excited Crigiee biradical, i.e.

$$>C=C< + O_3 \rightarrow >CO2[excited] + >C=O$$

Two reactions are generated for each C=C bond, involving formation of the biradical from each of the two groups around the bond. Therefore, it is necessary to know both the total rate constant and the fraction of biradical formation at each of the groups around the bond.

1. Assigned O_3 Rate constants

Rate constants for reaction with O_3 have been measured for most of the VOCs in the current mechanism for which O_3 reactions are assumed to be non-negligible. Table 16 lists the rate parameter assignments for all VOCs for which this is the case, and indicates the source of the assignments. Again, this includes all VOCs in the current mechanism, not just those whose reactions can be processed by the mechanism generation system. As with the other reactions, almost all of the assignments are based on recommendations from various Atkinson reviews (Atkinson and Carter, 1984; Atkinson, 1994, 1997a).

2. Estimated Total Rate Constants

As discussed by Atkinson and Carter (1984), ozone + alkene rate constants tend to be quite variable depending on the structure of the compound, even if grouped according to the number of substitutents on each side of the double bond. This is shown on Figure 2, which shows a comparison of the T=300K rate constants for the various monoalkenes tabulated by Atkinson (1997a), with a separate plot for each type of double bond structure. Note that cyclohexenes (which tend to have higher O_3 rate constants) and terpenes (whose structures the mechanism generation system cannot presently handle) are not shown. It can be seen that there is variability in the rate constants, particularly for the 1,1-disbustituted compounds. It is interesting to note that the more highly branched compounds tend to have the lowest rate constants, suggesting that steric effects may be important.

Fortunately, measured O_3 rate constants are available for most of the alkenes that are important in current emissions, which tend to be the lower molecular weight compounds. However, it is still necessary to have a method to estimate rate constants for those compounds where no data are available, even if it is uncertain. For this purpose, we use the average of the rate constants for the reactions at the various types of double bonds, as shown on Figure 2, and as summarized on Table 17. Table 16, shows the discrepancies between the experimental and estimated values for all the alkenes in the current mechanism. The anomalously low value for 3,4-dietlyl-2-hexene (which may be low because of steric hindrance) was not used when computing the average for -CH=C<. Although there is variability, the averages are probably appropriate as best estimates for compounds whose rate constants are not known, at least for use by the mechanism generation system at its current state of development. Obviously, compounds with large steric effects need to be estimated on a case-by-case basis.

[10] Reactions of O_3 with alkynes are included as assigned reactions for special reactants (see Section III.E.4), but are not automatically generated by the system.

Table 15. Assigned mechanisms for the reactions of NO_3 radicals with compounds for which estimates could not be made, or where experimental data or other considerations indicate that the general estimates may not be appropriate.

Reactant and Products	Factor	Documentation
1,3-Butadiene [CH2=CH-CH=CH2]		
CH2=CH-CH[.]-CH2-ONO2	100.0%	Terminal addition assumed to dominate because of formation of resonance-stabilized radical.
Isoprene [CH2=CH-C(CH3)=CH2]		
CH2=CH-C[.](CH3)-CH2-ONO2	100.0%	Mechanism of Carter and Atkinson (1996) is assumed.
Crotonaldehyde [CH3-CH=CH(CHO)]		
CH3-CH=CH(CO.)	45.0%	Assumed to occur with the same rate constant as the analogous reaction for methacrolein.
CH3-CH[.]-CH(ONO2)-CHO	27.5%	Fraction reacted based on total rate constant, estimated rate for abstraction from -CHO, and assumption that addition at each side of the double bond is equal.
CH3-CH(ONO2)-CH[.]-CHO	27.5%	See above.
Methacrolein [CH2=C(CHO)-CH3]		
HNO3 + CH2=C(CO.)-CH3	50.0%	Mechanism of Carter and Atkinson (1996) is assumed.
CH3-C[.](CHO)-CH2-ONO2	50.0%	See above.
Hydroxy Methacrolein [CH2=C(CHO)-CH2-OH]		
HNO3 + CH2=C(CO.)-CH2-OH	50.0%	Mechanism of Carter and Atkinson (1996) is assumed.
HO-CH2-C[.](CHO)-CH2-ONO2	50.0%	See above.
Isoprene Product #1 [CH3-C(CHO)=CH(CH2-OH)]		
CH3-C[.](CHO)-CH(ONO2)-CH2-OH	100.0%	Mechanism of Carter and Atkinson (1996) is assumed. Abstraction from -CHO is estimated to occur only ~4% of the time.
Isoprene Product #2 [CH3-C(CHO)=CH-CH2-OH]		
CH3-C[.](CHO)-CH(ONO2)-CH2-OH	100.0%	Mechanism of Carter and Atkinson (1996) is assumed. Abstraction from -CHO is estimated to occur only ~4% of the time.
Isoprene Product #3 [HCO-CH=C(CH3)-CH2-OH]		
HCO-CH(ONO2)-C[.](CH3)-CH2-OH	100.0%	Mechanism of Carter and Atkinson (1996) is assumed. Abstraction from -CHO is estimated to occur only ~4% of the time.

Table 16. Rate constant and temperature dependence parameter assignments used for reactions of VOCs with O_3 in the present mechanism.

Compound	Model Name	k(300)	A	Ea	Ref	Est'd	
		(cm^3 $molec^{-1}$ s^{-1})		kcal/mole		k(300)	(diff)
Ethene	ETHENE	1.68e-18	9.14e-15	5.127	1	1.68e-18	0%
Propene	PROPENE	1.05e-17	5.51e-15	3.732	1	1.01e-17	-4%
1-Butene	1-BUTENE	1.00e-17	3.36e-15	3.466	1	1.01e-17	1%
Isobutene	ISOBUTEN	1.17e-17	2.70e-15	3.243	1	1.18e-17	1%
cis-2-Butene	C-2-BUTE	1.28e-16	3.22e-15	1.924	1	1.15e-16	-10%
trans-2-Butene	T-2-BUTE	1.95e-16	6.64e-15	2.104	1	1.15e-16	-41%
1-Pentene	1-PENTEN	1.04e-17	3.36e-15	3.445	2	1.01e-17	-3%
2-Methyl-1-Butene	2M-1-BUT	1.66e-17	2.70e-15	3.037	3	1.18e-17	-29%
2-Methyl-2-Butene	2M-2-BUT	4.08e-16	2.87e-15	1.162	4	3.48e-16	-15%
3-Methyl-1-Butene	3M-1-BUT	1.14e-17	3.36e-15	3.388	2	1.01e-17	-12%
1-Hexene	1-HEXENE	1.14e-17	3.36e-15	3.388	2	1.01e-17	-12%
Cis-3-Hexene	C-3-C6E	1.53e-16	3.22e-15	1.816	5	1.15e-16	-25%
Trans-3-Hexene	T-3-C6E	1.74e-16	6.64e-15	2.170	6	1.15e-16	-34%
2-Methyl-1-Pentene	2M1-C5E	1.55e-17	2.70e-15	3.075	3	1.18e-17	-24%
3-Methyl-1-Pentene	3M1-C5E	5.12e-18	3.36e-15	3.867	2	1.01e-17	97%
4-Methyl-1-Pentene	4M1-C5E	9.57e-18	3.36e-15	3.494	2	1.01e-17	6%
Cis-3-Methyl-2-Hexene	C3M2-C5E	4.56e-16	2.87e-15	1.096	4	3.48e-16	-24%
Trans 3-Methyl-2-Hexene	T3M2-C5E	5.66e-16	2.87e-15	0.967	4	3.48e-16	-39%
23-Dimethyl-1-Butene	23M1-BUT	1.35e-17	2.70e-15	3.160	3	1.18e-17	-12%
3,3-Dimethyl-1-Butene	33M1-BUT	5.43e-18	3.36e-15	3.832	2	1.01e-17	86%
2,3-Dimethyl-2-Butene	23M2-BUT	1.14e-15	3.03e-15	0.584	1	6.74e-16	-41%
2-Ethyl-1-Butene	2E1-BUT	1.35e-17	2.70e-15	3.160	3	1.18e-17	-12%
1-Heptene	1-HEPTEN	1.25e-17	3.36e-15	3.337	2	1.01e-17	-19%
2,3,3-trimethyl-1-Butene	233M1BUT	8.63e-18	2.70e-15	3.426	3	1.18e-17	37%
1-Octene	1-OCTENE	1.45e-17	3.36e-15	3.246	2	1.01e-17	-30%
Cis-4-Octene	C-4-C8E	9.73e-17	3.22e-15	2.086	5	1.15e-16	18%
Trans-4-Octene	T-4-C8E	1.44e-16	6.64e-15	2.285	6	1.15e-16	-20%
Trans 2,5-Dimethyl 3-Hexene	T25M3C6E	4.24e-17	6.64e-15	3.013	6	1.15e-16	>100%
Trans 2,2-Dimethyl 3-Hexene	T22M3C6E	4.34e-17	6.64e-15	2.998	6	1.15e-16	>100%
2,4,4-trimethyl-2-Pentene	244M2C5E	1.43e-16	2.87e-15	1.788	4	3.48e-16	>100%
3-Methyl-2-Isopropyl-1-Butene	3M2I1C4E	3.45e-18	2.70e-15	3.972	3	1.18e-17	>100%
1-Decene	1-C10E	9.67e-18	3.36e-15	3.488	2	1.01e-17	4%
Cis-5-Decene	C-5-C10E	1.23e-16	3.22e-15	1.948	5	1.15e-16	-6%
3,4-Diethyl-2-Hexene	34E2-C6E	4.39e-18	2.87e-15	3.864	4	3.48e-16	>100%
Cyclopentene	CYC-PNTE	5.61e-16	1.80e-15	0.696	1	1.15e-16	-79%
1-Methyl cyclohexene	1M-CC5E	6.76e-16	2.70e-15	0.825	3	3.48e-16	-49%
Cyclohexene	CYC-HEXE	8.33e-17	2.88e-15	2.112	1	1.15e-16	38%
1-Methyl Cyclohexene	1M-CC6E	1.68e-16	2.87e-15	1.690	4	3.48e-16	>100%
4-Methyl Cyclohexene	4M-CC6E	8.40e-17	2.88e-15	2.107	7	1.15e-16	37%
1,2-Dimethyl Cyclohexene	12M-CC6E	2.11e-16	3.03e-15	1.589	8	6.74e-16	>100%
1,3-Butadiene	13-BUTDE	6.64e-18	1.34e-14	4.537	1		
Isoprene	ISOPRENE	1.34e-17	7.86e-15	3.802	1		
a-Pinene	A-PINENE	8.80e-17	1.01e-15	1.455	1		
3-Carene	3-CARENE	3.78e-17	1.01e-15	1.958	9		
b-Pinene	B-PINENE	1.54e-17	1.01e-15	2.493	9		
Sabinene	SABINENE	8.74e-17	1.01e-15	1.459	9		
d-Limonene	D-LIMONE	2.04e-16	3.71e-15	1.729	10		
2-Methyl-2-Butene-3-ol	MBUTENOL	9.30e-18			18	1.01e-17	9%

Table 16 (continued)

Compound	Model Name	k(300) (cm^3 $molec^{-1}$ s^{-1})	A	Ea kcal/mole	Ref	Est'd k(300)	(diff)
2-(Cl-methyl)-3-Cl-Propene	CL2IBUTE	3.90e-19			11		
Styrene	STYRENE	1.71e-17			12		
Acetylene	ACETYLEN	8.61e-21	2.00e-14	8.739	13		
Methyl Acetylene	ME-ACTYL	1.56e-20	1.00e-14	7.970	14		
Ethyl Acetylene	ET-ACTYL	2.15e-20	1.00e-14	7.780	14		
2-Butyne	2-BUTYNE	2.15e-20	1.00e-14	7.780	15		
Methylvinyl ketone	MVK	4.74e-18	7.51e-16	3.020	12		
Methacrolein	METHACRO	1.19e-18	1.36e-15	4.200	12		
Isoprene Product #1	IP-MHY1	1.00e-17			16		
Isoprene Product #2	IP-MHY2	1.00e-17			16		
Isoprene Product #3	IP-HMY	1.00e-17			16		
Hydroxy Methacrolein	HOMACR	1.19e-18	1.36e-15	4.200	17		
Crotonaldehyde	CROTALD	9.00e-19			11		
Acrolein	ACROLEIN	3.07e-19	1.36e-15	5.006	19		

References

1 Rate constant expression recommended by Atkinson (1997a)

2 T=298K rate constant recommended by Atkinson (1997a). Temperature dependence estimated by assuming the A factor is the same as for 1-butene.

3 T=298K rate constant recommended by Atkinson (1997a). Temperature dependence estimated by assuming the A factor is the same as for isobutene.

4 T=298K rate constant recommended by Atkinson (1997a). Temperature dependence estimated by assuming the A factor is the same as the average of those for isobutene and 2,3-dimethyl-2-butene.

5 T=298K rate constant recommended by Atkinson (1997a). Temperature dependence estimated by assuming the A factor is the same as for cis-2-butene.

6 T=298K rate constant recommended by Atkinson (1997a). Temperature dependence estimated by assuming the A factor is the same as for trans-2-butene.

7 T=298K rate constant recommended by Atkinson (1997a). Temperature dependence estimated by assuming the A factor is the same as for cyclohexene.

8 T=298K rate constant recommended by Atkinson (1997a). Temperature dependence estimated by assuming the A factor is the same as for 2,3-dimethyl-2-butene.

9 T=298K rate constant recommended by Atkinson (1997a). Temperature dependence estimated by assuming the A factor is the same as for a-pinene.

10 T=298K rate constant recommended by Atkinson (1997a). Temperature dependence estimated by assuming the A factor is the sum of those for a-pinene and isobutene.

11 Rate constant recommended by Atkinson and Carter (1984)

12 Rate constant recommended by Atkinson (1994).

13 T=298K rate constant is from Atkinson and Aschmann (1984), as recommended by IUPAC (Atkinson et al, 1999). The temperature dependence is estimated based on assuming the A factor is roughly twice that for O3 + ethylene.

14 T=298K rate constant is from Atkinson and Aschmann (1984). The temperature dependence is estimated based on assuming the A factor is roughly twice that for O3 + propene.

15 Assumed to have approximately the same rate constant as 1-butyne, based on data given by Atkinson and Carter (1984).

16 Rate constant estimated by Carter and Atkinson (1996)

17 Estimated to have the same rate constant as methacrolein (Carter and Atkinson, 1996)

18 Average of 291K rate constant of Grosjean and Grosjean (1994) and the 298K rate constant of Fantechi et al (1998).

19 Rate constant at 298K of 2.9e-19 recommended by Atkinson (1994). Activation energy assumed to be the same as used for methacrolein.

Figure 2. Comparison of O_3 + alkene rate constants for alkenes with the same configurations of constituents about the double bond.

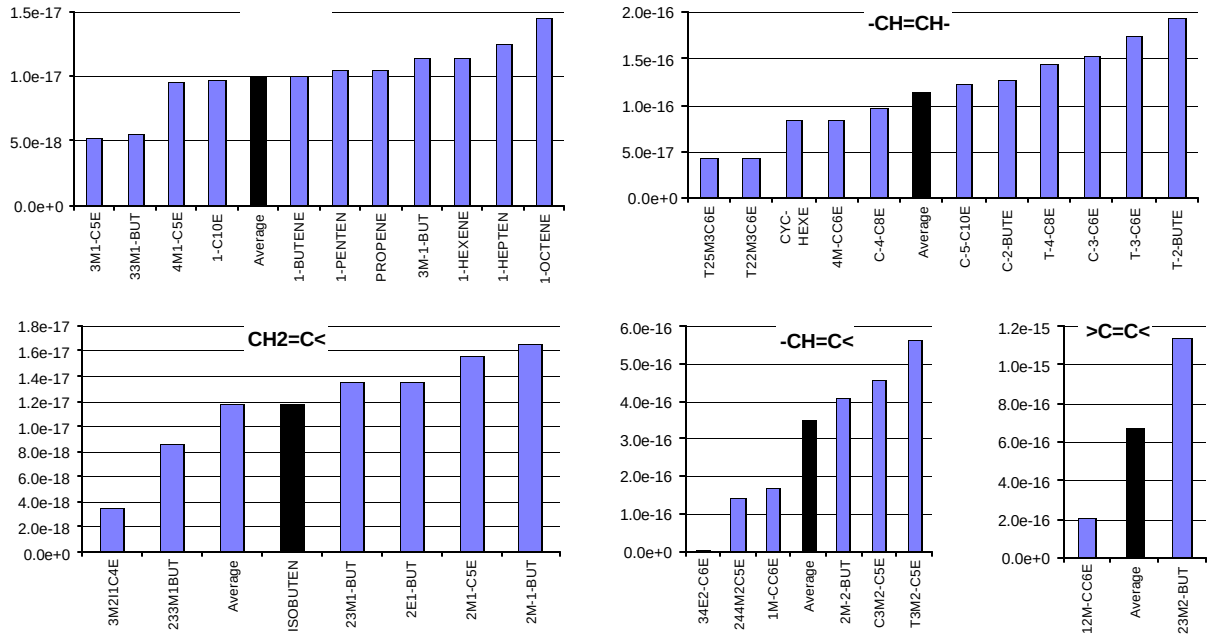

3. Branching Ratios for Biradical Formation

Since the biradical and carbonyl formation in the initial O_3 reaction can occur on two different positions in unsymmetrical molecules, it is necessary to specify their relative importances. Information concerning this can be obtained from the measured yields of the primary carbonyl products, which are summarized by Atkinson (1997a). The averages of the primary yield data given by Atkinson (1997a) are summarized on Table 18 through Table 20 for the olefins with the various types of unsymmetrical groups where such data are available. In most cases the sum of these primary product yields are within experimental uncertainty of unity, indicating that these products account for the total O_3 + alkene reactions. (The main exceptions are propene [Table 18] and isobutene [Table 19], where higher than unit yields can be attributed to formaldehyde formation from the secondary reactions of the excited biradical.) Atkinson (1997a) also summarizes carbonyl yield data for symmetrical alkenes (not shown here), and in most of those cases near-unit yields of the expected single carbonyl product are observed.

For alkenes with CH_2=CH- groups, Table 18 indicates that the data for most alkenes are consistent with assuming equal probability for each of the two possible reaction modes. This is therefore assumed when generating O_3 reaction mechanisms for all alkenes of this type. The major exception appears to be highly branched compounds such as 3,3-dimethyl-1-butene, where steric effects may tend to reduce biradical formation on the most substituted side. Since the current mechanism generation system is not capable of assessing steric effects, such compounds need to be handled on a case-by-case basis. However, present assignments are not made for such compounds because they are not important in current emissions inventories. The average error in assuming equal splits for the compounds where data are available is less than 10%, and the absolute value of the percentage error is less than 15%.

Table 17. Summary of rate constant estimates for reactions of O_3 at alkene groups.

Groups	Estimated Total Rate Constant (300K) (cm3 molec-1 s-1)	
CH2=CH-	1.01e-17	Average of 300K values for propene, 1-butene, 3-methyl-1-butene, 1-pentene, 1-hexene, 3-methyl-1-pentene, 3,3-dimethyl-1-butene, 4-methyl-1-pentene, 1-heptene, 1-octene, and 1-decene (Atkinson, 1997a).
CH2=C<	1.18e-17	Average of 300K values for isobutene, 2-methyl-1-butene, 23-dimethyl-1-butene, 2-ethyl-1-butene, 2-methyl-1-pentene, 2,3,3-trimethyl-1-butene, 3-methyl-2-isopropyl-1-butene, and 3,4-diethyl-2-hexene (Atkinson, 1997a).
-CH=CH-	1.15e-16	Average of 300K values for trans-2-butene, cis-2-butene, trans-3-hexene, cis-3-hexene, cis-4-octene, trans-4-octene, trans 2,5-dimethyl 3-hexene, trans 2,2-dimethyl 3-hexene, cis-5-decene, cyclohexene, and 4-methyl cyclohexene (Atkinson, 1997a).
-CH=C<	3.48e-16	Average of 300K values for 2-methyl-2-butene, cis-3-methyl-2-hexene, trans 3-methyl-2-hexene, 2,4,4-trimethyl-2-pentene, and 1-methyl cyclohexene (Atkinson, 1997a).
>C=C<	6.74e-16	Average of 300K values for 2,3-dimethyl-2-butene and 1,2-dimethyl cyclohexene (Atkinson, 1997a).

For alkenes with CH_2=C< groups, Table 19 indicates that the data are more consistent with assuming that fragmentation to formaldehyde + the disubstituted is essentially twice as probable as fragmentation to the ketone + $HCHO_2$ in essentially all cases. Steric effects appear to be less important in affecting this generalization, as suggested by the data for 2,3,3-trimethyl-1-butene. Therefore, the O_3 reactions of alkenes of this type are generated based on assuming that ketone + $HCHO_2$ formation occurs 33.3% of the time, as indicated on the table. This gives an average error of less than 5% and an average absolute percentage error of less than 15%.

For alkenes with -CH=C< groups, Table 20 indicates that aldehyde + disubstituted biradical formation occurs a larger fraction of the time than formation of the ketone + the monosubstituted biradical, but the limited data indicate somewhat variable ratios. For mechanism estimation and generation purposes, we assume that ketone + monosubstituted biradical formation occurs 30% of the time, as indicated on the table. This gives an average error of 10% and an average absolute percentage error of slightly less than 20% for the three compounds that were studied.

Atkinson (1997a) gives no information concerning primary carbonyl yields from unsymmetrical molecules with -CH=CH- or >C=C< groups – only data for symmetrical molecules are tabulated. For estimation and mechanism generation purposes, we assume equal probability for the two modes of reaction in such cases. The data for the other unsymmetrical molecules indicate that this is probably a good approximation, with the possible exception of molecules that are highly branched on one side where steric effects may come into play.

Table 18. Experimental and estimated yields of primary carbonyl products and OH radicals from the reactions of O_3 with alkenes with CH_2=CH- groups.

	Experimental			Estimated		OH Yield		
	HCHO	RCHO	Sum	RCHO	Error	Expt.	Est'd.	Error
CH2=CH- Average		0.54		0.50	-8%			-6%
Propene	0.71	0.48	1.20	0.50	3%	0.33	0.32	-3%
1-Butene	0.63	0.35	0.98	0.50	30%	0.41	0.32	-22%
1-Pentene	0.55	0.52	1.07	0.50	-4%	0.37	0.32	-14%
1-Hexene	0.54	0.53	1.07	0.50	-5%	0.32	0.32	0%
1-Heptene	0.52	0.55	1.07	0.50	-9%	0.27	0.32	19%
1-Octene	0.50	0.51	1.01	0.50	-2%	0.32	0.32	0%
1-Decene	0.53	0.49	1.02	0.50	2%			
3-Methyl-1-Butene	0.50	0.51	1.01	0.50	-2%			
3-Methyl-1-Pentene	0.39	0.63	1.03	0.50	-26%			
4-Methyl-1-Pentene	0.44	0.71	1.15	0.50	-41%			
3,3-Dimethyl-1-Butene	0.32	0.67	0.99	0.50	-34%			
Cyclohexene						0.68	0.52	-24%

Table 19. Experimental and estimated yields of primary carbonyl products and OH radicals from the reactions of O_3 with alkenes with CH_2=C< groups.

	Experimental			Estimated		OH Yield		
	HCHO	R-CO-R'	Sum	R-CO-R'	Error	Expt.	Calc	Error
CH2=C< Average		0.34		0.33	-2%			4%
Isobutene	0.98	0.32	1.29	0.33	4%	0.84	0.71	-16%
2-Methyl-1-Butene	0.64	0.28	0.92	0.33	16%	0.83	0.71	-15%
2-Methyl-1-Pentene	0.62	0.32	0.94	0.33	3%			
2-Ethyl-1-Butene	0.49	0.30	0.80	0.33	9%			
23-Dimethyl-1-Butene	0.72	0.38	1.10	0.33	-14%	0.5	0.71	41%
2,3,3-trimethyl-1-Butene	0.64	0.35	0.99	0.33	-6%			
3-Methyl-2-Isopropyl-1-Butene	0.61	0.43	1.03	0.33	-28%			

Table 20. Experimental and estimated yields of primary carbonyl products and OH radicals from the reactions of O_3 with alkenes with -CH=C< groups.

	Experimental			Estimated		OH Yield		
	RCHO	R-CO-R'	Sum	R-CO-R'	Error	Expt.	Calc	Error
-CH=C< Average		0.27		0.30	10%			-8%
2-Methyl-2-Butene	0.72	0.34	1.05	0.30	-13%	0.91	0.84	-8%
2,4,4-Trimethyl-2-Pentene	0.84	0.19	1.03	0.30	38%			
3,4-Diethyl-2-Hexene	0.71	0.29	0.99	0.30	4%			
1-Methyl Cyclohexene						0.90	0.84	-7%

Table 18 through Table 20 also show measured yields of OH radicals, which are believed to be formed from secondary radicals of the biradical intermediates (see Section III.K). If it is assumed that the OH yields from the excited $HCHO_2$, $RCHO_2$, and $RR'CO_2$ biradicals are independent of the molecule from which they are formed, then these OH yields should be consistent with the assumed branching ratios and the OH yields assumed for the various types of biradicals. As discussed in Section III.K, the current mechanism assumes that OH yields from excited $HCHO_2$, CH_3CHO_2, and $RR'CO_2$ biradicals are respectively 12%, 52%, and 100%, based primarily on recommendations and data discussed by Atkinson (1997a). The "Calc'd" OH yields on Table 18 through Table 20 show the yields for the various molecules derived based on these assumptions, where they can be compared with the experimental data. In most cases these are consistent with the experimental data, with the percentage errors being no greater than those for the estimated carbonyl yields. Therefore, the estimates based on carbonyl yields and OH yields are self-consistent. However, as discussed in Section III.K, the experimental and estimated OH yields for the C_{4+} 1-alkenes are not consistent with the environmental chamber reactivity data for these compounds, and lower adjusted OH yields have to be used for the purpose of reactivity predictions. However, these adjustments do not affect the assumed branching ratios for the initial O_3 + alkene reactions.

4. Assigned Mechanisms for Initial O_3 Reactions

As with the other reactions discussed above, explicit assignments are used for the initial reactions for those VOCs where estimates cannot be made, where available experimental data indicate the estimates are inappropriate, or where alternative estimates are used. The explicitly assigned branching ratios for the initial O_3 reactions that are currently incorporated in the system are summarized on Table 21, along with the basis for the various assignments that are used.

F. Reactions with O^3P

O^3P atoms can react with compounds with C=C double bonds, forming an excited adduct that may decompose in various ways or undergo collisional stabilization. Although these reactions are generally of negligible importance under most ambient atmospheric conditions, they have been found to be non-negligible in some of the environmental chamber experiments used for mechanism evaluation,

Table 21. Assigned mechanisms for the reactions of O_3 with compounds for which estimates could not be made, or where experimental data or other considerations indicate that the general estimates may not be appropriate.

Reactant and Products	Factor	Documentation
2-Methyl-3-Buten-2-ol [CH2=CH-C(CH3)(OH)-CH3]		
CH3-C(OH)(CHOO[excited])-CH3 + HCHO	30.0%	Based on product data of Alvarado et al (1999).
CH2OO[excited] + CH3-C(CHO)(OH)-CH3	70.0%	See above.
1,3-Butadiene [CH2=CH-CH=CH2]		
HCHO + CH2=CH-CHOO[excited]	50.0%	Estimated mechanism.
CH2=CH-CHO + CH2OO[excited]	50.0%	Estimated mechanism.
Isoprene [CH2=CH-C(CH3)=CH2]		
HCHO + CH2=CH-COO[excited]-CH3	20.0%	Mechanism of Carter and Atkinson (1996) is assumed.
HCHO + CH2=C(CHOO[excited])-CH3	20.0%	See above.
CH2=C(CHO)-CH3 + CH2OO[excited]	39.0%	See above.
CH2=CH-CO-CH3 + CH2OO[excited]	16.0%	See above.
O2 + *C(CH=CH2)(CH3)-CH2-O-*	2.5%	See above.
O2 + *CH(C(CH3)=CH2)-CH2-O-*	2.5%	See above.
Acetylene [HC::CH]		
HCO-CHOO[excited]	100.0%	The initially formed primary ozonide is assumed to rearrange to the Crigiee biradical via an O-O bond scission. [a]
Methyl Acetylene [HC::C-CH3]		
CH3-COO[excited]-CHO	50.0%	The initially formed primary ozonide is assumed to rearrange to the Crigiee biradical via an O-O bond scission. Equal probability of formation of each possible isomer is assumed. [a]
CH3-CO-CHOO[excited]	50.0%	See above.
Ethyl Acetylene [HC::C-CH2-CH3]		
CH3-CH2-COO[excited]-CHO	50.0%	The initially formed primary ozonide is assumed to rearrange to the Crigiee biradical via an O-O bond scission. Equal probability of formation of each possible isomer is assumed. [a]
CH3-CH2-CO-CHOO[excited]	50.0%	See above.
2-Butyne [CH3-C::C-CH3]		
CH3-CO-COO[excited]-CH3	100.0%	The initially formed primary ozonide is assumed to rearrange to the Crigiee biradical via an O-O bond scission. [a]
Methacrolein [CH2=C(CHO)-CH3]		
HCHO + CH3-COO[excited]-CHO	10.0%	Mechanism of Carter and Atkinson (1996) is assumed.
CH3-CO-CHO + CH2OO[excited]	90.0%	See above
Hydroxy Methacrolein [CH2=C(CHO)-CH2-OH]		
HCO-CO-CH2-OH + CH2OO[excited]	90.0%	Mechanism of Carter and Atkinson (1996) is assumed.
HCHO + HCO-COO[excited]-CH2-OH	10.0%	See above
Isoprene Product #1 [CH3-C(CHO)=CH(CH2-OH)]		
CH3-CO-CHO + HO-CH2-CHOO[excited]	90.0%	Mechanism of Carter and Atkinson (1996) is assumed.
HCO-CH2-OH + CH3-COO[excited]-CHO	10.0%	See above

Table 21 (continued)

Reactant and Products	Factor	Documentation
CH3-CO-CHO + HO-CH2-CHOO[excited]	90.0%	Mechanism of Carter and Atkinson (1996) is assumed.
HCO-CH2-OH + CH3-COO[excited]-CHO	10.0%	See above
Isoprene Product #3 [HCO-CH=C(CH3)-CH2-OH]		
CH3-CO-CH2-OH + HCO-CHOO[excited]	90.0%	Mechanism of Carter and Atkinson (1996) is assumed.
HCO-CHO + CH3-COO[excited]-CH2-OH	10.0%	See above
Methylvinyl ketone [CH2=CH-CO-CH3]		
HCHO + CH3-CO-CHOO[excited]	5.0%	Mechanism of Carter and Atkinson (1996) is assumed.
CH3-CO-CHO + CH2OO[excited]	95.0%	See above

[a] Although the biradical excitation energies are almost certainly different from those formed in the reactions of O3 with acroleins, because of lack of availabale information it is assumed to react to form the same products, and thus is represented by the same species.

where NO_2 concentrations tend to be higher under ambient conditions[11]. They may also be non-negligible in plumes that have higher NO_x concentrations than ambient. For these reasons, O^3P + alkene reactions are included in the current mechanism and are supported by the mechanism generation system.

1. Assigned O^3P Rate Constants

The rate constant assignments used for the O^3P reactions that are incorporated in the present mechanism are given on Table 22, where they are compared for the estimated values for those VOCs for which estimates can be made. The table also indicates the source of the rate constant assignments, which in most cases are from Atkinson (1997a).

2. Estimated O^3P Rate Constants

Since the reactions of alkenes with O^3P and OH radicals are both believed to involve primarily addition to the double bond, one might expect the rate constants for these reactions to be correlated. This is indeed the case for most of the alkenes where both rate constants have been measured, as is shown on Figure 3, which gives a log-log plot of O^3P and OH radical rate constants for the alkenes listed on Table 22. The line shows the least squares fit for the log-log plot for the monoalkenes, which was used for the purpose of estimating O^3P rate constants for those alkenes for which data are not available. This is given by:

$$\ln(kO^3P) = 19.160 + 1.864\ k(OH) \qquad (II)$$

where kO^3P and kOH are the O^3P and OH radical rate constants in $cm^3\ molec^{-1}\ s^{-1}$. (Note that the third digits are significant since they are being used to compute logrithms.) Although the dialkens and the terpenes were not used when deriving this fit, Table 22 and Figure 3 show that the above equation performs reasonably well in predicting their rate constants in most cases. Including the terpenes and

[11] Reactions with O_3P increase in importance as NO_2 concentrations increase because NO_2 photolysis is the primary source of O^3P.

Table 22. Rate constant and temperature dependence parameter assignments used for reactions of VOCs with O^3P atoms in the present mechanism.

Compound	Model Name	k(300) (cm^3 $molec^{-1}$ s^{-1})	A	Ea kcal/mole	Ref	Est'd k(300) k	(diff)
Ethene	ETHENE	7.42e-13	1.04e-11	1.574	1		
Propene	PROPENE	4.01e-12	1.18e-11	0.644	1	3.91e-12	-2%
1-Butene	1-BUTENE	4.22e-12	1.25e-11	0.648	1	5.43e-12	29%
Isobutene	ISOBUTEN	1.69e-11			2	1.36e-11	-20%
cis-2-Butene	C-2-BUTE	1.76e-11			2	1.62e-11	-8%
trans-2-Butene	T-2-BUTE	2.18e-11			2	2.04e-11	-6%
1-Pentene	1-PENTEN	4.69e-12	1.48e-11	0.686	3	5.42e-12	16%
cis-2-Pentene	C-2-PENT	1.70e-11			2	2.09e-11	23%
3-Methyl-1-Butene	3M-1-BUT	4.18e-12	1.32e-11	0.686	3	5.55e-12	33%
2-Methyl-2-Butene	2M-2-BUT	5.10e-11			2	3.62e-11	-29%
1-Hexene	1-HEXENE	4.69e-12	1.48e-11	0.686	3	7.37e-12	57%
2,3-Dimethyl-2-Butene	23M2-BUT	7.64e-11			2	5.60e-11	-27%
Cyclopentene	CYC-PNTE	2.10e-11			2	2.23e-11	6%
Cyclohexene	CYC-HEXE	2.00e-11			2	2.26e-11	13%
1-Methyl Cyclohexene	1M-CC6E	9.00e-11			2	3.71e-11	-59%
1,3-Butadiene	13-BUTDE	1.98e-11			2		
Isoprene	ISOPRENE	3.60e-11			4		
a-Pinene	A-PINENE	3.20e-11			2		
3-Carene	3-CARENE	3.20e-11			2		
b-Pinene	B-PINENE	2.70e-11			2		
d-Limonene	D-LIMONE	7.20e-11			2		

References

1 Rate constant expression from Atkinson and Lloyd (1984). T=298K value is consistent with recommendation of Atkinson (1997a).

2 Rate constant from Atkinson (1997a). Temperature dependence is expected to be small.

3 T=298K rate constant from Atkinson (1997a). Activation energy estimated from propene and 1-butene, as given by Atkinson and Lloyd (1984).

4 Rate constant from Paulson et al (1995).

dialkenes, the average discrepancy is around 25%, and all the discrepancies in all cases except for d-limonene are less than 60%.

3. Estimated Mechanisms for O^3P Reactions

The mechanisms for the reactions of O^3P with the simpler alkenes have been recently reviewed by Atkinson (1997a), though the discussion there is based primarily on the earlier review of Atkinson and Lloyd (1984). The reaction presumably proceeds by O adding to the double bond forming an excited oxide, which can either be collisionally stabilized, undergo a 1,2-H shift to a carbonyl compound and then be stabilized, or decompose in various ways. Neglecting reactions requiring pentavalent transition states that are chemically unreasonable (e.g., formation of isobutyraldehyde from O^3P + 2-butenes), the alternative reaction routes given by Atkinson and Lloyd (1984) and Atkinson (1997a) can be classified as follows:

Figure 3. Plot of OH radical vs. O^3P rate constants for VOCs in the mechanism where both rate constants are available. Rate constants are for T=300K.

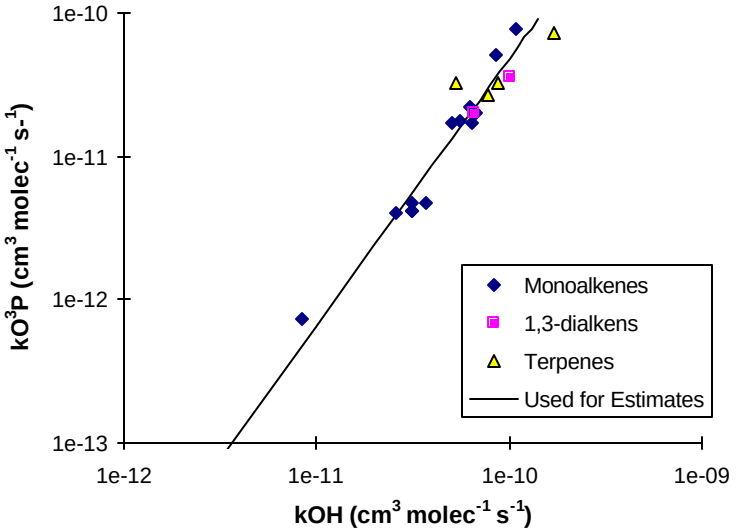

$$O^3P + >C=C< + M \rightarrow \text{oxide} + M \quad \text{(S1)}$$

$$O^3P + >C=C'H- + M \rightarrow >CH-C'O- + M \quad \text{(S2a)}$$

$$O^3P + -CH=C-< + M \rightarrow -CO-CH< + M \quad \text{(S2b)}$$

$$O^3P + -CX=C'< \rightarrow [-CX(O\cdot)-C(\cdot)<] \rightarrow X\cdot + -CO-C(\cdot)< \quad \text{(D1a)}$$

$$O^3P + >C=C'X- \rightarrow [>C(\cdot)-C'(O\cdot)X-] \rightarrow >C(\cdot)-C'O- + X. \quad \text{(D1b)}$$

$$O^3P + -CH=C'< \rightarrow [-CO-C'H<]^* \rightarrow \cdot CO- + >C'H\cdot \quad \text{(D2a)}$$

$$O^3P + >C=C'H- \rightarrow [>CH-C'O-]^* \rightarrow >CH\cdot + \cdot CO- \quad \text{(D2b)}$$

Where, for unsymmetrical molecules, C' refers to the carbon that has the greater number of substitutents.

Branching ratios estimated or interpolated based on these data are given in Table 23, where the branching ratio designations used are as indicated above, and footnotes indicate the source of the estimated mechanisms. Note that these ratios are applicable to one atmosphere total pressure only – the mechanism generation system currently does not support predicting the effects of total pressure on these yields[12]. Atkinson (1997a) and Atkinson and Lloyd (1994) gave no recommendations for compounds of with CH_2=C<, -CH=C<, or >C=C<, and highly approximate estimates are made based on considerations

[12] Ignoring these pressure dependences is unlikely to introduce significant errors in tropospheric simulations because NO_2 concentrations are expected to be sufficiently low at higher altitudes that reactions of O^3P with alkenes is expected to be negligible.

Table 23. Estimated branching ratios for the reactions of O^3P with alkenes, based on the recommendations of Atkinson (1997a) and Atkinson and Lloyd (1984). Note that these ratios are not used in the final mechanism because of unsatisfactory results when simulating environmental chamber experiments.

Compound	Branching Ratio							Notes
	S1	S2a	S2b	D1a	D1b	D2a	D2b	
CH2=CH2								
Ethene	0%	0%		60%		40%		1
CH2=CH-								
Propene	30%	30%	0%	20%	0%	20%	0%	2
1-Butene	45%	40%	0%	15%	0%	0%	0%	2
C5 Alkenes	50%	45%	0%	5%	0%	0%	0%	3
C6+ Alkenes	55%	45%	0%	0%	0%	0%	0%	3
CH2=C<								
Isobutene	40%	-	30%	0%	15%	15%	-	4
C5 Alkenes	50%	-	38%	0%	6%	6%	-	3
C6 Alkenes	56%	-	40%	0%	2%	2%	-	3
C7+ Alkenes	60%	-	40%	0%	0%	0%	-	3
-CH=CH-								
2-Butenes	50%	20%		30%		0%		5
C5 Alkenes	64%	24%		12%		0%		3
C6 Alkenes	72%	24%		4%		0%		3
C7+ Alkenes	76%	24%		0%		0%		3
-CH=C<								
2-Methyl-2-Butene	50%	-	38%	6%	6%	0%	-	4
C6 Alkenes	56%	-	40%	2%	2%	0%	-	3
C7+ Alkenes	60%	-	40%	0%	0%	0%	-	3
>C=C<								
2,3-Dimethyl-2-Butene	96%		-	2%	2%		-	4
C7+ Alkenes	100%		-	0%	0%		-	3

Notes

1 Based on Atkinson (1997a) recommendation, ignoring ketene formation, which is lumped with the D2 decomposition route

2 Based on Atkinson (1997a) and Atkinson and Lloyd (1984) recommendation. Numbers rounded to nearest 5%

3 Based on extrapolating from data for lower molecular weight alkenes, assuming that stabilization will increase with the size of the molecule increases.

4 Estimated based on recommended mechanisms given by Atkinson and Lloyd (1994) for other alkenes.

5 Based on the Atkinson (1997a) and Atkinson and Lloyd (1984) recommendation, with the chemically unreasonable 20% CH3 shift represented by increasing oxide formation and decomposition eacy by 10%.

of data given by Atkinson and Lloyd (1994) for other compounds[13]. As indicated on the table, stabilization is assumed to become increasingly important for higher molecular weight compounds, and to dominate for C_{7+} alkenes.

Although the branching ratios shown on Table 23 represent our current best estimates based on available product data (Atkinson, 1997a), it was found that using these branching ratios gave unsatisfactory results when conducting model simulations of the available chamber database. This was found to be the case even after reasonable adjustment of the other uncertain parameters in the mechanism that affect radical initiation or termination processes. In order to fit the data, it was necessary to assume much lower radical yields from these O^3P reactions, i.e., that stabilization is much more important than indicated by the available product data. In particular, the model significantly overpredicts the reactivity of 1-butene and 1-hexene if any radical formation in the O^3P reaction is assumed, and consistent fits to the chamber data cannot be obtained unless it is assumed that radical formation from O^3P + propene is also negligible. In addition, assuming only 50% fragmentation in the O^3P + ethene rather than the recommended 100% removes biases in the simulation of the large database of ethene experiments.

The reason for this apparent inconsistency between the chamber data and the O^3P branching ratios indicated by the available product data is unknown, and needs to be investigated. Although O^3P reactions are not important under most atmospheric conditions, they are non-negligible in many of the chamber experiments used for mechanism evaluation, and using incorrect O^3P + alkene mechanisms may compensate for other errors in the mechanism. However, no reasonable adjustments of the other uncertainties in the alkene mechanisms that involve radical initiation/termination processes (such as nitrate yields from the peroxy radicals formed in the OH reaction, radical yields from the biradicals formed in the O_3 reaction, or radical generation in the alkene + NO_3 reactions) could be found to give satisfactory fits to the chamber data using the recommended O^3P branching ratios. Therefore, adjusted branching ratios, assuming no radical formation from C_{3+} alkenes and assuming only 50% fragmentation from ethene, are used in the current version of the mechanism that is developed in this work. These adjusted yields are given on Table 24.

4. Assigned Mechanisms for Dialkenes

Although it is expected that the reactions of O^3P with alkynes are unimportant and therefore are ignored in the mechanism, their reactions with isoprene and 1,3-butadiene may be non-negligible under some conditions, and need to be specified explicitly. The assigned O^3P mechanisms for these compounds are shown on Table 25. The O^3P + isoprene mechanism is based on that of Carter and Atkinson (1996), and the mechanism for 1,3-butadiene is assumed to be analogous. The current system does not have assigned mechanisms for any other VOCs.

G. Photolysis Reactions

The previous mechanism represented all photoreactive VOCs (e.g., aldehydes, ketones, and organic nitrates) either explicitly or using the lumped molecule approach, so mechanisms for photolysis reactions were all derived on a case-by-base basis. However, the lumped molecule approach has proven to

[13] It is probable that improved estimates could be made for some of these compounds by reviewing the product data literature. This review was not carried out because of the relatively low importance of these O^3P reactions in most atmospheric simulations, and because in any case the branching ratios had to be revised to fit the chamber data.

Table 24. Adjusted branching ratios for the reactions of O^3P with alkenes that are found to give best fits to the available chamber database and are used in the final version of the mechanism developed in this work.

Groups	Branching Ratio				
	S1	S2a	S2b	D1a+D1b	D2a+D2b
CH_2=CH_2	25%	25%		20%	30%
CH_2=CH-	55%	45%	0%	0%	0%
CH_2=C>	60%	-	40%	0%	0%
-CH=CH-	76%	24%		0%	0%
-CH=C<	60%	-	40%	0%	0%
>C=C<	100%	-		0%	-

Table 25. Assigned mechanisms for the reactions of O^3P atoms with the dialkenes in the current mechanism.

Reactant and Products	Factor	Documentation
Isoprene [CH2=CH-C(CH3)=CH2]		
C(CH=CH2)(CH3)-CH2-O-	50.0%	As assumed by Carter and Atkinson (1996). Products represented by epoxides. Most of the reaction is assumed to occur at the more substituted position.
CH(C(CH3)=CH2)-CH2-O-	25.0%	See above.
CH2=CH-CO-CH2. + CH3.	25.0%	Fragmentation mechanism and yield as assumed by Carter and Atkinson (19896). Approximately 25% radical yield also necessary to obtain satisfactory fit to data with updated mechanism.
1,3-Butadiene [CH2=CH-CH=CH2]		
CH(CH=CH2)-CH2-O-	75.0%	Assumed to be analogous to the isoprene mecanism of Carter and Atkinson (1996). Products represented by epoxides.
CH2=CH-CH[.]-CHO + H.	25.0%	Analogous to the fragmentation mechanism in the isoprene system as assumed by Carter and Atkinson (1996).

be unsatisfactory for the higher ketones (Carter et al, 2000a) and is therefore not used in this mechanism for the higher aldehydes, ketones, and nitrates. Instead, specific mechanistic assignments are made for these compounds, based on generated mechanisms for their reactions with OH radicals, NO_3 (for aldehydes), and photolyses. Specific mechanistic assignments are also made for the OH radical and photolysis reactions of organic nitrates, which were used for determining the lumped organic nitrate mechanism as discussed in Section II.C.2. The estimation and generation of their initial reactions with OH radicals and NO_3 were discussed above. This section discusses the estimation and generation of their initial photolysis reactions

Photolysis rates for the aldehydes, α-dicarbonyls, vinyl ketones and organic nitrates are estimated by assuming that they have the same absorption cross sections and quantum yields as the most chemically similar lower molecular weight analogue that is in the base mechanism. In the case of the simple ketones, it is assumed that the overall quantum yield decreases with the size of the molecule, based on overall quantum yields which give best fits of model simulations to environmental chamber data for methyl ethyl ketone, methyl propyl ketone, methyl isobutyl ketone, and methyl amyl ketone (see Section V and Appendix B). The specific assignments are as summarized on Table 26, along with footnotes indicating the derivations of the assignments and the groups used by the mechanism generation system to classify compounds according to photolysis type.

Note that if the molecule has groups bonded to the carbonyl or nitrate groups that are different than those indicated on the table, then the system cannot currently generate photolysis reactions for compounds with that structure. If the molecule has more than one photoreactive center (e.g., CH_3-CO-CH_2CHO), then the photolysis reaction is assumed to occur only at the most reactive center, based on an assumed reactivity ordering of α-dicarbonyls > unsaturated aldehydes or ketones > aldehydes > ketones > nitrates. This obviously is an approximation and it would be much better if such multifunctional molecules could be handled on a case-by-case basis if information were available.

1. Default Carbonyl Photolysis Mechanisms

Although the actual mechanisms for the photolysis reactions of the higher molecular weight carbonyl compounds may well be more complex (Calvert and Pitts, 1966), unless information is available otherwise, it is assumed that all photolyses of carbonyls proceed by breaking the weakest CO-C bond. In the case of aldehydes (including glyoxals) this means the reaction is assumed to always proceed via

$$R\text{-}CHO + h\nu \rightarrow R\cdot + HCO\cdot$$

(where "R". would be R'CO in the case of glyoxals) and in the case of α-dicarbonyl ketones it is assumed always to proceed via

$$R\text{-}CO\text{-}CO\text{-}R' + h\nu \rightarrow RCO\cdot + R'CO\cdot$$

In the case of unsymmetrical ketones, two possible reactions are considered:

$$R\text{-}CO\text{-}R' + h\nu \rightarrow R\cdot + R'CO\cdot$$

$$R\text{-}CO\text{-}R' + h\nu \rightarrow RCO\cdot + R'\cdot$$

In this case, the pathway with the lowest estimated heat of reaction is assumed to 100% of the time, regardless of the differences between them. This gives a prediction that is consistent with the assumed photolysis mechanism for methyl ethyl ketone in the base mechanism.

2. Unsaturated Carbonyl Photolysis

Somewhat different photolysis mechanisms are assigned for acrolein, methacrolein and methyl vinyl ketone, based on the mechanisms for the latter two given by Carter and Atkinson (1996). The base mechanism listing gives the assignments and documentation in the cases of methacrolein and MVK. In the case of acrolein, the following initial photolysis mechanism is used, which is derived by analogy to the Carter and Atkinson (1996) mechanism for methacrolein.

Table 26. Summary of assignments of absorption cross sections and quantum yields for carbonyl and organic nitrate photolysis reactions.

Compound Type	Phot. Set	Q.Yield	Notes	Group Definition used to Determine Type
Aldehydes	C2CHO	-	1,2	-CHO groups bonded to -CH_3, -CH_2-, -CH< or -C<
Ketones (4 groups)	KETONE	0.15	3,4	-CO- groups bonded to -CH_3, -CH_2-, -CH< or -C<, with a total of 4 groups in the molecule.
Ketones (5 groups.)	KETONE	0.10	3,5	As above, but 5 groups in the molecule
Ketones (6 groups.)	KETONE	0.05	3,6	As above, but 6 groups in the molecule
Ketones (7 groups.)	KETONE	0.02	3,7	As above, but 7 groups in the molecule
Ketones (8 groups.)	KETONE	0.01	3,8	As above, but 8 groups in the molecule
Ketones (9+ groups.)	No photolysis		3,9	As above, but more than 8 groups in the molecule
Alkyl Glyoxal	MGLY_ADJ	-	1,4	-CHO- broups bonded to -CO-
Dialkyl Glyoxyl	BACL_ADJ	-	1,5	-CO- groups bonded to -CO-
Acrolein	ACROLEIN	2.0e-3	3,6	CH2=CH-CHO only.
Other Acroleins	ACROLEIN	4.1e-3	3,7	-CHO groups bonded to -CH= or >C=
Vinyl Ketone	ACROLEIN	2.1e-3	3,8	-CO- groups bonded to -CH= or >C=
Ester or Acid	No photolysis		9	-CO- or -CHO- groups bonded to -O- or -OH
Organic Nitrates	IC3ONO2	1.0	10	-ONO_2 groups bonded to -CH_3, -CH_2- -CH< or -C<

Notes

1 The wavelength dependent quantum yields are given with the absorption cross sections in the photolysis set. See base mechanism documentation and mechanism listing.
2 Assumed to have same photolysis rate as propionaldehyde.
3 The photolysis set gives the absorption cross sections only, which are given with the base mechanism listing. The wavelength-independent quantum yield is shown on the table.
4 Overall quantum yield adjusted based on model simulations of environmental chamber experiments with methyl ethyl ketone (Carter et al, 2000a).
5 Overall quantum yield adjusted based on model simulations of environmental chamber exp eriments with methyl propyl ketone (Carter et al, 2000e).
6 Overall quantum yield adjusted based on model simulations of environmental chamber experiments with methyl isobutyl ketone (Carter et al, 2000a).
7 Overall quantum yield adjusted based on model simulations of environmental chamber experiments with 2-heptanone (Carter et al, 2000e).
8 Estimated to have an overall quantum yield which is half that estimated for ketones with seven groups.
9 Photodecomposition is estimated to be unimportant for ketones with nine or more groups.
4 Assumed to have the same photolysis rate as methyl glyoxal.
5 Assumed to have the same photolysis rate as biacetyl.
6 Overall quantum yield adjusted to fit model simulations of O3, NO, acrolein, and formaldehyde in acrolein - NOx chamber runs ITC941, 943, and 944.
7 Assumed to have same photolysis rate as methacrolein. See base mechanism documentation.
8 Assumed to have same photolysis rate as methyl vinyl ketone. See base mechanism documentation.
9 Photolysis assumed to be negligible, based on absorption cross section data given by Calvert and Pitts (1966).
10 All alkyl nitrates are assumed to photolyze at the same rate and with a unit quantum yield. Absorption cross sections used are those recommended by IUPAC (Atkinson et al, 1997, 1999) for isopropyl nitrate.

$$CH_2=CH\text{-}CHO + h\nu \rightarrow HCO\cdot + CH_2=CH\cdot \quad (34\%)$$

$$CH_2=CH\text{-}CHO + h\nu \rightarrow H\cdot + CH_2=CH\text{-}CO\cdot \quad (33\%)$$

$$CH_2=CH\text{-}CHO + h\nu \rightarrow CO + CH_3CH: \quad (33\%)$$

The subsequent reactions of the radicals or carbenes formed are discussed in the following sections.

For the other unsaturated aldehydes, including specifically those used to derive the mechanism for the ISOPROD model species, the default mechanism, based on assuming 100% HCO· formation is used. The current mechanism has no mechanistic assignments for unsaturated ketones other than MVK, and in general specific assignments would need to be given for the individual compounds.

3. Organic Nitrate Photolysis

As discussed in Section II.C.2, although organic nitrate products are represented using the lumped molecule approach, the mechanism for the generic organic nitrate model species used for this purpose is derived based on generated mechanisms for individual organic nitrate compounds. The rates of their photolysis reactions are determined as shown on Table 26, which indicates that all organic nitrates are assumed to photolyze using the absorption cross sections recommended by IUPAC (Atkinson et al, 1997, 1999) for isopropyl nitrate. As discussed there, the quantum yield for NO_2 formation is assumed to be unity. In view of this, all organic nitrate photolysis reactions are represented by the general mechanism

$$RONO_2 + h\nu \rightarrow RO\cdot + NO_2$$

The subsequent reactions of the alkoxy radicals are then derived using the general methods discussed in Section III.J.

H. Reactions of Carbon Centered Radicals

Carbon-centered radicals are any radicals containing the groups CH3., -CH2., -CH[.]-, >C[.]-, HCO., -CO., =CH., or =C[.]. Except as indicated below or in Table 27, these are assumed to react exclusively by O_2 addition, forming the corresponding peroxy group. The general exceptions are as follows:

- Vinylic radicals are assumed to react via the mechanism

  $$H_2C=CH\cdot + O_2 \rightarrow HCHO + HCO.$$

  based on the data of Slagle et al (1984). Except as indicated below, substituted vinylic radicals are assumed to react analogously, e.g.,

  $$>C=C(\cdot)X + O_2 \rightarrow >C=O + XCO.$$

  Where -X is -H or any non-radical group. The exceptions are radicals of the type HO-C=C· formed in the reactions of OH with acetylenes, where specific mechanistic assignments are made as indicated below in Table 27.

- α-Hydroxy alkyl radicals are assumed to react by O_2 abstraction from the -OH, forming HO_2 and the corresponding carbonyl compound, e.g.,

  $$>C(\cdot)\text{-}OH + O_2 \rightarrow >C=O + HO_2$$

Table 27. Mechanistic assignments for carbon-centered radicals that are assumed not to react as estimated for general carbon-centered radicals.

Reactant	Product(s)	Yield	Notes
OH-Substituted Vinylic Radicals (from OH + Acetylenes)			
HO-CH=CH.	HCO-OH + HCO. HCO-CHO + OH	33% 67%	1
CH3-C[.]=CH(OH)	HCO-OH + CH3-CO. CH3-CO-CHO + OH	33% 67%	2
CH3-C[.]=CH-OH	HCO-OH + CH3-CO. CH3-CO-CHO + OH	33% 67%	2
CH3-C(OH)=C[.]-CH3	CH3-CO-OH + CH3-CO. CH3-CO-CO-CH3 + OH	33% 67%	2
CH3-CH2-C[.]=CH-OH	HCO-OH + CH3-CH2-CO. CH3-CH2-CO-CHO + OH	33% 67%	2
Allylic Radicals			
CH2=CH-C[.](CH3)-CH2-OH	CH2=CH-C[OO.](CH3)-CH2-OH HO-CH2-C(CH3)=CH-CH2OO. HO-CH2-C(CH3)=CH(CH2OO.)	67% 16.5% 16.5%	3,4
CH2=C(CH3)-CH[.]-CH2-OH	CH2=C(CH3)-CH[OO.]-CH2-OH CH3-C(CH2OO.)=CH(CH2-OH) CH3-C(CH2OO.)=CH-CH2-OH	59.2% 20.4% 20.4%	3,5
HO-CH2-C(CH2.)=CH(CH2-OH)	CH2=C(CH2-OH)-CH[OO.]-CH2-OH	100%	3,6
C(CH3)=CH-O-CH2-CH[.]-	*O-CH=C(CH3)-CH=CH-* + HO2.	100%	3,7
C[.](CH3)-CH=CH-O-CH2-	*O-CH=C(CH3)-CH=CH-* + HO2.	100%	3,7
CH2=CH-C[.](CH3)-CH2-ONO2	.OOCH2-CH=C(CH3)-CH2-ONO2	100%	3,8
CH2=CH-CH[.]-CH2-OH	CH2=CH-CH[OO.]-CH2-OH HO-CH2-CH=CH-CH2OO. HO-CH2-CH=CH(CH2OO.)	50% 25% 25%	9
CH2=CH-CH[.]-CH2-ONO2	.OOCH2-CH=CH-CH2-ONO2 .OOCH2-CH=CH(CH2-ONO2)	50% 50%	3,10
Allylic Radical Precursors			
C(CH3)(OH)-CH2-O-CH2-CH[.]-	H2O + *C(CH3)=CH-O-CH2-CH[.]-*	100%	3,7
CH(OH)-C[.](CH3)-CH2-O-CH2-	H2O + *C[.](CH3)-CH=CH-O-CH2-*	100%	3,7

Notes

1 Estimated mechanism is based on the data of Hatakeyama et al (1986) and modeling acetylene environmental chamber runs Carter et al (1997c).

2 Estimated by analogy with assumed reactions of HO-CH=CH. from acetylene.

3 Ratios of reaction of O2 at different positions of the allylic radical is assumed to be as discussed by Carter and Atkinson (1996).

4 The relative importance of this reaction is based on observed yields of methyl vinyl ketone in the reactions of OH radicals with isoprene.

Table 27 (continued)

5 The relative importance of this reaction is based on observed yields of methyl vinyl ketone in the reactions of OH radicals with methacrolein.

6 This reaction is assumed to dominate to be consistent with results of API-MS isoprene + OH product studies of Kwok et al (1995), which indicate that C5-dihydroxycarbonyls, the predicted products of the competing reactions, are not formed.

7 It is necessary to assume this radical reacts as shown in order to explain the observed formation of 3-methyl furan from the reaction of OH radicals with isoprene (Carter and Atkinson, 1996).

8 Assumed to dominate over addition at the least substituted end of the allylic radical to be consistent with product data, as discussed by Carter and Atkinson (1996). Formation of only one of the two possible cis-trans isomers is shown because the reactions of the other isomer are expected to give the same products.

9 Equal probablity of addition at either radical center of the allylic radical is assumed.

10 100% terminal addition to allylic radical is assumed, to be consistent with mechanism assumed for isoprene (Carter and Atkinson, 1996). Equal probablity of cis and trans formation is assumed.

The assumption that this reaction dominates for α-hydroxy radicals is based on results of product studies of reactions of alcohols and other OH-substituted compounds in the presence of O_2.

- α-Nitroxy alkyl radicals, which can be formed in the reactions of NO_3 radicals with alkenes, are assumed to undergo rapid unimolecular decomposition to NO_2 and the corresponding carbonyl compound, e.g.,

$$>C(\cdot)\text{-}ONO_2 \rightarrow >C=O + NO_2$$

This is assumed to be an extremely rapid decomposition based on its high estimated exothermicity, combined with the expectation that the decomposition should not have a large activation energy. However, experimental (and theoretical) verification of this assumption would be useful.

- Carbenes are assumed to react with O_2, forming an excited Crigiee biradical, e.g.,

$$>C[:]- + O_2 \rightarrow >CO2[excited]-$$

Although the excitation energy is almost certainly different than those formed in O_3 + alkene reactions, since information to the contrary is not available, the excited Crigiee biradicals are assumed to react with the same mechanism, and are therefore represented by the same species in the mechanism generation system. The reactions of Crigiee biradicals are discussed in Section III.K.

In addition to the above general exceptions, specific mechanistic assignments are made for some of the unsaturated carbon-centered radicals formed in the reactions of the special reactants that are currently supported by the system. These assignments are indicated on Table 27, along with footnotes documenting the reasons for the assignments. As shown there, there are three types of radicals that are considered, as follows:

1) OH-substituted vinylic radicals formed by OH addition to acetylenes whose mechanisms are assigned based on the assumed mechanism for acetylene (Carter et al, 1997c);

2) various allylic radicals where O_2 can add at more than one radical center, where the branching ratio assignments are based primarily on data from isoprene product studies (Carter and Atkinson, 1996); and

3) precursors to allylic radicals that are assumed to react with O_2 by abstraction forming HO_2 and allylic radicals, in order to account for the formation of 3-methyl furan from the reactions of OH with isoprene (Carter and Atkinson, 1996).

Note that the assignments for the allylic radicals that are based on product data are not always consistent with each other [e.g., addition of O_2 to the least substituted position is assumed for the nitrate-substituted radicals, while the opposite assumption is made for HO-CH2-C(CH2.)=CH(CH2-OH) to be consistent with product data]. Thus, these must be considered to be highly uncertain.

Although one might expect radicals of the type R-O-C(O)· to rapidly decompose to R· + CO_2, Kirchner et al (1997) and Christensen et al (1999) reported synthesizing $CH_3OC(O)OONO_2$ from the reaction of Cl_2 with methyl formate, which is only possible if $CH_3OC(O)$· lasts long enough to react with O_2 to form $CH_3OC(O)OO$·. In addition, model simulations of reactivity experiments with methyl isobutyrate, which is predicted to form $CH_3OC(O)$· radicals in high yields, cannot fit the data if this decomposition is assumed (Carter et al, 2000a). Therefore, we assume that these radicals do not decompose, but instead add O_2 to form radicals of the type ROC(O)OO·, which can react with NO_2 to form PAN analogues of the type $ROC(O)OONO_2$, as observed by Kirchner et al (1997) and Christensen et al (1999).

I. Reactions of Peroxy Radicals

Peroxy radicals are critical intermediates in almost all the generated mechanisms. Although under atmospheric conditions they can react with NO_2, NO_3, HO_2, and other peroxy radicals, the current version of the system only generates their reactions with NO. This is because reaction with NO is the major fate of peroxy radicals under conditions where reactions of VOCs contribute to tropospheric ozone, and the current base mechanism uses condensed approaches to represent the effects of the other reactions (see Section II.B.4). The reactions of non-acyl peroxy radicals with NO_2 are ignored because they are assumed to be rapidly reversed by the thermal decomposition of the peroxynitrate formed. The reactions of acyl peroxy radicals with NO_2 are not considered because acyl peroxy radicals are represented by lumped species so their reactions do not need to be generated. The products of peroxy + NO_3 and peroxy + peroxy reactions are represented by lumped species, so they are not considered in the mechanism generation system.

The main factor that needs to be determined when generating reactions of peroxy radicals with NO is the branching ratio between formation of NO_2 and the corresponding alkoxy radical, or addition and rearrangement forming the organic nitrate, e.g.

$$RO_2\cdot + NO \rightarrow RO\cdot + NO_2 \qquad (A)$$

$$RO_2\cdot + NO + M \rightarrow RONO_2 + M. \qquad (N)$$

The rate constant ratio $k_N/(k_A+k_N)$ is referred to as the "nitrate yield" in the subsequent discussion. This is a potentially important factor affecting a VOC's atmospheric impact because nitrate formation (process "N") is a radical termination process and can significantly inhibit radical levels if it is sufficiently important compared to propagation (process "A). Unfortunately, except for secondary peroxy radicals formed from the C_3-C_{10} n-alkanes, direct information concerning nitrate yields is extremely limited, and

nitrate yields have to be either estimated or (for those few cases where this is possible) adjusted to fit overall reactivity observed in environmental chamber experiments.

For the peroxy radicals formed from alkane photooxidations, the previous version of the mechanisms used yields estimated by Carter and Atkinson (1989b). These are based on data for nitrate yields from reactions of OH with C_3-C_8 n-alkanes and several C_5 and C_6 branched alkanes at ambient temperature and pressure, and on nitrate yields at different temperatures and pressures from OH reactions of several C_5 and C_7 alkanes. The data indicate that nitrate yields from alkyl peroxy radicals increase with the size of the molecule from less than 5% for C_3 to ~33% for C_8 (with an apparent upper limit of 40-50% for larger molecules), and also increase with decreasing temperature and decrease with decreasing pressure. This suggests that the rate of the nitrate formation reaction is governed by similar factors affecting other three-body reactions, whose temperature and pressure dependences can be parameterized using a modified version of the "Troe" falloff expression that is currently used in the evaluations. Based on this, Carter and Atkinson (1989b) used the following parameterization to fit the nitrate yield data for the secondary alkyl peroxy radicals:

$$Y_{sec}(n_C, T, M) = (k_N/k_R) / [1 + (k_N/k_R)] \qquad (III)$$

where Y_{sec} is the nitrate yield for secondary alkyl radicals with n_C carbons at temperature T (in ^oK) and total pressure M (in molecules cm^{-3}), and the rate constant ratio k_N/k_R is derived from

$$k_N/k_R = \{R_0(T,n_C)\cdot M/[1 + R_0(T,n_C)\cdot M/R_\infty(T)]\}\cdot F^Z \qquad (IV)$$

where

$$R_0(T,n_C) = \alpha \cdot e^{\beta\cdot n_C} \cdot (T/300)^{-m_0}$$

$$R_\infty(T) = R_\infty^{300} \cdot (T/300)^{-m_\infty}$$

$$Z = \{1 + [\log_{10}\{R_0(T,n_C)\cdot M)/R_\infty(T)\}]^2\}^{-1}$$

and α, β, R_∞^{300}, m_0, m_∞, and F are empirical parameters that are optimized to fit the data. Based on the data available at the time, Carter and Atkinson (1989b) derived α=1.94 x 10^{-22} cm^3 $molecule^{-1}$, β=0.97, R_∞^{300}=0.826, m_0=0, m_∞=8.1, and F=0.411. The limited (and somewhat inconsistent) data for primary and tertiary peroxy radicals indicate that lower nitrate yields are formed from these radicals, and Carter and Atkinson (1989b) recommended using scaling factors of 0.4±0.05 and 0.3±0.15 for secondary and tertiary peroxy radicals, respectively.

Most of the data concerning the effects of nitrate yields on carbon number come from the measurements of Atkinson et al (1982b, 1984), and the temperature and pressure effects data come from Atkinson et al (1983b). More recently, using improved chromatographic methods, Arey et al (2000) remeasured the nitrate yields from the C3-C8 n-alkanes. They obtained significantly lower nitrate yields for the C5+ radicals, and Atkinson and co-workers (unpublished results, 1999) also obtained lower nitrate yields from n-decane than estimated using the parameterization of Carter and Atkinson (1989b). For example, the new data indicate a nitrate yield of 24% for the C_8 secondary peroxy radicals, compared to the previous measurement of ~33%. As discussed below, these lower nitrate yields resulted in the model being able to fit chamber data without having to make the chemically unreasonable assumption that hydroxy-substituted C_{6+} peroxy radicals formed after alkoxy radical isomerizations did not form nitrates when they reacted with NO, as had to be made in previous versions of the mechanism (Carter, 1990; Carter and Atkinson, 1985). Therefore, the earlier nitrate yields of Atkinson et al (1982b, 1983b, 1984), which are all based on similar analytical methods, appear to be high.

Because of this, the parameter values of Carter and Atkinson (1989b) are no longer appropriate for general estimation purposes and need to be re-derived to be consistent with the new data. To determine temperature and pressure effects, we assume that the data of Atkinson et al (1983b) are valid in a relative sense (i.e., the errors are in the nitrate calibrations), so relative changes with temperature and pressure are still correct, and based on this corrected the earlier data to be consistent with the remeasured yields at atmospheric temperature and pressure. Table 28 gives the nitrate yield data that were used to re-derive the parameterization, along with footnotes giving the source of the data or how they were derived. These include all the new data currently available from Atkinson's laboratory, together with the pentyl and heptyl nitrate yields at varying temperatures and pressures from Atkinson et al (1983b), corrected to be consistent with the new data. The temperature and pressure effects data for the branched secondary alkyl nitrate data from Atkinson et al (1983b) (see also Carter and Atkinson, 1989b) were not used because there are no more recent data available to correct the yields, and because the pentyl and heptyl nitrate data should be a sufficient basis for the optimization.

The new parameter values were derived using a non-linear optimization procedure to minimize the quantity

$$\text{Fit Error} = \sum_{\text{Measurement Data}} \text{Weight} \left(\frac{(\text{Estimated Nitrate Yield}) - (\text{Corrected Measured Nitrate Yield})}{\text{Maximum } (0.1, \text{Corrected Measured Nitrate Yield})} \right)^2$$

where "Weight" is the relative weight given to the measurement in determining the total error, as shown on Table 28. The expression in the denominator was used to weight the points because minimizing absolute errors resulted in giving undue weight to the somewhat uncertain data obtained at the lowest temperature causing the derivation of unreasonable optimized parameters. Minimizing simply relative errors put undue weight on the lowest nitrate yields, which have the highest experimental uncertainty and are least important in affecting reactivity predictions. The parameter obtained in the optimization were as follows:

$\alpha = 3.94 \times 10^{-22}$ cm^3 molecule^{-1}
$\beta = 0.705$
$R_\infty^{300} = 0.380$
$m_0 = 2.15$
$m_\infty = 6.36$
$F = 0.745$

Note that the above value of R_∞^{300}, which is essentially the upper limit nitrate yield for high molecular weight compounds at ambient temperatures, is a factor of 1.6 lower than the upper limit derived from the previous parameterization. On the other hand, nitrate yield predictions for lower molecular weight compounds under ambient conditions are not as significantly affected.

Table 28 shows the nitrate yields estimated using these reoptimized parameters. These are used as the basis for the secondary nitrate yields estimates in the current mechanism, except as indicated below. A comparison for the experimental and calculated values for these data is also shown on Figure 4. It can be seen that reasonably good fits are obtained, though there may be a slight tendency for the parameterization to underpredict the yields at the lowest temperature and highest pressure.

Table 28. Alkyl nitrate yield data from the reactions of NO with secondary alkyl radicals that were used to derive the parameters to estimate secondary alkyl nitrate yields as a function of temperature, pressure, and carbon number.

Compound or Radical	nC	T (K)	P (molec cm^3)	Yield				Fit	
				Uncor	Corr	Notes	Calc	Weight	Error
Total nitrate yield from compound									
Propane	3	300	2.37e+19		4.0%	1,2	5.0%	100%	11%
n-Butane	4	300	2.37e+19		8.3%	1,2	7.9%	100%	-4%
n-Pentane	5	300	2.37e+19	13.4%	11.5%	1,2	11.4%	100%	0%
n-Hexane	6	300	2.37e+19		15.0%	1,2	15.3%	100%	2%
n-Heptane	7	300	2.37e+19	29.1%	18.7%	1,2	18.9%	100%	1%
n-Octane	8	300	2.37e+19		23.6%	1,2	21.8%	100%	-7%
n-Decane	10	300	2.37e+19		24.1%	2,3	25.0%	100%	4%
Cyclohexane	6	300	2.37e+19		16.5%	4	15.3%	100%	-7%
Yield of specific radicals at varying T and P									
2-Pentyl from	5	284	2.52e+19	15.8%	13.5%	5	14.3%	5%	6%
n-pentane	5	284	1.21e+19	10.6%	9.1%		9.7%	5%	6%
	5	284	5.27e+18	6.8%	5.8%		5.5%	5%	-3%
	5	300	1.63e+19	9.9%	8.5%		9.5%	5%	10%
	5	300	1.13e+19	9.5%	8.1%		7.7%	5%	-4%
	5	300	4.96e+18	6.0%	5.1%		4.5%	5%	-7%
	5	300	1.82e+18	3.1%	2.7%		2.0%	5%	-7%
	5	328	2.18e+19	8.2%	7.0%		7.8%	5%	8%
	5	326	1.19e+19	6.4%	5.5%		5.9%	5%	5%
	5	327	4.46e+18	3.9%	3.3%		3.2%	5%	-2%
	5	337	2.12e+19	7.9%	6.8%		6.9%	5%	2%
3-Pentyl from	5	284	2.52e+19	17.4%	14.9%	3,4	14.3%	5%	-4%
n-pentane	5	284	1.21e+19	12.0%	10.3%		9.7%	5%	-6%
	5	284	5.27e+18	7.5%	6.4%		5.5%	5%	-9%
	5	300	1.63e+19	10.7%	9.2%		9.5%	5%	3%
	5	300	1.13e+19	10.3%	8.8%		7.7%	5%	-11%
	5	300	4.96e+18	5.9%	5.0%		4.5%	5%	-6%
	5	300	1.82e+18	3.1%	2.7%		2.0%	5%	-7%
	5	328	2.18e+19	8.4%	7.2%		7.8%	5%	6%
	5	326	1.19e+19	6.6%	5.6%		5.9%	5%	3%
	5	327	4.46e+18	4.4%	3.8%		3.2%	5%	-6%
	5	337	2.12e+19	8.1%	6.9%		6.9%	5%	0%
2-Heptyl from	7	284	2.52e+19	29.8%	19.1%		23.9%	2.5%	25%
n-heptane	7	285	1.18e+19	24.9%	16.0%		18.6%	2.5%	16%
	7	283	5.43e+18	16.3%	10.5%		13.6%	2.5%	30%
	7	284	1.97e+18	11.5%	7.4%		7.4%	2.5%	1%
	7	300	1.14e+19	23.1%	14.8%		15.1%	2.5%	2%
	7	300	5.15e+18	14.6%	9.4%		10.8%	2.5%	14%
	7	300	1.80e+18	10.1%	6.5%		5.9%	2.5%	-6%
	7	323	2.21e+19	20.4%	13.1%		13.5%	2.5%	3%
	7	323	1.06e+19	16.3%	10.5%		10.9%	2.5%	4%

Table 28 (continued)

Compound or Radical	nC	T (K)	P (molec cm^3)	Yield Uncor	Yield Corr	Yield Notes	Yield Calc	Fit Weight	Fit Error
	7	324	4.65e+18	10.4%	6.7%		7.7%	2.5%	10%
	7	321	1.79e+18	7.1%	4.6%		4.7%	2.5%	2%
	7	339	2.11e+19	15.9%	10.2%		10.7%	2.5%	5%
	7	342	4.52e+18	8.9%	5.7%		6.1%	2.5%	4%
3-Heptyl from	7	284	2.52e+19	35.2%	22.6%		23.9%	2.5%	6%
n-heptane	7	285	1.18e+19	29.1%	18.7%		18.6%	2.5%	-1%
	7	283	5.43e+18	19.6%	12.6%		13.6%	2.5%	8%
	7	284	1.97e+18	14.1%	9.1%		7.4%	2.5%	-16%
	7	300	1.14e+19	29.3%	18.8%		15.1%	2.5%	-20%
	7	300	5.15e+18	17.7%	11.4%		10.8%	2.5%	-5%
	7	300	1.80e+18	12.2%	7.8%		5.9%	2.5%	-19%
	7	323	2.21e+19	22.6%	14.5%		13.5%	2.5%	-7%
	7	323	1.06e+19	17.9%	11.5%		10.9%	2.5%	-5%
	7	324	4.65e+18	12.2%	7.8%		7.7%	2.5%	-1%
	7	321	1.79e+18	8.8%	5.7%		4.7%	2.5%	-9%
	7	339	2.11e+19	17.2%	11.1%		10.7%	2.5%	-3%
	7	342	4.52e+18	9.6%	6.2%		6.1%	2.5%	0%
4-Heptyl from	7	284	2.52e+19	31.4%	20.2%		23.9%	2.5%	18%
n-heptane	7	285	1.18e+19	26.5%	17.0%		18.6%	2.5%	9%
	7	283	5.43e+18	17.6%	11.3%		13.6%	2.5%	20%
	7	284	1.97e+18	12.1%	7.8%		7.4%	2.5%	-3%
	7	300	1.14e+19	23.6%	15.2%		15.1%	2.5%	0%
	7	300	5.15e+18	15.3%	9.8%		10.8%	2.5%	10%
	7	300	1.80e+18	10.5%	6.7%		5.9%	2.5%	-8%
	7	323	2.21e+19	20.0%	12.9%		13.5%	2.5%	5%
	7	323	1.06e+19	16.0%	10.3%		10.9%	2.5%	6%
	7	324	4.65e+18	10.2%	6.6%		7.7%	2.5%	11%
	7	321	1.79e+18	7.3%	4.7%		4.7%	2.5%	0%
	7	339	2.11e+19	15.3%	9.8%		10.7%	2.5%	9%
	7	342	4.52e+18	8.4%	5.4%		6.1%	2.5%	7%

Notes

1 Nitrate yields for secondary radicals derived from total secondary nitrate yield from reactions of the n-alkane, divided by the fraction of formation of secondary radicals, as estimated using the method of Kwok and Atkinson (1995).

2 Total secondary nitrate yields from Arey et al (2000).

3 Total secondary nitrate yield from Atkinson (unpublished data, 1999).

4 Aschmann et al. (1997).

5 Nitrate yields relative to nitrate yields at ~300K and 1 atm total pressure from Atkinson et al (1983), as tabulated by Carter and Atkinson (1989). Data placed on an absolute basis using the ~300K, 1 atm total secondary nitrate yield data from Arey et al (2000), divided by the fraction of formation of secondary radicals as estimated by the method of Kwok and Atkinson (1995).

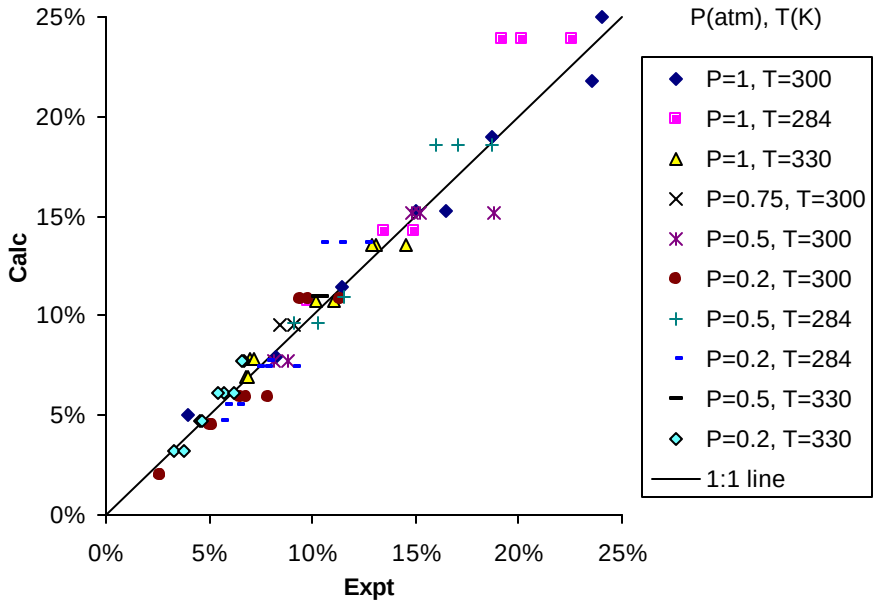

Figure 4. Plots of experimental vs calculated secondary alkyl nitrate yields that were used to optimize the parameters for estimation purposes.

The data summarized by Carter and Atkinson (1989b) indicate that the parameterization that fits the data for secondary alkyl nitrates does not perform well in predicting the limited nitrate yield data for primary and tertiary peroxy radicals. In addition, the presence of -OH, -O-, -CO-, ester, or other groups may also affect nitrate yields. Available information concerning nitrate yields that can serve as a basis for deriving estimates for substituted and non-secondary peroxy radicals is given in Table 29. As indicated on the table, most of these "nitrate yields" are not results of direct measurements, but results of optimizations of nitrate yield parameters in order to fit environmental chamber data. Although these chamber data are highly sensitive to this parameter, this is obviously a highly uncertain "measurement" because the results can be affected by other uncertainties in the VOCs' mechanisms, as well in the ability of the model to simulate the conditions of the experiment (see Section V). Nevertheless, for most types of radicals this provides the only information available from which general estimates can be derived.

Table 29 shows that the estimates for secondary alkyl peroxy radicals (shown in the Y_{sec} column on the table) generally perform very poorly in fitting the data for these substituted or other radicals, in most cases overpredicting the observed or adjusted yields. This means that some correction is needed when estimating nitrate yields for substituted or non-secondary peroxy radicals. Carter and Atkinson (1989b) recommended using a correction factor for the purpose of estimating primary and tertiary nitrate yields, This is equivalent to assuming that

$$Y_i\,(n_C, T, M) = Y_{sec}\,(n_C, T, M) \cdot f_i \qquad (V)$$

where Yi is the yield computed for radicals of type i, Y_{sec} is the yield for secondary alkyl radicals computed as shown above, and f_i is a correction factor for this type of radical. This method, if generally applied, would mean that substitution or radical structure affects nitrate yields in a way that does not

Table 29. Alkyl nitrate yield assignments used in the current mechanism, including data used to derive general estimation methods for primary, tertiary, and substituted peroxy radicals.

Compound and Radical	Nitrate Yield			Ref.
	Value Used	Estimated Y_{sec}	Estimated Y_{corr}	
Propane				
CH3-CH2-CH2OO.	2.0%	5.0%	0.0%	1
CH3-CH[OO.]-CH3	4.0%	5.0%	5.0%	2
Neopentane				
CH3-C(CH3)(CH2OO.)-CH3	5.1%	11.4%	6.4%	1
2,2,4-Trimethyl Pentane [b]				
CH3-C(CH3)(CH3)-CH2-C[OO.](CH3)-CH3	10.2%	21.8%	17.2%	3
CH3-C(CH3)(CH2OO.)-CH2-C(CH3)(OH)-CH3	10.2%	21.8%	17.2%	3
CH3-C(CH3)(CH3)-CH[OO.]-CH(CH3)-CH3	12.9%	21.8%	21.9%	3
CH3-C(CH3)(CH2OO.)-CH2-CH(CH3)-CH3	10.2%	21.8%	17.2%	3
CH3-C(CH3)(CH3)-CH2-CH(CH2OO.)-CH3	10.2%	21.8%	17.2%	3
CH3-C[OO.](CH3)-CH2-C(CH3)(CH3)-CH2-OH	10.2%	21.8%	17.2%	3
CH3-C(CH3)(OH)-CH2-C(CH3)(CH2OO.)-CH2-OH	10.2%	21.8%	17.2%	3
CH3-C(CH3)(OH)-CH2-C[OO.](CH3)-CH3	7.9%	19.0%	13.4%	3
CH3-C(OH)(CH2OO.)-CH2-C(CH3)(OH)-CH3	7.9%	19.0%	13.4%	3
CH3-CH(CH3)-CH2-C[OO.](CH3)-CH3	7.9%	19.0%	13.4%	3
CH3-C(CH3)(CH3)-CH2-CH[OO.]-CH3	11.2%	19.0%	19.0%	3
CH3-C(CH3)(CH2OO.)-CH2-CH(OH)-CH3	7.9%	19.0%	13.4%	3
CH3-C(CH3)(OH)-CH2-CH(CH2OO.)-CH3	7.9%	19.0%	13.4%	3
2-Methyl Butane				
CH3-C[OO.](CH3)-CH2-CH3	5.2%	11.4%	6.4%	1
CH3-CH(CH3)-CH[OO.]-CH3 [a]	14.1%	11.4%	11.4%	1
Propene				
CH3-CH[OO.]-CH2-OH	1.5%	5.0%	0.0%	4
CH3-CH(CH2OO.)-OH	1.8%	5.0%	0.0%	4
1-Butene				
CH3-CH2-CH(CH2OO.)-OH	3.1%	7.9%	3.9%	5
CH3-CH2-CH[OO.]-CH2-OH	2.2%	7.9%	3.9%	5
1-Hexene				
CH3-CH2-CH2-CH2-CH(CH2OO.)-OH	6.6%	15.3%	9.6%	6
CH3-CH2-CH2-CH2-CH[OO.]-CH2-OH	4.9%	15.3%	9.6%	6
Cis-2-Butene				
CH3-CH(OH)-CH[OO.]-CH3	3.5%	7.9%	3.9%	7
Isoprene				
HO-CH2-C(CH3)=CH-CH2OO.	8.8%	11.4%	6.4%	8
HO-CH2-C(CH3)=CH(CH2OO.)	8.8%	11.4%	6.4%	8
CH2=CH-C[OO.](CH3)-CH2-OH	8.8%	11.4%	6.4%	8
CH3-C(CH2OO.)=CH(CH2-OH)	8.8%	11.4%	6.4%	8

Table 29 (continued)

Compound and Radical	Nitrate Yield			Ref.
	Value Used	Estimated Y_{sec}	Estimated Y_{corr}	
CH3-C(CH2OO.)=CH-CH2-OH	8.8%	11.4%	6.4%	8
CH2=C(CH3)-CH[OO.]-CH2-OH	8.8%	11.4%	6.4%	8
CH2=CH-C(OH)(CH2OO.)-CH3	8.8%	11.4%	6.4%	8
CH2=C(CH3)-CH(CH2OO.)-OH	8.8%	11.4%	6.4%	8
T-Butyl Alcohol				
CH3-C(OH)(CH2OO.)-CH3	7.0%	7.9%	3.9%	9
MTBE				
CH3-C(CH3)(CH3)-O-CH2OO.	7.0%	11.4%	6.4%	10
CH3-C(CH3)(CH2OO.)-O-CH3	7.0%	11.4%	6.4%	10
Ethoxy Ethanol				
CH3-CH[OO.]-O-CH2-CH2-OH	2.5%	7.9%	3.9%	11
CH3-CH2-O-CH[OO.]-CH2-OH	2.5%	7.9%	3.9%	11
HO-CH2-CH2-O-CH2-CH2OO.	2.5%	7.9%	3.9%	11
Carbitol				
HO-CH2-CH2-O-CH2-CH2-O-CH2-CH2OO.	12.2%	15.3%	9.6%	12
CH3-CH[OO.]-O-CH2-CH2-O-CH2-CH2-OH	12.2%	15.3%	9.6%	12
CH3-CH2-O-CH[OO.]-CH2-O-CH2-CH2-OH	12.2%	15.3%	9.6%	12
CH3-CH2-O-CH2-CH[OO.]-O-CH2-CH2-OH	12.2%	15.3%	9.6%	12
CH3-CH2-O-CH2-CH2-O-CH[OO.]-CH2-OH	12.2%	15.3%	9.6%	12
Methyl Acetate				
CH3-CO-O-CH2OO.	1.5%	5.0%	0.0%	13
2-Butoxyethanol				
HO-CH2-CH2-O-CH2-CH2-CH2-CH2OO.	11.8%	15.3%	9.6%	14
CH3-CH[OO.]-CH2-CH2-O-CH2-CH2-OH	11.8%	15.3%	9.6%	14
CH3-CH2-CH[OO.]-CH2-O-CH2-CH2-OH	11.8%	15.3%	9.6%	14
CH3-CH2-CH2-CH[OO.]-O-CH2-CH2-OH	11.8%	15.3%	9.6%	14
CH3-CH2-CH2-CH2-O-CH[OO.]-CH2-OH	11.8%	15.3%	9.6%	14
Ethyl Acetate				
CH3-CO-O-CH2-CH2OO.	4.0%	7.9%	3.9%	15
CH3-CO-O-CH[OO.]-CH3	4.0%	7.9%	3.9%	15
CH3-CH2-O-CO-CH2OO.	4.0%	7.9%	3.9%	15
Dimethyl Succinate (DBE-4)				
CH3-O-CO-CH2-CH2-CO-O-CH2OO.	8.0%	15.3%	9.6%	16
CH3-O-CO-CH2-CH[OO.]-CO-O-CH3	8.0%	15.3%	9.6%	16
CH3-O-CO-CH2-CH(OH)-CO-O-CH2OO.	8.0%	15.3%	9.6%	16
Dimethyl Glutyrate (DBE-5)				
CH3-O-CO-CH2-CH2-CH2-CO-O-CH2OO.	14.8%	19.0%	13.4%	17
CH3-O-CO-CH2-CH2-CH[OO.]-CO-O-CH3	14.8%	19.0%	13.4%	17
CH3-O-CO-CH2-CH[OO.]-CH2-CO-O-CH3	14.8%	19.0%	13.4%	17
CH3-O-CO-CH2-CH2-CH(OH)-CO-O-CH2OO.	14.8%	19.0%	13.4%	17

Table 29 (continued)

Compound and Radical	Nitrate Yield			Ref.
	Value Used	Estimated Y_{sec}	Estimated Y_{corr}	
Methyl Isobutyrate				
CH3-CH(CH2OO.)-CO-O-CH3	6.4%	11.4%	6.4%	18
CH3-C[OO.](CH3)-CO-O-CH3	6.4%	11.4%	6.4%	18
CH3-CH(CH3)-CO-O-CH2OO.	6.4%	11.4%	6.4%	18
t-Butyl Acetate				
CH3-C(CH3)(CH2OO.)-O-CO-CH3	12.0%	15.3%	9.6%	19
CH3-C(CH3)(CH3)-O-CO-CH2OO.	12.0%	15.3%	9.6%	19
Propylene Carbonate [b]				
CH(CH3)-O-CO-O-CH[OO.]-	1.2%	7.9%	3.9%	20
C[OO.](CH3)-CH2-O-CO-O-	1.2%	7.9%	3.9%	20
CH(CH2OO.)-CH2-O-CO-O-	1.2%	7.9%	3.9%	20
CH3-CO-O-CO-O-CH2OO.	1.2%	7.9%	3.9%	20
CH3-CH[OO.]-O-CO-O-CHO	1.2%	7.9%	3.9%	20
Isobutene				
CH3-C[OO.](CH3)-CH2-OH	10.0%	7.9%	3.9%	21
n-Butyl Acetate				
CH3-CO-O-CH2-CH2-CH2-CH2OO.	10.0%	15.3%	9.6%	22
CH3-CO-O-CH2-CH2-CH[OO.]-CH3	10.0%	15.3%	9.6%	22
CH3-CH2-CH[OO.]-CH2-O-CO-CH3	10.0%	15.3%	9.6%	22
CH3-CH2-CH2-CH[OO.]-O-CO-CH3	10.0%	15.3%	9.6%	22
CH3-CH2-CH2-CH2-O-CO-CH2OO.	10.0%	15.3%	9.6%	22
Methyl Pivalate				
CH3-C(CH3)(CH2OO.)-CO-O-CH3	13.0%	15.3%	9.8%	23
CH3-C(CH3)(CH3)-CO-O-CH2OO.	13.0%	15.3%	9.8%	23
Methyl Isopropyl Carbonate				
CH3-CH(CH2OO.)-O-CO-O-CH3	4.5%	11.4%	6.5%	24
CH3-C[OO.](CH3)-O-CO-O-CH3	4.5%	11.4%	6.5%	24
CH3-CH(CH3)-O-CO-O-CH2OO.	4.5%	11.4%	6.5%	24
Cyclohexanone				
CH2-CH2-CH2-CH2-CO-CH[OO.]-	15.0%	15.3%	9.6%	25
CH2-CH2-CH2-CO-CH2-CH[OO.]-	15.0%	15.3%	9.6%	25
CH2-CH2-CO-CH2-CH2-CH[OO.]-	15.0%	15.3%	9.6%	25
1-Methoxy-2-Propanol				
CH3-CH(OH)-CH[OO.]-O-CH3	1.6%	7.9%	3.9%	26
CH3-CH(OH)-CH2-O-CH2OO.	1.6%	7.9%	3.9%	26

[a] Experimental value is probably high. Not used for determining best fit parameters.

[b] Other uncertainties in the mechanism affect the nitrate yield that gives the best fits to the mechanism to such an extent that the adjusted yield for this compound was not used to determine the best fit parameters.

Table 29 (continued)

References

1 Based on nitrate yield data tabulated by Carter and Atkinson (1989).

2 Based on 2-propyl nitrate yields from propane from Arey et al (2000), corrected fraction of 2-propyl formation estimated using the method of Kwok and Atkinson (1995).

3 Nitrate yields from C_7 and C_8 peroxy radicals formed from 2,2,4-trimethyl pentane reduced by a factor of 1.7 to fit results of environmental chamber reactivity experiments.

4 Based on nitrate yield data from propene from Shepson et al (1985) and O'Brien et al (1998), corrected for estimated fraction of reaction from terminal position based on data of Cvetanocic (1976).

5 Based on nitrate yield data from 1-butene from O'Brien et al (1998), corrected for estimated fraction of reaction from terminal position based on data of Cvetanocic (1976) for propene.

6 Based on nitrate yield data from 1-hexene from O'Brien et al (1998), corrected for estimated fraction of reaction from terminal position based on data of Cvetanocic (1976) for propene.

7 Based on nitrate yield data from cis-2-butene from Muthuramu et al (1993) and O'Brien et al (1998).

8 Adjusted to fit environmental chamber reactivity data for isoprene.

9 Adjusted to fit environmental chamber reactivity data for t-butanol..

10 Adjusted to fit environmental chamber reactivity data for MTBE.

11 Adjusted to fit environmental chamber reactivity data for ethoxy ethanol.

12 Adjusted to fit environmental chamber reactivity data for carbitol.

13 Adjusted to fit environmental chamber reactivity data for methyl acetate.

14 Adjusted to fit environmental chamber reactivity data for 2-butoxyethanol.

15 Adjusted to fit environmental chamber reactivity data for ethyl acetate.

16 Adjusted to fit environmental chamber reactivity data for DBE-4.

17 Adjusted to fit environmental chamber reactivity data for DBE-5.

18 Adjusted to fit environmental chamber reactivity data for methyl isobutyrate.

19 Adjusted to fit environmental chamber reactivity data for t-butyl acetate.

20 Adjusted to fit environmental chamber reactivity data for propylene carbonate.

21 Adjusted to fit environmental chamber data for isobutene.

22 Adjusted to fit environmental chamber reactivity data for n-butyl acetate.

23 Adjusted to fit environmental chamber reactivity data for methyl pivalate.

24 Adjusted to fit environmental chamber reactivity data for methyl isopropyl carbonate.

25 Adjusted to fit environmental chamber reactivity data for cyclohexanone.

26 Adjusted to fit environmental chamber reactivity data for 1-Methoxy-2-Propanol.

depend on the size of the radical. An alternative approach is to adjust the carbon number used to estimate the yields, i.e.,

$$Y_i (n_C, T, M) = Y_{sec} (n_C - n_i, T, M) \quad \text{(VI)}$$

where n_i is a correction term used to derive an "effective carbon number" for radicals of type i. This would predict that the effects of substitution or structure tend to become less important as the size of the radical increases, since the parameterization predicts that the nitrate yield becomes less dependent on n_C as n_C increases.

Figure 5 shows plots of the observed or adjusted overall nitrate yields derived for compounds forming non-secondary or substituted peroxy radicals against secondary nitrate yields (Y_{sec}) calculated for the same number of carbons using Equations (III and IV)[14]. It can be seen that in most cases the ratio of the observed or adjusted yields to Y_{sec} range from ~0.4 to 1, with no apparent dependence of the ratio on the nature of the radical or its substituents. The best fit line for all the data corresponds to a correction factor of ~0.65, if the constant correction factor method (Equation V) is employed, with an uncertainty of approximately a factor of 1.6. Because of the lack of a clear dependence of the correction on the type of radical, the most appropriate approach is probably to use this factor for all substituted or non-secondary radicals.

However, if the constant correction factor method (Equation V) is employed, then the model tends to overpredict the ozone reactivities of high molecular weight alkanes (e.g., n-octane and n-dodecane) in environmental chamber reactivity experiments. Better fits are obtained if higher nitrate yields from the C_{8+} OH-substituted peroxy radicals formed in the oxidations of these compounds (following 1,4-H shift isomerizations, as discussed in Section III.J.2) are assumed than predicted using Equation (V) and f=0.65. This suggests that the effects of substitution may decrease as the size of the radical increases, as is predicted by the "effective carbon number" adjustment approach (Equation VI). Therefore, "effective carbon number" adjustment this approach is adopted in this work.

The best fits to the available experimental or adjusted nitrate yield data for are obtained by using Equation (VI) with the carbon numbers reduced by ~1.5 for non-secondary or substituted peroxy radicals, with no apparent dependence of the reduction on the type of radical or its substituents. Figure 6 shows the performance of this method in estimating overall nitrate yields for compounds forming substituted or non-secondary peroxy radicals that are used as the basis for deriving our estimates. The 1:1 line and lines showing a factor of 1.6 uncertainty range are also shown. A comparison of Figure 5 and Figure 6 shows that the carbon number adjustment method performs about as well (or poorly) as the factor adjustment method, with the data being an insufficient basis for choosing between them. However, the use of Equation (VI) with a carbon number reduction of 1.5 for all non-secondary or substituted radicals is preferred because of its superior performance in simulating the overall reactivities of the higher n-alkanes.

There are several cases where the observed or adjusted nitrate yields are not well fit by either method. These include $CH_3C(OH)(CH_3)CH_2OO\cdot$ from t-butanol, $CH_3C(OO\cdot)(CH_3)CH_2OH$ from isobutene, and $CH_3C(O)OC(CH_3)(CH_3)CH_2OO\cdot$ from t-butyl acetate, where the estimated yields are considerably lower than those that must be assumed for model simulations to fit the chamber data. On the other hand, the estimates tend to underpredict nitrate yields that were measured in the reactions of OH radicals with 1-butene and 1-hexene (O'Brein et al, 1998). It is interesting to note that the cases where the nitrate yields are higher than estimated all have the radical center is at or near a quaternary carbon.

[14] The adjusted nitrate yield for methyl isobutyrate, whose mechanism is highly uncertain, is not shown.

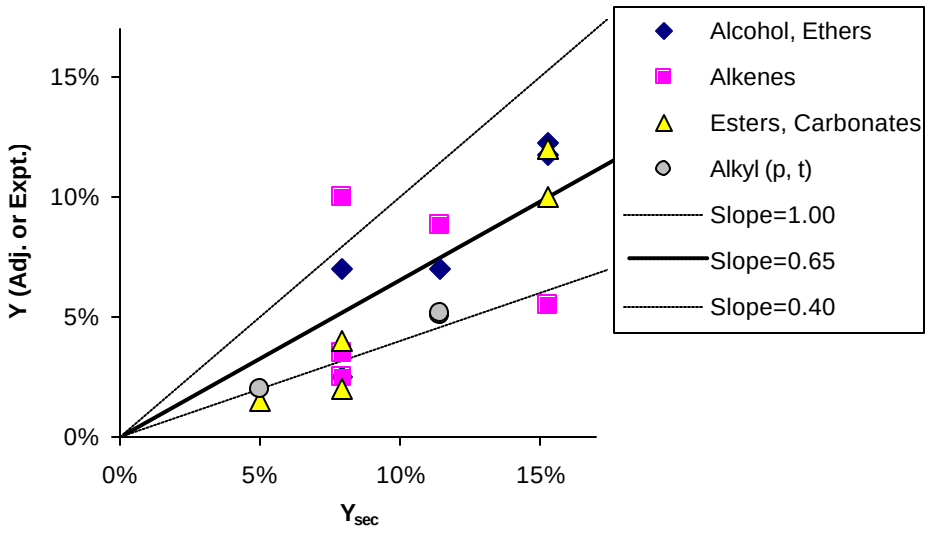

Figure 5. Plots of observed or adjusted overall nitrate yields against Y_{sec} values derived using Equations (III and IV) for compounds forming non-secondary and substituted peroxy radicals.

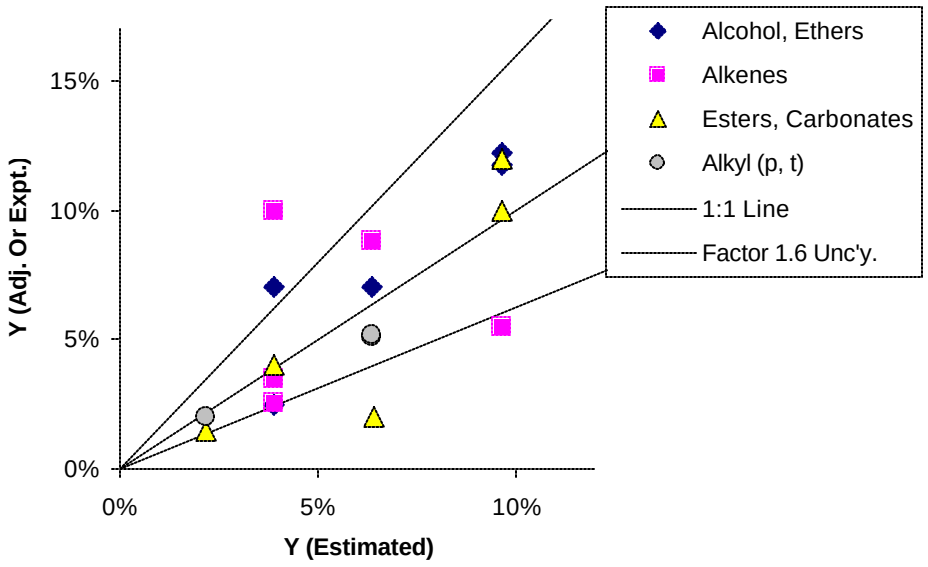

Figure 6. Plots of observed or adjusted overall nitrate yields for compounds forming non-secondary and substituted peroxy radicals against overall nitrate yields estimated using Equation (VI) and a carbon number reduction of 1.5.

However, the alkyl nitrate yield data for neopentyl, 2-methyl-2-butyl and 2-methyl-2-pentyl (Carter and Atkinson, 1989b) are reasonably consistent with the predictions using the estimated corrections discussed above, so no general conclusions can be made for radicals with this structure. The reason why the nitrate yields from radicals formed from 1-butene and 1-hexene are too low is unclear, and the possibility of experimental problems cannot necessarily be ruled out.

The approach adopted in this work to use Equation (VII) with a carbon number reduction of 1.5 to derive the correction factors for estimating nitrate yields in cases of non-secondary or substituted radicals where no data are available, and to use explicit assignments for those radicals (including the outliers discussed above) for which available data indicate the estimates are not appropriate. These assignments are indicated on the "value used" column on Table 29.

J. Reactions of Alkoxy Radicals

Alkoxy radicals are also critical intermediates in the photooxidation mechanisms of most VOCs, and the variety of possible reactions that higher molecular weight alkoxy radicals can undergo is a major source of the complexity (and uncertainty) in the generated photooxidation mechanisms for most VOCs. Primary and secondary alkoxy radicals can react with O_2, C_{2+} alkoxy radicals can react via β-scission forming smaller molecules and radicals, long chain alkoxy radicals can undergo H-shift isomerizations ultimately forming disubstituted radicals, and certain substituted alkoxy radicals can undergo other reactions. Knowledge of the rate constants or branching ratios for all these processes need to be specified to generate the mechanisms. Unfortunately, relevant information concerning these processes is highly limited, and estimates are usually necessary. The methods used to estimate the various rate constants or branching ratios, and the specific assignments that are used in those cases where data are available, are discussed in this section.

1. Reaction with O_2

Primary and secondary alkoxy radicals can react with O_2, forming HO_2 and the corresponding carbonyl compound.

$$RCH_2O\cdot + O_2 \rightarrow RCHO + HO_2$$

$$RR'CO\cdot + O_2 \rightarrow R\text{-}CO\text{-}R' + HO_2$$

Absolute rate constants for these reactions are available only for methoxy, ethoxy, and isopropoxy radicals, and the IUPAC recommended rate parameters (Atkinson et al, 1998) are given on Table 30. Non-Arrhenius temperature dependences are observed and the A factors are much lower than expected for an abstraction reaction, possibly indicating a complex mechanism. However, the A factors are reasonably consistent for the reactions of the different radicals, increasing as expected with the number of abstractable hydrogens, though the A factor per hydrogen for isopropoxy is approximately half that of ethoxy (3.0×10^{-14} cm^3 $molec^{-1}$ s^{-1}).

For estimation purposes, we assume that all primary alkoxy radicals react with O_2 with the same A factor as does ethoxy, and that all secondary alkoxy + O_2 A factors are the same as for isopropoxy radicals:

$$A(O_2, \text{primary } RO\cdot) = 6.0 \times 10^{-14} \text{ cm}^3 \text{ molec}^{-1} \text{ s}^{-1}$$

$$A(O_2, \text{secondary } RO\cdot) = 1.5 \times 10^{-14} \text{ cm}^3 \text{ molec}^{-1} \text{ s}^{-1}$$

Table 30. Recommended kinetic parameters for reactions of alkoxy radicals with O_2.

Radical	n	A	A/n	K(298)	ΔH_r	Ea
		(cm^3 $molec^{-1}$ s^{-1})			(kcal/mol)	
CH3O.	3	7.20e-14	2.40e-14	1.92e-15	-26.28	2.15
CH3-CH2O.	2	6.00e-14	3.00e-14	9.48e-15	-32.03	1.09
CH3-CH[O.]-CH3	1	1.50e-14	1.50e-14	7.67e-15	-35.82	0.40

From Atkinson (1997a), Table 9

Because the low A factors and non-Arrhenius behavior these estimates must be considered to be uncertain, and quantitative data are clearly needed for other alkoxy radicals.

Table 30 shows that the apparent activation energies for the alkoxy + O_2 reaction appear to be correlated with the heat of reaction. In fact, a plot of the activation energy vs. ΔH_r (not shown) indicates that X perhaps by coincidence X the data for these three radicals fall almost exactly on a straight line, which is given by:

$$Ea(O_2) = 6.96 + 0.183\ \Delta H_r(O_2) \qquad \text{(VIII)}$$

where $Ea(O_2)$ is the activation energy and $\Delta H_r(O_2)$ is the heat of reaction[15] This therefore can be used to estimate activation energies, and therefore rate constants, for any alkoxy + O_2 reaction.

However, the above equation cannot be used for estimating activation energies for reactions of O_2 with alkoxy radicals such as $CH_3OCH_2O\cong$, whose reaction with O_2 are sufficiently exothermic that Equation (VIII) predicts a negative activation energy. In those cases, we assume for estimation purposes that no alkoxy + O_2 reaction has an activation energy that is less than the a certain minimum value, which should be somewhere between 0 and 0.4 kcal/mole. We assume that the actual minimum is near the high end of this range, or 0.4 kcal/mole. Therefore, for estimation purposes we use:

$$Ea(O_2) = \max [\ 0.4,\ 6.96 + 0.183\ \Delta H_r(O_2)\ ] \qquad \text{(IX)}$$

Note that the 0 to 0.4 kcal/mole range for the minimum activation energy amounts to an uncertainty in the rate constant of a factor of ~2 for highly exothermic alkoxy + O_2 reactions. This is not a large uncertainty given the uncertainty in assuming that the A factors for the O_2 reactions are the same for all primary or all secondary alkoxy radicals.

The estimates for the reactions of O_2 with the saturated hydrocarbon alkoxy radicals (i.e, alkoxy radicals containing only $-CH_3$, $-CH_2-$, >CH-, or >C< groups) are probably the least uncertain because they are the most similar to the simple alkoxy radicals used as the basis for the estimate. These estimates become increasingly uncertain for the oxygenated radicals with significantly higher reaction exothermicities (i.e., the reaction of O_2 with $CH_3OCH_2O\cong$ has an estimated ΔH_r of -46.6 kcal/mole, compared to -35.8 for isopropoxy). The estimates used here predict that these highly exothermic alkoxy + O_2 reactions have 298K rate constants of ~3 x 10^{-14} cm^3 $molec^{-1}$ s^{-1} for primary radicals and ~8 x 10^{-15} cm^3

[15] Heats of reaction are estimated by group additivity as discussed in Section IV.A.5, based primarily on the thermochemical groups in the NIST (1994) database. Some reactants or products had groups that are not in the NIST (1994) database, and the thermochemical contributions of these groups had to be estimated. Tabulated heats of reaction may be uncertain by at least 2 kcal/mole.

molec^{-1} s^{-1} for secondary radicals. However, the possibility that these rate constants may be orders of magnitude higher cannot be ruled out. For example, if the approach of Atkinson (1997a), which uses a relationship between the rate constant (not the activation energy) and the heat of reaction, estimates the rate constant for the reaction of O_2 with, for example, $CH_3OCH_2O\cong$, to be ~3.7 x 10^{-13} cm^3 molec^{-1} s^{-1}, which is a factor of ~12 higher than the estimation approach discussed above. This, of course, would imply that the effective A factors for these highly exothermic reactions are significantly higher than for those radicals whose rate constants have been measured – which we assume is not the case.

2. H-Shift Isomerizations

Long chain alkoxy radicals can react unimolecularly by abstraction by the alkoxy center from a C-H bond elsewhere in the radical, via a cyclic transition state, forming a hydroxy-substituted carbon-centered radical, e.g.,

$$CH_3CH_2CH_2CH_2O\cdot \rightarrow \quad \cdot CH_2CH_2CH_2CH_2OH$$

Rate constants for these reactions can be estimated based on activation energies for bimolecular H-atom abstractions by alkoxy radicals plus ring strain energies for the cyclic transition states, and estimates of A factors (Carter et al, 1976; Baldwin et al, 1977; Carter and Atkinson, 1985; Atkinson, 1994). The results indicate that 1,4-H shift reactions (such as shown above), involving a relatively unstrained 6-member ring transition state, will be relatively rapid and should dominate over competing processes, at least for the hydrocarbon alkoxy radicals formed in alkane photooxidation systems. On the other hand, the estimates indicate that hydrogen shifts involving strained transition states, such as 1,3-H shifts involving a 5 member ring, as well as those involving more strained rings, are not likely to be sufficiently rapid to be important. Therefore except for the "ester rearrangement" reaction discussed below, only 1,4 H shift isomerizations are considered when the estimated mechanisms are generated.

The only data available concerning rates of 1,4-H shift isomerizations of alkoxy radicals are rate constants relative to competing alkoxy + O_2 or decomposition reactions. Although the rate constants for the competing reactions have also not been measured, they can be estimated in the case of the O_2 reactions as discussed above. Table 31 lists the isomerization reactions whose rate have been determined relative to the competing O_2 reaction, together with the rate constant ratios as summarized by Atkinson (1997a). Table 31 also shows the A factors estimated by Atkinson (1997a) and the corresponding activation energies, which are based on assuming

$$A(isom) = 8.0 \times 10^{10} \times (\text{number of abstractable hydrogens}) \text{ sec}^{-1}.$$

This is based on the previous estimates of Baldwin et al (1977), and is incorporated in the 1,4-H shift estimates used in this work.

The limited number of species for which isomerization rate constants have been measured and the relative imprecision of the data for 2-hexoxy provide an inadequate data base from which to derive a general estimation method for the activation energies. It is reasonable to assume that the activation energy will be correlated with the C-H bond dissociation energy for the bond that is being attacked by the alkoxy center. To provide a somewhat larger database in this regard, it is useful to look at available kinetic information for a bimolecular analogue for this reaction, namely the H-atom abstraction reactions of methoxy radicals. Table 31 lists the rate constants or Arrhenius parameters found for such reactions in the NIST kinetics database (NIST, 1989). The Arrhenius parameters have been estimated for those species where temperature dependence information was not given by using the average of those determined for

Table 31. Rate constants for H abstraction reactions by alkoxy radicals.

Reaction	BDE [a] (kcal)	A [b]	Ea (kcal)	T (K)	k(T)	Refs [c]
Alkoxy Isomerizations (sec^{-1})						
1-Butoxy [d]	101.4	2.4e+11	8.42	298	1.60e+5	1,2
2-Pentoxy [d]	101.4	2.4e+11	8.16	298	2.50e+5	1,2
3-Hexoxy	101.4	2.4e+11	8.04	298	3.05e+5	2,3
2-Hexoxy	98.1	1.6e+11	6.44	298	3.05e+6	2,4
Methoxy + RH Reactions (cm^3 $molec^{-1}$ sec^{-1})						
CH_4	104.9	2.6e-13	8.84			5
C_2H_6 -> i-C_2H_5	101.2	4.0e-13	7.09			5
C_3H_8 -> i-C_3H_7	98.6	2.4e-13	4.57			6
$(CH_3)_2CHCH(CH_3)_2$	96.8	1.7e-13	4.11	373	6.64e-16	7,8
CH_3OH -> CH_2OH	98.1	5.0e-13	4.07			9
CH_3CHO	85.9	8.4e-14	0.63	298	2.88e-14	8,10
Alkoxy Isomerization Group Rate Constants for estimations (sec^{-1})						
-CH_3	101.4	2.4e+11	8.49	298	1.44e+5	2,11
-CH_2-	98.1	1.6e+11	6.33	298	3.63e+6	2,11
-CH<	96.8	8.0e+10	5.51	298	7.29e+6	2,11
-CHO	85.9	8.0e+10	5.75	299	5.02e+6	2,12

[a] Bond dissociation energies are derived from the NIST (1994) thermochemical database or from heats of formation given in the IUPAC evaluation (Atkinson et al, 1997).

[b] Underlined A, Ea, T, or k data are experimental measurements. Data not underlined are estimates.

[c] Notes and references:

1 Rate constant recommended by Atkinson (1997a)

2 A factors estimated for general alkoxy radical isomerizations by Atkinson (1997a), based on earlier estimates of Baldwin et al (1977)

3 Use middle value of range given by Eberhard et a. (1995). Varies from 1.8 - 4.3 x 10^5 sec^{-1}.

4 Use middle value of range given by Eberhard et a. (1995). Varies from 1.4 - 4.7 x 10^6 sec^{-1}.

5 Tsang and Hampson (1986)

6 Tsang (1988)

7 Alcock and Mile (1975)

8 A factor per abstracted hydrogen is assumed to be the average of that for the methoxy + ethane, propane and propane (to isopropyl) reactions.

9 Tsang (1987)

10 Weaver et al, (1975), Kelly and Keicklen (1978). These report rate constant ratios relative to methoxy + O2 of 14-15. Placed on an absolute basis using the methoxy + O2 rate constant.

11 Activation energy derived from correlation between methoxy + RH rate constants and BDE, with an added 1.6 kcal/mole "strain" correction for consistency with data for isomerization reactions, as discussed in the text.

12 Activation energy estimated from that estimated for the methoxy + acetaldehyde reaction, plus the 1.6 kcal/mole "strain" correction used for the other groups, plus an additional 3.5 kcal/mole "strain" correction for reactions with -CO- groups in the transition state, derived as discussed in the text.

methoxy + methane and methoxy + ethane. The measured (IUPAC, 1997) or estimated (NIST, 1994) bond dissociation energies (BDE's) for the C-H bond being attacked are also shown in the Table.

Figure 7 shows plots of the activation energies for the internal or bimolecular alkoxy H-atom abstraction reactions against the relevant bond dissociation energy. [Data for the methoxy + isobutane reaction are inconsistent (NIST 1998), so they are not included.] It can be seen that if the methoxy + acetaldehyde data are not included, then a reasonably good straight line relationship is obtained. The limited data for the isomerization reactions are consistent with the relationship for the bimolecular methoxy reactions, with an offset of 1.6 kcal/mole. Although this offset is probably not outside the uncertainties of the BDE or activation energy determinations, it could also be rationalized as ring strain in the 6-member ring transition state for the isomerization reaction.

The solid line shown on Figure 7 is the least squares line through the data for the methoxy abstraction reactions, with the data for acetaldehyde not being used when determining the fit. The measurement for acetaldehyde is excluded because abstractions from (CO)-H bonds apparently do not have the same correlation with the bond energies as abstractions from hydrocarbon C-H bonds.

The dotted line on Figure 7 shows the line for the methoxy reaction offset by 1.6 kcal/mole to agree with the data for the isomerizations of the butoxy, pentoxy, and hexoxy radicals. Therefore, this can be used as a basis for estimating activation energies for alkoxy radical isomerizations in general, or at least those involving abstractions from alkyl C-H bonds.

The rate constants for any isomerization reaction can be estimated using a generalization of the structure-reactivity approach derived by Atkinson (Atkinson, 1987, Kwok and Atkinson, 1995, Atkinson, 1997a) for estimating OH radical reactions. In this approach, reaction by H-abstraction at each type of group, whether -CH3, -CH2-, -CH<, or -CHO is given by a group rate constant for that group, multiplied by an appropriate correction factor for each substituent other than methyl groups (whose correction factor is 1.0 by definition). Note that the substituting corrections are assumed to be due only to the substituting affecting the activation energy, not the A factor (Kwok and Atkinson, 1995; Atkinson, 1997a).

Obviously a large kinetic database is necessary to derive the substituent correction factors, and this is not available for these alkoxy radical abstraction reactions. However, if we assume that (1) the substituent corrections are due only to the substituent affecting the activation energy and not the A factor, and (2) the activation energy is linearly related to the bond dissociation energy for both the OH and the alkoxy radical abstraction reactions, then one can derive the substituent correction factors for the alkoxy reactions from those for the corresponding OH radical reaction. The latter have been derived by Kwok and Atkinson (1996) using the large kinetic database for OH radical reactions. The first assumption is reasonable, and is already incorporated in the way the Atkinson estimation methods derive temperature dependences. The second assumption is already incorporated in our alkoxy radical estimation methods discussed above, but needs to be examined in the case of OH radical rate constants.

The 298K group rate constants used in estimating OH radical reactions and parameters used by Kwok and Atkinson (1996) to determine their temperature dependences, are given in Table 9. Kwok and Atkinson (1996) gave the temperature dependences in the form $k=C\ T^2\ \exp(-B/T)$, but these can be recast to the Arrhenius activation energy (adjusted to be valid for T around 298K), to place it on the same basis as used for the alkoxy radical reactions. The corresponding activation energies are 1.82, 0.68, -0.20, and -0.62 kcal/mole for -CH3, -CH2-, -CH<, and -CHO, respectively. These activation energies are plotted against the bond dissociation energies associated with the group on Figure 7. It can be seen that the activation energies are reasonably well fit by a linear relationship with the bond dissociation energy for reactions at alkyl C-H bonds, but not for reaction at -CHO groups. In the case of OH radicals, the

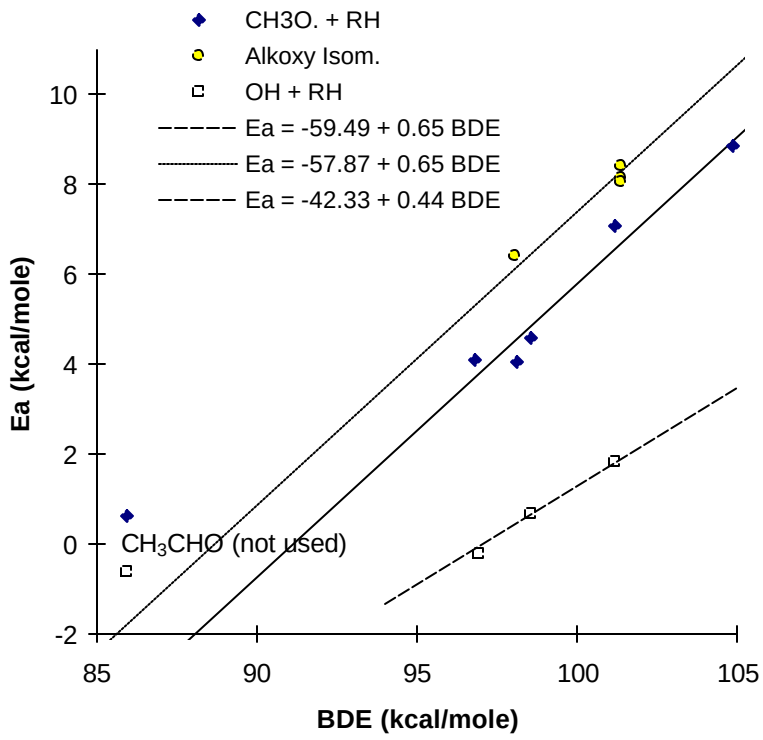

Figure 7. Plot of activation energies vs bond dissociation energies for methoxy abstraction reactions, alkoxy radical isomerizations, and OH abstraction reactions.

correlation breaks down for bond dissociation energies less than ~95 kcal/mole because there is essentially no energy barrier for bonds weaker than that. However, for stronger bonds, the correlation between group activation energy and BDE seems to hold reasonably well.

It is of interest to note that the slope for the line relating Ea to BDE for the alkoxy reactions is somewhat greater than that for the OH reactions, by a factor of ~1.5. This means that the activation energies for the alkoxy reactions would be more sensitive to substituents than is the case for OH reactions, as might be expected given the slower rates of these reactions. If these linear relationships between Ea and BDE are assumed to hold for the substituted species, this suggests that the group correction factors for the alkoxy radical isomerizations (F_{isom}) should be related to those for the OH radical reactions (F_{OH}) by

$$F_{isom} \approx f_{OH}^{1.5} \qquad (X)$$

Thus, the group correction factors given by Kwok and Atkinson (1996) for estimating rate constants for OH radical reactions can be used as a basis for estimating alkoxy radical isomerization reactions.

The dotted line on Figure 7 was derived to fit data primarily for radicals that have a -CH2- attached to the -CH3 group where the reaction is occurring. The OH group correction factor at ~300K for a -CH2- substituent is 1.23, which from Equation (X) corresponds to a correction factor of 1.5 for alkoxy radical reactions. This corresponds to an activation energy reduction of 0.18 kcal/mole. This means that the intercept for the line adjusted to fit the activation energy for these radicals (the dotted line on Figure

7) should be increased by 0.18 for the purpose of estimating group rate constants, which are defined based on -CH_3 substituents. Based on this, the activation energies for group rate constants for alkoxy radical isomerizations involving abstractions from -CH3, -CH2- and -CH< can be estimated from

$$Ea\ (group\ isom) = -57.87 + 0.65\ BDE + 0.18 = 57.69 + 0.65\ BDE \qquad (XI)$$

where BDE is the bond dissociation energy for the breaking bond. To place the BDE's on the same basis as those used to derive the equation, the BDE's for Equation (XII) should be calculated for groups with one -CH2- substituent, with the other substituents, if any, being CH3 groups.

Table 31 shows the activation energies for the various alkyl groups derived using Equation (XI), along with their corresponding A factors and 298K rate constants. In the case of -CHO groups, the activation energy is estimated from the estimated methoxy + acetaldehyde activation energy, plus the estimated 1.6 kcal/mole strain energy, derived as discussed above, plus an additional 3.5 kcal/mole of strain for reactions with -CO- groups in the cyclic transition state, derived as discussed in Section III.J.4, below. These group rate constants, together with the substituent factors derived for Equation (XI) using the substituent factors for estimating OH radical rate constants from Table 9, above, can then be used for estimating isomerization rate constants for any alkoxy radicals where the abstraction is at the given group.

As indicated above, a comparison of the activation energies for the bimolecular methoxy reactions with the estimated activation energies for isomerization of butoxy, pentoxy and hexoxy suggests that the ring strain for these isomerizations is ~1.6 kcal/mole. Note that this is reasonably consistent with the ring strain given by Benson (1976) for a six member ring with one oxygen. However, the strain may be different if the ring in the transition state involves groups other than just -CH2-. We assume that there is no strain difference if the transition state ring also has -CH< or >C< groups, but this does not appear to be the case if the ring also contains -O-, -CO- or -O-CO- groups. In particular, predictions are more consistent with available data if activation energies for isomerization involving -O-, -CO- or -O-CO- in the transition states are increased by an additional ~3.5 kcal/mole. Before giving the basis for this, which is discussed in Section III.J.4, it is necessary to first discuss the rate constant estimates for the competing decomposition reactions. This is given in the following section.

3. Beta Scission Decomposition

The most common unimolecular reactions of alkoxy radicals are β-scission decompositions. These involve breaking the C-C bond next to the alkoxy group, forming a carbonyl compound and a carbon center radical (where the latter will react further, as discussed above). For primary, secondary, and tertiary alkoxy radicals, the respective reactions are:

$$RCH_2O\cdot \rightarrow R\cdot + HCHO$$

$$RCH(O\cdot)R' \rightarrow RCHO + R'\cdot \ \underline{or}\ R'CHO + R\cdot$$

$$RC(O\cdot)(R')R'' \rightarrow R\text{-}CO\text{-}R' + R''\cdot \ \underline{or}\ R\text{-}CO\text{-}R'' + R'\cdot \ \underline{or}\ R'\text{-}CO\text{-}R'' + R\cdot$$

Note that for secondary and tertiary radicals there may be more than one possible reaction route, if the R, R' and/or R" substituents are different.

No direct measurements of absolute rate constants for alkoxy radical decompositions are available, but information is available concerning ratios of these rate constants relative to those for other alkoxy radical reactions. The only information concerning temperature dependent rate constants come from the measurements relative to alkoxy + NO reactions, whose absolute rate constants are known or can

be estimated (Atkinson, 1994, and references therein). Based on these data, Atkinson (1994, 1997b) recommends estimating the Arrhenius A factors using

$$A = 2.0 \times 10^{14} \cdot n \text{ sec-1}, \qquad \text{(XIII)}$$

where n is the reaction path degeneracy. The recommended decomposition rate constants and kinetic parameters are summarized on Table 32. The A factors derived using Equation (XIII) are assumed to be applicable to all alkoxy radical decompositions. Table 32 also gives alkoxy radical decomposition rate constants obtained from rate constant ratios obtained from results of various mechanistic and product studies, and placed on an absolute basis using estimates for the competing decomposition reactions. This is discussed below.

Table 33 lists the various alkoxy radicals for which relevant data are available concerning the branching ratios for their various competing reactions, or at least concerning upper or lower limits for those branching ratios. These are determined from product yields observed in various studies of OH radical + organic + NO_x systems where these alkoxy radicals are expected to be formed, as indicated in the comments on the table. In some cases product yield ratios can be used to derive ratios of rate constants involving an alkoxy radical decomposition; these are indicated in Table 33 and the relevant data are also included in Table 32. (In those cases Table 32 also gives the radical number used on Table 33 to aid the reader in finding the data on that radical.) In many other cases, only upper or lower branching ratios can be derived. For example, lower limits for a reaction route can be based on observing high yields of a product expected from a reaction, and upper limits for another route can be inferred from the failure to observe an expected product from the reaction. Many of the upper or lower limit estimates are subjective and approximate, and probably in many cases they could be refined based on a detailed analysis of the experimental methods. However, these approximate upper and lower limit data are useful for assessing the overall performance of the estimation methods because of the relatively large number and variety of reactions involved.

Table 33 also includes the heats of reaction for the various reactions where relevant and the estimated rate constants and corresponding branching ratios for the competing reactions. (The predictions for the O_2 reactions and the isomerizations are as discussed in the previous section, the predictions for the decompositions are discussed below.) An indication of how well the predicted branching ratios agree with the observed ratios is also shown. Table 34 gives a subset of the information on Table 33, organized by alkoxy reaction type rather than by radical. This is useful for obtaining an indication of how well the estimates are performing for a particular type of reaction. For that reason, Table 34 includes results using several alternative assumptions, which are discussed below.

Based on the approach used by Atkinson (1996), the activation energies for the decomposition reactions are estimated assuming

$$Ea \text{ (decomposition)} = EaA + EaB \cdot \Delta H_r \qquad \text{(XIV)}$$

where EaA and EaB are parameters which are assumed to depend only on the type of radical which is formed in the decomposition. The derivation of these parameters for the various types of decomposition reactions is discussed below.

We will first consider decompositions forming methyl radicals, for which, as shown on Table 32, there are the most extensive and best characterized data. These come in two groups: decompositions of hydrocarbon alkoxy radicals (i.e., alkoxy radicals containing only $-CH_3$, $-CH_2-$, >CH-, or >C< groups) which tend to be endothermic by ~5 to ~13 kcal/mole and relatively slow, and decompositions of alkoxy

Table 32. Summary of measured or estimated rate constants for alkoxy radical decompositions.

Reaction	Rate Parameters [a]				Relative to			Note	Ea (est.)	
	DH_r	A	Ea	k(298)	Type	Ratio	k(ref) [b]		Value	Err
Reactions forming CH3.										
CH3-CH2O. -> CH3. + HCHO	13.04	2.0e+14	20.20	3.1e-1	k(NO)		-	[c]	19.8	-0.4
CH3-CH[O.]-CH3 -> CH3-CHO + CH3.	7.86	4.0e+14	17.60	5.0e+1	k(NO)		-	[c]	17.5	-0.1
CH3-CH2-CH[O.]-CH3 -> CH3-CH2-CHO + CH3.	7.63	2.0e+14	16.60	1.3e+2	k(NO)		-	[c]	17.4	0.8
CH3-C[O.](CH3)-CH3 -> CH3-CO-CH3 + CH3.	4.98	7.5e+14	16.20	9.9e+2	k(NO)		-	[c,d]	16.2	0.0
CH3-C[O.](CH3)CH2-CH3 -> CH3-CH2-CO-CH3 + CH3.	4.82	4.0e+14	18.30	1.5e+1	k(NO)		-	[c,e,f]	16.2	-2.1
CH3-C(CH3)(CH3)-O-CH[O.]-CH3 -> CH3. + CH3-C(CH3)(CH3)-O-CHO	-4.81	2.0e+14	12.30	1.9e+5	k(O2)	4.85	3.9e+4	23 [f]	11.9	-0.4
CH3-CH2-O-CH[O.]-CH3 -> CH3-CH2-O-CHO + CH3.	-4.81	2.0e+14	11.49	7.5e+5	k(O2)	19	3.9e+4	13 [f]	11.9	0.4
CH3-CO-O-CH2-CH2-O-CH[O.]-CH3 -> CH3. + CH3-CO-O-CH2-CH2-O-CHO	-4.81	2.0e+14	11.92	3.6e+5	k(O2)	9.3	3.9e+4	30 [f]	11.9	0.0
CH3-CH[O.]-O-CH2-CH2-OH -> CH3. + HCO-O-CH2-CH2-OH	-4.81	2.0e+14	12.33	1.8e+5	k(O2)	4.62	3.9e+4	16 [f]	11.9	-0.4
Reactions forming CH3-CH2. and CH3-CH2-CH2.										
CH3-CH2-CH[O.]-CH3 -> CH3-CHO + CH3-CH2.	6.94	2.0e+14	13.58	2.2e+4	k(O2)	0.56	3.9e+4	11 [f]	14.3	0.7
CH3-CH2-CH[O.]-CH2-CH3 -> CH3-CH2-CHO + CH3-CH2.	6.71	4.0e+14	13.92	2.5e+4	k(O2)	0.63	3.9e+4	18 [f]	14.2	0.3
CH3-CH2-CH2-CH[O.]-CH3 -> CH3-CH2-CH2. + CH3-CHO	6.13	2.0e+14	14.10	9.1e+3	k(NO)		-	[c]	13.9	-0.2
CH3-C[O.](CH3)-CH2-CH3 -> CH3-CO-CH3 + CH3-CH2.	4.06	2.0e+14	13.90	1.3e+4	k(NO)		-	[c]	13.0	-0.9
Reactions forming CH3-C[.](CH3)-CH3										
CH3-C(CH3)(CH2O.)-CH3 -> HCHO + CH3-C[.](CH3)-CH3	10.40	2.0e+14	11.16	1.3e+6	k(O2)	39	3.4e+4	6 [f]	11.2	0.0
Reactions forming alpha-Hydroxy Alkyl Radicals										
HO-CH2-CH2O. -> HO-CH2. + HCHO	11.79	2.0e+14	12.62	1.1e+5	k(O2)	3.59	3.1e+4	1 [f]	12.6	0.0
CH3-CH(CH3)-CH[O.]-CH2-OH -> CH3-CH(CHO)-CH3 + HO-CH2.	7.15	2.0e+14	11.48	7.6e+5	kd($R_2CH.$)	2.45	3.1e+5	20 [f]	10.6	-0.9
Reactions forming $CH_3C(O)CH_2$. Radicals										
CH3-CO-CH2-CH[O.]-CH3 -> CH3-CHO + CH3-CO-CH2.	3.86	2.0e+14	12.38	1.7e+5	k(O2)	4.26	3.9e+4	19 [f]	12.9	0.6
Reactions forming Alkoxy Radicals										
CH3-C[O.](CH3)-O-CH3 -> CH3-CO-CH3 + CH3O.	9.50	2.0e+14	11.90	3.7e+5	kd(CH3.)	0.15	2.5e+6	36 [f]	12.6	0.7
CH3-CH(CH3)-CH2-O-C[O.](CH3)-CH3 -> CH3-CH(CH2O.)-CH3 + CH3-CO-CH3	9.29	2.0e+14	11.69	5.4e+5	kd(CH3.)	0.21	2.5e+6	46 [f]	12.5	0.8
CH3-C[O.](CH3)-O-CH2-CH3 -> CH3-CH2O. + CH3-CO-CH3	9.28	2.0e+14	11.26	1.1e+6	kd(CH3.)	0.44	2.5e+6	39 [f]	12.5	1.3
Reactions forming R-CO-O. Radicals										
CH3-C[O.](CH3)-O-CO-CH3 -> CH3-CO-CH3 + CH3-CO2.	10.73	2.0e+14	16.72	1.1e+2?	kd(CH3.)	0.32	3.5e+2?	41 [f]	16.7	0.0

[a] Data from Table 33 unless noted otherwise. Rate constants and A factors in units of sec-1, and Ea;s and heats of reaction are in units of kcal/mole. Underlined Ea from references, otherwise Ea's computed from tabiuated k(298) and A. These parameters are explicitly assigned for this radical in the mechanism generation system, unless indicated otherwise.

[b] k(ref) for O_2 reaction is $k(O_2)[O_2]$ for $[O_2] = 5.16 \times 10^{18}$ molec cm^{-3} at 1 atm and 298K.

[c] Atkinson (1997b). Relative to $k(RO+NO) = 2.3 \times 10^{-11} \exp(150/T)$.

[d] High pressure limit. Batt and Robinson (1987) calculate that rate constant under atmospheric conditions is ~80% of this. However, to fit chamber data, the A factor for atmospheric modeling is increased to from 6.0 to 7.5×10^{14} sec-1.

[e] Not used when computing best fit parameters for reactions forming methyl radicals. No explicit assignments made for this radical.

[f] Number is the radical number on Table 33 from which the data are taken. See footnotes to that table for documentation.

Table 33. Experimental and estimated branching ratios for radicals where relevant data are available.

Radical [a] Reaction	Type	DH_r (kcal)	Estimated [b] k (s^{-1})	%	Expt. Branching [c] Min	Exp'd	Max	Fit [d]	k Ratios [e] Expt	Calc
1 HO-CH2-CH2O.									kd/kO2	
HO-CH2-CH2O. + O2 -> HO2. + HCO-CH2-OH	O2	-30.6	3.10e+4	22%	15%	22%	30%	ok		
HO-CH2-CH2O. -> HO-CH2. + HCHO	D	11.8	1.11e+5	78%	70%	78%	85%	ok	3.59	3.59
Based on product data for ethene, as recommended by Atkinson (1997a).										
2 CH3-CO-CH2O.										
CH3-CO-CH2O. + O2 -> CH3-CO-CHO + HO2.	O2	-26.9	1.01e+4	0%	0%		25%	ok		
CH3-CO-CH2O. -> HCHO + CH3-CO.	D	2.6	1.74e+9	0%	75%	100%	100%	Low		
Based on data of Jenkin et al (1993) indicating that decomposition dominates.										
3 CH3-CO-O-CH2O.										
CH3-CO-O-CH2O. + O2 -> CH3-CO-O-CHO + HO2.	O2	-30.1	2.70e+4	65%	55%	65%	75%	ok	k(estr)/kO2	
CH3-CO-O-CH2O. -> CH3-CO-OH + HCO.	Estr	-3.0	1.46e+4	35%	25%	35%	45%	ok	0.54	0.54
Based on product yields for OH + methyl acetate (Christensen et al, 2000).										
4 CH3-O-CH2-O-CH2O.										
CH3-O-CH2-O-CH2O. + O2 -> HO2. + CH3-O-CH2-O-CHO	O2	-46.6	1.58e+5	96%	75%	100%	100%	ok		
CH3-O-CH2-O-CH2O. -> CH3-O-CH2O. + HCHO	D	13.3	6.50e+3	4%	0%	0%	25%	ok		
The observed products from OH + dimethoxy methane given by Sidebottom et al (1997), which are consistent with the data of Wallington et al (1997), include CH3-O-CH2-O-CHO, and account for essentially all the reaction. This means that decomposition must not be important.										
5 CH3-CH2-O-CO-CH2O.										
CH3-CH2-O-CO-CH2O. + O2 -> CH3-CH2-O-CO-CHO + HO2.	O2	-23.3	3.23e+3	14%	30%	75%	100%	Low		
CH3-CH2-O-CO-CH2O. -> HCHO + CH3-CH2-O-CO.	D	13.5	1.39e+1	0%	0%	0%	70%	ok		
CH3-CH2-O-CO-CH2O. -> CH3-CH[.]-O-CO-CH2-OH	I(O)		1.99e+4	86%	0%	25%	70%	High		
The most reasonable explanation for the observation of ~25% of CH3-CH2-O-CO-CHO from ethyl 3-ethoxypropionate (Baxley et al, 1997) is to assume that this radical reacts with O_2 to a significant extent. This radical is predicted to be formed ~33% of the time.										
6 CH3-C(CH3)(CH2O.)-CH3									kd/kO2	
CH3-C(CH3)(CH2O.)-CH3 + O2 -> CH3-C(CH3)(CHO)-CH3 + HO2.	O2	-30.8	3.35e+4	3%	0%	3%	5%	ok		
CH3-C(CH3)(CH2O.)-CH3 -> HCHO + CH3-C[.](CH3)-CH3	D	10.4	1.31e+6	98%	75%	98%	100%	ok	39	39
Based on data summarized by Atkinson (1997b)										
7 CH3-C(CH3)(CH3)-O-CH2O.										
CH3-C(CH3)(CH3)O-CH2O. + O2 -> CH3-C(CH3)(CH3)O-CHO + HO2.	O2	-46.6	1.58e+5	97%	65%	95%	100%	ok		
CH3-C(CH3)(CH3)O-CH2O. -> CH3-C[O.](CH3)CH3 + HCHO	D	14.3	3.09e+3	2%	0%	0%	25%	ok		
CH3-C(CH3)(CH3)O-CH2O. -> CH3-C(CH3)(CH2.)O-CH2-OH	I(O)		1.59e+3	1%	0%	0%	25%	ok		
Based on observation of t-butyl formate as the major product from MTBE (Tuazon et al, 1991b; Smith et al, 1991).										
8 CH3-CH(CH2O.)-O-CO-CH3										
CH3-CH(CH2O.)-O-CO-CH3 + O2 -> HO2. + CH3-CH(CHO)-O-CO-CH3	O2	-30.8	3.37e+4	41%	0%	0%	75%	ok		
CH3-CH(CH2O.)-O-CO-CH3 -> CH3-CO-O-CH[.]-CH3 + HCHO	D	12.8	4.93e+4	59%	25%	100%	100%	ok		
Necessary to assume decomposition is non-negligible to explain observation of acetic acid as a 9% product from isopropyl acetate (Tuazon et al, 1998b).										
9 CH3-CH[O.]-CH2-OH										
CH3-CH[O.]-CH2-OH + O2 -> HO2. + CH3-CO-CH2-O	O2	-34.6	2.68e+4	1%						
CH3-CH[O.]-CH2-OH -> HO-CH2. + CH3-CHO	D	6.6	5.19e+6	99%	85%	100%	100%	ok		
Based on product data for propene, as discussed by Atkinson (1997a).										

Table 33 (continued)

Radical [a] Reaction	Type	DH_r (kcal)	Estimated [b] k (s^{-1})	%	Expt. Branching [c] Min	Exp'd	Max	Fit [d]	k Ratios [e] Expt	Calc
10 CH3-O-CH[O.]-O-CH3										
CH3-O-CH[O.]-O-CH3 + O2 -> CH3-O-CO-O-CH3 + HO2.	O2	-53.3	3.94e+4	0%	50%	84%	95%	Low	kd/kO2	
CH3-O-CH[O.]-O-CH3 -> CH3-O-CHO + CH3O.	D	-1.7	9.07e+8	100%	0%	16%	50%	High	0.2	2e+4
Based on CH3-O-CHO / CH3-O-CO-O-CH3 yield ratios from dimethoxy methane (Sidebottom et al, 1997), assuming they are both formed from the CH3-O-CH[O.]-CH3 radical.										
11 CH3-CH2-CH[O.]-CH3										
CH3-CH2-CH[O.]-CH3 + O2 -> CH3-CH2-CO-CH3	O2	-36.0	3.94e+4	86%	46%	64%	76%	High	kd/kO2	
CH3-CH2-CH[O.]-CH3 -> CH3-CHO + CH3-CH2.	D	6.9	6.46e+3	14%	24%	36%	54%	Low	0.56	0.16
CH3-CH2-CH[O.]-CH3 -> CH3-CH2-CHO + CH3.	D	7.6	3.43e+1	0%						
Average of rate constant ratios reported by Carter et al (1979) and Cox et al (1981) as given by Atkinson (1997b).										
12 CH3-CH(OH)-CH[O.]-CH3										
CH3-CH(OH)-CH[O.]-CH3 + O2 -> CH3-CH(OH)-CO-CH3 + HO2	O2	-34.8	2.91e+4	0%	0%	0%	0%	ok		
CH3-CH(OH)-CH[O.]-CH3 -> CH3-CHO + CH3-CH[.]-OH	D	2.9	2.56e+9	100%	100%	100%	100%	ok		
CH3-CH(OH)-CH[O.]-CH3 -> CH3-CH(OH)-CHO + CH3.	D	9.1	1.18e+1	0%						
Based on upper limit yields of hydroxy carbonyls from OH + trans-2-butene (Atkinson, personal communication, 1999). Similar results were obtained from OH + trans-3-hexene.										
13 CH3-CH2-O-CH[O.]-CH3										
CH3-CH2-O-CH[O.]-CH3 + O2 -> CH3-CH2-O-CO-CH3 + HO2.	O2	-49.4	3.94e+4	8%	0%	5%	10%	ok		
CH3-CH2-O-CH[O.]-CH3 -> CH3-CH2O. + CH3-CHO	D	10.1	7.44e+4	16%	0%	0%	15%	High	kd/kO2	
CH3-CH2-O-CH[O.]-CH3 -> CH3-CH2-O-CHO + CH3.	D	-4.8	3.54e+5	76%	60%	95%	100%	ok	19.00	8.99
CH3-CH2-O-CH[O.]-CH3 -> CH3-CH(OH)O-CH2-CH2.	I(O)		5.31e+2	0%	0%	0%	25%	ok		
Based on ethyl formate from diethyl ether in 92% (Wallington and Japar, 1991) or 66% (Eberhard et al, 1993) yields and ethyl acetate in 4% yield (Eberhard et al, 1993) Average of yields for ethyl formate used in computing yield ratio. (Acetaldehyde also observed, but could be formed in other ways)										
14 CH3-CO-O-CH[O.]-CH3										
CH3-CO-O-CH[O.]-CH3 + O2 -> CH3-CO-O-CO-CH3 + HO2.	O2	-32.9	1.61e+4	4%	0%	0%	10%	ok		
CH3-CO-O-CH[O.]-CH3 -> CH3-CH(OH)-O-CO-CH2.	I(OCO)		6.72e+1	0%	0%	0%	10%	ok		
CH3-CO-O-CH[O.]-CH3 -> CH3-CO-OH + CH3-CO.	Estr	-8.4	3.54e+5	96%	95%	100%	100%	ok		
Product data from Tuazon et al (1998b) on OH + ethyl acetate indicates that the ester rearrangement must dominate in this reaction.										
15 CH3-CH(OH)-CH[O.]-O-CH3										
CH3-CH(OH)-CH[O.]-O-CH3 + O2 -> HO2. + CH3-CH(OH)-CO-O-CH3	O2	-48.5	3.94e+4	0%	0%	0%	15%	ok		
CH3-CH(OH)-CH[O.]-O-CH3 -> CH3-CH[.]-OH + CH3-O-CHO	D	-9.8	3.14e+13	100%	80%	100%	100%	ok		
CH3-CH(OH)-CH[O.]-O-CH3 -> CH3O. + CH3-CH(OH)-CHO	D	11.5	2.57e+4	0%	0%	0%	15%	ok		
Based on observation of 59% yield of methyl formate and 56% yield of acetaldehyde from 1-methoxy-2-propanol (Tuazon et al, 1998a). This radical is predicted to be formed ~55% of the time, and the observed products account for ~98% of the overall reaction.										
16 CH3-CH[O.]-O-CH2-CH2-OH										
CH3-CH[O.]-O-CH2-CH2-OH + O2 -> HO2. + CH3-CO-O-CH2-CH2-OH	O2	-49.4	3.94e+4	7%	5%	18%	30%	ok	kd/kO2	
CH3-CH[O.]-O-CH2-CH2-OH -> CH3. + HCO-O-CH2-CH2-OH	D	-4.8	3.54e+5	64%	70%	82%	100%	Low	4.62	8.99
CH3-CH[O.]-O-CH2-CH2-OH -> HO-CH2-CH2O. + CH3-CHO	D	10.1	7.39e+4	13%	0%	0%	25%	ok		
CH3-CH[O.]-O-CH2-CH2-OH -> CH3-CH(OH)-O-CH2-CH[.]-OH	I(O)		8.80e+4	16%	0%	0%	25%	ok		

Table 33 (continued)

Radical [a] Reaction	Type	DH_r (kcal)	Estimated [b] k (s^{-1})	%	Expt. Branching [c] Min	Exp'd	Max	Fit [d]	k Ratios [e] Expt	Calc
Based on the observed formation of 36% HO-CH2-CH2-O-CHO and 8% CH3-CO-O-CH2-CH2-OH from 2-ethoxy ethanol (Stemmler et al, 1996). This radical is predicted to be formed ~36% of the time. The observed products account for essentially all the reaction.										
17 CH3-CH2-O-CH[O.]-CH2-OH										
CH3-CH2-O-CH[O.]-CH2-OH + O2 -> HO2. + CH3-CH2-O-CO-CH2-OH	O2	-48.3	3.94e+4	0%	0%	0%	25%	ok		
CH3-CH2-O-CH[O.]-CH2-OH -> CH3-CH2O. + HCO-CH2-OH	D	11.5	2.48e+4	0%	0%	0%	25%	ok		
CH3-CH2-O-CH[O.]-CH2-OH -> HO-CH2. + CH3-CH2-O-CHO	D	-6.1	6.36e+10	100%	75%	100%	100%	ok		
Based on the observed formation of ~43% ethyl formate from 2-ethoxy ethanol (Stemmler et al, 1996). This radical is predicted to be formed ~36% of the time. The observed products account for essentially all the reaction.										
18 CH3-CH2-CH[O.]-CH2-CH3										
CH3-CH2-CH[O.]-CH2-CH3 + O2 -> CH3-CH2-CO-CH2-CH3 + HO2.	O2	-36.3	3.94e+4	72%	42%	61%	74%	ok	kd/kO2	
CH3-CH2-CH[O.]-CH2-CH3 -> CH3-CH2-CHO + CH3-CH2.	D	6.7	1.53e+4	28%	26%	39%	58%	ok	0.63	0.39
Based on data of Atkinson et al (1995).										
19 CH3-CO-CH2-CH[O.]-CH3										
CH3-CO-CH2-CH[O.]-CH3 + O2 -> CH3-CO-CH2-CO-CH3 + HO2.	O2	-38.1	3.94e+4	38%	10%	19%	30%	High	kd/kO2	
CH3-CO-CH2-CH[O.]-CH3 -> CH3-CHO + CH3-CO-CH2.	D	3.9	6.37e+4	62%	70%	81%	90%	Low	4.3	1.6
CH3-CO-CH2-CH[O.]-CH3 -> CH3-CO-CH2-CHO + CH3.	D	5.8	1.35e+2	0%	0%	0%	10%	ok		
CH3-CO-CH2-CH[O.]-CH3 -> CH3-CH(OH)-CH2-CO-CH2.	I(CO)		2.53e+2	0%	0%	0%	10%	ok		
Based on ratios of acetaldehyde to 2,4-pentadione yields from OH + 2-pentanone (Atkinson et al, 2000b).										
20 CH3-CH(CH3)-CH[O.]-CH2-OH										
CH3-CH(CH3)-CH[O.]-CH2-OH + O2 -> CH3-CH(CH3)-CO-CH2-OH + HO2	O2	-34.4	2.52e+4	1%	0%	0%	10%	ok	kd/kd(R2CH.)	
CH3-CH(CH3)-CH[O.]-CH2-OH -> HCO-CH2-OH + CH3-CH[.]-CH3	D	8.1	3.11e+5	8%	15%	29%	50%	Low	2.45	11.26
CH3-CH(CH3)-CH[O.]-CH2-OH -> CH3-CH(CHO)-CH3 + HO-CH2.	D	7.2	3.50e+6	91%	50%	71%	90%	High		
Based on yields of 2-methyl propanal, acetone, and glycolaldehyde from OH + 3-methyl-1-butene (Atkinson et al, 1998), assuming that OH addition occurs an estimated ~65% of the time at the 1-position relative to total OH addition.										
21 CH3-CH2-CH2-CH[O.]-O-CH3										
CH3-CH2-CH2-CH[O.]-O-CH3 + O2 -> HO2. + CH3-CH2-CH2-CO-O-CH3	O2	-49.7	3.94e+4	0%	0%	0%	30%	ok		
CH3-CH2-CH2-CH[O.]-O-CH3 -> CH3-CH2-CH2. + CH3-O-CHO	D	-6.5	1.45e+8	100%	50%	66%	100%	ok		
CH3-CH2-CH2-CH[O.]-O-CH3 -> CH3O. + CH3-CH2-CH2-CHO	D	10.3	6.04e+4	0%	0%	0%	30%	ok		
CH3-CH2-CH2-CH[O.]-O-CH3 -> CH3-O-CH(OH)-CH2-CH2-CH2.	I		1.96e+5	0%	0%	0%	30%	ok		
Based on observations of 43% propionaldehyde and 51% methyl formate from methyl n-butyl ether (Aschmann and Atkinson, 1999). This radical is predicted to be formed ~71% of the time. The observed products account for ~70% of the reaction.										
22 CH3-CH(CH3)-O-CH[O.]-CH2-OH										
CH3-CH(CH3)-O-CH[O.]-CH2-OH + O2 -> HO2. + CH3-CH(CH3)-O-CO-CH2-OH	O2	-48.3	3.94e+4	0%	0%	0%	15%	ok		
CH3-CH(CH3)-O-CH[O.]-CH2-OH -> CH3-CH[O.]-CH3 + HCO-CH2-OH	D	12.4	1.36e+4	0%	0%	0%	15%	ok		
CH3-CH(CH3)-O-CH[O.]-CH2-OH -> HO-CH2. + CH3-CH(CH3)-O-CHO	D	-6.1	6.36e+10	100%	80%	100%	100%	ok		
CH3-CH(CH3)-O-CH[O.]-CH2-OH -> CH3-CH(CH2.)-O-CH(OH)-CH2-OH	I(O)		1.06e+3	0%	0%	0%	15%	ok		
Based on formation of 57% isopropyl formate from 2-isopropoxy ethanol (Aschmann and Atkinson, 1999). This radical is predicted to be formed ~30% of the time, and the observed products account for essentially all the reaction routes.										
23 CH3-C(CH3)(CH3)-O-CH[O.]-CH3										
CH3-C(CH3)(CH3)O-CH[O.]-CH3 + O2 -> CH3-C(CH3)(CH3)O-CO-CH3 + HO2.	O2	-49.4	3.94e+4	9%	0%	17%	25%	ok		

Table 33 (continued)

Radical [a] Reaction	Type	DH_r (kcal)	Estimated [b] k (s^{-1})	%	Expt. Branching [c] Min	Exp'd	Max	Fit [d]	k Ratios [e] Expt	Calc
CH3-C(CH3)(CH3)-O-CH[O.]-CH3 -> CH3-C[O.](CH3)-CH3 + CH3-CHO	D	11.1	3.51e+4	8%	0%	0%	20%	ok	kd/kO2	
CH3-C(CH3)(CH3)-O-CH[O.]-CH3 -> CH3. + CH3-C(CH3)(CH3)-O-CHO	D	-4.8	3.54e+5	82%	70%	83%	100%	ok	3.3	9.0
CH3-C(CH3)(CH3)O-CH[O.]-CH3 -> CH3-C(CH3)(CH2.)O-CH(OH)CH3	I(O)		1.59e+3	0%	0%	0%	20%	ok		
Based on observed t-butyl formate and t-butyl acetate yields from ETBE (Smith et al, 1992).										
24 CH3-CH2-CH[O.]-CH2-O-CO-CH3										
CH3-CH2-CH[O.]-CH2-O-CO-CH3 + O2 -> HO2. + CH3-CH2-CO-CH2-O-CO-CH3	O2	-34.8	2.91e+4	89%	25%	50%	100%	ok		
CH3-CH2-CH[O.]-CH2-O-CO-CH3 -> CH3-CH2. + CH3-CO-O-CH2-CHO	D	8.4	2.15e+3	7%	0%		75%	ok		
CH3-CH2-CH[O.]-CH2-O-CO-CH3 -> CH3-CO-O-CH2. + CH3-CH2-CHO	D	8.8	1.57e+3	5%	0%		75%	ok		
Based on observed formation of ~15% CH3-CH2-CO-CH2-O-CO-CH3 from n-butyl acetate (Veillerot et al. 1995). This radical predicted to be formed ~30% of the time. Only ~30% of the reaction route are accounted for, and the yields are only approximate.										
25 CH3-CO-O-CH2-CH2-CH[O.]-CH3										
CH3-CO-O-CH2-CH2-CH[O.]-CH3 + O2 -> HO2. + CH3-CO-CH2-CH2-O-CO-CH3	O2	-36.0	3.94e+4	62%	25%	65%	100%	ok		
CH3-CO-O-CH2-CH2-CH[O.]-CH3 -> CH3-CO-O-CH2-CH2. + CH3-CHO	D	5.2	2.41e+4	38%	0%	35%	75%	ok		
CH3-CO-O-CH2-CH2-CH[O.]-CH3 -> CH3. + CH3-CO-O-CH2-CH2-CHO	D	7.9	2.76e+1	0%	0%		75%			
Based on observed formation of ~15% CH3-CO-CH2-CH2-O-CO-CH3 from n-butyl acetate (Veillerot et al. 1995). This radical predicted to be formed ~23% of the time. Only ~30% of the reaction route are accounted for, and the yields are only approxmiate.										
26 CH3-CH2-CH2-CH[O.]-O-CO-CH3										
CH3-CH2-CH2-CH[O.]-O-CO-CH3 + O2 -> CH3-CH2-CH2-CO-O-CO-CH3 + HO2.	O2	-33.2	1.75e+4	3%	0%	0%	65%	ok		
CH3-CH2-CH2-CH[O.]-O-CO-CH3 -> CH3-CO-O-CHO + CH3-CH2-CH2.	D [e]	10.0	2.01e+4	4%	0%	0%	65%	ok		
CH3-CH2-CH2-CH[O.]-O-CO-CH3 -> CH3-CH2-CH2-CHO + CH3-CO2.	D	11.6	5.85e+1	0%	0%	0%	65%	ok		
CH3-CH2-CH2-CH[O.]-O-CO-CH3 -> CH3-CO-O-CH(OH)-CH2-CH2-CH2.	I		1.96e+5	36%	35%	100%	100%	ok		
CH3-CH2-CH2-CH[O.]-O-CO-CH3 -> CH3-CO-OH + CH3-CH2-CH2-CO.	Estr	-8.1	3.07e+5	57%	0%	0%	65%	ok		
CH3-CH2-CH2-CH[O.]-O-CO-CH3 -> CH3-CH2-CH2-CH(OH)-O-CO-CH2.	I(OCO)		6.72e+1	0%	0%	0%	65%	ok		
Environmental chamber reactivity data for n-butyl acetate can only be fit by model simulations if it is assumed that the isomerization reaction occurs a significant fraction of the time..										
27 CH3-CH2-CH2-CH[O.]-O-CH2-CH2-OH										
CH3-CH2-CH2-CH[O.]-O-CH2-CH2-OH + O2 -> HO2. + CH3-CH2-CH2-CO-O-CH2-CH2-OH	O2	-49.7	3.94e+4	0%	0%	0%	25%	ok		
CH3-CH2-CH2-CH[O.]-O-CH2-CH2-OH -> CH3-CH2-CH2. + HCO-O-CH2-CH2-OH	D	-6.5	1.45e+8	100%	50%	100%	100%	ok		
CH3-CH2-CH2-CH[O.]-O-CH2-CH2-OH -> HO-CH2-CH2O. + CH3-CH2-CH2-CHO	D	10.1	7.06e+4	0%	0%	0%	25%	ok		
CH3-CH2-CH2-CH[O.]-O-CH2-CH2-OH -> HO-CH2-CH2-O-CH(OH)-CH2-CH2-CH2.	I		1.96e+5	0%	0%	0%	25%	ok		
CH3-CH2-CH2-CH[O.]-O-CH2-CH2-OH -> CH3-CH2-CH2-CH(OH)-O-CH2-CH[.]-OH	I(O)		8.80e+4	0%	0%	0%	25%	ok		
Based on observations of propionaldehyde and HO-CH2-CH2-O-CHO in ~20% yields from 2-butoxy ethanol by Tuazon et al. (1998), with somewhat higher yields observed by Stemmler et al. (1997b). This radical is believed to be formed ~20% of the time.										
28 CH3-CH2-CH2-CH2-O-CH[O.]-CH2-OH										
CH3-CH2-CH2-CH2-O-CH[O.]-CH2-OH + O2 -> HO2. + CH3-CH2-CH2-CH2-O-CO-CH2-OH	O2	-48.3	3.94e+4	0%	0%	0%	25%	ok		
CH3-CH2-CH2-CH2-O-CH[O.]-CH2-OH -> CH3-CH2-CH2-CH2O. + HCO-CH2-OH	D	11.6	2.46e+4	0%	0%	0%	25%	ok		
CH3-CH2-CH2-CH2-O-CH[O.]-CH2-OH -> HO-CH2. + CH3-CH2-CH2-CH2-O-CHO	D	-6.1	6.36e+10	100%	80%	100%	100%	ok		
CH3-CH2-CH2-CH2-O-CH[O.]-CH2-OH -> CH3-CH2-CH[.]-CH2-O-CH(OH)-CH2-OH	I(O)		1.83e+4	0%	0%	0%	25%	ok		

Table 33 (continued)

Radical [a] Reaction	Type	DH_r (kcal)	Estimated [b] k (s^{-1})	%	Expt. Branching [c] Min	Exp'd	Max	Fit [d]	k Ratios [e] Expt	Calc
Based on observations of n-butyl formate from 2-butoxy ethanol with yields of 57% (Tuazon et al, 1998) or ~35% (Stemmler et al., 1997b). This radical is believed to be formed ~50% of the time.										
29 CH3-CH2-O-CH[O.]-CH2-O-CO-CH3										
CH3-CH2-O-CH[O.]-CH2-O-CO-CH3 + O2 -> HO2. + CH3-CH2-O-CO-CH2-O-CO-CH3	O2	-48.3	3.94e+4	0%	0%	0%	30%	ok		
CH3-CH2-O-CH[O.]-CH2-O-CO-CH3 -> CH3-CH2O. + CH3-CO-O-CH2-CHO	D	11.5	2.48e+4	0%	0%	0%	30%	ok		
CH3-CH2-O-CH[O.]-CH2-O-CO-CH3 -> CH3-CO-O-CH2. + CH3-CH2-O-CHO	D	-3.6	1.63e+7	100%	50%	90%	100%	ok		
CH3-CH2-O-CH[O.]-CH2-O-CO-CH3 -> CH3-CO-O-CH2-CH(OH)-O-CH2-CH2.	I(OCO)		5.31e+2	0%	0%	0%	30%	ok		
Based on observed yield of ethyl formate (33%) from 2-ethoxyethyl acetate (Wells et al., 1996). This is somewhat lower than the predicted 44% formation for this radical, but within the uncertainty of the estimate.										
30 CH3-CO-O-CH2-CH2-O-CH[O.]-CH3										
CH3-CO-O-CH2-CH2-O-CH[O.]-CH3 + O2 -> HO2. + CH3-CO-O-CH2-CH2-O-CO-CH3	O2	-49.4	3.94e+4	8%	5%	10%	25%	ok		
CH3-CO-O-CH2-CH2-O-CH[O.]-CH3 -> CH3-CO-O-CH2-CH2O. + CH3-CHO	D	10.1	7.39e+4	15%	0%	0%	25%	ok	kd/kO2	
CH3-CO-O-CH2-CH2-O-CH[O.]-CH3 -> CH3. + CH3-CO-O-CH2-CH2-O-CHO	D	-4.8	3.54e+5	72%	50%	90%	100%	ok	9.3	9.0
CH3-CO-O-CH2-CH2-O-CH[O.]-CH3 -> CH3-CH(OH)-O-CH2-CH[.]-O-CO-CH3	I(O)		2.72e+4	6%	0%	0%	25%	ok		
Based on yields of CH3-CO-O-CH2-CH2-O-CHO (37%) and CH3-CO-O-CH2-CH2-O-CO-CH3 (4%) from 2-ethoxyethyl acetate (Wells et al, 1996). This radical is predicted to be formed ~36% of the time, which is consistent with these product yields.										
31 CH3-CH(CH3)-O-CH[O.]-CH(CH3)-CH3										
CH3-CH(CH3)-O-CH[O.]-CH(CH3)-CH3 + O2 -> HO2. + CH3-CH(CH3)-O-CO-CH(CH3)-CH3	O2	-49.2	3.94e+4	0%	0%	0%	25%	ok		
CH3-CH(CH3)-O-CH[O.]-CH(CH3)-CH3 -> CH3-CH[O.]-CH3 + CH3-CH(CHO)-CH3	D	11.4	2.75e+4	0%	0%	0%	25%	ok		
CH3-CH(CH3)-O-CH[O.]-CH(CH3)-CH3 -> CH3-CH[.]-CH3 + CH3-CH(CH3)-O-CHO	D	-6.1	1.14e+10	100%	50%	100%	100%	ok		
CH3-CH(CH3)-O-CH[O.]-CH(CH3)-CH3 -> CH3-CH(CH3)-CH(OH)-O-CH(CH2.)-CH3	I(O)		5.31e+2	0%	0%	0%	25%	ok		
Based on observation of 48% yield of t-butyl formate from isobutyl isopropyl ether (Stemmler et al, 1997a). This radical is predicted to be formed ~33% of the time.										
32 CH3-CH2-O-CO-CH2-CH[O.]-O-CH2-CH3										
CH3-CH2-O-CO-CH2-CH[O.]-O-CH2-CH3 + O2 -> HO2. + CH3-CH2-O-CO-CH2-CO-O-CH2-CH3	O2	-51.8	3.94e+4	0%	0%	0%	20%	ok		
CH3-CH2-O-CO-CH2-CH[O.]-O-CH2-CH3 -> CH3-CH2-O-CO-CH2. + CH3-CH2-O-CHO	D	-5.8	8.34e+7	100%	50%	84%	100%	ok		
CH3-CH2-O-CO-CH2-CH[O.]-O-CH2-CH3 -> CH3-CH2O. + CH3-CH2-O-CO-CH2-CHO	D	8.0	3.46e+5	0%	0%	16%	20%	ok		
CH3-CH2-O-CO-CH2-CH[O.]-O-CH2-CH3 -> CH3-CH2-O-CO-CH2-CH(OH)-O-CH2-CH2.	I(O)		5.31e+2	0%	0%	0%	20%	ok		
Based on yield ratios for ethyl formate and CH3-CH2-O-CO-CH2-CHO from ethyl 3-ethoxypropionate (Baxley et al, 1997). Total yield is ~42%, while predicted amount of this radical formed is ~50%.										
33 CH3-CH2-O-CO-CH2-CH2-O-CH[O.]-CH3										
CH3-CH2-O-CO-CH2-CH2-O-CH[O.]-CH3 + O2 -> HO2. + CH3-CH2-O-CO-CH2-CH2-O-CO-CH3	O2	-49.4	3.94e+4	8%	0%	0%	50%	ok		
CH3-CH2-O-CO-CH2-CH2-O-CH[O.]-CH3 -> CH3-CH2-O-CO-CH2-CH2O. + CH3-CHO	D	10.1	7.39e+4	16%	0%	0%	50%	ok		
CH3-CH2-O-CO-CH2-CH2-O-CH[O.]-CH3 -> CH3. + CH3-CH2-O-CO-CH2-CH2-O-CHO	D	-4.8	3.54e+5	75%	50%	75%	100%	ok		
CH3-CH2-O-CO-CH2-CH2-O-CH[O.]-CH3 -> CH3-CH(OH)-O-CH2-CH[.]-CO-O-CH2-CH3	I(O)		2.32e+3	0%	0%	0%	50%	ok		
Based on formation of 30% CH3-CH2-O-CO-CH2-CH2-O-CHO from ethyl 3-ethoxypropionate (Baxley et al, 1977). Note that this radical is predicted to be formed 40% of the time, so the observed yield is higher than maximum predicted.										
34 CH3-O-CO-CH2-CH[O.]-CH2-CO-O-CH3										
CH3-O-CO-CH2-CH[O.]-CH2-CO-O-CH3 + O2 -> CH3-O-CO-CH2-CO-CH2-CO-O-CH3 + HO2.	O2	-40.5	3.94e+4	38%	90%	100%	100%	Low		

Table 33 (continued)

Radical [a] / Reaction	Type	DH_r (kcal)	Estimated [b] k (s^{-1})	%	Expt. Branching [c] Min	Exp'd	Max	Fit [d]	k Ratios [e] Expt	Calc
CH3-O-CO-CH2-CH[O.]-CH2-CO-O-CH3 -> CH3-O-CO-CH2-CHO + CH3-O-CO-CH2.	D	4.8	6.34e+4	62%	0%	0%	10%	High		
Necessary to assume that reaction with O2 dominates for model simulations of dimethyl glutarate (DBE-5) chamber experiments. The observation of CH3-O-CO-CH2-CO-CH2-CO-O-CH3 as a product of the OH + DBE-5 reaction (Tuazon et al, 1999) also indicates that the O2 reaction is important.										
35 CH3-O-CO-CH2-CH2-CH[O.]-CO-O-CH3										
CH3-O-CO-CH2-CH2-CH[O.]-CO-O-CH3 + O2 -> CH3-O-CO-CH2-CH2-CO-CO-O-CH3 + HO2.	O2	-28.1	3.57e+3	77%	0%	10%	10%	High		
CH3-O-CO-CH2-CH2-CH[O.]-CO-O-CH3 -> CH3-O-CO-CHO + CH3-O-CO-CH2-CH2.	D	15.0	1.67e+1	0%	0%	0%	10%	ok		
CH3-O-CO-CH2-CH2-CH[O.]-CO-O-CH3 -> CH3-O-CO-CH2-CH2-CHO + CH3-O-CO.	D	9.5	2.80e+2	6%	0%	0%	10%	ok		
CH3-O-CO-CH2-CH2-CH[O.]-CO-O-CH3 -> CH3-O-CO-CH2-CH2-CH(OH)-CO-O-CH2.	I(OCO)		7.88e+2	17%	80%	90%	100%	Low		
Isomerization is assumed to dominate by analogy with the assumptions made for CH3-O-CO-CH2-CH[O.]-CO-O-CH3 radicals. This also results in somewhat better fits of model simulations to dimethyl glutarate (DBE-5) reactivity experiments. Reaction with O2, predicted to be the major competing process, is arbitrarily assumed to occur ~10% of the time.										
36 CH3-C[O.](CH3)-O-CH3										
CH3-C[O.](CH3)-O-CH3 -> CH3-O-CO-CH3 + CH3.	D	-6.5	2.51e+6	96%	50%	87%	95%	High	kd/kd(CH_3)	
CH3-C[O.](CH3)-O-CH3 -> CH3-CO-CH3 + CH3O.	D	9.5	1.13e+5	4%	5%	13%	25%	Low	0.15	0.05
Based on ratios of methyl acetate to acetone yields from MTBE (Tuazon et al, 1991, Smith et al, 1991)										
37 CH3-C[O.](CHO)-CH2-OH										
CH3-C[O.](CHO)-CH2-OH -> HCO-CO-CH2-OH + CH3.	D	19.0	7.13e-3	0%	0%	0%	25%	ok		
CH3-C[O.](CHO)-CH2-OH -> CH3-CO-CH2-OH + HCO.	D	-0.7	1.53e+7	94%	75%	100%	100%			
CH3-C[O.](CHO)-CH2-OH -> CH3-CO-CHO + HO-CH2.	D	8.9	9.82e+5	6%	0%	0%	25%	ok		
Based on observations of hydroxyacetone as a major product in the reaction of OH with methacrolein (Tuazon and Atkinson, 1990). This and products from other radicals formed believed to account for all the reaction routes.										
38 *C[O.](CH3)-CH2-O-CO-O-*										
C[O.](CH3)-CH2-O-CO-O- -> *CH2-O-CO-O-CO-* + CH3.	D [e]	11.1	7.40e+1	0%	0%	0%	20%	ok		
C[O.](CH3)-CH2-O-CO-O- -> CH3-CO-O-CO-O-CH2.	D [e]	4.9	8.61e+5	99%	75%	100%	100%	ok		
C[O.](CH3)-CH2-O-CO-O- -> CH3-CO-CH2-O-CO2.	D	5.6	5.12e+3	1%	0%	0%	20%	ok		
Necessary to assume that the decomposition to CH3-CO-O-CO-O-CH2. dominates in order for model to fit results of propylene carbonate reactivity chamber experiments.										
39 CH3-C[O.](CH3)-O-CH2-CH3										
CH3-C[O.](CH3)-O-CH2-CH3 -> CH3. + CH3-CH2-O-CO-CH3	D	-6.5	2.51e+6	95%	0%	69%	100%	ok		
CH3-C[O.](CH3)-O-CH2-CH3 -> CH3-CH2O. + CH3-CO-CH3	D	9.3	1.33e+5	5%	0%	31%	100%	ok	0.44	0.05
CH3-C[O.](CH3)-O-CH2-CH3 -> CH3-C(CH3)(OH)-O-CH2-CH2.	I(O)		5.31e+2	0%						
Based on ratios of acetone and ethyl acetate yields from ETBE (Smith et al, 1992), assuming they are all formed from this radical, which is estimated to be formed 5% of the time. (Total yields of both are ~6%). This is uncertain.										
40 CH3-C[O.](CH3)-CO-O-CH3										
CH3-C[O.](CH3)-CO-O-CH3 -> CH3-O-CO-CO-CH3 + CH3.	D	12.2	1.16e+0	0%	0%	0%	50%	ok		
CH3-C[O.](CH3)-CO-O-CH3 -> CH3-CO-CH3 + CH3-O-CO.	D	5.7	4.62e+3	85%	50%	100%	100%	ok		
CH3-C[O.](CH3)-CO-O-CH3 -> CH3-C(CH3)(OH)-CO-O-CH2.	I(O)		7.88e+2	15%	0%	0%	50%	ok		
It is necessary to assume that the decomposition to CH3-O-CO. is a major route in order for model to simulate results of methyl isobutyrate reactivity experiments (Carter et al, 2000a).										

Table 33 (continued)

Radical [a] / Reaction	Type	DH_r (kcal)	Estimated [b] k (s^{-1})	%	Expt. Branching [c] Min	Exp'd	Max	Fit [d]	k Ratios [e] Expt	Calc
41 CH3-C[O.](CH3)-O-CO-CH3										
CH3-C[O.](CH3)-O-CO-CH3 -> CH3-CO-O-CO-CH3 + CH3.	D [e]	10.0	3.48e+2	66%	50%	76%	90%	ok	kd/kd(CH_3)	
CH3-C[O.](CH3)-O-CO-CH3 -> CH3-CO-CH3 + CH3-CO2.	D	10.7	1.09e+2	21%	10%	24%	50%	ok	0.32	0.31
CH3-C[O.](CH3)-O-CO-CH3 -> CH3-C(CH3)(OH)-O-CO-CH2.	I(OCO)		6.72e+1	13%	0%	0%	25%	ok		
Based on yields of acetone and acetic anhydride from isopropyl acetate and t-butyl acetate (Tuazon et al. 1998b).										
42 CH3-C[O.](CH3)-O-CH2-CH2-OH										
CH3-C[O.](CH3)-O-CH2-CH2-OH -> CH3. + CH3-CO-O-CH2-CH2-OH	D	-6.5	2.51e+6	92%	60%	90%	100%	ok		
CH3-C[O.](CH3)-O-CH2-CH2-OH -> HO-CH2-CH2O. + CH3-CO-CH3	D	9.3	1.32e+5	5%	0%	0%	20%	ok		
CH3-C[O.](CH3)-O-CH2-CH2-OH -> CH3-C(CH3)(OH)-O-CH2-CH[.]-OH	I(O)		8.80e+4	3%	0%	0%	20%	ok		
Based on formation of 44% CH3-CO-O-CH2-CH2-OH from 2-isopropoxy ethanol (Aschmann and Atkinson, 1999). This radical is predicted to be formed ~50% of the time, and the observed products account for essentially all the reaction routes.										
43 CH3-C[O.](CH3)-O-CO-O-CH3										
CH3-C[O.](CH3)-O-CO-O-CH3 -> CH3-O-CO-O-CO-CH3 + CH3.	D [e]	10.0	3.48e+2	74%	50%	75%	100%	ok		
CH3-C[O.](CH3)-O-CO-O-CH3 -> CH3-CO-CH3 + CH3-O-CO2.	D	10.6	1.21e+2	26%	0%	25%	50%	ok		
Necessary to assume decomposition forming acetone is slow to be consistent with acetone formation observed in methyl isopropyl carbonate environmental chamber experiments. This also results in somewhat better fits of the model to the data, without having to make large adjustments to the overall nitrate yield.										
44 CH3-CH(CH3)-O-C[O.](CH3)-CH3										
CH3-CH(CH3)-O-C[O.](CH3)-CH3 -> CH3-CH[O.]-CH3 + CH3-CO-CH3	D	10.1	7.28e+4	3%	0%		20%	ok		
CH3-CH(CH3)-O-C[O.](CH3)-CH3 -> CH3. + CH3-CH(CH3)-O-CO-CH3	D	-6.5	2.51e+6	97%	80%	100%	100%	ok		
CH3-CH(CH3)-O-C[O.](CH3)-CH3 -> CH3-C(CH3)(OH)-O-CH(CH2.)-CH3	I(O)		1.06e+3	0%	0%		20%	ok		
Based on observations of isopropyl acetate as major product (nearly 100% yield) from di-isopropyl acetate (Wallington et al, 1993).										
45 CH3-C(CH3)(CH3)-O-C[O.](CH3)-CH3										
CH3-C(CH3)(CH3)-O-C[O.](CH3)-CH3 -> CH3-C[O.](CH3)-CH3 + CH3-CO-CH3	D	10.3	6.27e+4	2%	0%	0%	20%	ok		
CH3-C(CH3)(CH3)-O-C[O.](CH3)-CH3 -> CH3. + CH3-C(CH3)(CH3)-O-CO-CH3	D	-6.5	2.51e+6	97%	75%	100%	100%	ok		
CH3-C(CH3)(CH3)-O-C[O.](CH3)-CH3 -> CH3-C(CH3)(CH2.)-O-C(CH3)(OH)-CH3	I(O)		1.59e+3	0%	0%	0%	20%	ok		
Based on observed 85% yield of isopropyl acetate from di-t-butyl ether (Langer et al, 1996).										
46 CH3-CH(CH3)-CH2-O-C[O.](CH3)-CH3										
CH3-CH(CH3)-CH2-O-C[O.](CH3)-CH3 -> CH3-CH(CH2O.)-CH3 + CH3-CO-CH3	D	9.3	1.32e+5	5%	0%	18%	40%	ok	kd/kd(CH_3)	
CH3-CH(CH3)-CH2-O-C[O.](CH3)-CH3 -> CH3. + CH3-CH(CH3)-CH2-O-CO-CH3	D	-6.5	2.51e+6	94%	40%	82%	100%	ok	0.21	0.05
CH3-CH(CH3)-CH2-O-C[O.](CH3)-CH3 -> CH3-C(CH3)(OH)-O-CH2-C[.](CH3)-CH3	I(O)		2.70e+4	1%	0%	0%	30%	ok		
Based on 6% yields of CH3-CH(CHO)-CH3 and 28% of CH3-CH(CH3)-CH2-O-CO-CH3 from isopropyl isobutyl ether (Stemmler et al, 1997a), assuming that the former is formed from subsequent reactions from this radical. This radical is predicted to be formed ~50% of the time.										
47 CH3-CH(CH3)-O-CH2-C[O.](CH3)-CH3										
CH3-CH(CH3)-O-CH2-C[O.](CH3)-CH3 -> CH3-CH(CH3)-O-CH2. + CH3-CO-CH3	D	3.7	6.96e+4	13%	0%	0%	25%	ok		
CH3-CH(CH3)-O-CH2-C[O.](CH3)-CH3 -> CH3. + CH3-CH(CH3)-O-CH2-CO-CH3	D	6.2	1.93e+2	0%	0%	0%	25%			
CH3-CH(CH3)-O-CH2-C[O.](CH3)-CH3 -> CH3-C(CH3)(OH)-CH2-O-C[.](CH3)-CH3	I(O)		4.81e+5	87%	75%	100%	100%	ok		
Based on observed formation of ~25% of CH3-C(CH3)(OH)-CH2-O-CO-CH3 from isobutyl isopropyl ether (Stemmler et al, 1997a), which can only be formed by the isomerization reaction. However, this radical is predicted to be formed only ~8% of the time.										

Table 33 (continued)

Radical [a] Reaction	Type	DH_r (kcal)	Estimated [b] k (s^{-1})	%	Expt. Branching [c] Min	Exp'd	Max	Fit [d]	k Ratios [e] Expt	Calc
48 CH3-C(CH3)(OH)-CH2-O-C[O.](CH3)-CH3										
CH3-C(CH3)(OH)-CH2-O-C[O.](CH3)-CH3 -> CH3-C(OH)(CH2O.)-CH3 + CH3-CO-CH3	D	9.3	1.32e+5	5%	0%	0%	25%	ok		
CH3-C(CH3)(OH)-CH2-O-C[O.](CH3)-CH3 -> CH3. + CH3-C(CH3)(OH)-CH2-O-CO-CH3	D	-6.5	2.51e+6	95%	75%	100%	100%	ok		
Based on observed formation of ~25% of CH3-C(CH3)(OH)-CH2-O-CO-CH3 from isobutyl isopropyl ether (Stemmler et al, 1997a), which can only be formed by this reaction. However, this radical is predicted to be formed only ~5% of the time.										

[a] Radicals are given in order of primary, secondary, and then tertiary. Within each type, radicals are sorted first by carbon number, then by molecular weight.

[b] Rate constants estimated for T=298K using recommended parameters as discussed in the text. Units are sec-1. Unimolecular rate constants for O2 reaction calculated assuming [O2] = 5.18 x 10-18 molec cm-3. "%" is the estimated percentage of the radical which reacts with this reaction.

[c] Minimum, expected, and maximum fractions for this reaction route relative to all reactions of this radical, based on analysis of the experimental data. Minimum and maximum values are subjective estimates. Underlined branching ratios are used for explicit estimates for this radical -- overriding the temperature-dependent rate constant estimates.

[d] "High" means that the estimated branching ratio is greater than the maximum value estimated from analysis of the experimental data; "Low" means that the estimated ratio is lower than the minimum; "ok" means that the estimated branching ratio lies between the minimum and maximum considered consistent with the experimental data.

[e] Rate constant ratios that can be used for quantitative rate constant estimates.

[f] The activation energy is reduced by 2 kcal/mole for reactions that form products with -CO-O-CO- groups. If this correction were not applied, the estimated rate constant would be a factor of ~30 lower.

radicals with a-O groups such as formed in photooxidations of ethers, which are exothermic by ~5 kcal/mole and tend to be much more rapid. Note that the rate constants for the latter are uncertain because of uncertainty in the estimates for the O_2 reaction used to place the experimental rate constant ratio on an absolute basis. It is possible that the O_2 reaction is significantly faster than estimated in this work, in which case these decompositions will also be faster.

Figure 8 shows plots of the estimated activation energy for selected decompositions reactions vs. the estimated heats of reaction. It can be seen that the data for reactions forming methyl radicals fall reasonably well on a straight line, if the point for the 2-methyl-2-butoxy radical, which seems to be somewhat inconsistent with the other data, is excluded. The least squares line (excluding the point for 2-methyl-2-butoxy) is

$$Ea \text{ (decomp. to CH3.)} = 14.05 + 0.44\ \Delta H_r \qquad \text{(XV)}$$

where Ea is the activation energy and ΔH_r is the estimated heat of reaction, both in kcal/mole. This corresponds to EaA = 14.05 kcal/mole and EaB = 0.44. These are used for estimating activation energies for all the alkoxy radical decompositions forming methyl radicals.

Figure 8 shows that Equation (XV) overpredicts the activation energies for reactions forming ethyl and propyl radicals. However, the data for these decompositions are reasonably well fit if EaB is assumed to be the same as form reactions forming methyl radicals, and EaA is reduced to 11.25 kcal/mole, i.e.,

$$Ea \text{ (decomp. to RCH2.)} = 11.25 + 0.44\ \Delta Hr \qquad \text{(XVI)}$$

Although the data are not sufficient to determine whether the EaB for decompositions forming these radicals is necessarily the same as for those forming methyl, this is assumed for lack of sufficient data to determine otherwise. Likewise, the single measurement for a decomposition forming tertiary radicals is fit

using EaA = 6.58 kcal/mole, and the least uncertain measurement for a decomposition forming $HOCH_2\cong$ is

Table 34. Experimental and estimated branching ratios for radicals where relevant data are available, sorted by type of reaction. Estimated branching ratios derived using alternative mechanistic assumptions are also shown.

Reaction Type and Reaction	Rad. [a]	Hr (kcal)	Estimated k (min^{-1})	%	Expt. Fract React. Min	Exp'd	Max	Estimation vs Experimental
Estimates using Recommended Parameters								
Decomposition Forming CH3.								
CH3-CH2-O-CH[O.]-CH3 -> CH3-CH2-O-CHO + CH3.	13	-4.81	3.54e+5	76%	60%	95%	100%	ok
CH3-CH[O.]-O-CH2-CH2-OH -> CH3. + HCO-O-CH2-CH2-OH	16	-4.81	3.54e+5	64%	70%	82%	100%	Low: 64% vs 70%
CH3-C(CH3)(CH3)-O-CH[O.]-CH3 -> CH3. + CH3-C(CH3)(CH3)-O-CHO	23	-4.81	3.54e+5	82%	70%	83%	100%	ok
CH3-CO-O-CH2-CH2-O-CH[O.]-CH3 -> CH3. + CH3-CO-O-CH2-CH2-O-CHO	30	-4.81	3.54e+5	72%	50%	90%	100%	ok
CH3-CH2-O-CO-CH2-CH2-O-CH[O.]-CH3 -> CH3. + CH3-CH2-O-CO-CH2-CH2-O-CHO	33	-4.81	3.54e+5	75%	50%	75%	100%	ok
CH3-C[O.](CH3)-O-CH3 -> CH3-O-CO-CH3 + CH3.	36	-6.51	2.51e+6	96%	50%	87%	95%	High: 96% vs 95%
CH3-C[O.](CH3)-O-CH2-CH3 -> CH3. + CH3-CH2-O-CO-CH3	39	-6.51	2.51e+6	95%	0%	69%	100%	ok
CH3-C[O.](CH3)-O-CO-CH3 -> CH3-CO-O-CO-CH3 + CH3.	41	9.99	3.48e+2	66%	50%	76%	90%	ok
CH3-C[O.](CH3)-O-CH2-CH2-OH -> CH3. + CH3-CO-O-CH2-CH2-OH	42	-6.51	2.51e+6	92%	60%	90%	100%	ok
CH3-CH(CH3)-O-C[O.](CH3)-CH3 -> CH3. + CH3-CH(CH3)-O-CO-CH3	44	-6.51	2.51e+6	97%	80%	100%	100%	ok
CH3-C(CH3)(CH3)-O-C[O.](CH3)-CH3 -> CH3. + CH3-C(CH3)(CH3)-O-CO-CH3	45	-6.51	2.51e+6	97%	75%	100%	100%	ok
CH3-CH(CH3)-CH2-O-C[O.](CH3)-CH3 -> CH3. + CH3-CH(CH3)-CH2-O-CO-CH3	46	-6.51	2.51e+6	94%	40%	82%	100%	ok
CH3-C(CH3)(OH)-CH2-O-C[O.](CH3)-CH3 -> CH3. + CH3-C(CH3)(OH)-CH2-O-CO-CH3	48	-6.51	2.51e+6	95%	75%	100%	100%	ok
Decomposition Forming RCH2.								
CH3-CH2-CH[O.]-CH3 -> CH3-CHO + CH3-CH2.	11	6.94	6.46e+3	14%	24%	36%	54%	Low: 14% vs 24%
CH3-CH2-CH[O.]-CH2-CH3 -> CH3-CH2-CHO + CH3-CH2.	18	6.71	1.53e+4	28%	26%	39%	58%	ok
CH3-CH2-CH2-CH[O.]-O-CH3 -> CH3-CH2-CH2. + CH3-O-CHO	21	-6.54	1.45e+8	100%	50%	66%	100%	ok
CH3-CO-O-CH2-CH2-CH[O.]-CH3 -> CH3-CO-O-CH2-CH2. + CH3-CHO	25	5.17	2.41e+4	38%	0%	35%	75%	ok
CH3-CH2-CH2-CH[O.]-O-CH2-CH2-OH -> CH3-CH2-CH2. + HCO-O-CH2-CH2-OH	27	-6.54	1.45e+8	100%	50%	100%	100%	ok
Decomposition Forming R2CH.								
CH3-CH(CH3)-O-CH[O.]-CH(CH3)-CH3 -> CH3-CH[.]-CH3 + CH3-CH(CH3)-O-CHO	31	-6.09	1.14e+10	100%	50%	100%	100%	ok
Decomposition Forming R3C.								
CH3-C(CH3)(CH2O.)-CH3 -> HCHO + CH3-C[.](CH3)-CH3	6	10.40	1.31e+6	98%	75%	98%	100%	ok
Decomposition Forming RO. (Rate constants estimated to minimize bias [Equation (XX)].								
CH3-O-CH2-O-CH2O. -> CH3-O-CH2O. + HCHO	4	13.34	6.50e+3	4%	0%	0%	25%	ok
CH3-C(CH3)(CH3)O-CH2O. -> CH3-C[O.](CH3)CH3 + HCHO	7	14.34	3.09e+3	2%	0%	0%	25%	ok
CH3-O-CH[O.]-O-CH3 -> CH3-O-CHO + CH3O.	10	-1.67	9.07e+8	100%	0%	16%	50%	High: 100% vs 50%
CH3-CH2-O-CH[O.]-CH3 -> CH3-CH2O. + CH3-CHO	13	10.06	7.44e+4	16%	0%	0%	15%	High: 16% vs 15%
CH3-CH(OH)-CH[O.]-O-CH3 -> CH3O. + CH3-CH(OH)-CHO	15	11.49	2.57e+4	0%	0%	0%	15%	ok
CH3-CH[O.]-O-CH2-CH2-OH -> HO-CH2-CH2O. + CH3-CHO	16	10.07	7.39e+4	13%	0%	0%	25%	ok
CH3-CH2-O-CH[O.]-CH2-OH -> CH3-CH2O. + HCO-CH2-OH	17	11.54	2.48e+4	0%	0%	0%	25%	ok

Table 34 (continued)

Reaction Type and Reaction	Rad. [a]	Hr (kcal)	Estimated k (min^{-1})	%	Expt. Fract React. Min	Exp'd	Max	Estimation vs Experimental
CH3-CH2-CH2-CH[O.]-O-CH3 -> CH3O. + CH3-CH2-CH2-CHO	21	10.34	6.04e+4	0%	0%	0%	30%	ok
CH3-CH(CH3)-O-CH[O.]-CH2-OH -> CH3-CH[O.]-CH3 + HCO-CH2-OH	22	12.35	1.36e+4	0%	0%	0%	15%	ok
CH3-C(CH3)(CH3)-O-CH[O.]-CH3 -> CH3-C[O.](CH3)-CH3 + CH3-CHO	23	11.07	3.51e+4	8%	0%	0%	20%	ok
CH3-CH2-CH2-CH[O.]-O-CH2-CH2-OH -> HO-CH2-CH2O. + CH3-CH2-CH2-CHO	27	10.13	7.06e+4	0%	0%	0%	25%	ok
CH3-CH2-CH2-CH2-O-CH[O.]-CH2-OH -> CH3-CH2-CH2-CH2O. + HCO-CH2-OH	28	11.55	2.46e+4	0%	0%	0%	25%	ok
CH3-CH2-O-CH[O.]-CH2-O-CO-CH3 -> CH3-CH2O. + CH3-CO-O-CH2-CHO	29	11.54	2.48e+4	0%	0%	0%	30%	ok
CH3-CO-O-CH2-CH2-O-CH[O.]-CH3 -> CH3-CO-O-CH2-CH2O. + CH3-CHO	30	10.07	7.39e+4	15%	0%	0%	25%	ok
CH3-CH2-O-CO-CH2-CH[O.]-O-CH2-CH3 -> CH3-CH2O. + CH3-CH2-O-CO-CH2-CHO	32	7.99	3.46e+5	0%	0%	16%	20%	ok
CH3-CH2-O-CO-CH2-CH2-O-CH[O.]-CH3 -> CH3-CH2-O-CO-CH2-CH2O. + CH3-CHO	33	10.07	7.39e+4	16%	0%	0%	50%	ok
CH3-C[O.](CH3)-O-CH3 -> CH3-CO-CH3 + CH3O.	36	9.50	1.13e+5	4%	5%	13%	25%	Low: 4% vs 5%
CH3-C[O.](CH3)-O-CH2-CH3 -> CH3-CH2O. + CH3-CO-CH3	39	9.28	1.33e+5	5%	0%	31%	100%	ok
CH3-C[O.](CH3)-O-CO-CH3 -> CH3-CO-CH3 + CH3-CO2.	41	10.73	1.09e+2	21%	10%	24%	50%	ok
CH3-C[O.](CH3)-O-CH2-CH2-OH -> HO-CH2-CH2O. + CH3-CO-CH3	42	9.29	1.32e+5	5%	0%	0%	20%	ok
CH3-CH(CH3)-O-C[O.](CH3)-CH3 -> CH3-CH[O.]-CH3 + CH3-CO-CH3	44	10.09	7.28e+4	3%	0%	0%	20%	ok
CH3-C(CH3)(CH3)-O-C[O.](CH3)-CH3 -> CH3-C[O.](CH3)-CH3 + CH3-CO-CH3	45	10.29	6.27e+4	2%	0%	0%	20%	ok
CH3-CH(CH3)-CH2-O-C[O.](CH3)-CH3 -> CH3-CH(CH2O.)-CH3 + CH3-CO-CH3	46	9.29	1.32e+5	5%	0%	18%	40%	ok
CH3-C(CH3)(OH)-CH2-O-C[O.](CH3)-CH3 -> CH3-C(OH)(CH2O.)-CH3 + CH3-CO-CH3	48	9.29	1.32e+5	5%	0%	0%	25%	ok
Decomposition Forming RCO.								
CH3-CO-CH2O. -> HCHO + CH3-CO.	2	2.59	1.74e+9	0%	75%	100%	100%	Low: 0% vs 75%
CH3-CH2-O-CO-CH2O. -> HCHO + CH3-CH2-O-CO.	5	13.50	1.39e+1	0%	0%	0%	70%	ok
Decomposition forming HCO.								
CH3-C[O.](CHO)-CH2-OH -> CH3-CO-CH2-OH + HCO.	37	-0.66	1.53e+7	94%	75%	100%	100%	ok
Decomposition Forming a-Hydroxy Radicals								
HO-CH2-CH2O. -> HO-CH2. + HCHO	1	11.79	1.11e+5	78%	70%	78%	85%	ok
CH3-CH[O.]-CH2-OH -> HO-CH2. + CH3-CHO	9	6.62	5.19e+6	99%	85%	100%	100%	ok
CH3-CH(OH)-CH[O.]-CH3 -> CH3-CHO + CH3-CH[.]-OH	12	2.87	2.56e+9	100%	100%	100%	100%	ok
CH3-CH(OH)-CH[O.]-O-CH3 -> CH3-CH[.]-OH + CH3-O-CHO	15	-9.80	3.14e+13	100%	80%	100%	100%	ok
CH3-CH2-O-CH[O.]-CH2-OH -> HO-CH2. + CH3-CH2-O-CHO	17	-6.05	6.36e+10	100%	75%	100%	100%	ok
CH3-CH(CH3)-CH[O.]-CH2-OH -> CH3-CH(CHO)-CH3 + HO-CH2.	20	7.15	3.50e+6	91%	50%	71%	90%	High: 91% vs 90%
CH3-CH(CH3)-O-CH[O.]-CH2-OH -> HO-CH2. + CH3-CH(CH3)-O-CHO	22	-6.05	6.36e+10	100%	80%	100%	100%	ok
CH3-CH2-CH2-CH2-O-CH[O.]-CH2-OH -> HO-CH2. + CH3-CH2-CH2-CH2-O-CHO	28	-6.05	6.36e+10	100%	80%	100%	100%	ok
Decompositions Forming ROCH2.								
CH3-CH2-CH[O.]-CH2-O-CO-CH3 -> CH3-CO-O-CH2. + CH3-CH2-CHO	24	8.84	1.57e+3	5%	0%		75%	ok
CH3-CH(CH3)-O-CH2-C[O.](CH3)-CH3 -> CH3-CH(CH3)-O-CH2. + CH3-CO-CH3	47	3.74	6.96e+4	13%	0%	0%	25%	ok
Decompositions Forming ROCH[.]R								

Table 34 (continued)

Reaction Type and Reaction	Rad. [a]	Hr (kcal)	Estimated k (min^{-1})	%	Expt. Fract React. Min	Exp'd	Max	Estimation vs Experimental
CH3-CH(CH2O.)-O-CO-CH3 -> CH3-CO-O-CH[.]-CH3 + HCHO	8	12.81	4.93e+4	59%	25%	100%	100%	ok
Decomposition Forming RO-CO-CH2. or R-CO-O-CH2.								ok
CH3-CH2-O-CH[O.]-CH2-O-CO-CH3 -> CH3-CO-O-CH2. + CH3-CH2-O-CHO	29	-3.60	1.63e+7	100%	50%	90%	100%	ok
CH3-CH2-O-CO-CH2-CH[O.]-O-CH2-CH3 -> CH3-CH2-O-CO-CH2. + CH3-CH2-O-CHO	32	-5.80	8.34e+7	100%	50%	84%	100%	ok
Decompositions forming RO-CO.								
CH3-CH2-O-CO-CH2O. -> HCHO + CH3-CH2-O-CO.	5	13.50	1.39e+1	0%	0%	0%	70%	ok
CH3-C[O.](CH3)-CO-O-CH3 -> CH3-CO-CH3 + CH3-O-CO.	40	5.69	4.62e+3	85%	50%	100%	100%	ok
Isomerizations (no -O- or -CO- in transition state ring)								
CH3-CH2-CH2-CH[O.]-O-CH2-CH2-OH -> HO-CH2-CH2-O-CH(OH)-CH2-CH2-CH2.	27		1.96e+5	0%	0%	0%	25%	ok
Isomerizations with -O- or -CO- in transition state ring (3.5 kcal/mole strain energy assumed)								
CH3-C(CH3)(CH3)O-CH2O. -> CH3-C(CH3)(CH2.)O-CH2-OH	7		1.59e+3	1%	0%	0%	25%	ok
CH3-CH2-O-CH[O.]-CH3 -> CH3-CH(OH)O-CH2-CH2.	13		5.31e+2	0%	0%	0%	25%	ok
CH3-CH[O.]-O-CH2-CH2-OH -> CH3-CH(OH)-O-CH2-CH[.]-OH	16		8.80e+4	16%	0%	0%	25%	ok
CH3-CO-CH2-CH[O.]-CH3 -> CH3-CH(OH)-CH2-CO-CH2.	19		2.53e+2	0%	0%	0%	10%	ok
CH3-CH2-CH2-CH[O.]-O-CH3 -> CH3-O-CH(OH)-CH2-CH2-CH2.	21		1.96e+5	0%	0%	0%	30%	ok
CH3-C(CH3)(CH3)O-CH[O.]-CH3 -> CH3-C(CH3)(CH2.)O-CH(OH)CH3	23		1.59e+3	0%	0%	0%	20%	ok
CH3-CH2-CH2-CH[O.]-O-CH2-CH2-OH -> CH3-CH2-CH2-CH(OH)-O-CH2-CH[.]-OH	27		8.80e+4	0%	0%	0%	25%	ok
CH3-CH2-CH2-CH2-O-CH[O.]-CH2-OH -> CH3-CH2-CH[.]-CH2-O-CH(OH)-CH2-OH	28		1.83e+4	0%	0%	0%	25%	ok
CH3-CO-O-CH2-CH2-O-CH[O.]-CH3 -> CH3-CH(OH)-O-CH2-CH[.]-O-CO-CH3	30		2.72e+4	6%	0%	0%	25%	ok
CH3-CH2-O-CO-CH2-CH[O.]-O-CH2-CH3 -> CH3-CH2-O-CO-CH2-CH(OH)-O-CH2-CH2.	32		5.31e+2	0%	0%	0%	20%	ok
CH3-CH2-O-CO-CH2-CH2-O-CH[O.]-CH3 -> CH3-CH(OH)-O-CH2-CH[.]-CO-O-CH2-CH3	33		2.32e+3	0%	0%	0%	50%	ok
CH3-C[O.](CH3)-O-CO-CH3 -> CH3-C(CH3)(OH)-O-CO-CH2.	41		6.72e+1	13%	0%	0%	25%	ok
CH3-C[O.](CH3)-O-CH2-CH2-OH -> CH3-C(CH3)(OH)-O-CH2-CH[.]-OH	42		8.80e+4	3%	0%	0%	20%	ok
CH3-CH(CH3)-O-C[O.](CH3)-CH3 -> CH3-C(CH3)(OH)-O-CH(CH2.)-CH3	44		1.06e+3	0%	0%	0%	20%	ok
CH3-C(CH3)(CH3)-O-C[O.](CH3)-CH3 -> CH3-C(CH3)(CH2.)-O-C(CH3)(OH)-CH3	45		1.59e+3	0%	0%	0%	20%	ok
CH3-CH(CH3)-CH2-O-C[O.](CH3)-CH3 -> CH3-C(CH3)(OH)-O-CH2-C[.](CH3)-CH3	46		2.70e+4	1%	0%	0%	30%	ok
CH3-CH(CH3)-O-CH2-C[O.](CH3)-CH3 -> CH3-C(CH3)(OH)-CH2-O-C[.](CH3)-CH3	47		4.81e+5	87%	75%	100%	100%	ok
Estimates using alternative assumptions (see text)								
Decomposition Forming RO. (Rate constants estimated to best fit data on Table 32 [Equation (XIX)].)								
CH3-O-CH2-O-CH2O. -> CH3-O-CH2O. + HCHO	4	13.34	1.49e+4	9%	0%	0%	25%	ok
CH3-C(CH3)(CH3)O-CH2O. -> CH3-C[O.](CH3)CH3 + HCHO	7	14.34	3.14e+4	17%	0%	0%	25%	ok
CH3-O-CH[O.]-O-CH3 -> CH3-O-CHO + CH3O.	10	-1.67	6.55e+4	0%	0%	16%	50%	ok
CH3-CH2-O-CH[O.]-CH3 -> CH3-CH2O. + CH3-CHO	13	10.06	1.19e+5	0%	0%	0%	15%	ok
CH3-CH(OH)-CH[O.]-O-CH3 -> CH3O. + CH3-CH(OH)-CHO	15	11.49	1.20e+5	1%	0%	0%	15%	ok

Table 34 (continued)

Reaction Type and Reaction	Rad. [a]	Hr (kcal)	Estimated k (min^{-1})	%	Expt. Fract React. Min	Exp'd	Max	Estimation vs Experimental
CH3-CH[O.]-O-CH2-CH2-OH -> HO-CH2-CH2O. + CH3-CHO	16	10.07	1.20e+5	0%	0%	0%	25%	ok
CH3-CH2-O-CH[O.]-CH2-OH -> CH3-CH2O. + HCO-CH2-OH	17	11.54	1.24e+5	0%	0%	0%	25%	ok
CH3-CH2-CH2-CH[O.]-O-CH3 -> CH3O. + CH3-CH2-CH2-CHO	21	10.34	1.70e+5	30%	0%	0%	30%	High: 30% vs 30%
CH3-CH(CH3)-O-CH[O.]-CH2-OH -> CH3-CH[O.]-CH3 + HCO-CH2-OH	22	12.35	2.18e+5	100%	0%	0%	15%	High: 100% vs 15%
CH3-C(CH3)(CH3)-O-CH[O.]-CH3 -> CH3-C[O.](CH3)-CH3 + CH3-CHO	23	11.07	2.92e+5	0%	0%	0%	20%	ok
CH3-CH2-CH2-CH[O.]-O-CH2-CH2-OH -> HO-CH2-CH2O. + CH3-CH2-CH2-CHO	27	10.13	3.03e+5	11%	0%	0%	25%	ok
CH3-CH2-CH2-CH2-O-CH[O.]-CH2-OH -> CH3-CH2-CH2-CH2O. + HCO-CH2-OH	28	11.55	3.41e+5	0%	0%	0%	25%	ok
CH3-CH2-O-CH[O.]-CH2-O-CO-CH3 -> CH3-CH2O. + CH3-CO-O-CH2-CHO	29	11.54	3.51e+5	12%	0%	0%	30%	ok
CH3-CO-O-CH2-CH2-O-CH[O.]-CH3 -> CH3-CO-O-CH2-CH2O. + CH3-CHO	30	10.07	3.57e+5	47%	0%	0%	25%	High: 47% vs 25%
CH3-CH2-O-CO-CH2-CH[O.]-O-CH2-CH3 -> CH3-CH2O. + CH3-CH2-O-CO-CH2-CHO	32	7.99	3.57e+5	46%	0%	16%	20%	High: 46% vs 20%
CH3-CH2-O-CO-CH2-CH2-O-CH[O.]-CH3 -> CH3-CH2-O-CO-CH2-CH2O. + CH3-CHO	33	10.07	3.57e+5	43%	0%	0%	50%	ok
CH3-C[O.](CH3)-O-CH3 -> CH3-CO-CH3 + CH3O.	36	9.50	3.59e+5	48%	5%	13%	25%	High: 48% vs 25%
CH3-C[O.](CH3)-O-CH2-CH3 -> CH3-CH2O. + CH3-CO-CH3	39	9.28	5.45e+5	0%	0%	31%	100%	ok
CH3-C[O.](CH3)-O-CO-CH3 -> CH3-CO-CH3 + CH3-CO2.	41	10.73	6.37e+5	20%	10%	24%	50%	ok
CH3-C[O.](CH3)-O-CH2-CH2-OH -> HO-CH2-CH2O. + CH3-CO-CH3	42	9.29	6.37e+5	20%	0%	0%	20%	ok
CH3-CH(CH3)-O-C[O.](CH3)-CH3 -> CH3-CH[O.]-CH3 + CH3-CO-CH3	44	10.09	6.37e+5	20%	0%	0%	20%	High: 20% vs 20%
CH3-C(CH3)(CH3)-O-C[O.](CH3)-CH3 -> CH3-C[O.](CH3)-CH3 + CH3-CO-CH3	45	10.29	6.41e+5	20%	0%	0%	20%	High: 20% vs 20%
CH3-CH(CH3)-CH2-O-C[O.](CH3)-CH3 -> CH3-CH(CH2O.)-CH3 + CH3-CO-CH3	46	9.29	1.67e+6	2%	0%	18%	40%	ok
CH3-C(CH3)(OH)-CH2-O-C[O.](CH3)-CH3 -> CH3-C(OH)(CH2O.)-CH3 + CH3-CO-CH3	48	9.29	4.38e+9	100%	0%	0%	25%	High: 100% vs 25%
Isomerizations with -O- in transition state ring (Estimates assuming no excess ring strain energy)								
CH3-C(CH3)(CH3)O-CH2O. -> CH3-C(CH3)(CH2.)O-CH2-OH	7		2.15e+5	29%	0%	0%	25%	High: 29% vs 25%
CH3-CH2-O-CH[O.]-CH3 -> CH3-CH(OH)O-CH2-CH2.	13		6.46e+5	80%	0%	0%	25%	High: 80% vs 25%
CH3-CH[O.]-O-CH2-CH2-OH -> CH3-CH(OH)-O-CH2-CH[.]-OH	16		6.46e+5	57%	0%	0%	25%	High: 57% vs 25%
CH3-CO-CH2-CH[O.]-CH3 -> CH3-CH(OH)-CH2-CO-CH2.	19		4.31e+5	13%	0%	0%	10%	High: 13% vs 10%
CH3-CO-CH2-CH[O.]-CH3 -> CH3-CH(OH)-CH2-CO-CH2.	19		9.32e+4	47%	0%	0%	10%	High: 47% vs 10%
CH3-C(CH3)(CH3)O-CH[O.]-CH3 -> CH3-C(CH3)(CH2.)O-CH(OH)CH3	23		6.46e+5	18%	0%	0%	20%	ok
CH3-CH2-CH2-CH[O.]-O-CH2-CH2-OH -> CH3-CH2-CH2-CH(OH)-O-CH2-CH[.]-OH	27		2.15e+5	0%	0%	0%	25%	ok
CH3-CH2-CH2-CH2-O-CH[O.]-CH2-OH -> CH3-CH2-CH[.]-CH2-O-CH(OH)-CH2-OH	28		9.19e+5	63%	0%	0%	25%	High: 63% vs 25%
CH3-CO-O-CH2-CH2-O-CH[O.]-CH3 -> CH3-CH(OH)-O-CH2-CH[.]-O-CO-CH3	30		1.08e+7	95%	0%	0%	25%	High: 95% vs 25%
CH3-CH2-O-CO-CH2-CH[O.]-O-CH2-CH3 -> CH3-CH2-O-CO-CH2-CH(OH)-O-CH2-CH2.	32		3.49e+7	18%	0%	0%	20%	ok
CH3-CH2-O-CO-CH2-CH2-O-CH[O.]-CH3 -> CH3-CH(OH)-O-CH2-CH[.]-CO-O-CH2-CH3	33		7.26e+6	0%	0%	0%	50%	ok
CH3-C[O.](CH3)-O-CO-CH3 -> CH3-C(CH3)(OH)-O-CO-CH2.	41		2.15e+5	0%	0%	0%	25%	ok
CH3-C[O.](CH3)-O-CH2-CH2-OH -> CH3-C(CH3)(OH)-O-CH2-CH[.]-OH	42		1.06e+7	78%	0%	0%	20%	High: 78% vs 20%

Table 34 (continued)

Reaction Type and Reaction	Rad. [a]	Hr (kcal)	Estimated k (min^{-1})	%	Expt. Fract React. Min	Exp'd	Max	Estimation vs Experimental
CH3-CH(CH3)-O-C[O.](CH3)-CH3 -> CH3-C(CH3)(OH)-O-CH(CH2.)-CH3	44		1.89e+8	100%	0%	0%	20%	High: 100% vs 20%
CH3-C(CH3)(CH3)-O-C[O.](CH3)-CH3 -> CH3-C(CH3)(CH2.)-O-C(CH3)(OH)-CH3	45		3.49e+7	92%	0%	0%	20%	High: 92% vs 20%
CH3-CH(CH3)-CH2-O-C[O.](CH3)-CH3 -> CH3-C(CH3)(OH)-O-CH2-C[.](CH3)-CH3	46		3.49e+7	99%	0%	0%	30%	High: 99% vs 30%

[a] Radical number on Table 33

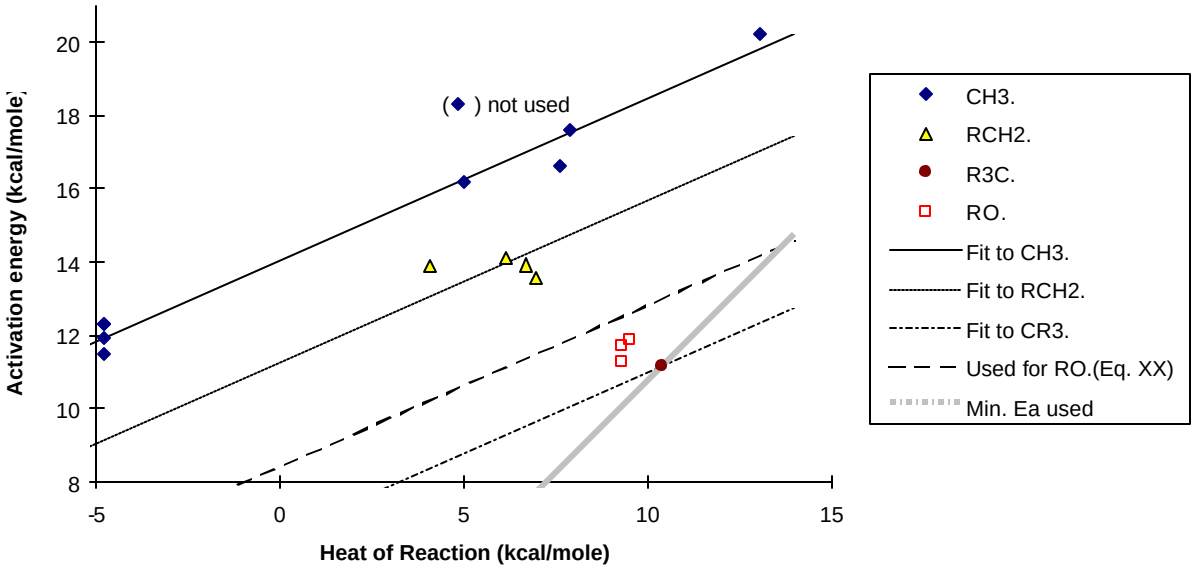

Figure 8. Plots of estimated or measured activation energies vs. heats of reaction for various alkoxy radical decompositions.

fit using EaA = 7.42 kcal/mole, if it is assumed that the same EaB is applicable for reactions assuming these radicals as well. Thus,

$$Ea \text{ (decomp. to } R_3C.) = 6.58 + 0.44\ \Delta H_r \quad \text{(XVII)}$$

$$Ea \text{ (decomp. to } HOCH_2\cong) = 7.43 + 0.44\ \Delta Hr \quad \text{(XVIII)}$$

can be used to estimate activation energies for these types of decompositions.

Quantitative information concerning decompositions forming alkoxy radicals is sparse, though as shown on Table 33 and Table 34 there are a number of cases where upper or lower limit estimates can be obtained. As shown on Table 32, the only quantitative information concerns two radicals where decomposition to an alkoxy radical competes with a decomposition forming a methyl radical. If equation (XIII) and (XV) are used to estimate the Arrhenius parameters and thus the rate constants for these competing decompositions to methyl radicals, then the rate constants forming alkoxy radicals can be placed on an absolute basis. If this is assumed, and if the same EaB is used as assumed for the reactions forming alkyl or $HOCH_2\cong$ radicals, then a value of EaA = 7.42 kcal/mole can be derived, i.e.,

$$Ea \text{ (decomp to RO. - initial estimate)} = 7.50 + 0.44\ \Delta H_r \quad \text{(XIX)}$$

Note that using Equation (XIX) gives a reasonably good fit to the data for the decomposition determined relative to the O_2 reaction, even though this was not used in the derivation of Equation (XIX).

However, although use of Equation (XIX) to predict alkoxy-forming decomposition activation energies gives good fits to the limited quantitative product yield data, Table 34 shows that there are many cases where it results in predictions which are inconsistent with upper limit data concerning the relative importance of this reaction (see "rate constants estimated to best fit data on Table 32" in the "alternative assumptions" section of the table). In particular, use of Equation (XIX) appears to be biased towards overpredicting the relative importance of this reaction. Such a bias is not acceptable as a basis for deriving a general methodology for deriving estimated VOC reaction mechanisms, and if uniformly good predictions cannot be obtained, at a minimum the prediction method should be as likely to underpredict as overpredict.

To obtain unbiased estimates for the relative importances of these decompositions, an optimization was performed to minimize the cases where the estimates were outside of the estimated upper and lower limit ranges, as well as to minimize the discrepancies between estimated and experimental quantitative yield ratios[16]. This optimization was done in two ways: one where EaA was adjusted and EaB was held fixed at the 0.44 value as assumed for the reactions forming alkyl radicals, and the other where both EaA and EaB were optimized. However, the qualities of the fits were not significantly different in either case, so for consistency with the estimates for the other reactions we will only use the data where we assumed EaB = 0.44. The results of this optimization yielded EaA = 8.44 kcal/mole, i.e.,

$$Ea \text{ (decomp to RO. - recommended)} = 8.43 + 0.44\ \Delta H_r \quad \text{(XX)}$$

This resulted in overpredicting the apparent activation energies for the three alkoxy-forming decompositions on Table 32 by ~1 kcal/mole each, which corresponds to an underprediction of the 298K rate

[16] The data for the $CH_3OCH(O\cdot)OCH_3$ radical, where the estimates appear to fail by orders of magnitude more than was the case for any other radicals, were not used in the optimization.

constant by a factor of ~6. However, use of Equation (XX) for predicting activation energies for alkoxy-forming decompositions is preferred over Equation (XIX) because the latter removes the apparent bias towards overpredicting upper limit rate constants. In particular, this gives only three cases (as opposed to six for Equation XIX) where the prediction is outside the estimation is outside the estimated uncertainty range of the experimental data.

The estimates discussed above do not cover all the types of radicals that may be formed in alkoxy radical decompositions, and methods are needed to estimate EaA values for cases where there are no data. Atkinson (1997b) observed that there is an apparent correlation between the EaA and the ionization potential of the radical formed, and used this to derive a general estimation method for all alkoxy radical decompositions. Plots of the EaA values obtained as discussed above against ionization potential of the radical formed is shown on Figure 9. The IP's used are given in Table 35 and are from the NIST (1994) database. It can be seen that the three points for the alkyl (methyl, ethyl, propyl and t-butyl) radicals are reasonably well fit by a straight line, which is given by

$$\text{EaA (decomp. to hydrocarbon radicals)} = -8.73 + 2.35\ \text{IP} \qquad \text{(XXI)}$$

where EaA is in kcal/mole and IP is the ionization potential of the radical formed in eV. When combined with Equation (XIV), and using EaB = 0.44 as discussed above, this yields

$$\text{Ea (decomp. to hydrocarbon radicals)} = -8.73 + 2.35\ \text{IP} + 0.44\ \Delta H_r \qquad \text{(XXII)}$$

where IP is in eV and Ea and ΔH_r is in kcal/mole. This is close to the general relationship derived by Atkinson (1997a), which is

$$\text{Ea (general decompositions)} = -8.1 + 2.4\ \text{IP} + 0.36\ \Delta H_r. \qquad \text{(XXIII)}$$

The small differences between these equations are due to the fact that in this work the EaB parameter is determined using only the reactions forming methyl radicals, and that Atkinson (1996) did not include the exothermic decompositions of the radicals from the ether systems in his analysis, but did include the reaction forming $HOCH_2\cong$.

Figure 9 shows that Equation (XXI) overpredicts the EaA for the reaction forming $HOCH_2\cong$ by 1.65 kcal/mole, resulting in an underprediction of the 298K rate constant by a factor of ~16. However, it can be argued that the discrepancy is not large considering the data and the assumptions behind the empirical correlations. Equation (XXI) clearly fails in the case of reactions forming alkoxy radicals, overpredicting activation energies by over 4.5 kcal/mole and the decomposition rate constants by three orders of magnitude. For that reason, we conclude that Equations (XXI) should only be used for reactions forming carbon-centered radicals. For substituted radicals the actual data should be used to derive EaA estimates whenever possible.

Based on these considerations, together with the availability of IP data, Equation (XXI) can therefore be used to derive the EaA parameters for decompositions forming secondary alkyl radicals ($R_2CH\cong$), and a modified version of Equation (XXI), where the EaA is reduced by 1.65 kcal/mole so its predictions are consistent with the data for the reaction forming $HOCH_2O\cong$, can be used to estimate EaA for reactions forming $CH_3C(.)OH$. In the case of reactions forming HCO and RC(O)· radicals, predictions that are reasonably consistent with the limited upper and lower limit data (see Table 34) if the EaA predicted using Equation (XXI) is reduced by ~2 kcal/mole. These estimates are given on Table 35, together with the EaA values derived for the decompositions discussed above, and the associated ionization potentials. Obviously, these EaA estimates are the least uncertain for secondary alkyl radicals, are highly uncertain for formyl and acetyl radicals.

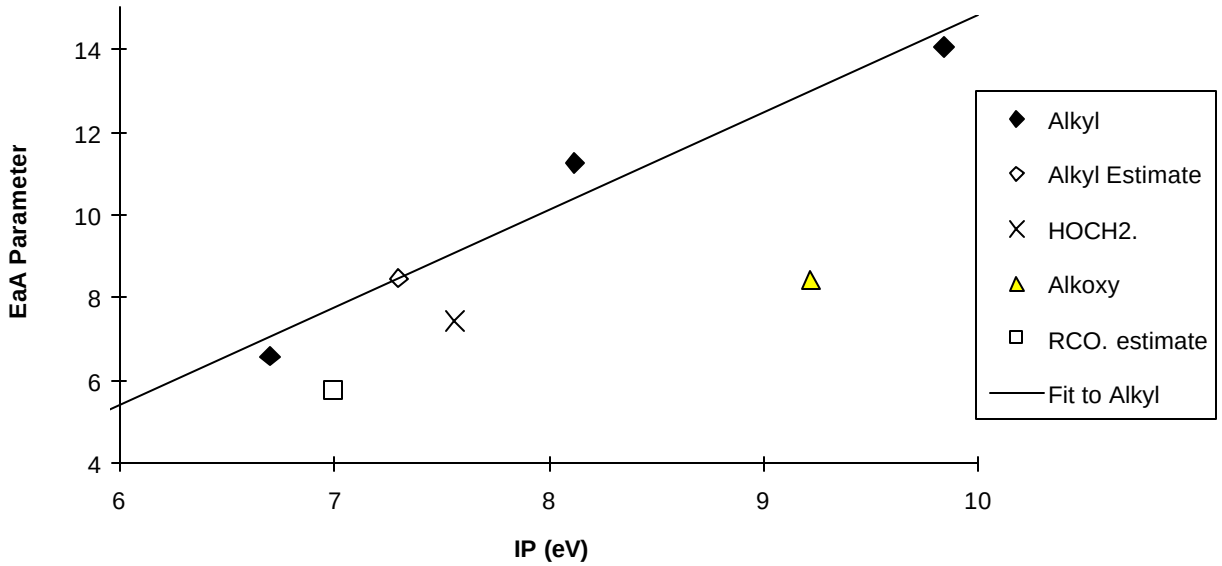

Figure 9. Plots of the EaA parameter used in Equation (XIV) to predict activation energies from heats of reactions for various types of alkoxy radical decompositions vs. the ionization potential of the radical formed. These are based on assuming all lines have the same slope as fits the data for reactions forming methyl radicals.

Available IP data and Equation (XXI) (or the modified version of it) can also be used to derive an EaA for reactions forming CH_3OCH_2≅ radicals, which presumably could also be applied to reactions forming other radicals of the type $ROCH_2$≅. However, applying this approach to reactions forming these radicals predict that this type of reaction is extremely rapid (having rate constants > 10^9 sec^{-1}) in at least two cases where available data are inconsistent with this reaction dominating (see Table 34 and radicals 24 and 48 on Table 33). Predictions are more consistent with the data if the activation energies are derived assuming the same EaA as employed for reactions forming alkyl RCH_2≅ radicals. For other radicals, Equation (XII) is either not applicable or cannot be used because of lack of available IP data.

For reactions forming substituted alkyl radicals (i.e., reactions forming radicals with non-alkyl substituents) we assume that ß- or further substituents on the radical formed have no effect, and make various estimates concerning the effects of various types of a-substituents, based on highly uncertain assumptions or fits to a very limited data base. In several cases, adjustments were made so the predictions would be consistent with product data or with environmental chamber reactivity data for several compounds. For example, it was initially assumed that decompositions forming RC(O)O≅ radicals have the same parameters as those forming simple alkoxy (RO≅) radicals, but,, as indicated on Table 35, better fits to product and environmental chamber data for several compounds were obtained if a much higher EaA value was used. These estimates, which are obviously very uncertain, are summarized on Table 35.

Although this is not the case with any of the radicals listed on Table 33, there may be cases where Equation (XIV) and the recommended EaA and EaB values may predict unreasonably low or negative

activation energies. For general estimation purposes, we assume a minimum decomposition energy of ~0.75 kcal/mole. Thus if Equation (XIV) predicts a lower activation energy lower than that, 0.75

Table 35. Summary of ionization potentials and EaA parameters used to estimate activation energies for alkoxy radical decompositions from the heats of reactions.

Type of radical Formed [a]	IP [b] (eV)	EaA (kcal $mole^{-1}$)	Derivation of EaA
CH_3.	9.84	14.05	Derived from least squares fits of Ea vs Hr as discussed in the text (Equation (XV). The EaB derived from these data are assumed to be applicable for all alkoxy radical decompositions.
RCH_2.	8.12	11.25	Derived to by adjusting EaA to fit the data as discussed in the text (Equation (XVI).
RCH[.]R	7.30	8.46	EaA is estimated from the IP using Equation (XXI). See text.
R_2C[.]R	6.70	6.58	Derived to by adjusting EaA to fit the data as discussed in the text (Equation (XVII).
RO.	9.22	8.43	Derived to minimize errors and biases in predictions of relative product yield data as discussed in the text (Equation XX).
OH	13.00	8.43	EaA assumed to be the same as derived for decompositions forming alkoxy radicals. This is highly uncertain.
HCO.	~8.8? [c]	9.99	Estimated from the IP using Equation (XXI), with the intercept reduced by 2.0 kcal/mole to give predictions which are more consistent with the limited available upper and lower limit data. Highly uncertain and may be upper limit.
R'C(O).	7.00	5.76	(see above)
R'C(O)O.		12.00	Necessary to assume that decompositions forming RCO2. radicals are slow to be consistent with product data from reaction of OH with isopropyl and t-butyl acetates, and for model simulations to fit chamber data for propylene carbonate. The EaA value used is the lowest value that is consistent with the data for propylene carbonate.
$HOCH_2$.	7.56	7.43	Derived to by adjusting EaA to fit the data as discussed in the text (Equation (XVIII).
RCH[.]OH	6.70	5.41	Estimated from the IP using Equation (XXI), with the intercept reduced by 1.65 kcal/mole to correctly predict the data for the decomposition of HOCH2CH2O. to HOCH2.
R_2C[.]OH		4.21	Ratio of EaA for R_2C[.]OH to R2C[.]R assumed to be the same as ratio of EaA's for RCH[.]OH to RCH[.]R.
R'OCH_2.	6.94	11.25	Better fits to available data are obtained if reactions forming $ROCH_2$. Radicals have the same activation energies as those forming RCH_2 radicals.
RCH[.]OR'		7.46	R'O- substitution assumed to reduce EaA by 1 kcal/mole relative to alkyl substitution to fit data for a minor product from isopropyl acetate. This is highly uncertain, and the data are also consistent with reducing EaA even further.
R_2C[.]OR'		5.58	R'O- substitution assumed to reduce EaA by 1 kcal/mole to be consistent with assumption made when estimating EaA for RCH[.]OR'. This is highly uncertain.
ROC(O).		12.00	Derived to be such that this decomposition is predicted to be minor for CH3-O-CO-CH2-CH[O.]-CO-O-CH3 radicals, but is the dominant process for CH3-C[O.](CH3)-CO-O-CH3, for model predictions to be consistent with environmental chamber reactivity data for dimethyl succinate (DBE-4) and methyl isobutyrate, respectively.
$XC(O)CH_2$.		11.25	For lack of available data, R'C(O)- and HC(O)- substitution is assumed to have no effect on EaA.
RCH[.]C(O)X		8.46	(see above)
R_2C[.]C(O)X		6.58	(see above)

[a] "R" is any substituent where the radical center is bonded to a non-carbonyl carbon. "R'" is any substituent other than H. "X" is any substituent, including H.

Table 35 (continued)

[b] IP data from NIST (1994) and is given for the methyl substituted species except where indicated.

[c] Not in NIST database. Entry of "8.8?" given in Lange's handbook of chemistry (1985).

kcal/mole is used. Although the possibility of a lower minimum cannot be ruled out, the data for the decomposition of neopentoxy and $HOCH_2CH_2O\cong$ radicals tend to rule out the minimum being higher than this.

The above discussion, based on the use of Equation (XIV), incorporates the assumption that the activation energy for the decomposition only depends on the nature of the radical formed and the overall heat of reaction. With appropriate choices of EaA, as shown on Table 35, this gives predictions which, though not always consistent with the data to within the experimental uncertainty, are at least good to within an order of magnitude in most cases. Note that this assumption implies that the activation energy does not depend on the nature of the carbonyl compound that is formed. This appears to work in the case of reactions forming aldehydes, ketones, or esters, which includes most of the reactions listed on Table 33.

However, this assumption appears to fail in the case of reactions where the carbonyl group formed is in an anhydride or carbonate anhydride, i.e., is contained in a -C(O)OC(O)- structure. The data of Tuazon et al (1989b) indicate that the $CH_3C[O.](CH_3)OC(O)CH_3$ radical formed in the reactions of OH radicals with t-butyl and isopropyl acetates (radical 41 on Table 33) decomposes to a significant extent to form acetic anhydride and methyl radicals, while Equation (XIV) and the parameters that fit the data for most of the other methyl radical-forming reactions predict that this reaction is sufficiently slow that the competing isomerization pathway, which is not observed, would dominate[17]. In addition, reactivity and product data recently obtained from a methyl isopropyl carbonate can only be explained if an analogous reaction of a carbonate-containing radical (Radical 43 on Table 33) is much more rapid than predicted by these estimates (Carter et al, 2000d). The data of Tuazon et al (1998b), together with the estimated rate constant for the competing decomposition of $CH_3C[O.](CH_3)OC(O)CH_3$ to acetone and $CH_3CO_2\cdot$, can be predicted if the reactions forming anhydride products have a 2 kcal/mole lower reaction energy than predicted using Equation (XIV), and the methyl isopropyl carbonate environmental chamber data are also better fit if this is assumed.

Therefore, for estimating activation energies for β-scission decompositions that form carbonyl compounds with -C(O)OC(O)- structures, the following modified version of Equation (XIV) is employed:

$$Ea \text{ (decomposition forming } R\cdot + \text{-CO-O-CO-)} = EaA - 2 \text{ kcal/mole} + EaB \cdot \Delta H_r \qquad \text{(XXIV)}$$

where EaA is derived based on the radical, R·, that is formed as shown on Table 35, and the same EaB value is used as assumed for all other reactions. This is obviously uncertain because it is derived based on highly uncertain estimates for competing rate constants, and is based on only a limited number of reactions. However, employing this correction means that the mechanism estimation system gives branching ratio predictions that are consistent with the limited data that are currently available.

[17] The decomposition is predicted to dominate even after the ring strain correction of 3.5 kcal/mole for transition states containing -O- or -CO- groups is added, as discussed in Section III.J.4.

One area where the estimation methods discussed above clearly fails is the predictions of the branching ratios of the $CH_3OCH(O\cdot)OCH_3$ radical (radical 10 on Table 33). The data of Sidebottom et al (1997) indicate that decomposition and O_2 reaction occur at competitive rates (with O_2 reaction being somewhat more important), while the estimation methods derived in this work predict that decomposition will dominate by orders of magnitude. It is unclear whether the problem is with the estimation of the O_2 reaction, the estimates of the decomposition rates, the thermochemical estimates, or (least likely) the experimental data or its interpretation. Until data are available for other similar radicals with similar discrepancies between the estimates and the data, it is unclear what, if any, adjustments may be appropriate. Therefore, estimates for reactions of alkoxy radicals with two alkoxy substituents near the radical center must be considered suspect. However, dimethoxy methane is the only compound of this structure in the current detailed mechanism, and because of the experimental data of Sidebottom et al (1997) it is not necessary to use estimates to determine its mechanism.

The decomposition activation energy and rate constant estimates discussed in this section are obviously highly uncertain in many (if not most) cases, being based in many cases on very uncertain alkoxy + O_2 rate constants, employing many highly uncertain and untested assumptions, and not giving satisfactory predictions in all cases. Clearly, additional data are needed, particularly for reactions of oxygen-containing alkoxy radicals, to test, refine, and improve these estimates and the many assumptions they incorporate. Indeed, it may not be possible to develop a totally satisfactory estimation method that can accurately predict rate constants for the full variety of these reactions, without carrying out detailed theoretical calculations for each system. Thus, rate constants or branching ratios derived from experimental data should always be used whenever possible when developing reaction mechanisms for atmospheric reactivity predictions. However, when no data are available, we have no choice but to use estimates such as those discussed in this section.

4. Isomerization Corrections

As discussed above, when estimating alkoxy radical isomerization rate constants, an additional 3.5 kcal/mole is added to the activation energy if the cyclic transition state contains -O-, -C(O)- or -OC(O)- groups. The need for this correction is shown on Table 34, which compares the experimental and predicted upper and lower limit branching ratios for these isomerizations with and without this correction. It can be seen that if the additional 3.5 kcal/mole is not added to the activation energy, there are 8 cases where isomerization is predicted to be important where the experimental data indicate it is not. This overprediction of the importance of isomerization is removed when the additional 3.5 kcal/mole activation energy is assumed. On the other hand, if a strain energy of greater than that is assumed, then the estimation becomes inconsistent with the observation that the $CH_3CH(CH_3)$-$OCH_2C(O\cong)(CH_3)CH_3$ reacts primarily by isomerization (Stemmler et al, 1997a).

Note that if it is assumed that the reactions of O_2 with the O-substituted alkoxy radicals are much more rapid than estimated in this work, as predicted, for example, by the estimation method of Atkinson (1997a), then many of the competing decompositions would also be predicted to be faster, and this isomerization strain correction may not be necessary. Obviously this isomerization correction, as well as all our estimates concerning the decomposition reactions, would need to be revisited if new data indicate that our estimates concerning these alkoxy + O_2 reactions are incorrect.

5. Ester Rearrangement

Tuazon et al (1998b) and Christensen et al (2000) recently reported data indicating that α-ester-substituted alkoxy radicals undergo a second type of hydrogen shift isomerization, where the hydrogen α

to the alkoxy center shifts, via a 5-member ring transition state, to the ester carbonyl oxygen atom, forming an acid and an acyl radical, e.g.,

$$RCH(O\cdot)\text{-}O\text{-}CO\text{-}R' \rightarrow RC(O)\cdot + O{=}C(OH)\text{-}R'.$$

In order to account for the product data in the reactions of OH + methyl (Christensen et al, 2000) and ethyl (Tuazon et al, 1998b) acetates, it is necessary to assume that this "ester rearrangement" reaction occurs at a non-negligible or rapid rate. Therefore, this reaction must be taken into account when generating mechanisms for esters.

The available data give some limited information upon which to base quantitative estimates for the rate constants for these reactions. In the case of the alkoxy radical formed from methyl acetate [CH_3-CO-O-$CH_2O\cdot$], the product data reported by Christensen et al (2000) indicated that the ester rearrangement occurs at a rate that is about 0.54 times that of the competing reaction with O_2 under ambient conditions. Based on the 298K rate constant for the reaction of O_2 with this radical estimated as discussed in Section III.J.1, this gives a 298K rate constant for the ester rearrangement to be 1.5×10^{-4} sec^{-1}. In the case of the radical formed from ethyl acetate [$CH_3CH(O\cdot)O$-CO-CH_3], the data of Tuazon et al (1998b) indicate that the ester rearrangement dominates over the competing reactions of this alkoxy radical (primarily reaction with O_2 and decomposition to CH_3CHO and $CH_3CO_2\cdot$), which are estimated to have a total rate constant of $\sim 5 \times 10^4$ sec^{-1} under atmospheric conditions. This means that the ester rearrangement for this radical must have a rate constant of at least $\sim 3 \times 10^5$ sec^{-1} under ambient conditions. The differences in these two rate constants can be explained if it is assumed that the ester rearrangement rate constant depends on the heat of reaction. In particular, the ester rearrangement for the radical formed from methyl acetate is estimated to be endothermic by ~3 kcal/mole, while the more rapid ester rearrangement of the radical formed from ethyl acetate is estimated to be endothermic by ~8.4 kcal/mole.

To obtain a rough estimate of temperature dependence, we assume that these ester rearrangements have an A factor of 8×10^{10} sec^{-1}, which is approximately the same as that used for 1,4-H shift isomerizations, based on expected similarities in the structure of the transition states. As with the decomposition reactions discussed above, the activation energy is assumed to linearly dependent on the heat of reaction, i.e.,

$$Ea(\text{ester rearrangement}) = EaA^{estr} + EaB^{estr} \cdot \Delta H_r \qquad \text{(XXV)}$$

where ΔH_r is the heat of reaction of the rearrangement. Obviously, the one quantitative rate constant derived from the methyl acetate data and the lower limit from the ethyl acetate data are insufficient to uniquely determine EaA^{estr} and EaB^{estr}. However, the results of the environmental chamber reactivity experiments for n-butyl acetate (Carter et al, 2000a; see also Section V.B) can only be fit by model simulations if the ester rearrangement for $CH_3CH_2CH_2CH(O\cdot)$-O-CO-CH_3 (radical 26 on Table 33) is of comparable rate or slower than the competing isomerization to $\cdot CH_2CH_2CH_2CH(OH)$-O-CO-CH_3, which means that this ester rearrangement, with an estimated ΔH_r of -8.1 kcal/mole, should have an estimated 298K rate constant of $\sim 3 \times 10^5$ sec-1 or less. To be consistent with this as well as the methyl and ethyl acetate product data discussed above, we assume that

$$EaA^{estr} = 10.23 \text{ kcal/mole}$$

and

$$EaB^{estr} = 0.35,$$

which yields

$$k(\text{ester rearrangement}) = 8 \times 10^{10}\ e^{-(10.23+0.35\Delta Hr)/RT} \qquad \text{(XXVI)}$$

Obviously, this is highly uncertain, and more quantitative information concerning relative rates of competing reactions involving this rearrangement, or at least more upper or lower limit data, would significantly reduce the uncertainty of these estimates.

Tuazon et al (1998b) saw no evidence that the analogous ester rearrangement reaction involving a 6-member ring transition state that might be expected to occur in the t-butyl acetate system, e.g.,

$$\cdot OCH_2C(CH_3)_2O\text{-}CO\text{-}CH_3 \rightarrow HC(O)C(\cdot)(CH_3)CH_3 + O{=}C(OH)\text{-}CH_3$$

in fact occurs to any significant extent. Of course, this could be because the competing decomposition to HCHO + $CH_3C(\cdot)$(CH3)-O-CO-CH_3 is predicted to be very fast, with an estimated rate constant of ~3 x 10^7 sec^{-1}. Nevertheless, we tentatively assume that these reactions are not important, and the possibility that they may occur is not presently incorporated in the mechanism generation system. However, the possibility that this occurs needs to be investigated.

6. Acyloxy Radicals

Acyloxy radicals are radicals of the form RC(O)O· or HC(O)O·. It is expected that the decomposition of RC(O)O· to R· and CO_2,

$$RC(O)O\cdot \rightarrow R\cdot + CO_2$$

should be rapid, based on thermochemical considerations, so this is assumed to be its major fate when it is generated in the mechanisms. In the case of HC(O)O·, the it is assumed to be consumed by rapid reaction with O_2.

$$HC(O)O\cdot + O_2 \rightarrow HO_2 + CO_2$$

Although it is also possible that it may primarily decompose to H· + CO_2, under atmospheric conditions the net effect would be the same because the major fate of H· atoms is reaction with O_2, forming HO_2.

7. Explicit Alkoxy Reaction Assignments

Because of the uncertainties in estimating alkoxy radical rate constants, explicit assignments of alkoxy radical rate constants or branching ratios are used rather than estimates whenever there are sufficient data available to make such assignments. These are shown on Table 30 through Table 33, above, where Table 30 contains the explicit assignments for the three measured alkoxy + O_2 reactions, Table 31 shows the assignments used for the butoxy and pentoxy isomerizations, Table 32 shows the assignments for those decompositions where quantitative rate constant assignments could be made, and Table 33 shows the assignments where the available data are appropriate for assigning branching ratios only. Note that many of these are quite uncertain, in most cases being based on highly indirect determinations or adjustments in complex mechanisms to fit reactivity data in chamber experiments, and having highly uncertain, usually estimated, reference rate constants. Note also that the system does not incorporate temperature dependence estimates for those reactions on Table 33 where only branching ratio assignments could be made, so the estimates may not be applicable for temperatures much different from ~300K. Nevertheless, these are less uncertain than the rate constants or branching ratios that have to be based entirely on estimates.

The reactions of isoprene, isoprene products and alkynes involve the formation of radicals whose mechanisms cannot be estimated because of lack of available thermochemical data, so explicit assignments have to be made in those cases so reactions of those compounds could be generated. These assignments are listed on Table 36, along with footnotes indicating the basis for the assignments. Note that those for radicals formed from isoprene and its products are based on estimates incorporated in the isoprene and isoprene products mechanism of Carter and Atkinson (1996), and those for other radicals are based on analogy for reactions of similar radicals for which estimates could be made.

8. Thermochemical Assignments Used in Estimates

Many of the estimates of alkoxy radical rate constants discussed above require a knowledge or estimate of the heats of reaction for the reactions being considered. These are estimated using the group additivity methods of Benson (1976), using updated group additivity data that were obtained primarily from the NIST (1994) thermochemical database. Although that database is extensive, it is not sufficient for many of the reactions that need to be considered, and assignments or estimates for additional groups had to be added. Table 37 and Table 38 give a complete listing of the thermochemical group assignments currently incorporated in the database. Table 37 gives the data obtained from the NIST (1994) database,and Table 38 gives the thermochemical assignments that were added for this work, indicating the source of the assignments.

Note that there were insufficient resources in this project to comprehensively review the available and most up-to-date thermochemical group data, so some of the assignments shown on Table 38 may not necessarily represent the state of the art, and they probably can be improved significantly in some cases. However, given the other uncertainties of the estimation methods discussed above, it is suspected that this probably does not represent the largest source of uncertainty involved, at least in most cases.

The more significant problem with the thermochemical assignment database in the current mechanism generation system is a lack of assignments for certain groups, which limits the overall scope of the mechanism generation system. In particular, the limited number of assignments for halogenated groups (particularly those containing radicals) means that mechanisms cannot be generated for most halogenated compounds. Also, the lack of assignments for unsaturated radicals means the system cannot automatically generate mechanisms for abstraction reactions from alkenes [which are believed to be non-negligible for longer chain alkenes (Atkinson, 1997a)] or reactions of OH or NO_3 radicals with dialkenes. Lack of thermochemical group estimates also prevents mechanisms from being generated for certain highly substituted groups as well. Because of this, improving the thermochemical database must be a priority when this system is updated.

K. Reactions of Crigiee Biradicals

Crigiee biradicals, i.e., species of the type >C[·]OO·, are assumed to be formed in the reactions of O_3 with alkenes or alkynes, and by the reactions of carbenes (which are assumed to be formed in the photolyses of some unsaturated compounds) with O_2. These radicals are believed to be formed with initial vibrational excitation, and can undergo various unimolecular decompositions or be collisionally stabilized. The ranges of excitation energies of the biradicals formed from the reactions of carbenes with O_2 or O_3 with alkynes are almost certainly different from those formed in the reactions of O_3 with alkenes, so in general one might expect the branching ratios for the decomposition and stabilization routes to differ depending on the source of the biradicals. However, because of lack of information concerning the former reactions we assume that they react with the same mechanism as determined from O_3 + alkene systems.

Table 36. Explicit assignments for reactions of alkoxy radicals whose mechanisms could not be estimated.

Radical	Products	Ratio	Notes
Isoprene Intermediates			
HO-CH2-C(CH3)=CH-CH2O.	HO-CH2-CH=C(CH3)-CH[.]-OH		1
HO-CH2-C(CH3)=CH(CH2O.)	HO-CH2-C(CH2.)=CH(CH2-OH)		1
CH2=C(CH2-OH)-CH[O.]-CH2-OH	CH2=C(CHO)-CH2-OH + HO-CH2.		1
CH2=CH-C[O.](CH3)-CH2-OH	CH2=CH-CO-CH3 + HO-CH2.		1
CH3-C(CH2O.)=CH(CH2-OH)	HO-CH2-C(CH3)=CH-CH[.]-OH		1
CH3-C(CH2O.)=CH-CH2-OH	CH3-C(CHO)=CH-CH2-OH + HO2.		1
CH2=C(CH3)-CH[O.]-CH2-OH	CH2=C(CHO)-CH3 + HO-CH2.		1
CH2=CH-C(OH)(CH2O.)-CH3	*C(CH3)(OH)-CH2-O-CH2-CH[.]-*		1
CH2=C(CH3)-CH(CH2O.)-OH	*CH(OH)-C[.](CH3)-CH2-O-CH2-*		1
CH2=CH-CO-CH2O.	HCHO + CH2=CH-CO.		1
Isoprene Product Intermediates			
HCO-CO-CH2O.	HCHO + HCO-CO.		1
.OCH2-CH=C(CH3)-CH2-ONO2	HCO-CH=C(CH3)-CH2-ONO2 + HO2.	80%	1
	HO-CH2-CH=C(CH3)-CH[.]-ONO2	20%	
Alkyne and Diene Intermediates			
CH3-CH[O.]-CO-CHO	CH3-CHO + HCO-CO.		2
CH3-CO-CO-CH2O.	HCHO + CH3-CO-CO.		3
CH2=CH-CH[O.]-CH2-OH	CH2=CH-CHO + HO-CH2.		4
HO-CH2-CH=CH(CH2O.)	HCO-CH=CH(CH2-OH) + HO2.		5
HO-CH2-CH=CH-CH2O.	HO-CH2-CH=CH-CH[.]-OH		6
CH2=CH-CH[O.]-CHO	CH2=CH-CHO + HCO.		7
.OCH2-CH=CH(CH2-ONO2)	HCO-CH=CH(CH2-ONO2) + HO2.		5
.OCH2-CH=CH-CH2-ONO2	HO-CH2-CH=CH-CH[.]-ONO2		6
CH2=CH-CH[O.]-CH2-ONO2	CH2=CH-CO-CH2-ONO2 + HO2.		8

Notes

1 As assumed by Carter and Atkinson (1996).

2 Assumed to be fast by analogy with estimated reactions for CH_3-CH[O.]-CO-R radicals.

3 Assumed to be fast by analogy with estimated reactions for CH_3-CO-CH_2O. radicals.

4 Assumed to be fast by analogy with estimated reactions for R-CH[O.]-CH_2-OH radicals.

5 Assumed to be fast based on lack of facile decomposition routes, and the fact that isomerization would involve a trans cyclic transition state.

6 Isomerization, which is permitted by the cis configuration, is expected to dominate.

7 Assumed to be fast by analogy with estimated reactions for R-CH[O.]-CHO radicals.

8 Reaction with O_2 estimated to be the major route based on the estimated mechanism for CH_3-CH2-CH[O.]-CH_2-ONO_2.

Table 37. Thermochemical group assignments used for estimating heats of reaction for rate constant estimation purposes that were obtained from the NIST (1994) database, or assigned as zero. Estimation methods and notation based on Benson (1976).

Group	kcal/mole	Group	kcal/mole	Group	kcal/mole
		From NIST (1994)			
C*_(C)	39.10	C_(C)(Cd)	-4.76	Cd_(Cd)(Cd)(Cd)	4.60
C*_(C)(C)	40.95	C_(C)(Cd)(O)	-6.50	Cd_(Cd)(Cd)(O)	8.90
C*_(C)(C)(C)	42.60	C_(C)(Cl)	-15.60	Cd_(Cd)(CO)	5.00
C*_(C)(O)	35.10	C_(C)(Cl)(Cl)	-18.90	Cd_(Cd)(CO)(O)	11.60
C*_(CO)	37.90	C_(C)(Cl)(Cl)(Cl)	-24.90	Cd_(Cd)(O)	8.60
C_(*CO)	-5.40	C_(C)(Cl)(F)(F)	-106.30	CO_(C)	-29.10
C_(*CO)(C)	-0.30	C_(C)(Cl)(O)	-21.60	CO_(C)(C)	-31.40
C_(*CO)(C)(C)	2.60	C_(C)(CO)	-5.20	CO_(C)(C*)	-31.40
C_(Br)(Br)(Br)(C)	3.90	C_(C)(CO)(Cl)	-22.00	CO_(C)(Cl)	-47.92
C_(Br)(C)	-5.40	C_(C)(F)	-51.50	CO_(C)(CO)	-29.20
C_(Br)(C)(C)	-3.40	C_(C)(F)(F)	-102.30	CO_(C)(F)	-95.50
C_(Br)(C)(C)(C)	-0.40	C_(C)(F)(F)(F)	-158.00	CO_(C)(I)	-20.00
C_(Br)(C)(Cl)	-10.10	C_(C)(I)	8.00	CO_(C)(O)	-35.10
C_(C)	-10.20	C_(C)(I)(I)	26.00	CO_(Cd)	-29.10
C_(C)(C)	-4.93	C_(C)(NO2)	-14.40	CO_(Cd)(O)	-32.00
C_(C)(C)(C)	-1.90	C_(C)(O)	-8.10	CO_(Cl)(O)	-49.20
C_(C)(C)(C)(C)	0.50	C_(C)(O)(O)	-16.30	CO_(CO)	-25.30
C_(C)(C)(C)(Cd)	1.68	C_(C)(O)(O)(O)	-29.60	CO_(CO)(Cl)	-40.15
C_(C)(C)(C)(Cl)	-12.80	C_(C)(O*)	6.10	CO_(CO)(O)	-29.30
C_(C)(C)(C)(CO)	1.40	C_(C)(O*)	6.10	CO_(O)	-32.10
C_(C)(C)(C)(F)	-48.50	C_(C*)	-10.08	CO_(O)(O)	-29.70
C_(C)(C)(C)(I)	13.00	C_(Cd)	-10.20	N_(C)(F)(F)	-7.80
C_(C)(C)(C)(NO2)	-11.70	C_(Cd)(Cd)	-4.29	O_(C)	-37.90
C_(C)(C)(C)(O)	-6.60	C_(Cd)(CO)	-3.80	O_(C)(C)	-23.20
C_(C)(C)(C)(O*)	8.60	C_(CO)	-10.20	O_(C)(C*)	-23.20
C_(C)(C)(Cd)	-1.48	C_(CO)(Cl)	-10.20	O_(C)(Cd)	-30.50
C_(C)(C)(Cl)	-14.80	C_(CO)(Cl)(Cl)	-12.00	O_(C)(CO)	-43.10
C_(C)(C)(Cl)(Cl)	-22.00	C_(CO)(Cl)(Cl)(Cl)	-11.80	O_(C)(NO2)	-19.40
C_(C)(C)(CO)	-1.70	C_(CO)(CO)	-7.60	O_(C)(O)	-4.50
C_(C)(C)(F)	-49.00	C_(I)(O)	3.80	O_(C*)	-37.90
C_(C)(C)(F)(F)	-97.00	C_(O)	-10.20	O_(Cd)(Cd)	-33.00
C_(C)(C)(I)	10.50	C_(O)(O)	-16.10	O_(Cd)(CO)	-45.20
C_(C)(C)(NO2)	-13.60	Cd_(C)(C)(Cd)	10.34	O_(CO)	-58.10
C_(C)(C)(O)	-7.20	Cd_(C)(Cd)	8.59	O_(CO)(CO)	-46.50
C_(C)(C)(O)(O)	-18.60	Cd_(C)(Cd)(Cd)	8.88	O_(CO)(O)	-19.00
C_(C)(C)(O*)	7.80	Cd_(C)(Cd)(CO)	7.50	O_(NO2)(O)	4.00
C_(C)(C*)	-4.95	Cd_(C)(Cd)(O)	10.30	O_(O)	-16.30
C_(C)(C*)(C)	-1.90	Cd_(Cd)	6.26	O_(O)(O)	14.70
C_(C)(C*)(C)(C)	1.50	Cd_(Cd)(Cd)	6.78		
		Assigned to Zero			
*CO_(C)	0.00	Cl_(C)	0.00	I_(CO)	0.00
*CO_(CO)	0.00	Cl_(CO)	0.00	NO2_(C)	0.00
Br_(C)	0.00	F_(C)	0.00	NO2_(O)	0.00
Br_(C*)	0.00	F_(CO)	0.00	ONO2_(C)	0.00
Br_(CO)	0.00	I_(C)	0.00		

Table 38. Thermochemical group assignments used for estimating heats of reaction for rate constant estimation purposes that were derived for this work. Estimation methods and notation based on Benson (1976).

Group	ΔH_f (kcal/mole)	Documentation
*CO_(O)	-4.20	The C-H bond energy in formates is estimated to be 95 kcal/mole or higher based on an assumed correlation between bond the dissociation energy and CO-H + OH rate constants.
*CO_(ONO2)	-19.40	Calculated from O_(C)(NO2) + *CO_(O), *CO_(O).
C*_(Br)(C)	41.78	Estimated using an assumed correlation between the OH radical rate constants and the bond dissociation energies for alkanes and methanol, and the OH radical rate constant estimated using group additivity.
C*_(C)(C)(CO)	42.25	Estimated assuming that the heat of reaction of CH3-C[.](CH3)-CHO + CH3-CH2-CHO = CH3-CH(CH3)-CHO + CH3-CH[.]-CHO is zero.
C*_(C)(C)(O)	31.50	Estimated assuming that the heat of reaction of CH3-C[.](CH3)OH + CH3-CH(CH3)CH3 + CH3-CH2-OH + CH3-CH[.]-CH3 = CH3-CH(CH3)OH + CH3-C[.](CH3)CH3 + CH3-CH[.]-OH + CH3-CH2-CH3 is zero.
C*_(C)(C)(ONO2)	12.10	Estimated assuming that the heat of reaction of CH3-C[.](ONO2)-CH3 = CH3-C[.](O-NO2)-CH3 is zero.
C*_(C)(CO)	38.58	Estimated assuming that the heat of reaction of CH3-CO-CH2. + CH3-CH2-CO-CH3 + CH3-CH2-CH3 + CH3-CH2-CH[.]-CH3 = CH3-CO-CH3 + CH3-CH[.]-CO-CH3 + CH3-CH2-CH2. + CH3-CH2-CH2-CH3 is zero.
C*_(C)(CO)(O)	32.46	Assumed that the carbonyl group does not affect the C..H bond dissociation energy.
C*_(C)(O)(O)	24.50	Estimated assuming that the heat of reaction of HO-CH(CH3)-OH + HO-CH[.]-CH3 = HO-C[.](CH3)-OH + HO-CH2-CH3 is zero.
C*_(C)(ONO2)	15.70	Calculated from O_(C)(NO2) + C*_(C)(O).
C*_(CO)(O)	34.95	Assumed to be the same as normal primary alcohols, i.e., that carbonyl group does not affect bond dissociation energy.
C*_(CO)(ONO2)	15.55	Estimated assuming that the heat of reaction of HCO-CH[.]-ONO2 = HCO-CH[.]-O-NO2 is zero.
C*_(O)	35.75	This was 33.7 kca/mole in the NIST database. Adjusted to agree with the heat of formation of .CH2OH given by IUPAC (1996)
C*_(O)(O)	29.93	Estimated assuming that the heat of reaction of HO-CH2-OH + HO-CH2. = HO-CH[.]-OH + HO-CH3 is zero.
C*_(ONO2)	16.35	Calculated from O_(C)(NO2) + C*_(O).
C_(*CO)(C)(C)(C)	5.70	CH3-C(CH3)(CH3)-CHO is assumed to have the same CO..H bond dissociation energy as CH3-CH(CH3)-CHO.
C_(*CO)(C)(C)(CO)	3.25	CH3-C(CH3)(CHO)-CO..H is assumed to have the same bond dissociation energy as CH3-CO..H.
C_(*CO)(C)(C)(O)	-0.98	CH3-C(CH3)(OH)CO..H is assumed to have the same bond dissociation energy as CH3-CO..H.
C_(*CO)(C)(CO)	0.15	CH3-CH(CHO)-CO..H is assumed to have the same bond dissociation energy as CH3-CO..H.
C_(*CO)(C)(CO)(O)	-3.85	CH3-C(OH)(CHO)-CO..H is assumed to have the same bond dissociation energy as CH3-CO..H.
C_(*CO)(C)(O)	-1.60	CH3-CH(CHO)-CO..H is assumed to have the same bond dissociation energy as CH3-CO..H.
C_(*CO)(C)(ONO2)	-20.53	CH3-CH(ONO2)-CHO is assumed to have the same (CO)..H bond dissociation energy as CH3-CH2-CHO.

Table 38 (continued)

Group	ΔH_f (kcal/mole)	Documentation
C_(*CO)(CO)	-2.41	HCO-CH2-CHO is assumed to have the same (CO)..H bond dissociation energy as CH3-CH2-CHO.
C_(*CO)(CO)(O)	-4.47	CH3-CH(CHO)-CO..H is assumed to have the same bond dissociation energy as CH3-CO..H.
C_(*CO)(CO)(ONO2)	-23.87	CH3-CH(CHO)-CO..H is assumed to have the same bond dissociation energy as CH3-CO..H.
C_(*CO)(O)	-1.76	CH3-O-CH2-CHO is assumed to have the same (CO)..H bond dissociation energy as CH3-CH2-CHO.
C_(*CO)(O)(O)	-10.70	HO-CH(OH)-CO..H is assumed to have the same bond dissociation energy as CH3-CO..H.
C_(*CO)(ONO2)	-21.17	HCO-CH2-ONO2 is assumed to have same (CO)..H bond dissociation energy as CH3-CH2-CHO.
C_(Br)(C)(CO)	4.00	The heat of reaction for CH3-CH(CHO)-Br + CH3. = CH3-CH(CHO)-CH3 + Br. is assumed to be the same as that for analogous reactions of CH3-CH(Cl)-Br.
C_(Br)(C)(O)	-2.50	The heat of reaction for CH3-CH(OH)-Br + CH3. = CH3-CH(OH)-CH3 + Br. is assumed to be the same as that for analogous reactions of CH3-CH(Cl)-Br.
C_(Br)(C)(O*)	12.50	The heat of reaction for CH3-CH[O.]-Br + CH3. = CH3-CH[O.]-CH3 + Br. is assumed to be the same as that for analogous reactions of CH3-CH(Cl)-Br.
C_(Br)(C*)	-6.67	The heat of reaction for .CH2-CH2-Br + CH3. = .CH2-CH2-CH3 + Br. is assumed to be the same as that for analogous reactions for alkyl groups.
C_(Br)(CO)	-6.27	The heat of reaction for CH3-CO-CH2-Br + CH3. = CH3-CO-CH2-CH3 + Br. is assumed to be the same as that for analogous reactions for alkyl groups.
C_(Br)(O)	-3.70	Estimated assuming that the heat of reaction of Br-CH2O. + CH3-OH = Br-CH2-OH + CH3O. is zero.
C_(Br)(O*)	10.79	The heat of reaction for .OCH2-Br + CH3. = .OCH2-CH3 + Br. is assumed to be the same as that for analogous reactions of CH3-CH(Cl)-Br.
C_(Br)(OO*)	9.30	Estimated assuming that the heat of reaction of Br-CH2OO. + CH3-O-OH = Br-CH2-O-OH + CH3OO. Is zero.
C_(C)(C)(C)(C*)	-1.20	Estimated assuming that the heat of reaction of CH3-C(CH3)(CH3)-CH3 = CH3-C(CH3)(CH3)CH2. + H. is 99.7.
C_(C)(C)(C)(NO2)	-11.70	Note in NIST database: “Benson's value -15.8”
C_(C)(C)(C)(ONO2)	-26.00	Calculated from O_(C)(NO2) + C_(C)(C)(C)(O).
C_(C)(C)(C)(OO*)	5.50	The bond dissociation energy for ROO..H is assumed to be 85.0 based on IUPAC heats of formation for CH3OO. and C2H5OO.
C_(C)(C)(C*)	-3.60	Estimated assuming that the heat of reaction of CH3-CH(CH3)CH3 = CH3-CH(CH3)CH2. + H. is 99.7
C_(C)(C)(C*)(CO)	-0.30	The bond dissociation energy for HO-CH(..H)-C(CH3)(CH3)-CHO is assumed to be the same as that for HO-CH[..H]-CH2-CHO.
C_(C)(C)(C*)(O)	-8.90	Estimated assuming that the heat of reaction of CH3-C(CH3)(OH)-CH2. + CH3-CH(OH)-CH3 = CH3-C(CH3)(OH)-CH3 + CH3-CH(OH)-CH2. Is zero.
C_(C)(C)(C*)(ONO2)	-28.30	Estimated assuming that the heat of reaction of .CH2-C(CH3)(CH3)-ONO2 = .CH2-C(CH3)(CH3)-O-NO2 is zero.
C_(C)(C)(CO)(CO)	-1.47	Estimated assuming that the heat of reaction of HCO-CH(CH3)-CHO + CH3-C(CH3)(CH3)-CHO = HCO-C(CH3)(CH3)-CHO + CH3-CH(CH3)-CHO is zero.
C_(C)(C)(CO)(O)	-5.70	Estimated assuming that the heat of reaction of CH3-C(OH)(CH3)-CHO + CH3-C(CH3)(CH3)CH3 = CH3-C(CH3)(CH3)CHO + CH3-C(OH)(CH3)-CH3 is zero.

Table 38 (continued)

Group	ΔH_f (kcal/mole)	Documentation
C_(C)(C)(CO)(O*)	9.50	Estimated assuming that the heat of reaction of CH3-C(OH)(CH3)CHO + CH3-C[O.](CH3)CH3 = CH3-C[O.](CH3)CHO + CH3-C(OH)(CH3)CH3 is zero.
C_(C)(C)(CO)(ONO2)	-25.10	Estimated assuming that the heat of reaction of CH3-C(CH3)(ONO2)-CO-CH3 = CH3-C(CH3)(O-NO2)-CO-CH3 is zero.
C_(C)(C)(NO2)	-13.60	Notation in NIST database: “Benson's value -15.1”
C_(C)(C)(O)(O*)	-3.40	Assumed to have same O..H bond dissociation energy as that for t-butanol.
C_(C)(C)(O)(ONO2)	-38.00	Calculated from O_(C)(NO2) + C_(C)(C)(O)(O).
C_(C)(C)(O)(OO*)	-6.50	The bond dissociation energy for ROO..H is assumed to be 85.0 based on IUPAC heats of formation for CH3OO. and C2H5OO.
C_(C)(C)(O*)(ONO2)	-23.80	Calculated from O_(C)(NO2) + C_(C)(C)(O)(O*).
C_(C)(C)(ONO2)	-26.60	Calculated from O_(C)(NO2) + C_(C)(C)(O).
C_(C)(C)(OO*)	4.90	The bond dissociation energy for ROO..H is assumed to be 85.0 based on IUPAC heats of formation for CH3OO. and C2H5OO.
C_(C)(C*)(CO)	-3.40	Estimated assuming that the heat of reaction of CH3-CO-CH(CH3)-CH2. + CH3-CH(CH3)-CH3 = CH3-CO-CH(CH3)-CH3 + CH3-CH(CH3)-CH2. is zero.
C_(C)(C*)(CO)(O)	-8.00	Estimated assuming that the heat of reaction of CH3-O-C(CH3)(CHO)-CH2. + CH3-O-C(CH3)(CH3)-CH3 = CH3-O-C(CH3)(CHO)-CH3 + CH3-O-C(CH3)(CH3)-CH2. is zero.
C_(C)(C*)(CO)(ONO2)	-27.40	HCO-C(CH3)(ONO2)-CH3 is assumed to have the same CH2..H bond dissociation energy as HCO-C(CH3)(OH)-CH3.
C_(C)(C*)(O)	-9.50	Assumed to have a C..H bond dissociation energy of 100.
C_(C)(C*)(O)(O)	-21.50	Difference between bond dissociation energy for CH3-C(OH)(OH)-CH(CH3)..H and CH3-C(CH3)(OH)-CH(CH3)..H is assumed to be the same as the difference between bond dissociation energy for CH3-C(CH3)(OH)-CH(CH3)..H and CH3-C(CH3)(CH3)-CH(CH3)..H.
C_(C)(C*)(ONO2)	-28.90	Calculated from O_(C)(NO2) + C_(C)(C*)(O).
C_(C)(Cd)(ONO2)	-25.90	Calculated from O_(C)(NO2) + C_(C)(Cd)(O).
C_(C)(Cl)(O*)	-6.60	The heat of reaction for CH3-CH[O.]-Cl + CH3. = CH3-CH[O.]-CH3 + Cl. is assumed to be the same as those for analogous reactions of compounds with the C_ClHO group.
C_(C)(Cl)(ONO2)	-41.00	Calculated from O_(C)(NO2) + C_(C)(Cl)(O).
C_(C)(CO)(CO)	-4.57	Estimated assuming that the heat of reaction of CH3-CO-CH2-CO-CH3 + CH3-CH2-CH(CH3)-CH2-CH3 = CH3-CO-CH(CH3)-CO-CH3 + CH3-CH2-CH2-CH2-CH3 is zero.
C_(C)(CO)(CO)(O)	-8.57	Estimated assuming that the heat of reaction of HCO-C(CH3)(OH)-CHO + HCO-C(CH3)(CH3)-CH3 = HCO-C(CH3)(CH3)-CHO + HCO-C(CH3)(OH)-CH3 is zero.
C_(C)(CO)(CO)(O*)	6.63	CH3-C[O..H](CHO)-CHO is assumed to have the same bond dissociation energy as CH3-C[O..H](CH3)-CH3.
C_(C)(CO)(O)	-6.32	Estimated assuming that the heat of reaction for CH3-CH2-OH + CH3-CHO = CH3-CH3 + HOCH2-CHO is the same as the heat of reaction for CH3-CH(OH)-CH3 + CH3-CH2-CHO -> CH3-CH(OH)-CHO + CH3-CH2-CH3.
C_(C)(CO)(O)(O)	-17.70	Estimated assuming that the heat of reaction of CH3-O-C(CHO)(CH3)-O-CH3 + CH3-O-C(CH3)(CH3)-CH3 = CH3-O-C(CH3)(CH3)-O-CH3 + CH3-O-C(CHO)(CH3)-CH3 is zero.
C_(C)(CO)(O)(O*)	-2.50	Radicals with this group are assumed to have the same O..H bond dissociation energy as analogous radicals formed from other tertiary alcohols.
C_(C)(CO)(O*)	7.87	An H-O bond dissociation energy of 104.2 is assumed.

Table 38 (continued)

Group	ΔH_f (kcal/mole)	Documentation
C_(C)(CO)(ONO2)	-25.72	Estimated assuming that the heat of reaction of CH3-CH(ONO2)-CO-CH3 = CH3-CH(O-NO2)-CO-CH3 is zero.
C_(C)(NO2)(NO2)	-9.90	Note in NIST database: "DIPPR value -16.5, No Benson H-value, this from literature".
C_(C)(O)(O)(ONO2)	-49.00	Calculated from O_(C)(NO2) + C_(C)(O)(O)(O).
C_(C)(O)(O*)	-2.10	The O..H bond dissociation energy is assumed to be the same as that for CH3-CH2-CH2-O..H.
C_(C)(O)(ONO2)	-35.70	Calculated from O_(C)(NO2) + C_(C)(O)(O).
C_(C)(O)(OO*)	-4.20	The bond dissociation energy for ROO..H is assumed to be 85.0 based on IUPAC heats of formation for CH3OO. and C2H5OO.
C_(C)(O*)(ONO2)	-21.50	Calculated from O_(C)(NO2) + C_(C)(O)(O*).
C_(C)(ONO2)	-27.50	Calculated from O_(C)(NO2) + C_(C)(O).
C_(C)(OO*)	3.34	Based on IUPAC heats of formation for CH3-CH2OO.
C_(C*)(Cl)	-18.01	The heat of reaction for .CH2-CH2-Cl + CH3. = .CH2-CH2-CH3 + Cl. is assumed to be the same as for analogous reactions of chloroalkanes.
C_(C*)(CO)	-6.90	The bond dissociation energy for H..CH2-CH2-CHO is assumed to be the same as that for H..CH2-CH2-CH3.
C_(C*)(CO)(O)	-8.02	Estimated assuming that the heat of reaction of HCO-CH(CH2.)OH + CH3-CH(CH3)CH3 = HCO-CH(CH3)OH + CH3-CH(CH2.)CH3 is zero.
C_(C*)(CO)(ONO2)	-27.42	HCO-CH(ONO2)-CH3 is assumed to have same CH2..H bond dissociation energy as HCO-CH(OH)-CH3.
C_(C*)(O)	-9.73	Estimated using heat of formation of n-propyl.
C_(C*)(O)(O)	-18.60	The bond dissociation energy for CH3-O-CH(OH)-CH2..H is assumed to be the same as for CH3-CH(OH)-CH2...H.
C_(C*)(ONO2)	-29.13	Calculated from O_(C)(NO2) + C_(C*)(O).
C_(Cd)(O)	-8.05	Set to give same estimated heat of formation for CH2=CH-CH2-OH as as tabulated by NIST at http://webbook.nist.gov/
C_(Cd)(O*)	5.25	CH2=CH-CH2-OH is assumed to have the same O..H bond dissociation energy as other primary alcohols.
C_(Cd)(OO*)	3.39	The O..H bond dissociation energy in allylic hydroperoxides is assumed to be the same as in alkyl hydroperoxides.
C_(Cl)(Cl)(O*)	-10.10	The heat of reaction of Cl-CH[O.]-Cl + CH3. = Cl-CH[O.]-CH3 + Cl. is assumed to be the same as for analogous reactions for dichlroralkanes.
C_(CO)(CO)(O)	-9.19	Estimated assuming that the heat of reaction of HCO-CH(OH)-CHO + HCO-CH(CH3)-CH3 = HCO-CH(CH3)-CHO + HCO-CH(OH)-CH3 is zero.
C_(CO)(CO)(O*)	5.81	Alcohols forming radicals with this group are assumed to have same O..H bond dissociation energy as other secondary alcohols.
C_(CO)(CO)(ONO2)	-28.59	Derived from the heat of formation of HCO-CH(O-NO2)-CHO.
C_(CO)(O)	-6.95	Estimated assuming Heat of reaction of -CO-CH2-CO- + CH2Cl2 = 2 -CO-CH2-Cl is the same as that for -CO-CH2-CO- + -O-CH2-O- = 2 -CO-CH2-O-.
C_(CO)(O)(O)	-15.42	Estimated assuming that the heat of reaction of HCO-CH(OH)-O-CH3 + CH3-CH(OH)-CH3 = HCO-CH(OH)-CH3 + CH3-CH(OH)-O-CH3 is zero.
C_(CO)(O)(O*)	-1.22	CH3-O-CH(OH)-CO-CH3 is assumed to have the same O..H bond dissociation energy as CH3-CH2-CH2-OH.
C_(CO)(O*)	7.24	Alcohols forming this radical are assumed to have the same O..H bond dissociation energy as CH3-CH2-CH2-O..H Note that this depends on highly uncertain assignment for C_(CO)O.
C_(CO)(ONO2)	-26.36	Calculated from O_(C)(NO2) + C_(CO)(O).
C_(CO)(OO*)	6.05	Estimated assuming that the heat of reaction of CH3-CO-CH2-O-OH + CH3OO. = CH3-CO-CH2OO. + CH3-O-OH is zero.

Table 38 (continued)

Group	ΔH_f (kcal/mole)	Documentation
C_(I)(ONO2)	-15.60	Calculated from O_(C)(NO2) + C_(I)(O).
C_(O)(O)(O)	-26.92	Based on average of the heats of formation of trimethoxy methane as tabulated by NIST at http://webbook.nist.gov/.
C_(O)(O)(O)(O)	-40.25	Based on average of the heats of formation of tetramethoxy methane tabulated by NIST at http://webbook.nist.gov/.
C_(O)(O)(O)(O*)	-25.05	Alcohols forming radicals with this group are assumed to have same O..H bond dissociation energy as other tertiary alcohols.
C_(O)(O)(O*)	-12.72	CH3-O-CH(OH)-O-CH3 is assumed to have the same O..H bond dissociation energy as CH3-O-CH(OH)-CH3.
C_(O)(O*)	-1.90	Alcohols forming radicals with this group are assumed to have same bond dissociation energy as CH3-CH2-CH2-O..H.
C_(O)(ONO2)	-35.50	Calculated from O_(C)(NO2) + C_(O)(O).
C_(O)(OO*)	-4.00	The bond dissociation energy for ROO..H is assumed to be 85.0 based on IUPAC heats of formation for CH3OO. and C2H5OO.
C_(O*)(ONO2)	-21.30	Calculated from O_(C)(NO2) + C_(O)(O*).
C_(ONO2)	-29.60	Calculated from O_(C)(NO2) + C_(O).
C_(OO*)	2.49	Estimated using IUPAC (1996) heats of formation for CH3OOH and CH3OO.
CO_(*CO)	-16.78	RCO-CO..H is assumed to have same bond dissociation energy as R-CO..H.
CO_(*CO)(C)	-20.77	CH3-CO-CO..H is assumed to have the same bond dissociation energy as CH3-CO..H.
CO_(*CO)(O)	-20.78	ROCO-CO..H is assumed to have same bond dissociation energy as RCO..H
CO_(Br)	-25.73	The heat of reaction of HCO-Br + CH3. = HCO-CH3 + Br. is assumed to be the same as analogous reactions of CH3-CH(Cl)-Br.
CO_(Br)(C)	-27.81	The heat of reaction of CH3-CO-BR + CH3. = CH3-CO-CH3 + Br. is assumed to be the same as analogous reactions of CH3-CH(Cl)-Br.
CO_(C)(Cd)	-34.06	Derived to fit the heats of formation for CH2=CH-CO-CH3 in the NIST database at http://webbook.nist.gov/.
CO_(C)(O*)	-39.36	Derived from the IUPAC heat of formation for CH3COOH, and the CRC O..H bond dissociation energy.
CO_(C)(OO*)	-30.91	Derived using the IUPAC heat of formation for CH3-C(O)OO.
CO_(C*)	-29.10	The C..H bond dissociation energy forming radicals with this group is assumed to be the same as CH3-CO-CH2..H.
CO_(C*)(CO)	-31.10	Estimated assuming that the heat of reaction of CH3-CO-CO-CH3 + CH3-CO-CH2. = CH3-CO-CO-CH2. + CH3-CO-CH3 is zero.
CO_(C*)(O)	-34.10	Estimated using correlation between the OH radical rate constants and bond dissociation energies for alkanes and methanol, and the OH radical rate constant estimated using group additivity.
CO_(Cl)	-45.84	The heat of reaction for HCO-Cl + CH3. = HCO-CH3 + Cl. is assumed to be the same as for analogous reaction of R-CO-Cl.
CO_(Cl)(ONO2)	-68.60	Calculated from O_(C)(NO2) + CO_(Cl)(O).
CO_(CO)(CO)	-26.89	The heat of reaction for elimination of CO from CH3-CO-CO-CO-CH3 is assumed to be the same as for elimination of CO from biacetyl.
CO_(CO)(O*)	-33.70	bond dissociation energy for HCO-CO-O..H assumed to be the same as for CH3-CO-O..H and HCO-O..H
CO_(O)(O*)	-34.10	Estimated assuming that the heat of reaction of CH3-CO-OH + CH3-O-CO2. = CH3-CO2. + CH3-O-CO-OH is zero.
CO_(O)(OO*)	-25.51	The bond dissociation energy for CH3-O-CO-OO..H is assumed to be same as for CH3-CO-OO..H.

Table 38 (continued)

Group	ΔH_f (kcal/mole)	Documentation
CO_(O*)	-36.84	Estimated assuming that the heat of reaction of CH3-CO-OH + HCO2. = CH3-CO2. + HCO-OH is zero.
O_(*CO)	-42.64	HCO-OH is assumed to have same (CO)..H bond dissociation energy as CH3-O-CHO.
O_(*CO)(C)	-27.30	The bond dissociation energy for H-CO-O-R is estimated to be relatively high (~100) based on low OH radical rate constants for formates. Highly uncertain.
O_(*CO)(CO)	-30.70	The bond dissociation energy for HCO-O-CO..H is assumed to be the same as that for CH3-O-CO..H.
O_(C)(NO2)	-19.40	Notation in NIST database: “Benson value = -14.9”.
O_(C*)(CO)	-40.65	The bond dissociation energy for H...CH2-O-CO- is assumed to be the same as for CH3-CH2..H.
O_(C*)(NO2)	-12.45	Estimated using correlation between the OH radical rate constants and bond dissociation energies for alkanes and methanol, and the OH radical rate constant estimated using group additivity.
O_(C*)(O)	-4.50	Estimated assuming that the heat of reaction of *CH(CH3)-O-C[.](CH3)-O-O-O-* + HO-CH2-CH3 = *CH(CH3)-O-CH(CH3)-O-O-O-* + HO-CH[.]-CH3 is zero.
O_(Cd)	-44.86	Derived to fit the heat of formation of CH2=CH-OH in the NIST database at http://webbook.nist.gov/.
O_(NO2)(O)	4.00	Notation in the NIST database: “Alan Baldwin's value”.
O_(O)(O*)	17.50	Estimated assuming that the heat of reaction of CH3-O-O-OH + CH3OO. = CH3-O-O-O. + CH3-O-OH is zero.
O_(O*)(ONO2)	14.00	Calculated from O_(C)(NO2) + O_(O)(O*).
ONO2_(C*)	6.95	Derived from the heat of reaction derived for .CH2-O-NO2.

1. $HCHO_2$ Biradicals

Atkinson (1997a) reviewed available information concerning reactions of O_3 with alkenes, and recommended the following mechanisms for the reactions of excited $HCHO_2$ biradicals:

$$HCHO_2(\text{excited}) + M \rightarrow HCHO_2(\text{stabilized}) \quad (37\%)$$

$$HCHO_2(\text{excited}) \rightarrow HCO + OH \quad (12\%)$$

$$HCHO_2(\text{excited}) \rightarrow CO_2 + H_2 \quad (13\%)$$

$$HCHO_2(\text{excited}) \rightarrow CO + H_2O \quad (38\%)$$

These branching ratios are used in the current mechanism. As indicated in Section II.B.2, the stabilized biradicals are assumed to react primarily with H_2O, forming the corresponding acid, i.e.,

$$HCHO_2(\text{stabilized}) + H_2O \rightarrow HC(O)OH + H_2O$$

2. $RCHO_2$ Biradicals

The reactions of substituted Crigiee biradicals are more uncertain. In the case of excited CH_3CHO_2., the following routes, discussed by Atkinson (1997a), appear to be the most reasonable to consider[18]:

$$CH_3CHOO(excited) + M \rightarrow CH_3CHOO(stabilized) + M \quad (A)$$

$$CH_3CHO_2(excited) \rightarrow CH_3\cdot + CO + OH \quad (B)$$

$$CH_3CHO_2(excited) \rightarrow CH_3\cdot + CO_2 + H\cdot \quad (C)$$

$$CH_3CHO_2(excited) \rightarrow CH_4 + CO_2 \quad (D)$$

Based on examination of the available literature, Atkinson (1997a) recommends assuming branching ratios of 15%, 54%, 17%, and 14% for pathways A-D, respectively. In the case of other substituted biradicals, this scheme can be generalized to

$$RCHOO(excited) + M \rightarrow RCHOO(stabilized) + M \quad (A')$$

$$RCHO_2(excited) \rightarrow R\cdot + CO + OH \quad (B')$$

$$RCHO_2(excited) \rightarrow R\cdot + CO_2 + H\cdot \quad (C')$$

$$RCHO_2(excited) \rightarrow RH + CO_2 \quad (D')$$

Note that Pathway B can account for much of the OH radical formation observed in the reactions of O_3 with 1-alkenes. The measured yields of OH radicals from the reactions of O_3 with 1-butene through 1-octene, as summarized by Atkinson (1997a) (see also Table 18, above), do not appear to be greatly different from that for the reaction of O_3 with propene, suggesting that the branching ratios may not change as the size of the biradical increases.

However, assuming the relatively high branching ratios recommended by Atkinson (1997a) for Pathways B and C results in positive biases in model simulations of the large data base of propene - NO_x environmental chamber experiments, and in significant overpredictions of O_3 formation rates in 1-butene - NO_x and (especially) 1-hexene - NO_x environmental chamber experiments. Although there are other uncertainties in the mechanisms that could be causing these discrepancies, reasonably consistent fits to the data cannot be obtained unless it is assumed that (1) somewhat lower radical yields (i.e., lower yields of Pathways B and C) are assumed for the excited CH_3CHOO reactions than recommended by Atkinson (1997a), and (2) the radical yields (i.e., the yields of Pathways B' and C') decrease as the size of the molecule increases. Note that both assumptions are inconsistent with the observed OH yields in the reactions of O_3 with 1-alkenes (Atkinson, 1997a – see also Table 18, above), so there is an apparent inconsistency between the laboratory measurements of the OH yields in the O_3 + alkene reactions and the results of modeling the 1-alkene - NO_x chamber experiments used to evaluate the mechanism.

The reason for this apparent inconsistency is unknown, and it might be due in part to the fact that NO_x is present in the environmental chamber experiments but not in the laboratory systems used to measure the OH yields. However, the possibility that the problems with modeling the 1-alkene chamber experiments using the Atkinson (1997a)-recommended branching ratios are due to other problems with

[18] Two other routes, involving formation of $CH_3O\cdot$ + HCO and CH_3OH + CO, are also given by Atkinson (1997a), but are not considered here because they do not involve chemically reasonable transition states for vibrationally excited molecules.

the mechanism certainly cannot be ruled out. Nevertheless, satisfactory fits to the available data cannot be obtained even after adjusting or making reasonable modifications in the other uncertain aspects of the alkene photooxidation mechanisms. Because the objective of this project is to develop a mechanism that correctly predicts O_3 reactivities and other impacts of VOCs in simulated smog systems, it is necessary to use branching ratios that give predictions that are consistent with the large environmental chamber data.

The adjusted branching ratios for the reactions of excited $RCHO_2$ biradicals that are used in the current version of the mechanism are summarized on Table 39. As shown there, to fit the chamber data the biradicals are assumed to be increasingly likely to be stabilized as the size of the "R" substituent on the radical is increased. For this purpose, the "size" of the substituent is defined as the number of groups used by the mechanism generation system to define the substituent, as indicated in Table 5, above. Note that for biradicals formed from unsubstituted alkenes the number of groups is the same as the number of carbons. Footnotes to the table indicate the rationalizations for the particular sets of branching ratios used.

3. R_2COO Biradicals

Available information on OH yields from reactions of O_3 with alkenes such as isobutene, 2-methyl-2-butene, 2,3-dimethyl-2-butene and other compounds (Atkinson, 1997a – see also Table 18, above) are most easily rationalized if it is assumed that most excited R_2COO react forming OH radicals in near-unit yields. In contrast with the case with 1-alkenes, model simulations assuming high radical yields in the reactions of O_3 with such alkenes are also reasonably consistent with the available chamber data, at least in the case of isobutene and several of the terpenes that are expected to form this type of biradical (see Section V and Appendix B). If one of the R groups has an α hydrogen, the reaction is assumed to proceed via rearrangement to an unsaturated hydroperoxide, which subsequently decomposes (Atkinson, 1997a):

$$>CH\text{-}C(\cdot)(OO\cdot)R \rightarrow >C=C(OOH)R \rightarrow >C=C(O\cdot)R + OH$$

$$>C=C(O\cdot)R \leftrightarrow >C(\cdot)C(O)R$$

Although other reactions probably occur to some extent, this is assumed to be the dominant reaction pathway for R_2COO biradicals which have the necessary α hydrogen. It may be that this reaction also occurs with the stabilized biradical, which may explain why there is no indication of decreased OH yield as the size of the molecule increases.

If the two substituents on the biradical are different and both have abstractable α hydrogens, then two possible OH-forming reactions can occur. In these cases, we estimate that the branching ratio is roughly proportional to the ratio of OH radical abstraction from the abstracted α hydrogens involved. This is uncertain because there is no experimental basis for this estimate.

The above mechanism cannot occur for those disubstituted Crigiee biradicals that do not have substituents with α hydrogens. It is also considered to be unlikely if the only substituent(s) with α hydrogens are -CHO groups, since it is expected that formation of a ketene hydroperoxide intermediate would involve a strained transition state. In those cases (which probably do not occur in many cases for the VOCs currently considered in the mechanism), we arbitrarily assume that 90% is stabilized and 10% decomposes to CO_2 + 2 R·.

Table 39. Adjusted branching ratios used for the reactions of excited $RCHO_2$ biradicals..

Pathway		Branching Ratio				
Number of Groups in R.		1	2	3	4	5+
Stabilization -> RC(O)OH	(A)	34%	89%	92%	95%	100%
R. + CO + OH	(B)	52%	11%	8%	5%	0%
R. + CO2 + H	(C)	0%	0%	0%	0%	0%
RH + CO2	(D)	14%	0%	0%	0%	0%
Notes		1	2	3	4	5

Notes

1 OH yield and methane formation (Pathways B and D) approximately as recommended by Atkinson (1997a). Radical formation from Pathway C is assumed to be negligible to improve fits of model simulation to propene - NOx chamber experiments, and fraction of stabilization (Pathway A) is increased accordingly.

2 Radical formation from Pathway (C) is assumed to be negligible and OH formation from Pathway (B) is reduced to improve fits of model simulations to 1-butene - NOx chamber experiments. Rest of reaction is assumed to be stabilization.

3 Branching ratios intermediate between those derived for the 1-butene and 1-hexene systems.

4 Model simulations are most consistent with results of 1-hexene - NOx chamber experiments if radical formation from the reactions of this biradical is assumed to involve no more than ~5% radical formation routes. The rest of the reaction is assumed to involve stabilization.

5 100% stabilization is assumed by extrapolation from the mechanisms assumed for the smaller biradicals.

4. Assigned Reactions of α-Carbonyl or Unsaturated Crigiee Biradicals

Carter and Atkinson (1996) gave estimated mechanisms for several α-carbonyl or unsaturated Crigiee biradicals that are different from the general mechanisms discussed above. In most cases, these are adopted in this work. These are summarized on Table 40. Note that the reactions shown for HC(O)CHOO, CH_2=CHCHOO, and CH_2=C(CH_3)CHOO are assigned mechanisms applicable for those biradicals only, while that shown for RC(O)CHOO is a general mechanism that is derived based on the mechanism assumed by Carter and Atkinson (1996) for CH_3C(O)CHOO, but is assumed to be applicable for all radicals of this type, regardless of the nature of the "R" group.

5. Stabilized Crigiee Biradicals

As discussed above, the major fate of stabilized Crigiee biradicals with α-hydrogens is assumed to be reaction with H_2O, forming the corresponding acid. This is consistent with the rate constant ratios cited by Atkinson (1997a) for the reactions of $HCHO_2$ with H_2O, HCHO, CO, and NO_2. The mechanism for the reactions of stabilized $HCHO_2$ with water appear to be complex and may involve some formation of H_2O_2 or other peroxides, but based on the discussion of Atkinson (2000) we assume that these competing processes are relatively minor compared to acid formation.

Table 40. Assigned mechanisms for the reactions of excited α-carbonyl or unsaturated Crigiee biradicals.

Reactant and Products	Factor	Documentation
R-CO-CHOO[excited]		
R-COO[excited]-CHO	100.0%	O-shifts of alpha-carbonyl biradicals, via a primary ozonide transition state, are assumed to be rapid if they form a more substituted biradical (Carter and Atkinson, 1996)
CH2=C(CH3)-CHOO[excited]		
CO2 + CH2=CH-CH3	25.0%	As assumed by Carter and Atkinson (1996).
CH2=C(CHOO[stab])-CH3	75.0%	See above.
CH2=CH-CHOO[excited]		
CO2 + CH2=CH2	25.0%	Assumed to be analogous to mechanism assumed for methyl-substituted radical formed from O3 + isoprene (Carter and Atkinson, 1996).
CH2=CH-CHOO[stab]	75.0%	See above.
HCO-CHOO[excited]		
CO + HCO. + OH	50.0%	Assumed that decomposition is much more facile than in the CH3-CHOO[excited] case because of the weaker H..CO and C..CO bonds. The two most likely decomposition routes are arbitrarily assumed to have equal probability.
HCO2. + HCO.	50.0%	See above.

The current mechanism does not predict significant formation of stabilized Crigiee biradicals that lack α hydrogens because as discussed in III.K.3 the excited precursor biradicals are assumed to primarily decompose. The only exceptions are R_2COO biradicals that lack the β-hydrogens needed to undergo the hydroperoxide rearrangement, which are rarely formed. The subsequent reactions of the stabilized biradicals of this type are ignored in the current mechanism.

L. Lumping Assignments

Once the reactions of a given VOC with OH, NO_3, O_3, etc. have been fully generated, the system summarizes the overall yields of all products (including the $NO \rightarrow NO_2$ conversion operator), so that each initial reaction of the VOC in the presence of NO_x can be represented by one overall process

$$X + VOC \rightarrow p_1\ HO_2 + p_2\ (NO \rightarrow NO_2\ \text{conversions}) + \sum_i p_i\ Product_i$$

Here X refers to the species reacting with the VOC (OH, hν, etc.), $product_i$ represents each of the products that are formed, and p_i represents its overall yield. Since many hundreds and even thousands of products might be formed in the reactions of larger molecules, it is clearly not possible that they all be represented explicitly in the model simulations. As discussed in Section II.C, above, the current mechanism represents most oxidation products using a limited number of model species based on various "lumped molecule" assignments.

These assignments, which provide the interface between the mechanism generation system discussed above and the base mechanism discussed in Section II, are summarized on Table 41. For each product that is formed in the overall reaction, the system checks the "lumping rules" associated with each model species in the order they are given on this table, and assigns the product to the first model species on the list whose associated rules describe the products being considered. Note that the last model species on the list is "INERT", which means that if the product satisfies none of the other criteria, it is treated as unreactive in the model. The total yield of each of the model species formed in the overall reaction are then summed up, and the overall reaction is then recast into the form

$$X. + VOC \rightarrow m_1\ HO2. + m_2\ RO2\text{-}R. + m_3\ R2O2. + \sum_i m_i\ ModSpe_i$$

where HO2., RO2-R., R2O2., or $ModSpe_i$ are model species in the base mechanism (see Table A-1 in Appendix A), and m_1, …, m_i are their corresponding yields. Reactions expressed in this way can be inserted directly into the mechanism, or the values of the overall rate constant and product yield parameters (the set of m_i's) can serve as a basis for deriving parameters for lumped parameter species used to represent the compound in complex mixtures (see Section VI).

Although most of Table 41 is reasonably self-explanatory, some explanation is needed concerning how overall yields of HO2., RO2-R., R2O2., and RO2-N. are determined. In the case of RO2-N., just determining if the product contains a nitrate (-ONO2) group is not always appropriate, since the starting reactant itself may contain nitrate groups, and nitrate-containing species are formed when NO_3 reacts with double bonds. Because of this, the system stores a flag with the product log whenever a RO_2+NO reaction forming a nitrate is generated, which can be used to determine if it is appropriate to represent the product by RO2-N. In the case of HO2., RO2-R., and RO2-N., the total yields are computed from the total HO_2 and total $NO \rightarrow NO_2$ counts as follows:

Condition:	[Total HO_2] ≥ [Total $NO \rightarrow NO_2$]	[Total $NO \rightarrow NO_2$] > [Total HO_2]
HO2. Yield =	[Total HO_2] - [Total $NO \rightarrow NO_2$]	0
RO2-R. yield =	[Total $NO \rightarrow NO_2$]	[Total HO_2]
R2O2. Yield =	0	[Total $NO \rightarrow NO_2$] - [Total HO_2]

Note that this is an approximate treatment, since the system lumps HO_2 that is formed with no NO to NO_2 conversions (e.g., in reactions of alcohols forming α-hydroxy alkyl groups) with extra NO to NO_2 conversions from another reaction pathway. However, the effect of this approximation should be small, and would only be non-negligible under low NO_x conditions where peroxy + peroxy reactions convert with NO to NO_2 conversion processes.

M. Generation of Mechanisms of Major Reactive Products

The representation of the major reactions of the oxidation products formed when a VOC reacts can have a significant impact on the calculated atmospheric impacts of the VOC if these products are sufficiently reactive. As discussed above, the standard method for representing the VOC's reactive oxidation products is to use the set of explicit or lumped product model species as discussed above. This obviously introduces inaccuracies in cases where the reactivities of the actual products formed are different than those of the model species used to represent them. These inaccuracies are minimized if a sufficiently comprehensive set of model species are used to represent the variety of types of organic products that can be formed, but they can never be completely eliminated unless fully explicit mechanisms are used.

Table 41. Summary of lumping assignments used to determine how individual explicit product species are represented in the base mechanism.

Model Species	Structure or Lumping Criteria
Radical Operators (see text)	
RO2-N.	Any organic nitrate that is formed in a RO2 + NO reaction
Total HO2	HO2.
Total NO → NO2	NO → NO2 conversion operator
Explicit Radicals	
CCO-O2.	CH3-CO[OO.]
C-O2.	CH3OO.
HO.	OH
Cl.	Cl.
TBU-O.	CH3-C[O.](CH3)-CH3
Lumped Radicals	
MA-RCO3.	Any compound containing a C=C double-bonded group next to a CO[OO.] group.
RCO-O2.	Any other compound containing a CO[OO.] group.
Explicit Products	
HNO3	HNO3
NO2	NO2
CO	CO
CO2	CO2
HCHO	HCHO
ACET	CH3-CO-CH3
GLY	HCO-CHO
HCOOH	HCO-OH
CCO-OH	CH3-CO-OH
Lumped Products	
CCHO	CH3-CHO or HO-CH2-CHO
RCHO	Any other compound containing a -CH2-, >CH- or >C< group next to a -CHO group.
MGLY	Any compound containing a -CO- next to a -CHO group.
BACL	Any compound containing a -CO- next to another -CO- group.
METHACRO	CH2=C(CHO)-CH3 or CH2=CH-CHO
MVK	Any compound containing CH2=CH-CO- groups except as indicated above.
ISOPROD	Any compound containing a C=C double-bonded group next to a -CHO or -CO- group except as indicated above, or 3-methyl furan.
RNO3	Any compound containing a -ONO2 group that reacts with OH faster than 5×10^{-13} cm^3 $molec^{-1}$ s^{-1}, that is not formed in a peroxy + NO reaction.
XN	Any other compound containing a -ONO2 group except as indicated above.
PROD2	Anything that reacts with OH faster than 5×10^{-12} cm^3 $molec^{-1}$ s^{-1}, except as indicated above.
RCO-OH	Any compound other than those listed above containing a -CO- group next to a -OH group. (Note that acids with $kOH > 5 \times 10^{-12}$ cm^3 $molec^{-1}$ s^{-1} are lumped with PROD2.)
MEK	Anything that reacts with OH faster than 5×10^{-13} cm^3 $molec^{-1}$ s^{-1}, except as indicated above.
INERT	Anything not satisfying any of the above criteria.

The ideal situation would be to represent all the major reactive products explicitly, but this is not practical because of the thousands of types of oxidation products that can be formed from the hundreds of types of VOCs emitted into actual atmospheres. A more practical solution is to derive the kinetic and mechanistic parameters of the lumped model species used to represent the particular set of products that they are being represented in any particular model application. As discussed in Section II.C.2, above, this approach is in fact used to derive the parameters for the PROD2 and RNO3 model species, *based on the assumption that the mixture of VOCs in the model simulation is reasonably well represented by the* "Base ROG mixture" used in the atmospheric reactivity calculations (Carter 1994a,b). In principle, the methods discussed in Section II.C.2 can be used to derive the appropriate PROD2 or RNO3 parameters for any mixture of VOCs, though the software to do this routinely has not yet been developed.

Adjusting the parameters for the lumped product species to be appropriate for modeling particular ambient mixtures does not necessarily solve the problem of inaccuracy in representing the products formed from individual VOCs when assessing their reactivities. This is because at least some types of individual VOCs whose reactivities are of interest may in some cases form quite different types of products than the mixture of VOCs that dominate current atmospheres. Therefore, use of standard mechanisms for lumped reactive products such as PROD2 or RCHO may not be the optimum representation of the reactions of the major products from such VOCs.

One approach to address this problem is to use the mechanism estimation and generation system to derive the mechanisms for the major products formed from any VOC whose reactivity is being assessed, and then represent the reactions of these products explicitly in the model. This is obviously not practical for representing all reacting VOCs in a model simulation, but may be feasible if only one VOC is of particular interest, such as in reactivity assessment calculations. This approach can be used if the VOC and its major product reactions can be processed using the current mechanism generation system, and if the VOC forms a manageable number of major reactive products. Furthermore, the latter requirement can be eliminated if products of similar reactivity ranges are lumped together and represented by lumped product model species whose parameters are derived based on the specific mixture of products from the VOC.

To address these issues, two separate mechanisms are derived for VOCs whose product reactions can be processed using the mechanism generation system. The "standard" or "lumped product" (LP) mechanisms are those derived as discussed in the previous sections, where all the VOC products are represented only using the standard set of model species described in Section II.C, as shown on Table 41. In the "adjusted product" (AP) mechanisms, the more reactive VOC products are represented using separate model species whose mechanisms are derived to represent the specific set of products predicted to be formed. Because of the large number of products predicted to be formed from some VOCs, the individual products are not all represented separately, but are used as the basis for deriving adjusted kinetic and mechanistic parameters for the lumped model species used to represent these products. Note that these adjusted mechanism lumped products are associated with the specific individual VOCs forming them, and are distinct from the lumped model species used to represent the products from the mixtures of other VOCs present in the simulation. Models that use adjusted product mechanisms for a VOC must include model species not only for the VOC itself, but also for the adjusted lumped product species used to represent their major reactive products.

The VOC mechanism listing in Table A-6 in Appendix A gives each of these mechanisms for all VOCs where this is applicable, as well as the mechanisms used for the major products in the adjusted product versions. The adjusted product (AP) mechanism is used in the reactivity assessment calculations for the individual VOCs (discussed in Section VII) and also in the simulations of the chamber

experiments for evaluating individual VOC mechanisms, as discussed in Section V. The lumped product (LP) mechanism is used in all other applications, such as representing the VOC when present in mixtures as discussed in Section VI. If no separate AP or LP mechanism is given for a VOC, it means that either an adjusted product mechanism could not be generated, or that the mechanism generation system determined that the major reactive products are adequately represented by the standard set of organic product model species. In these cases the same mechanism is used in reactivity or mechanism evaluation calculations as are used when representing the VOC in mixtures.

The mechanism generation system employs the following procedure to derive the adjusted product mechanisms for reactivity assessment of VOCs. Note that the first step is the same as employed when generating the lumped product version of the mechanism.

- The fully explicit mechanisms for the NO_x-air reactions of the subject VOC is generated, as discussed in Section III.A, and the lumped product model species corresponding to each of the explicit products that are predicted to be formed are determined.
- The products that are already adequately represented by the existing set of model species, or that are judged to have relatively low reactivity and thus not significantly affect the overall reactivity of the parent VOC, are represented in the same way as in the lumped product mechanism. The former includes compounds that are already represented explicitly (e.g., formaldehyde) or that are used as the basis for deriving the mechanism of the lumped model species used to represent them (e.g., propionaldehyde and methyl glyoxal). The latter include products that are represented by MEK, RCO-OH, RNO3, or INERT in lumped product mechanisms.
- The products that are represented by "reactive" lumped product model species (i.e., PROD2, RCHO, MGLY, BACL, METHACRO, ISO-PROD or MVK) are used to derive the mechanisms for adjusted versions of those model species that are specific to the individual VOC. If the VOC reacts in more than one way (e.g., reacts with O_3, NO_3, etc. as well as with OH), then separate model species are used to represent products from the different reactions, unless the products are exactly the same. These separate model species are given the name PRD1, PRD2, etc., starting with the reactive products formed in the OH reaction.
- The mechanisms of these VOC-specific product model species are derived by generating the mechanisms of all the individual compounds that they represent, deriving the lumped product representations of these mechanisms as discussed in Section III.L, and then determining the average kinetic and product yield parameters, weighted by the relative yields of the products. To minimize unnecessary processing for VOCs that form large numbers of products in very low yields, products with total yields of less than 2.5% are not used when computing the parameters for the VOC-specific lumped products. If all the products represented by a given type of model species are formed in less than 2.5% yield, then the standard lumped parameter model species is used, i.e., no separate VOC-specific product model species is created.
- The overall reaction mechanism of the VOC is then given in terms of yields of the standard lumped products representing the low reactivity VOCs and yields of the VOC-specific adjusted product model species derived as discussed above. Since the mechanisms of these adjusted product model species are in general different for each VOC, the mechanisms for these must also be specified as part of the overall adjusted product mechanism of the VOC. These are shown in Table A-6 in Appendix A for all VOCs for which explicit product mechanisms can be derived.

An illustrative example can be shown in the case of 2-hexanone, which can react with OH and by photolysis. The reactive products formed when generating the mechanism for this compound are as follows:

OH Products Represented by PROD2	Yield
$CH_3C(O)CH_2C(O)CH_2CH_2CH_2OH$	22.6%
$CH_3CH_2C(O)CH_2CH_2C(O)CH_3$	7.2%
$CH_3CH_2CH_2C(O)CH_2C(O)CH_3$	4.8%
$CH_3C(O)CH_2CH_2CH_2C(O)CH_3$	0.1%
OH Products Represented by RCHO	**Yield**
CH_3CH_2CHO	14.0%
$CH_3C(O)CH_2CHO$	13.8%
$CH_3CH(OH)CH_2CH_2CHO$	10.4%
$CH_3CH_2CH_2CH_2CHO$	9.2%
$CH_3CH_2CH_2CHO$	8.6%
$CH_3C(O)CH_2CH(OH)CH_2CH_2CHO$	1.6%
$CH_3C(O)CH_2CH_2CHO$	1.3%
Photolysis Products Represented by RCHO	**Yield**
$CH_3CH(OH)CH_2CH_2CHO$	87.4%

It can be seen that three adjusted product model species need to be used in the 2-hexanone adjusted product mechanism, one each to represent the PROD2 and RCHO products of the OH reaction and one to represent the RCHO product from the photolysis. These are as follows:

- The PRD1 model species is created to represent the PROD2 products from the OH reaction, with its yield set at 34.7%, and its mechanism is derived by generating those for $CH_3C(O)$-$CH_2C(O)CH_2CH_2CH_2OH$, $CH_3CH_2C(O)CH_2CH2C(O)CH_3$, and $CH_3CH_2CH_2C(O)CH_2C(O)CH_3$, with using weighting factors of 65.3%, 20.8%, and 13.9%, respectively. The contribution by $CH_3C(O)CH_2CH_2CH_2C(O)CH_3$ being ignored because its yield is less than 2.5%.
- The propionaldehyde (CH_3CH_2CHO) formed in 14% yield in the OH reaction is already well represented by the standard RCHO model species, since its mechanism is derived based on that of propionaldehyde (see Section II.C.2). Therefore, this product is represented by the formation of the standard RCHO model species in 14% yield. The PRD2 model species is created to represent the other OH products represented by RCHO, with a yield set at 44.9%. Its mechanism is derived based on the generated mechanisms for $CH_3C(O)CH_2CHO$, $CH_3CH(OH)CH_2CH_2CHO$, CH_3CH_2-CH_2CH_2CHO, and $CH_3CH_2CH_2CHO$ with weighting factors determined by their relative yields. The mechanisms for the other two products are not used because their yields are less than 2.5%.
- The PRD3 model species is created to represent the formed in the photolysis reaction that would otherwise be represented by RCHO, with a yield of 87.4% and a with the mechanism generated for $CH_3CH(OH)CH_2CH_2CHO$.

These mechanisms are shown on Table A-6 in Appendix A as the "AP" mechanism for 2-hexanone. Analogous procedures are used to generate the adjusted product mechanisms for the other VOCs whose product reactions can be processed using the mechanism generation system.

IV. PARAMETERIZED MECHANISMS

The mechanism generation system discussed in the previous system cannot be used for VOCs where the nature of the radical intermediates are unknown, or that involve formation of intermediates that cannot be processed by the present system. These include the aromatics (whose intermediates are highly uncertain and almost certainly involve highly unsaturated radicals for which thermochemical estimates cannot be made), terpenes (whose polycyclic structure cannot be represented by the current system), halogenated compounds (for which insufficient thermochemical information is available on the current database implemented with the system), and compounds containing groups, such as amins, for which general estimation methods have not been developed.

These VOCs must continue to be represented by parameterized or highly simplified mechanisms, as is the case in other mechanisms and previous versions of this mechanism. The representation and mechanisms used in these cases are discussed in this section.

A. Representation of Aromatics

Aromatic hydrocarbons are believed to react in the atmosphere primarily with OH radicals, forming a variety of ring-containing and fragmentation products (Atkinson, 1990, 2000, and references therein). Despite progress in recent years towards improving our understanding of the atmospheric chemistry of aromatic hydrocarbons (e.g., see Atkinson, 2000, and references therein), there is still insufficient understanding of the details of these mechanisms to derive, or even estimate, predictive mechanisms. Therefore, it is still necessary to use parameterized mechanisms, with yields of model species representing reactive uncharacterized products adjusted to fit chamber data, in order to represent the atmospheric reactions of this important class of compounds.

All current photochemical mechanisms are based on assuming that the reactions of OH radicals with aromatics involve two initial processes. The first, which is applicable only for aromatics with substituents about the ring, involves H-atom abstraction from the side group, ultimately forming primarily aromatic aldehydes and ketones, and possibly small yields of aromatic nitrates as well:

$$\text{OH + aromatic} \rightarrow H_2O + \text{(benzyl type radical, e.g., } \Phi CH_2\cdot)$$

$$\text{(benzyl type radical)} + O_2 \rightarrow \text{(benzyl peroxy type radical, e.g., } \Phi CH_2OO\cdot)$$

$$\text{(benzyl peroxy type radical) + NO} \rightarrow \text{aromatic nitrate, e.g., } \Phi CH_2ONO_2$$

$$\text{(benzyl peroxy type radical) + NO} \rightarrow NO_2 + \text{(benzyl oxy type radical, e.g., } \Phi CH_2O\cdot)$$

$$\text{(benzyl oxy type radical)} + O_2 \rightarrow HO_2 + \text{aromatic aldehyde or ketone, e.g., } \Phi CHO$$

The other reaction route, which is generally the more important (and also the most uncertain), involves addition of OH to the aromatic ring, ultimately forming phenols or cresols to some extent, but primarily forming various ring fragmentation products:

$$\text{OH + aromatic} \rightarrow \text{(OH-aromatic adduct)}$$

$$\text{(OH-aromatic adduct)} + O_2 \rightarrow HO_2 + \text{phenol or cresol}$$

$$\text{(OH-aromatic adduct)} + O_2 \rightarrow \text{(OH-aromatic-}O_2\text{ adduct)}$$

$$\text{(OH-aromatic-}O_2\text{ adduct) + NO} \rightarrow \text{uncharacterized nitrate products}$$

(OH-aromatic-O_2 adduct) + NO $\rightarrow$ NO_2 + (uncharacterized radical intermediates)

(uncharacterized radical intermediates) $\rightarrow \rightarrow$ HO_2 + α-dicarbonyls and other fragmentation products

Alternative mechanism formulations, e.g., assuming the OH-aromatic reacts with NO_2 at a rate competing with or exceeding its reaction with O_2, assuming radical intermediates react with NO_2 to form stable products, or assuming that additional NO to NO_2 conversions are involved in the formation of α-dicarbonyls or other fragmentation products, can also be considered. However, except for the naphthalenes and tetralin (discussed below), experience has shown that parameterizations based on these alternative mechanisms do not fit the available environmental chamber data as well as those based on the general reaction schemes shown above.

The exception to this general scheme is that as discussed below improved fits of model simulations to chamber data for naphthalene, 2,3-dimethyl naphthalene, and tetralin are obtained if it is assumed that at least some of the uncharacterized radical intermediates react in a manner analogous to a PAN precursor (e.g., acyl peroxy) radicals. This involves radicals where the reaction with NO_2 forming a relatively stable termination product, e.g.,

(uncharacterized radical intermediates) + NO_2 $\rightarrow$ (uncharacterized PAN analogue)

competes with the reaction with NO forming radical propagation products (shown above). Model calculations do not fit the chamber data for these compounds if it is assumed that there is no significant radical termination process, nor are the chamber data well fit if it is assumed that the extent of termination is not strongly affected by reaction conditions. The latter would be the case if the termination were due to organic nitrate formation from the reactions of peroxy radicals with NO, or to the formation of some intermediate, such as phenoxy radicals, that only reacts by a termination process.

Therefore, the parameterization used to represent the reactions of the aromatics in this version is similar to that employed previously (Carter et al, 1997a), except that, as discussed above in Sections II.C.1 and II.C.3, a larger number of model species are used to represent the reactions of the various known and uncharacterized aromatic ring fragmentation projects. In this version, all three of the α-dicarbonyl products from the methylbenzenes are represented explicitly, and three different model species are used to represent the non-photoreactive (DCB1) and the two types of photoreactive (DCB2 and DCB3) uncharacterized ring fragmentation products. In addition, the mechanisms for the DCB's are are estimated based roughly on those estimated for unsaturated dicarbonyls (see Section II.C.3), unlike the previous mechanism where they were based on reactions of α-dicarbonyls (Carter, 1990). In addition, to at least approximately fit chamber data for the naphthalenes and tetralin, the possibility for the formation of PAN precursor radicals, represented by the RCO-O2$\cdot$ model species, is also included in the parameterization.

In terms of model species used in the current mechanism, the overall reactions of the aromatics are represented as follows:

OH + aromatic $\rightarrow$ y_{RH} HO2. + y_{RR} RO2-R. + y_{NR} RO2-N. + y_{Q2} RCO-O2. +
y_{PH} PHEN + y_{CR} CRES + y_{BL} BALD + y_{K6} PROD2 +
y_{GL} GLY + y_{MG} MGLY + y_{BA} BACL + y_{D1} DCB1 + y_{D2} DCB2 + y_{D3} DCB3.

Here the y_{PH}, …, y_{D3} are the stoichiometric parameters that must be specified to define the mechanism. Note that the products shown in the first line represents the formation of various radical products and their effects of NO to NO_2 or organic nitrate formation from reactions of peroxy radicals, those shown in the second line represent the aromatic ring-retaining products (with PROD2 being used to represent aromatic

ketones such as methyl phenyl ketone that may be formed from ethylbenzene), and those in the third line represent the various known or uncharacterized ring fragmentation products.

Note that based on the reaction mechanism formulation discussed above, and considerations of factors such as radical conservation, relationships between some of the parameters can be derived, to reduce the number of parameters that have to be estimated or optimized. Radical conservation requires that

$$y_{RH} + y_{RR} + y_{RN} + y_{Q2} = 1.$$

If it is assumed that cresol or phenol formation occurs as shown above and that all the other processes involve a NO to NO_2 conversion, then

$$y_{RH} = y_{PH} + y_{CR}$$

This means that y_{RR} can be derived given the y_{Q2} value that best fits the data and the assigned phenol and cresol yields and the assigned nitrate yield (y_{RN}) parameter.

$$y_{RR} = 1 - (y_{PH} + y_{CR} + y_{Q2} + y_{RN}) \qquad \text{(XXVII)}$$

In addition, we assume that all the ring fragmentation processes, including those that form α-dicarbonyls, but probably excluding those involving involve formation of radicals represented by RCO-O2·, involve formation of some type of reactive dicarbonyl product. This implies that

$$\text{Total DCB Yield} = y_{D1} + y_{D2} + y_{D3} = 1 - (y_{Q2} + y_{NR} + y_{PH} + y_{CR} + y_{BL} + y_{K6}) \qquad \text{(XXVIII)}$$

This is used to derive y_{D1} given the optimized yields of y_{D1}, y_{D3}, and y_{Q2} and the assigned yields of the other parameters.

The stoichiometric yield parameters that were assigned or derived for the various aromatic compounds currently incorporated in the mechanism are summarized on Table 42. Footnotes to that table indicating the sources of the derivations are given on Table 43. As indicated in the footnotes, some of the product yield parameters are based on experimental data, some are estimated, and some are adjusted to fit chamber data. The adjustments were done by using a non-linear optimization method to minimize the sum of squares error between experimental and calculated values of the data indicated on the footnotes, with the errors normalized relative to the maximum values of the measurements for each experiment.

The following points are noted concerning these assignments and the resulting mechanisms for the various types of compounds.

1. Benzene

The glyoxal and phenol yields used were based on experimental data summarized by Atkinson (1997). Contrary to the previous version of the mechanisms (Carter, 1990; Carter et al, 1997a), the data are best fit if it is assumed that the uncharacterized ring fragmentation product does not photolyze to a significant extent. This change can be attributed to the fact that the photoreactivity of glyoxal is increased significantly in the present mechanism. This is based on results of modeling chamber studies of acetylene, where the reactivity of this compound could not be simulated unless significantly higher photoreactivity for glyoxal, its major photoreactive product, is assumed (Carter et al, 1997c; see also footnotes to Table A-2 in Table A-4). Therefore, only DCB1 is used to represent the uncharacterized fragmentation products from this compound.

Table 42. Summary of assigned and optimized stoichiometric yield parameters used to represent the reactions of the aromatics.

Parameters and Products		Benzene	Toluene	Ethyl Benzene	o-Xylene	m-Xylene	p-Xylene
OH abstraction pathway							
yBL	BALD		0.000		0.000	0.000	0.085
yK6	PROD2			0.000			
yNR	RO2-N.		0.129	0.000	0.000	0.000	0.008
Notes [b]		1	6,7	10	6,14	6,14	6,14
Phenol/Cresol patheay							
yPH	PHEN	0.000					
yCR	CRES		0.000	0.000	0.000	0.000	0.234
Notes		2,3	6	11	15	15	15
α-Dicarbonyl products							
yGL	GLY	0.084	0.084	0.207	0.207	0.207	0.116
yMG	MGLY		0.000	0.000	0.000	0.000	0.135
yBA	BACL				0.000		
Notes		4,3	8	11,12	8	8	8
Optimized Fragmentation Products							
yD2	DCB2		0.046		0.000	0.000	0.156
yD3	DCB3		0.046	0.000	0.000	0.000	0.057
Notes		5	9	13	16	17	18,19
Derived Yields [a]							
yRH	HO2.	0.236	0.600	0.236	0.236	0.236	0.234
yRR	RO2-R.	0.094	0.108	0.764	0.764	0.764	0.758
yD1	DCB1	0.000	0.016	0.764	0.764	0.764	0.460

Parameters and Products		1,2,3-Trimethyl Benzene	1,2,4-Trimethyl Benzene	1,3,5 Trimethyl Benzene	Naphthalene	Methyl Naphthalene	2,3-Dimethyl Naphthalene	Tetralin
OH abstraction pathway								
yBL	BALD	0.044	0.044	0.025				
yNR	RO2-N.	0.010	0.010	0.010	0.070	0.070	0.070	0.129
Notes [b]		20	20	20	24	29	24	31
Phenol/Cresol patheay								
yPH	PHEN				0.236			0.600
yCR	CRES	0.186	0.186	0.186		0.236	0.236	
Notes [b]		20	20	20	24	29	24	
α-Dicarbonyl products								
yGL	GLY	0.065	0.063	0.000	0.084	0.084	0.084	0.084
yMG	MGLY	0.166	0.364	0.621		0.038	0.076	
yBA	BACL		0.079		25	29	25,30	25
Notes [b]		8	8	8				
Optimized Fragmentation Products								
yD2	DCB2	0.077	0.000	0.097	0.049	0.076	0.103	0.046
yD3	DCB3	0.149	0.027	0.114	0.049	0.076	0.103	0.046
yQ2	RCO-O2.				0.479	0.539	0.600	0.163
Notes [b]		21	22	23	26,27,28	29	26,27,30	26,31
Derived Yields [a]								
yRH	HO2.	0.186	0.186	0.186	0.236	0.236	0.236	0.600
yRR	RO2-R.	0.804	0.804	0.804	0.215	0.155	0.094	0.108
yD1	DCB1	0.533	0.733	0.569	0.117	0.003	0 [c]	0.016

[a] Parameters calculated using Equations (XXVI) and (XXVII).

[b] Documentation notes are given on Table 43.

[c] Equation (XXVII) predicts a slightly negative DCB1 yield for this compound. Zero yield assumed.

Table 43. Documentation notes for the assigned and optimized stoichiometric yield parameters used to represent the reactions of the aromatics.

No.	Note
1	Organic nitrate yields from reaction of NO to OH - aromatic - O_2 adducts is assumed not to be significant
2	Glyoxal yields from Tuazon et al (1986).
3	See also yield data summarized by Atkinson (1994).
4	Phenol yield from Atkinson et al (1989).
5	Best fits to the D([O_3]-[NO]) data in benzene - NOx runs ITC560, ITC561, ITC562, ITC710, CTC159A, CTC159B, CTC160A, and CTC160B are obtained if yields of photoreactive DCB products are assumed to be negligible..
6	Aromatic aldehyde and and total phenolic product yields are averages of data tabulated by Atkinson (1994), except that the benzaldehyde and tolualdehyde yields of Gery et al (1987) are not used because they are substantially higher than the other measurements.
7	The approximate yield of organic nitrates in the RO_2+NO reaction are estimated from the benzyl nitrate yields tabulated by Atkinson (1994). Note that this corresponds to an approximately 9.5% yield from benzyl peroxy radicals, which is in the expected range for a molecule of this size.
8	Alpha-dicarbonyl yields are averages of data tabulated by Atkinson (1994), with low values from Shepson et al (1984) and the high values of Tagkagi et al (1980) excluded from the averages.
9	The DCB2 and DCB3 yields were adjusted to fit the concentration-time data for D([O_3]-[NO]) and toluene in toluene - NOx - air runs CTC079, CTC048, CTC026, CTC034, CTC065, DTC042B, DTC155A, DTC151A, DTC170A, and DTC042A.
10	The fraction reacted by abstraction from -CH_2- group is estimated from the rate constants for ethylbenzene and toluene, and from the benzaldehyde yield form toluene, assuming OH addition to the aromatic ring occurs with the same rate constant as with toluene. The expected abstraction product is benzophenone, which is very approximately represented in the mechanism by the lumped higher oxygenate product PROD2. The organic nitrate yield is estimated to be 10% of reaction of peroxy radical formed after abstraction from the -CH_2- group. Since abstraction is estimated to occur ~24% of the time and nitrate formation from the OH-aromatic-O_2 adducts is assumed to be negligible, this gives a 2.4% overall nitrate yield.
11	The phenolic product and alpha-dicarbonyl yields, relative to OH addition to aromatic ring, are assumed to be the same as for toluene
12	Methyl glyoxal is used to represent ethyl glyoxal.
13	The DCB2 and DCB3 yields were adjusted to fit the concentration-time data for D([O_3]-[NO]) and ethylbenzene in ethylbenzene - NOx - air runs CTC057, CTC092A, CTC092B, CTC098B, DTC223A, DTC223B, DTC224A, and DTC224B.
14	Nitrate yields for the xylenes are based approximately on the methylbenzyl nitrate yields tabulated by Atkinson (1994). The yields are consistent with 10-20% nitrate formation from reaction of NO with methylbenzyl peroxy radicals.
15	Phenolic product yields from Atkinson et al (1991).
16	The DCB2 and DCB3 yields were adjusted to fit the concentration-time data for D([O_3]-[NO]) and o-xylene in o-xylene - NOx - air runs CTC038, CTC039, CTC046, CTC068, CTC081, CTC091A, DTC207A, DTC207B, DTC208A, DTC208B, DTC209A, and DTC209B.
17	The DCB2 and DCB3 yields were adjusted to fit the concentration-time data for D([O_3]-[NO]) and and m-xylene in m-xylene - NOx - air runs CTC029, CTC035, CTC036, CTC094A, DTC193B, DTC192B, DTC206B, DTC295A, DTC188B, and DTC191B.
18	The DCB2 and DCB3 yields were adjusted to fit the concentration-time data for D([O_3]-[NO]) and p-xylene in p-xylene - NOx - air runs CTC041, CTC043, CTC044, CTC047, CTC070, DTC198A, DTC198B, and DTC199A.

Table 43 (continued)

No.	Note
19	Note that the apparent low photoreactive DCB yields from p-xylene and 1,2,4-trimethylbenzene can be attributed to the expected formation of diketone as well as dialdehyde products, where the diketones apparently do not photolyze as rapidly as dialdehydes.
20	The extent of reaction via abstraction from CH_3 groups is estimated from average rate constant per CH_3 group derived for toluene and the xylenes, which is 4.7×10^{-13} cm^3 $molec^{-1}$ s^{-1}. The overall yields of organic nitrates and phenolic products are estimated to be comparable to those for the xylenes, and to be similar for all isomers.
21	The DCB2 and DCB3 yields were adjusted to fit the concentration-time data for D([O_3]-[NO]) and the reactant aromatic in the 1,2,3-trimethylbenzene - NOx - air runs CTC054, CTC075, CTC076, DTC211A, DTC211B, DTC212A, DTC212B, DTC213A, and DTC213B.
22	The DCB2 and DCB3 yields were adjusted to fit the concentration-time data for D([O_3]-[NO]) and the reactant aromatic in the 1,2,4-trimethylbenzene - NOx - air runs CTC056, CTC091B, CTC093A, CTC093B, DTC201A, DTC201B, DTC203A, DTC203B, DTC204A, and DTC204B.
23	The DCB2 and DCB3 yields were adjusted to fit the concentration-time data for D([O_3]-[NO]) and the reactant aromatic in the 1,3,5-trimethylbenzene - NOx - air runs CTC030, CTC050, CTC071, CTC073, DTC194A, DTC194B, DTC195A, DTC195B, DTC196A, DTC196B, and DTC206A.
24	The naphthalenes are assumed to have the same yield of phenol-like products as benzene. Abstraction from the methyl group in the methyl naphthalenes is assumed to be relatively unimportant. However, model simulations of naphthalene - NOx and 2,3-dimethyl naphthalene runs are best fit by assuming relatively high nitrate yields of 12% and 7%, respectively, though assuming 7% overall yields for both compounds gives satisfactory fits to the data. Note that the actual reactions that this "nitrate formation" parameterization represents may be something other than nitrate formation from peroxy + NO.
25	The glyoxal yield from the naphthalenes and tetralin is assumed to be approximately the same as the glyoxal yield from o-xylene.
26	Since the only difference between DCB2 and DCB3 is the action spectrum of the photolysis reaction and since the available naphthalene, 2,3-dimethyl naphthalene and tetralin chamber experiments were all carried out using the same light source, the data are not sufficient to determine the yield ratio for these products. Based on the optimization results for the alkylbenzenes, where the optimized DCB2/DCB3 yield ratios varied from 0 to 3 with an average of about 1, we assume that the best fit yields for these two should be roughly equal for the naphthalenes and tetralins.
27	Satisfactory fits to the chamber data could not be obtained unless it was assumed that the ring fragmentation process included substantial formation of a peroxynitrate precursor, which was represented by the model species RCO-O2., the precursor of PAN2. See text.
28	The yields of RCO-O2. and DCB2 + DCB3 were optimized to fit D([O3]-[NO]) data for the naphthalene - NOx runs ITC751, ITC755, ITC756, ITC798, and ITC802.
29	No chamber data are available to derive a best fit mechanism for this compound. All its mechanistic parameters were derived by averaging those estimated or optimized for naphthalene and 2,3-dimethylnaphthalene.
30	The yields of RCO-O2. DCB2 + DCB3 and MGLY were optimized to fit D([O3]-[NO]) and PAN data for the 2,3-DMN - NOx runs ITC771, ITC774, ITC775, and ITC806. Best fits were obtained when the yield of the PAN precursor species was ~0.8, but using a value of 0.6, which is more consistent with the expected upper limit for ring opening, gave similar results. The DCB1 yield calculated using Equation XXIX was slightly negative, so a zero DCB1 yield is used.

Table 43 (continued)

No.	Note
31	Best fits to the chamber data are obtained if relatively high organic nitrate yields and high yields of phenol-like products are assumed. Higher nitrate yields could result if significant abstraction from -CH2- groups occurred, forming alkane-like peroxy radicals. It is also necessary to assume some formation of peroxynitrate precursors, represented by RCO-O2., to obtain satisfactory fits to the data, though the optimum yield for tetralin is less than derived for that for the naphthalenes. The total yield of phenol-like products was set at 0.6, which is reasonably consistent with the maximum value assuming that DCB, nitrate and peroxynitrate precursor formation account for the other pathways. The total alkyl nitrate yields, and yields of RCO-O2. and DCB2 + DCB3 from ring fragmentation were optimized to fit D([O3]-[NO]) data for the tetralin - NOx runs ITC739, ITC747, ITC748, ITC750, and ITC832.

Figure 10 shows plots of the $\Delta([O_3]-[NO])$ data for the benzene - NO_x experiments that were used for evaluating and deriving the mechanism for this compound. (See Section V for a summary of the model simulation methods and a more complete discussion of the evaluation results for all experiments used.) The results of model simulations using the assigned mechanism are also shown. It can be seen that the mechanism does not perform particularly well in simulating some of the data, tending to overpredict the rate of O_3 formation and NO oxidation in some of the xenon arc chamber runs and significantly underpredicting it in some of the blacklight chamber runs. However, no reasonable alternative parameterization that was examined resulted in a mechanism that better fit the data. Assuming any additional radical source from photolysis of uncharacterized products (or their reaction with O_3 for that matter) exacerbated the overprediction of the reactivity of the xenon arc chamber runs. Assuming higher radicals sources and countering them by increasing termination processes, such as using higher nitrate yield or assuming formation of products represented by PAN precursors (as found to improve simulations of data for the naphthalenes) did not solve the problem. Assuming alternative mechanisms such as formation of radicals that react with NO_2 also did not improve the fits.

More data are needed concerning the products formed in the photooxidation of benzene and their reactivities, including *direct* studies on the photoreactivity of glyoxal, before the uncertainties in the benzene photooxidation mechanism can be reduced. In addition, the possibility that there are experimental problems with some of the older ITC experiments, where the results appear to be inconsistent, cannot be ruled out. More comprehensive chamber data are needed to more unambiguously evaluate the mechanism for benzene. Although the model performs much better in simulating the data for the alkylbenzenes, and benzene is relatively unimportant in affecting atmospheric O_3 formation (because of its low reactivity and relatively low emissions amounts), the problems with the mechanism for what is presumably the simplest aromatic suggests fundamental problems with all aromatics mechanisms.

2. Methylbenzenes

The methylbenzenes (toluene, the xylenes and the trimethylbenzenes) are representative of the most important class of aromatic hydrocarbons in terms of both emissions and reactivity, and for that reason have the most extensive database of environmental chamber experiments for mechanism evaluation, as well information concerning yields of known products. The yields of phenolic products, benzaldehyde or tolualdehydes, and the α-dicarbonyls are based on experimental data summarized by Atkinson (1994). Averages of the reported data were used in those cases where more than one measurement is listed, though in some cases, measurements that appeared to fall outside the distribution of data from other studies were not used when computing the averages. The nitrate yields are somewhat

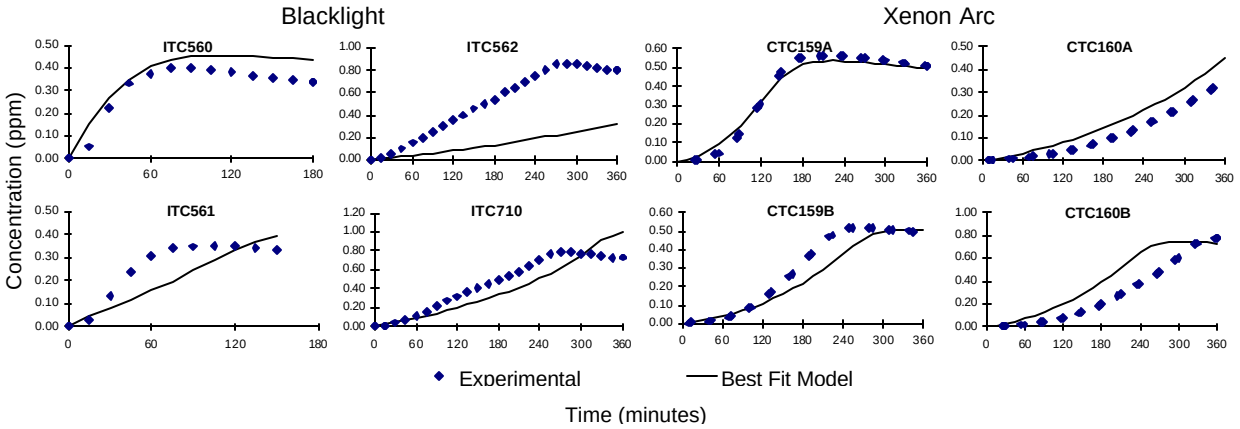

Figure 10. Plots of experimental and calculated $\Delta([O_3]-[NO])$ data for the experiments used to evaluate the benzene mechanism.

uncertain, but they appear to be relatively low and not highly important in affecting alkylbenzene reactivity.

As discussed above, the yields of model species DCB2 and DCB3, used to represent the uncharacterized photoreactive products, were optimized to fit the chamber data (see the footnotes to Table 42 in Table 43 for the specific data used). As discussed previously (Carter et al, 1997a) it is necessary to assume varying action spectra to fit the data in chambers with different light sources with data from chambers with both blacklight and xenon arc light source being used to determine their yields. Such data are available for all the methylbenzenes through the trimethylbenzenes, permitting their mechanisms to be optimized.

In contrast with benzene, the adjusted mechanism generally performs reasonably well in simulating the available chamber data, with no large or consistent differences in model performance in chambers with differing light sources. The performance of the model in simulating the individual alkylbenzene - NO_x chamber experiments is similar to that observed with previous versions of the mechanism (Carter et al, 1997a) and is presented in Section V.

3. Ethylbenzene

The mechanism for ethylbenzene is important because it is used as a surrogate (or surrogate species) for all the higher monoalkylbenzenes, such as propylbenzene or cumene. No product data for this compound is given by Atkinson (1994), and thus yields of all products had to be estimated. It is estimated that OH abstraction from the side group is more important than in the case of methylbenzenes because of the more reactive -CH_2- group, as indicated in the footnotes to Table 42 in Table 43. Other than that, the phenolic and α-dicarbonyl products are estimated based on those for toluene, reduced by the appropriate factor to correspond to the relatively lower fraction of reaction by OH addition to the aromatic ring.

As with the methylbenzenes, the DCB2 and DCB3 yields were adjusted to optimize the fit of model calculation to the chamber data, which also included experiments with both blacklight and xenon arc light sources. The model fit the data reasonably well (see Section V), performing comparably as the model for the methyl benzenes. However, it is interesting to note that the best fit DCB2 yield for

ethylbenzene is zero, while the yield for toluene is relatively high, being larger than that for DCB3 (see Table 42). On the other hand, the DCB3 yields for ethylbenzene and toluene are not greatly different. There is no obvious explanation for the large difference in DCB2 yields, which will have a significant effect on predicted reactivity, and suggests that estimates of comparable reactivity for aromatics with "comparable" structure may not always be reliable.

4. Naphthalenes and Tetralin

Relatively little is known about the details of the atmospheric reactions of naphthalenes and tetralins, except that appears that there are probably significant differences between the mechanisms for the alkylbenzenes and the naphthalenes (e.g., Atkinson, 2000, and references therein). The limited environmental chamber data for these compounds indicate that the naphthalenes and tetralin are considerably less reactive than the alkylbenzenes, despite their relatively high OH rate constants (Carter et al, 1981, 1987). Therefore, it is not appropriate to represent the naphthalenes and tetralins using general aromatic model species, and separate mechanisms are necessary to appropriately predict the reactivities of these compounds.

There was insufficient time and resources in this project to evaluate all available data for the naphthalenes (or tetralins) to determine the most appropriate parameterization for their mechanisms, so the parameterization used for the alkylbenzenes was used as the starting point. The yields of the phenolic products, organic nitrates, and α-dicarbonyls were very approximately estimated as discussed in the footnotes to Table 42 in Table 43, and optimizations were carried out to determine the best fit DCB2 + DCB3 yields. Because naphthalene and tetralin environmental chamber data are only available with a blacklight light source, it was not possible to separately optimize both products, so their yields were assumed to be the same (see footnotes to the table).

Although adjusting DCB2 and DCB3 yields was found to be sufficient to fit the chamber data for the alkylbenzene runs, this was found not to be the case when attempting to fit the mechanism to the data for the naphthalenes and tetralins. This is shown, for example, on Figure 11, which shows experimental and calculated $\Delta([O_3]-[NO])$ data for the naphthalene experiments. The calculated lines labeled "Optimize $y_{D2}=y_{D3}$" show the results of optimizing the photoreactive DCB yields only, using the initial estimates for the other parameters. It can be seen that the O_3 formation and NO oxidation rates in some runs are overpredicted and some are underpredicted, depending on the initial reactant concentrations. The results for 2,3-dimethyl naphthalene and tetralin are similar. In an attempt to improve the fits, a second set of optimizations were carried out where the nitrate yields, y_{NR}, were optimized along with the photoreactive DCB yields. This also did not result in acceptable fits to the data, as shown on the curves labeled "Optimize $y_{D2}=y_{D3}$, y_{NR}" on Figure 11. Reparameterizing mechanism to represent the possible formation of radicals that react with NO_2 to form termination products (such as phenoxy) and adjusting the yields of those radicals along with the photoreactive DCB yields gives similar results as adjusting the nitrate yields. Using alternative parameterizations where the product yields depend on the absolute NO_2 concentration (as would occur if radicals which react with both NO_2 and O_2 were involved) also did not yield acceptable fits to the data.

Improved fits of the parameterized model to the naphthalene, dimethylnaphthalene, and tetralin data were only obtained when it was assumed that the reactions involved the formation of radicals that in a manner to PAN precursors, which were represented in the model by RCO-O2·. The simulations of the naphthalene experiments using the best fit mechanism with the optimized PAN precursor and photoreactive DCB yields given on Table 42 are shown on Figure 11, where it can be seen that reasonably good performance in simulating the data is obtained. The results are similar for 2,3-dimethylnaphthalene

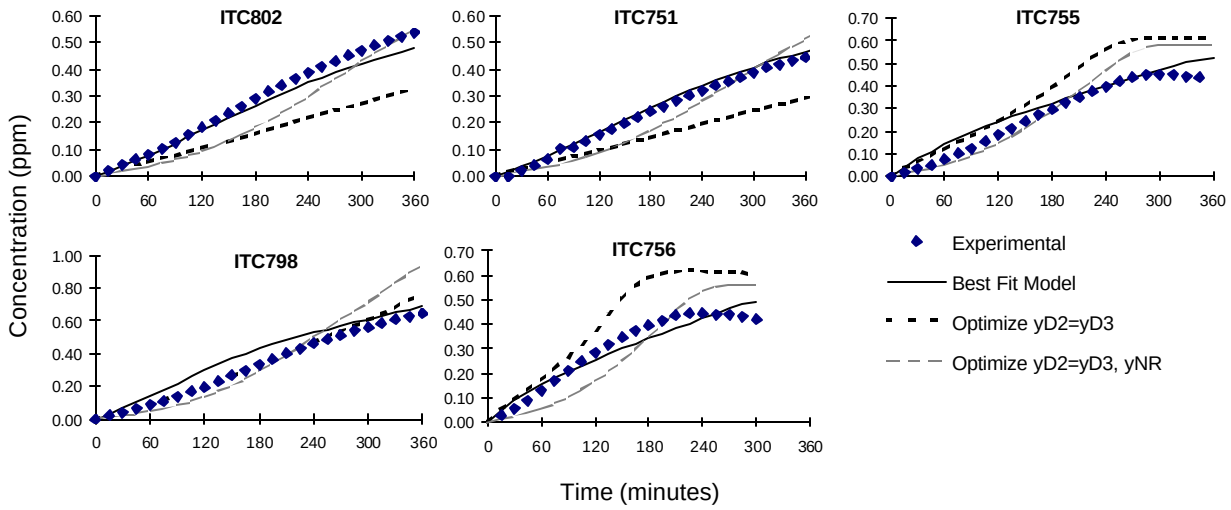

Figure 11. Plots of experimental and calculated $\Delta([O_3]-[NO])$ data for the naphthalene - NO_x used to derive the naphthalene mechanism.

and tetralin. However, in the case of 2,3-dimethylnaphthalene the yields of MGLY were also adjusted to optimize fits to the PAN data for these experiments, while for tetralin it was found that it was necessary also to adjust the overall nitrate yield for the model to satisfactorily simulate the data. The higher apparent nitrate yields in the case of tetralin could be due to reactions of radicals formed from OH abstractions from the non-aromatic ring.

These parameterized mechanisms for the naphthalenes and tetralin are clearly highly uncertain. Since the only currently available chamber data came from using a blacklight light source, the mechanism may not be correctly predicting the reactivity contributions of the photoreactive products in sunlight, where the spectrum is more similar to the xenon arc light sources. Perhaps more significantly, if the parameterizations employed do not correspond sufficiently well to the underlying chemistry of these compounds, the model may not be correctly extrapolating from the conditions of these experiments to the conditions of the atmosphere. However, these mechanisms represent our current best estimates at the present time.

5. Estimated Mechanisms for Other Aromatics

Table 8, above, shows that there are several other aromatic compounds whose OH rate constants are known, but for which no environmental chamber data are available for deriving mechanistic product yield parameters. These compounds are represented in the mechanism with model species using the appropriate measured rate constant, but with product yield parameters that are estimated based on those for most structurally similar compound(s) whose parameters are given in Table 42. These are as follows:

- Chlorobenzene (CL-BEN), dichlorobenzene (CL2-BEN) and nitrobenzene (NO2-BENZ) are assumed to have the same product yield parameters as derived for benzene.
- Parachlorobenzyltrifluoride (PCBTF) and trifluromethyl benzene (CF3-BEN) are assumed to have the same product yield parameters as derived for toluene.

- Isopropyl benzene (I-C3-BEN), n-propyl benzene (N-C3-BEN) and s-butyl benzene (S-C4-BEN) are assumed to have the same product yield parameters as derived for ethylbenzene.
- Monomethylnaphthalene (ME-NAPH) is assumed to have parameters that are averages of the corresponding parameters for naphthalene and 2,3-dimethylnaphthalene. The parameters so derived are shown on Table 42.

Obviously these estimates are uncertain, especially in view of the differences for the parameters for toluene and ethylbenzene, as discussed above. However, these provide the best available estimates concerning the mechanisms for these compounds, and at least incorporate their known OH rate constants. In this respect, their representation is presumed to be somewhat less uncertain than those aromatics that are not incorporated in the mechanism, but are represented by other aromatics using the "lumped molecule" approach (see Table C-1 in Appendix C).

B. Representation of Other Compounds

Table 44 shows the representation used for the reactions of the other compounds or classes of compounds that are incorporated in the present mechanism and that do not fall into the categories discussed above. The assignments for the various types of compounds are discussed in more detail below.

1. Terpenes

Terpenes are bicyclic alkenes or dialkenes or cyclic alkenes, and as such their reactions cannot be processed by the current mechanism generation system. The rate constants for their initial reactions are given above in Table 8 (for OH radicals), Table 13 (for NO_3 radicals) Table 16 (for O_3) and Table 22 (for O^3P atoms). Although some product data are available for their reactions with OH radicals and O_3 (see Atkinson, 1997a), the available information is not sufficient to completely determine their mechanisms. Their representation is therefore estimated based on simplified or parameterized mechanisms, or using mechanisms generated for similar monocyclic, monoalkene structures.

The terpenes whose reactions are represented in this mechanism are α- and β-pinenes, Δ^3-carene, d-limonene, and sabinene, the only terpenes for which environmental chamber data are available. The mechanisms used for these compounds, given in terms of model species in the base mechanism, are given in Table 44. The considerations used when deriving mechanisms for the terpenes are discussed below. The performance of these mechanisms in simulating the chamber data for these compounds is summarized in Section V.

Reaction with OH radicals. In the case of the reaction with OH radicals, the simplest mechanism would involve OH adding to the double bond, forming a β-hydroxy radical which will react with O_2 to form the corresponding peroxy radical. This then reacts with NO to form either the corresponding nitrate or alkoxy radical, and where the alkoxy radical can react in various ways, including decomposing to ultimately forming HO_2 and carbonyl compounds.

Table 44 Assigned mechanisms for terpenes and other non-aromatic compounds or groups of compounds that are not processed using the mechanism generation system.

Compound	Kinetic Parameters [a,b] A	Ea	B	Reaction [c] Reaction
				Assigned Mechanisms
α-Pinene	1.21e-11	0.882		A-PINENE + HO. = #.75 RO2-R. + #.25 RO2-N. + #.5 R2O2. + #.75 RCHO + #6.5 XC
	1.01e-15	1.455		A-PINENE + O3 = #.7 HO. + #.081 RO2-R. + #.321 RO2-N. + #1.375 R2O2. + #.298 RCO-O2. + #.051 CO + #.339 HCHO + #.218 RCHO + #.345 ACET + #.002 GLY + #.081 BACL + #.3 RCO-OH + #3.875 XC
	1.19e-12	0.974		A-PINENE + NO3 = #.75 NO2 + #.25 RO2-N. + #.75 R2O2. + #.75 RCHO + #6.25 XC + #.25 XN
	3.20e-11			A-PINENE + O3P = PROD2 + #4 XC
β-Pinene	2.38e-11	0.709		B-PINENE + HO. = #.75 RO2-R. + #.25 RO2-N. + #.5 R2O2. + #.75 HCHO + #.75 PROD2 + #3.25 XC
	1.01e-15	2.493		B-PINENE + O3 = #.34 HO. + #.09 HO2. + #.05 RO2-N. + #.2 R2O2. + #.2 RCO-O2. + #.375 CO + #.1 CO2 + #.25 HCHO + #.75 PROD2 + #.28 HCOOH + #3.595 XC
	2.51e-12			B-PINENE + NO3 = #.75 RO2-R. + #.25 RO2-N. + #.75 R2O2. + #.75 RNO3 + #4 XC + #.25 XN
	2.70e-11			B-PINENE + O3P = #.4 RCHO + #.6 PROD2 + #5.2 XC
3-Carene	1.64ε–11	0.994		3-CARENE + HO. = #.75 RO2-R. + #.25 RO2-N. + #.5 R2O2. + #.75 RCHO + #6.25 XC
	1.01e-15	1.958		3-CARENE + O3 = #.7 HO. + #.161 RO2-N. + #.539 R2O2. + #.482 CCO-O2. + #.058 RCO-O2. + #.058 HCHO + #.482 RCHO + #.3 RCO-OH + #5.492 XC
	9.10e-12			3-CARENE + NO3 = #.75 NO2 + #.25 RO2-N. + #.75 R2O2. + #.75 RCHO + #6.25 XC + #.25 XN
	3.20e-11			3-CARENE + O3P = PROD2 + #4 XC
d-Limonene	3.19ε–11	0.994		D-LIMONE + HO. = #.75 RO2-R. + #.25 RO2-N. + #.5 R2O2. + #.75 RCHO + #6.25 XC
	3.71e-15	1.729		D-LIMONE + O3 = #.7 HO. + #.161 RO2-N. + #.539 R2O2. + #.482 CCO-O2. + #.058 RCO-O2. + #.058 HCHO + #.482 RCHO + #.3 RCO-OH + #5.492 XC
	1.22e-11			D-LIMONE + NO3 = #.75 NO2 + #.25 RO2-N. + #.75 R2O2. + #.75 RCHO + #6.25 XC + #.25 XN
	7.20e-11			D-LIMONE + O3P = PROD2 + #4 XC
Sabinene	2.19e-11	0.994		SABINENE + HO. = #.75 RO2-R. + #.25 RO2-N. + #.5 R2O2. + #.75 HCHO + #.75 PROD2 + #3.25 XC
	1.01e-15	1.459		SABINENE + O3 = #.34 HO. + #.09 HO2. + #.05 RO2-N. + #.2 R2O2. + #.2 RCO-O2. + #.375 CO + #.1 CO2 + #.25 HCHO + #.75 PROD2 + #.28 HCOOH + #3.595 XC
	1.00e-11			SABINENE + NO3 = #.75 RO2-R. + #.25 RO2-N. + #.75 R2O2. + #.75 RNO3 + #4 XC + #.25 XN
	1.69e-11			SABINENE + O3P = #.4 RCHO + #.6 PROD2 + #5.2 XC

Table 44 (continued)

Compound	Kinetic Parameters [a,b] A	Ea	B	Reaction [c] Reaction
Styrene	5.80e-11			STYRENE + HO. = #.87 RO2-R. + #.13 RO2-N. + #.87 HCHO + #.87 BALD + #.26 XC
	1.71e-17			STYRENE + O3 = #.4 HCHO + #.6 BALD + #.6 HCOOH + #.4 RCO-OH + #1.6 XC
	1.51e-13			STYRENE + NO3 = #.22 NO2 + #.65 RO2-R. + #.13 RO2-N. + #.22 R2O2. + #.22 HCHO + #.22 BALD + #.65 RNO3 + #1.56 XC + #.13 XN
	1.76e-11			STYRENE + O3P = PROD2 + #2 XC
N-Methyl-2-Pyrrolidone	2.15e-11			NMP + HO. = #.92 HO2. + #.08 RO2-N. + #.46 RCHO + #.46 PROD2 + #.38 XC + XN
	1.26e-13			NMP + NO3 = #.92 HO2. + #.08 RO2-N. + #.92 PROD2 + #-1 XC + XN
				Adjusted Parameterized Mechanisms
Para Toluene Isocyanate	5.90e-12			P-TI + HO. = #.2 HO. + #.7 HO2. + #.15 MGLY + CRES
Toluene Diisocyanate	7.40e-12			TDI + HO. = #.5 HO. + CRES
Diphenylene Diisocyanate	1.18e-11			MDI + HO. = #.2 HO. + #.7 HO2. + #.15 MGLY + CRES
				"Placeholder" Mechanisms for Approximate Estimates [c]
Trichloro-ethylene	5.63e-13	-0.849		CL3-ETHE + HO. = RO2-R. + #.5 HCHO + #.5 RCHO
n-Propyl Bromide	1.18e-12			C3-BR + HO. = RO2-R. + #.5 HCHO + #.5 RCHO
n-Butyl Bromide	2.46e-12			C4-BR + HO. = RO2-R. + #.5 HCHO + #.5 RCHO
Methyl Chloride	3.15e-13	1.163	2	CH3-CL + HO. = RO2-R. + #.5 HCHO + #.5 RCHO
Dichloro-methane	7.69e-13	0.994	2	CL2-ME + HO. = RO2-R. + #.5 HCHO + #.5 RCHO
Methyl Bromide	2.34e-13	1.035	2	ME-BR + HO. = RO2-R. + #.5 HCHO + #.5 RCHO
Chloroform	5.67e-13	1.002	2	CHCL3 + HO. = RO2-R. + #.5 HCHO + #.5 RCHO
Ethyl Chloride	6.94e-13	0.302	2	C2-CL + HO. = RO2-R. + #.5 HCHO + #.5 RCHO
1,2-Dichloro-ethane	9.90e-13	0.813	2	12CL2-C2 + HO. = RO2-R. + #.5 HCHO + #.5 RCHO
1,1-Dichloro-ethane	2.60e-13			11CL2-C2 + HO. = RO2-R. + #.5 HCHO + #.5 RCHO
1,1,2-Trichloro-ethane	4.00e-13	0.413	2	112CL3C2 + HO. = RO2-R. + #.5 HCHO + #.5 RCHO
1,1,1-Trichloro-ethane	5.33e-13	2.244	2	111-TCE + HO. = RO2-R. + #.5 HCHO + #.5 RCHO
Ethyl Bromide	2.72e-11	2.671		C2-BR + HO. = RO2-R. + #.5 HCHO + #.5 RCHO
1,2-Dibromo-ethane	9.27e-13	0.839	2	11BR2-C2 + HO. = RO2-R. + #.5 HCHO + #.5 RCHO
Vinyl Chloride	1.69e-12	-0.839		CL-ETHE + HO. = RO2-R. + #.5 HCHO + #.5 RCHO
t-1,2-Dichloro-ethene	1.01e-12	-0.497		T-12-DCE + HO. = RO2-R. + #.5 HCHO + #.5 RCHO
Perchloro-ethylene	9.64e-12	2.403		CL4-ETHE + HO. = RO2-R. + #.5 HCHO + #.5 RCHO
Ethyl Amine	1.47e-11	-0.376		ET-AMINE + HO. = RO2-R. + #.5 HCHO + #.5 RCHO

Table 44 (continued)

Compound	Kinetic Parameters [a,b] A	Ea	B	Reaction [c] Reaction
Dimethyl Amine	2.89e-11	-0.491		DM-AMINE + HO. = RO2-R. + #.5 HCHO + #.5 RCHO
Trimethyl Amine	2.62e-11	-0.501		TM-AMINE + HO. = RO2-R. + #.5 HCHO + #.5 RCHO
Ethanolamine	3.15e-11			ETOH-NH2 + HO. = RO2-R. + #.5 HCHO + #.5 RCHO
Diethanol Amine	9.37e-11			ETOH2-NH + HO. = #.96 RO2-R. + #.04 RO2-N. + #.5 HCHO + #.5 RCHO
Triethanolamine	1.16e-10			ETOH3-N + HO. = #.905 RO2-R. + #.095 RO2-N. + #.5 HCHO + #.5 RCHO

[a] Rate constant given by A exp(-Ea/RT) $(T/300)^B$, where the rate constant and A factor are in cm^3 $molec^{-1}$ s^{-1} and the activation energy is in kcal/mole.

[b] See Table 8 for the derivation of the OH radical rate constants used.

[c] See text for a discussion of how the mechanisms were derived.

[d] These mechanisms are for approximate estimates only, and are based on assuming formation of relatively reactive products. They are not based on any evaluation of the chemistry of the compounds, and may not accurately predict their ozone impacts. See text.

$$\text{Terpene} + OH \rightarrow >C(\cdot)\text{-}C(OH)<$$

$$>C(\cdot)\text{-}C(OH)< + O_2 \rightarrow >C(OO\cdot)\text{-}C(OH)<$$

$$>C(OO\cdot)\text{-}C(OH)< + NO \rightarrow >C(ONO_2)\text{-}C(OH)<$$

$$>C(OO\cdot)\text{-}C(OH)< + NO \rightarrow NO_2 + >C(O\cdot)\text{-}C(OH)<$$

$$>C(O\cdot)\text{-}C(OH)< \rightarrow >C{=}O + \text{-}C(\cdot)(OH)\text{-}$$

$$\text{-}C(\cdot)(OH)\text{-} + O_2 \rightarrow HO_2 + >C{=}O$$

$$>C(O\cdot)\text{-}C(OH)< \rightarrow \text{other radicals (additional NO to } NO_2 \text{ conversions)}$$

If the decomposition involves breaking what was the double bond to form an α-hydroxy radical, which is the dominant process for most of the simpler alkenes, then no additional NO to NO_2 conversions would be involved. However, additional NO to NO_2 conversions may occur if other decompositions can compete, which are estimated to be non-negligible for compounds with similar structures as the terpenes. If the reacting double bond is in the ring, the carbonyl products would be expected to be bifunctional compounds with at least one aldehyde group, which is represented in the model by the RCHO model species. If the reacting double bond is a $=CH_2$ group outside the ring, then the products would be formaldehyde + a ketone, the latter represented by PROD2 in the model.

Therefore, for compounds with the double bond in the ring, such as α-pinene, Δ^3-carene, and d-limonene, the following parameterized mechanism is employed:

$$OH + \text{Terpene(ring d.bond)} \rightarrow y_N\ RO2\text{-}N\cdot + (1\text{-}y_N)\ \{RO2\text{-}R\cdot + RCHO\} + y_{R2O2}\ R2O2\cdot$$

where the nitrate yield, y_N, and the amount of extra NO to NO_2 conversions, y_{R2O2}, are determined based on model simulations of the available terpene - NO_x chamber data. For compounds with $=CH_2$ groups, such as β-pinene and sabinene, the parameterized mechanism is

$$OH + Terpene(=CH_2) \rightarrow y_N\ RO2\text{-}N\cdot + (1\text{-}y_N)\ \{RO2\text{-}R\cdot + HCHO + PROD2\} + y_{R2O2}\ R2O2\cdot$$

Best fits to most of the chamber data are obtained using y_N = 0.25 and y_{R2O2} = 0.5, and as indicated on Table 44 this is assumed for all the terpenes.

Reaction with O_3 The Crigiee biradicals expected to be formed in the reactions of O_3 with α-pinene, Δ^3-carene and d-limonene could all be represented in the mechanism generation system, so the overall O_3 reactions could be generated in the same way as used for the other alkenes, if the mechanism for the initial reaction is assigned. This is the approach used for these compounds. All three of these compounds have trisubstituted double bond in the ring, and as discussed above in Section III.E.3, it is assumed that the formation of -CO- + -CHOO[excited] and -CHO + -COO[excited]- occur respectively 30% and 70% of the time, based on ketone yields from acyclic trisubstituted alkenes. Although d-limonene has a second double bond outside the ring, it is assumed that most of the reaction occurs at the more substituted bond in the ring, and reactions at the second double bond is ignored when estimating the overall mechanism. Note that this procedure results in predicted OH yields of 70% for these compounds, which is reasonably close to the experimentally-determined values of 0.76-0.85 for α-pinene and 86% for d-limonene (Atkinson, 1997b). The overall processes generated in this way are shown in Table 44.

The mechanism generation system cannot be used as readily to estimate the reactions of O_3 with β-pinene and sabinene, since reaction to form formaldehyde + a Crigiee biradical with a bicyclic structure is expected to be formed to a non-negligible extent. However, the expected overall reactions of these biradicals are not expected to differ greatly with the structure, at least in terms of model species in the base mechanism. This is expected to be as follows,

$$\text{ring-COO[excited]-ring} \rightarrow \text{ring-C=C(OOH)-ring} \rightarrow OH + \text{ring-C(}\cdot\text{)-CO-ring}$$
$$\text{ring-C(}\cdot\text{)-CO-ring} + O_2 \rightarrow \text{ring-C(OO}\cdot\text{)-CO-ring}$$
$$\text{ring-C(OO}\cdot\text{)-CO-ring} + NO \rightarrow 0.2\ \text{ring-C}(ONO_2)\text{-ring} + 0.8\ \text{ring-C(O}\cdot\text{)-CO-ring}$$
$$\text{ring-C(O}\cdot\text{)-CO-ring} \rightarrow \text{-CO-chain-CO}\cdot$$

where the 20% nitrate yield is the value derived by the mechanism generation system for a substituted C_9 peroxy radical, such as expected to be formed in this case. Therefore, in terms of model species in the base mechanism, reaction of the terpene with O_3 to form this biradical yields the following overall process:

$$O_3 + Terpene(=CH_2) \rightarrow HCHO + OH + 0.2\ RO2\text{-}N\cdot + 0.8\ \{R2O2\cdot + RCO\text{-}O2\cdot\} \qquad (A)$$

Of course, part of the time the reaction would also involve formation of the cyclic ketone + HCHO2[excited], whose subsequent reactions are as discussed above. In this case, the overall process is

$$O_3 + Terpene(=CH_2) \rightarrow PROD2 + 0.12\ HO2 + 0.12\ OH + 0.5\ CO + 0.13\ CO2 + 0.37\ HCOOH \qquad (B)$$

The branching ratio for these two routes is derived based on assuming an overall OH yield of ~35%, which is the measured value for β-pinene and close to the measured values of 26% and 33% for sabinene (Atkinson, 1997a and references therein). This is predicted if Pathways (A) and (B) are assumed to occur respectively 25% and 75% of the time, which gives the following overall process:

$$O_3 + Terpene(=CH_2) \rightarrow 0.25\ HCHO + 0.75\ PROD2 + 0.34\ OH + 0.05\ RO2\text{-}N\cdot + 0.2\ R2O2\cdot$$
$$+ 0.2\ RCO\text{-}O2\cdot + 0.09\ HO2. + 0.375\ CO + 0.1\ CO2 + 0.28\ HCOOH$$

Note, however, that assuming ~75% ketone + HCHO2[excited] formation is not consistent with the observed yields of only 22-23% nopinone from β-pinene and 50% ketone from sabinene (Atkinson, 1997a, and references therein), so this is clearly an oversimplification of the actual mechanisms for these terpenes.

Reaction with NO_3 Radicals. The mechanisms for the terpene + NO_3 reactions are represented in a manner similar to that used for the OH reactions as discussed above, being based on assuming the following set of reactions:

$$\text{Terpene} + NO_3 \rightarrow >C(\cdot)\text{-}C(ONO_2)<$$

$$>C(\cdot)\text{-}C(ONO_2)< + O_2 \rightarrow >C(OO\cdot)\text{-}C(ONO_2)<$$

$$>C(OO\cdot)\text{-}C(ONO_2)< + NO \rightarrow >C(ONO_2)\text{-}C(ONO_2)<$$

$$>C(OO\cdot)\text{-}C(ONO_2)< + NO \rightarrow NO_2 + >C(O\cdot)\text{-}C(ONO_2)<$$

$$>C(O\cdot)\text{-}C(ONO_2)< \rightarrow >C{=}O + \text{-}C(\cdot)(ONO_2)\text{-}$$

$$\text{-}C(\cdot)(ONO_2)\text{-} \rightarrow >C{=}O + NO_2$$

The alkoxy radical estimation methods discussed above predict that the $>C(O\cdot)\text{-}C(ONO_2)<$ radicals of the types formed in these reactions should primarily decompose, so the possible competing reactions are not considered. As with the OH reaction, the carbonyls formed would either be a bifunctional aldehyde (represented by the RCHO model species) in the case of terpenes with double bonds in the ring, or formaldehyde + a ketone (represented by PROD2) in the case of terpenes with $=CH_2$ groups. If a the same overall nitrate yield is assumed as is used in the OH reaction (~25%), then the overall process is:

$$NO_3 + \text{Terpene(ring d.bond)} \rightarrow 0.25\ \{\text{RO2-N}\cdot + \text{XN}\} + 0.75\ \{\text{RCHO} + \text{R2O2}\cdot + \text{NO2}\}$$

for terpenes with the double bond in the ring, and

$$NO_3 + \text{Terpene}(=CH_2) \rightarrow 0.25\ \{\text{RO2-N}\cdot + \text{XN}\} + 0.75\ \{\text{HCHO} + \text{PROD2} + \text{R2O2}\cdot + \text{NO2}\}$$

for terpenes with $=CH_2$ groups.

Reaction with O^3P. As discussed above in Section III.F.3, it is assumed that the reactions of O^3P with the higher alkenes involve formation of ~60% of the corresponding oxide, and ~40% formation of a carbonyl compound. The oxide formed in the reactions of O^3P with the terpenes are represented by the PROD2 model species For terpenes with the double bond in the ring, the carbonyl product is expected to be primarily a ketone, which is also represented in the model by PROD2, while if the terpene has a $=CH_2$ group, the predicted product is an aldehyde, whose formation is represented by RCHO. Thus, the overall reactions are

$$O^3P + \text{Terpene(ring double bond)} \rightarrow \text{PROD2}$$

for terpenes with the double bond in the ring, and

$$O^3P + \text{Terpene}(=CH_2) \rightarrow 0.6\ \text{PROD2} + 0.4\ \text{RCHO}$$

for terpenes with $=CH_2$ groups.

2. Styrene

The mechanism used for the reactions of styrene is based on that derived by Carter et al (1999b) based on environmental chamber experiments employing that compound. Note that to fit the environmental chamber reactivity data it is necessary to assume that essentially no radical formation occurs in the O_3 reaction. The only modification to the mechanism of Carter et al (1999b) is that the nitrate yield for the OH reaction was increased from 10% to 13% to reduce biases in the model simulations of the mini-surrogate incremental reactivity experiments. The nitrate yield in the NO_3 reaction was also increased from 10% to 13%, since it is assumed to be the same in the OH reaction.

3. N-Methyl-2-Pyrrolidone

The mechanism for the reactions of N-methyl-2-pyrrolidone (NMP) is based on that derived by Carter et al (1996c), based on environmental chamber experiments employing that compound. The main differences are that the products 1-formyl-2-pyrrolidinone and N-methyl succimide were represented by PROD2 and RCHO, respectively, rather than by separate model species with parameterized mechanisms. In addition, the nitrate yields used in the mechanism had to be reduced from 15% to 8% for the model to give reasonably good simulations of the data. The fits of the model simulations to the chamber data are given in Appendix B (see also Section V).

4. Aromatic Isocyanates

Environmental chamber reactivity experiments have been carried out for toluene diisocyanate (TDI) (Carter et al, 1997i) and para-toluene isocyanate (P-TI) (Carter et al, 1999a), allowing simplified parameterized mechanisms for these compounds to be developed. Based on the P-TI mechanism, a simplified estimated mechanism for the structurally similar (and commercially more important) compound methylene diphenylene diisocyanate (MDI) was also derived (Carter et al, 1999a). Although the details of the atmospheric reactions of these compounds are unknown, highly simplified mechanisms, such as those shown on Table 44, were shown to simulate the data reasonably well (Carter et al, 1997i, 1999a).

These parameterized aromatic isocyanate mechanisms were incorporated in the updated mechanism and reoptimized to fit the chamber data. In the case of TDI, the OH yield in had to be increased from 0.3 to 0.6 in order to simulate the data approximately as well as the mechanism reported by Carter et al (1997i). In other words, with the updated base mechanism the chamber data are fit with a parameterized model with considerably less radical termination than the model used with the SAPRC-97 mechanism. In the case of P-TI, the extent of radical termination (which in any case is considerably less than for TDI) did not have to be readjusted, but the yield of product compounds represented by methyl glyoxal was reduced from 0.3 to 0.15. The reoptimized mechanisms are shown on Table 44, along with the estimated MDI mechanism, which was derived from the P-TI mechanism as discussed by Carter et al (1999a).

5. Halogenated Compounds

Although we have previously carried out experimental studies of the ozone reactivities of chloropicrin (CCl_3ONO_2) (Carter et al, 1997h), n-propyl and n-butyl bromides (Carter et al, 1997d) and trichloroethylene (Carter et al, 1996d), and developed mechanisms for those compounds that were evaluated using the data obtained, satisfactory fits of the model to chamber data were obtained only for chloropicrin. In particular, no reasonable adjustments of uncertain portions of the mechanisms would result in satisfactory fits to the data for the alkyl bromides (Carter et al, 1997d) or trichloroethylene

(Carter et al, 1996d), especially after the times in the experiment when O_3 formation began. Additional data are needed, with chemically simpler systems, before mechanisms can be developed that can reliably predict ozone impacts of halogenated compounds.

Because the explicit mechanisms with the ClO_x or BrO_x chemistry did not adequately fit the data for two of the three compounds studied, it was decided that our knowledge of these systems is not sufficient to include this chemistry in the base mechanism. Instead, a highly simplified and parameterized "placeholder" mechanism is used in the current mechanism to provide very rough estimates of the approximate range of reactivities of halogenated compounds under MIR conditions, given their OH radical rate constants. This parameterized mechanism, which is shown on Table 44, is based on the assumption that the overall reactions involve at least one NO to NO_2 conversion, form relatively reactive products (which are represented by formaldehyde and the lumped higher aldehyde), and do not involve any significant radical termination processes such as nitrate formation. The appropriate OH rate constant for the compound, given on Table 8 is used in conjunction with the placeholder mechanism given on Table 44.

Note that this mechanism is not appropriate for chloropicrin because it does not represent VOCs that are photoreactive. The reactions of chloropicrin are not represented in the current version of the mechanism, since the necessary ClO_x chemistry has not yet been incorporated in the base mechanism.

The performance of the placeholder mechanisms in simulating the reactivities of the two other halogenated compounds that were studied was evaluated by simulating the results of the incremental reactivity experiments. The results, which are given in Appendix B (see also Section V), indicate that the simplified mechanism performs remarkably well in simulating the experiments with trichloroethylene, especially in the higher NO_x experiments that are more representative of MIR conditions. The simulations of the higher NO_x reactivity experiments with the alkyl bromides were variable, with some experiments being reasonably well simulated, and others with the O_3 reactivity being overestimated by about a factor of 1.5-2. The parameterized mechanism performed very poorly in simulating the reactivities of these compounds under low NO_x conditions, with the model predicting they enhance O_3 in all cases, while O_3 was not enhanced in the low NO_x trichloroethylene runs, and inhibited in the low NO_x runs with the bromides.

Based on the results of this evaluation with a very limited number of compounds, it is possible that the parameterized mechanism may give at least rough estimates of reactivities under MIR (i.e., relatively high NO_x) conditions, but would likely significantly overestimate ozone impacts of such compounds under low NO_x conditions, where many may actually be O_3 inhibitors. Appropriately representing reactivities of these compounds under low NO_x conditions would require incorporating ClO_x or BrO_x reactions into the mechanism, and a better understanding of how they interact with the VOCs and NO_x species under ambient conditions, as well as how they interact with the chamber walls.

6. Amines

There are a number of amines and alcohol amines in the emissions inventories, and an ability to estimate at least their approximate ranges of reactivities, at least under MIR conditions, would be desirable. However, there is insufficient information available to derive or estimate atmospheric reaction mechanisms for amines, and no environmental chamber data available that are suitable for deriving parameterized mechanisms. For that reason, no attempt was made to derive or estimate mechanisms for these compounds. Instead, as with halogenated compounds, simplified and parameterized "placeholder" mechanisms were used for this purpose. These are given on Table 44. As with the amines, the placeholder mechanisms are based on the assumption that there is at least one NO to NO_2 conversion, that relatively

reactive products, represented by formaldehyde and the lumped higher aldehyde, are formed, and that no significant radical termination occurs for C_1-C_3 compounds. For the higher molecular weight alcohol amines, the nitrate yield is estimated based on that for a substituted, non-secondary peroxy radical with the same number of carbons (see Section III.I).

Since it assumes relatively reactive products and no inhibition other than the expected nitrate formation for the higher molecular weight compounds, the mechanism may be biased towards overpredicting the reactivities of these compounds. However, until more data are available this cannot be adequately assessed. In any case, reactivities estimated using these mechanisms must be considered to be highly uncertain.

C. Unrepresented Compounds

Although Table 8 includes OH radical rate constants for the atmospheric reactions of representatives of other classes of organic compounds, including several sulfur- and silicon-containing compounds, these are not represented in the current version of the mechanism. With the exception of several volatile siloxanes (Carter et al, 1992), which were shown to be ozone inhibitors under all conditions, there is insufficient information available to develop or evaluate mechanisms for these compounds. Although highly approximate estimated mechanisms could be developed in some cases, there was insufficient time and resources available to carry this out for this version of the mechanism.

V. MECHANISM EVALUATION

The base mechanism and the mechanisms for the individual VOCs were evaluated by comparing results of model simulations of with results of primarily indoor environmental chamber experiments carried out at the University of California at Riverside. These include not only experiments from the large data base of UCR chamber experiments through 1993 (Carter et al, 1995d), but also the large number of experiments carried out subsequently at CE-CERT. These include the experiments used in the development and evaluation of the SAPRC-97 mechanism (Carter et al, 1997a), and reactivity studies of a wide variety of individual VOCs (Carter et al, 1996a-d, 1997b-g,i, 1999a,b, 2000b-g), and studies of representative consumer product VOCs (Carter et al, 2000a). The experiments used in the evaluation, and references to the reports documenting the experiments, are summarized on Table B-1 in Appendix B. These consisted of the following:

- 76 characterization runs, including 3 pure air runs, 8 acetaldehyde - air runs to determine NO_x offgasing effects, and 65 CO - NO_x or n-butane - NO_x experiments to measure the chamber radical source.
- 481 single VOC runs involving 37 types of VOCs.
- 447 incremental reactivity experiments involving 87 types of VOCs or mineral spirits or solvent samples. These experiments consisted of determining the effect of adding the VOC or sample to a "base case" reactive organic gas (ROG) - NO_x "surrogate" mixture simulating ambient mixtures. The types of incremental reactivity experiments used in this evaluation, and the codes used to identify them in the tables and figures in Appendix B, are indicated on Table 45.
- 673 mixture runs involving various types of simple or complex mixtures or ambient ROG surrogates. Most of these (556 runs) were "base case" surrogate - NO_x runs carried out in conjunction with the incremental reactivity experiments. The types of mixtures or surrogates employed, and the codes used to identify them in Appendix B, are indicated on Table 45.

The environmental chambers used to generate the data used in this evaluation are summarized on Table 46. Note that a two- or three-letter code is used to designate each chamber. The individual experiments in any given chamber are numbered sequentially, and as shown on Table B-1, the runs are designated by the chamber code followed by the run number. Note that the DTC, OTC, and (for most runs) the CTC had dual reactors where two mixtures could be irradiated simultaneously. In those cases, the suffix "A" or "B" is used to indicate the reactor used to obtain the data. For incremental reactivity experiments, the designation refers to the reactor where the test VOC was added, with the understanding that the other reactor contained the same mixture without the added VOC.

There is also a large database of outdoor environmental chamber experiments that were carried out at the University of North Carolina that can be used for mechanism evaluation. These have been used for evaluations of the SAPRC-90 (Carter and Lurmann, 1991) and other (e.g., Carter and Lurmann, 1990; Gery et al, 1988) mechanisms, as well as for evaluation of the detailed isoprene mechanism of Carter and Atkinson (1996). Unfortunately, there was insufficient time to conduct a comprehensive evaluation of this mechanism using the UNC chamber data base, because of the need to update and re-evaluate the chamber model for that chamber. However, results of previous evaluation studies have shown that mechanisms that perform reasonably well in simulating the UCR indoor chamber data base also perform reasonably well in simulating the UNC chamber data (Carter and Lurmann, 1990, 1991; Carter and Atkinson, 1996).

Table 45. Designations used for types of incremental reactivity experiments and complex mixtures in the summaries of the evaluation experiments and results.

Designation	Description
	Types of Incremental Reactivity Experiments
MR3	Experiments using the 3-component "mini-surrogate" at relatively high NO_x levels. This type of experiment was used in our first major experimental incremental reactivity study (Carter et al, 1993a), and is still used as part of our experimental protocol to evaluate VOC reactivity. This employs relatively high NOx levels and uses an ethene, n-hexane, and m-xylene mixture as a simple representation of ambient VOCs. As discussed by Carter et al (1995b), experiments using this surrogate are very sensitive to effects of VOCs on radical levels (e.g., aspects of the mechanism that affect radical initiation or inhibition).
MR8	Experiments using the 8-component "full surrogate" at relatively high NO_x levels. This type of experiment was first employed by Carter et al (1995b) as a more realistic representation of maximum incremental reactivity (MIR) conditions than the mini-surrogate system, and that is also used as part of our standard experimental protocol to evaluate reactivity. Like the mini-surrogate, this also employs relatively high NOx conditions, but uses a mixture as of of n-butane, n-octane, ethene, propene, trans-2-butene, toluene, m-xylene, and formaldehyde as a more realistic representation of ambient conditions. Incremental reactivities measured using these experiments have been shown to give the best correlation to atmospheric MIR's than the other types of surrogate - NOx systems we employ for reactivity studies (Carter et al, 1995b).
R8	Experiments using the 8-component "full surrogate" at lower NO_x levels. This uses the same surrogate mixture as the "MR8" experiments, but with NO_x levels reduced by a factor of ~2. This type of experiment was also developed by Carter et al (1995b) and is also used as part of our standard experimental protocol to evaluate reactivity. These experiments evaluate the effects of VOCs on O3 formation under conditions where NOx is limited.
MRE	Experiments using ethene alone as the ROG surrogate, at relatively high NO_x levels. This was used in the study of Carter et al (1995b) when evaluating the effects of using simplified surrogate systems, and in some experiments to evaluate reactivities of terpenes. It has not been used subsequently because evaluation results are highly sensitive to the ability of the model to simulate the base case experiment, which tend to be variable.
MR4	Similar to "MR3" except that toluene and 1,3,5-trimethylbenzene is used in place of m-xylene. This was used in some recent experiments as an alternative to the standard mini-surrogate because the more rapidly reacting 1,3,5-trimethylbenzene gives a somewhat better measure of the effects of the VOC on radical levels. It is not widely used because the results are similar to those using the standard mini-surrogate, and use of the standard surrogate gives better comparability to the large existing data base.
R3	Experiments using the standard "MR3" mini-surrogate, but at lower NOx levels than the standard mini-surrogate. This was used in a few cases as part of specialized studies, or because of errors in reactant injections.
RE	Experiments using ethene as the surrogate and carried out under NOx limited conditions. This was used in a few experiments with terpenes (i.e., ethene + terpene experiments were carried out to evaluate terpene mechanisms).
RX	Experiments using other miscellaneous or non-standard surrogate - NO_x mixtures for the base case. These were used either for special studies, because gas chromatographic interferences prevented use of the standard surrogate, or because of injection errors.

Table 45 (continued)

Designation	Description
	Types of Simple Mixtures
MIX-A	Mixture of alkanes
MIX-E	Mixture of alkenes
MIX-AE	Mixture of alkanes and alkenes
MIX-AO	Mixtures of alkanes and oxygenates (generally aldehydes)
MIX-RO	Mixtures of aromatics and oxygenates (generally aldehydes)
MIX-AR	Mixtures of alkanes and aromatics
MIX-ER	Mixtures of alkenes and aromatics
	Ambient Surrogate Mixtures used in Base Case Incremental Reactivity Experiments.
SURG-3M	Base case for the "MR3" incremental reactivity experiments. Employed the standard 3-component "mini-surrogate" at relatively high NO_x concentrations.
SURG-8M	Base case for the "MR8" incremental reactivity experiments. Employed the standard 8-component "full surrogate" at relatively high NO_x concentrations.
SURG-8	Base case for the "R8" incremental reactivity experiments. Employed the standard 8-component "full surrogate" at lower NO_x concentrations.
SURG-3	Base case for the "R3" incremental reactivity experiments. Employed the standard 3-component "mini-surrogate" at lower NO_x concentrations.
SURG-4M	Base case for the "MR4" incremental reactivity experiments. Employed the modified version of the 3-component "mini-surrogate" at relatively high NO_x concentrations.
SURG-X	Base case for the "MRX" incremental reactivity experiments. Employed various miscellaneous surrogates, usually (but not always) at relatively high NO_x concentrations.
	Ambient Surrogate Mixtures used in Various Complex Mixture Experiments.
SURG-4	Experiments in the ITC chamber using a 4-component surrogate, low NO_x mixture used in the early incremental reactivity study of Carter and Atkinson (1987).
SURG-4R	Modified versions of the "SURG-4" mixture used in the study of Carter and Atkinson (1987).
SURG-7	A surrogate mixture of seven hydrocarbons used in several runs in the SAPRC EC (Pitts et al, 1979).
SURG-8S	A surrogate mixture of 8 hydrocarbons used in the "multi-day effects" study of Carter et al (1984b).

Table 46. Summary of environmental chambers used to obtain the data used for mechanism evaluation.

Chamber ID	Light Source	Type	Volume (liters)	Surface	RH	Period for Runs	Additional Information
ITC	Blacklight	Single	~6400	Semi-collapsible 2 mil FTP Teflon bag held by frame	~50%	1982-86	See Carter et al (1995d)
ETC	Blacklight	Single	~3000	Semi-collapsible 2 mil FTP Teflon bag held by frame	Dry	1989-93	See Carter et al (1995d)
DTC	Blacklight	Dual	2 x ~5000	Two semi-collapsible 2 mil FTP Teflon bags held by frames	Dry	1993-99	See Carter et al (1995d)
EC	25 KW Xenon Arc	Single	5774	Teflon coated aluminum, evacuable cylinder	~50%	1975-84	See Carter et al (1995d)
XTC	4 x 6 KW Xenon Arc	Single	~5000	Semi-collapsible 2 mil FTP Teflon bag held by frame	Dry	1993	See Carter et al (1995d)
CTC (11-82)	4 x 6 KW Xenon Arc	Single	~5000	Semi-collapsible 2 mil FTP Teflon bag held by frame	Dry	1994-95	Very similar to XTC.
CTC (83+)	4 x 6 KW Xenon Arc	Dual	2 x ~2500	Two semi-collapsible 2 mil FTP Teflon bags held by frames	Dry	1995-99	Similar to XTC except dual bags.
OTC	Sunlight	Dual	2 x ~20,000	Dividable and completely collapsible 2 mil FEP Teflon bag.	Dry	1992-93	See Carter et al (1995c,d)

Data from seven different chambers were used in these evaluations, and their major characteristics are summarized in Table 46. As indicated on the table, most of these chambers are described in detail by Carter et al (1995d), or references therein. The only exception is the CTC, which is the most recently constructed of these chambers. This is essentially the XTC after it was moved from SAPRC to CT-CERT, and employed the same light source and general design.

A. Chamber Simulation Methods

Evaluations of mechanisms using chamber data require an appropriate representation of the conditions of the chamber experiments that affect the simulation results. These include initial reactant concentrations, physical conditions such as temperature and dilution, light intensity and spectrum, and the major wall effects such as the chamber radical source, O_3 decays, NO_x offgasing, etc. These considerations are discussed in detail elsewhere (e.g., Carter and Atkinson, 1990, 1991; Carter et al, 1995c,d, 1997a), and generally the approach employed in this work was similar. This is summarized briefly in the following sections.

1. Light Characterization

Light characterization requires specification of both the intensity and the spectrum of the light source used in the experiments. As discussed by Carter et al (1995c,d) for indoor chamber runs, this is determined by the NO_2 photolysis rate (usually derived from results of NO_2 actinometry experiments), and the relative spectral distribution of the light source. For blacklight chambers the spectrum is assumed to be constant and the spectrum recommended by Carter et al (1995d) is used. For xenon arc chambers, the spectrum tends to vary with time, and the spectrum used for modeling is based on measurements made during or around the time of the experiment as discussed by Carter et al (1995d). For the outdoor

chamber, the spectrum was calculated as a function of solar zenith angle as described by Carter et al. (1995c).

For the blacklight chambers and the EC, the NO_2 photolysis rates were determined by carrying out periodic NO_2 actinometry experiments, with the values assigned to individual runs being based on the trends or averages of the measurements carried out around the time of the experiment (Carter et al, 1995d, 1997a). For the XTC and CTC, the relative trends in light intensity with time were determined primarily using absolute spectral intensity measurements, whose data were placed on an absolute basis using occasional in-chamber steady-state or Cl_2 actinometry measurements (Carter et al, 1995d, 1997a). For the outdoor chamber, the absolute light intensities were obtained using continuous UV radiometer and total solar radiometer (TSR) data. These were used to derive absolute spectra for calculating photolysis rates by fitting outputs of a solar radiation model to these measurements (Carter et al, 1995c).

For the DTC and CTC experiments carried out since 1994, a check on the accuracy of the light intensity assignments can be obtained from the trends of the results of the many replicate "base case" experiments carried out in conjunction with the incremental reactivity experiments. As the light intensity gradually decreases over time, the rate of O_3 formation and NO oxidation also decrease accordingly, and these rates take step increases when the changes are made that increase the light intensity. There are two periods when the trends of the results of these experiments were not consistent with the photolysis rates as indicated by the NO_2 actinometry or spectral intensity results. One case involved DTC runs 624-647 that were carried out using 75% lights (Carter et al, 1999c), but no runs in this group were used in this evaluation. The other case consisted of the CTC runs after CTC170, which includes a number of runs used in this evaluation. For these experiments, the rates of decrease in the rates of NO oxidation and O_3 formation in the base case runs decreased more rapidly with time than did the light intensity as measured by NO_2 actinometry or spectral measurements made outside the chamber (Carter et al, 1999b). On the other hand, the Cl_2 actinometry measurements made inside the chamber, though less precise than the other measurement methods, were consistent with the trend in base case surrogate reactivity results. This suggests that the chamber walls may be contributing to the decreasing intensity trend. For these CTC runs, the method for assigning NO_2 photolysis rates was adjusted to be consistent with the trend in replicate base case surrogate results (Carter et al, 1999b).

2. Representation of Chamber Wall Effects

The chamber wall effects that were represented in the simulations of these experiments were the chamber radical source (Carter et al, 1982), NO_x offgasing, heterogeneous formation of HONO from NO_2, N_2O_5 hydrolysis, O_3 dark decay, and background effects causing excess NO to NO_2 conversions. These are represented by the following psuedo-reactions:

$$\text{Walls} + h\nu \rightarrow \text{HONO} \qquad \text{(RN)}$$

$$\text{Walls} + NO_2 + h\nu \rightarrow 0.5\ \{\text{HONO} + \text{Wall-}NO_x\} \qquad \text{(RS)}$$

$$\text{Walls} + NO_2 \rightarrow y_{HONO}\ \text{HONO} + (1\text{-}y_{HONO})\ \text{Wall-}NO_x \qquad \text{(}NO_2\text{W)}$$

$$N_2O_5 + \text{walls} \rightarrow 2\ \text{Wall-}NO_x \qquad \text{(}N_{25}\text{I)}$$

$$N_2O_5 + H_2O + \text{walls} \rightarrow 2\ \text{Wall-}NO_x \qquad \text{(}N_{25}\text{S)}$$

$$\text{Walls} + O_3 \rightarrow (\text{loss of } O_3) \qquad \text{(}O_3\text{W)}$$

Note that "Wall-NO_x" in the above reactions is an inert counter species that was used to account for nitrogen balance only, since it undergoes no subsequent reaction in the model. The rate constants for

these processes, and the stoichiometric parameter y_{HONO} were assigned based on the results of appropriate characterization runs or estimates as indicated on Table 47. See Carter and Lurmann (1990, 1991) and Carter et al (1995d) for a more detailed discussion of how these processes are represented in chamber models and how their rate parameters are derived.

The formation of HONO from the walls (Reaction RN) was used to represent both the chamber radical source and NO_x offgasing, because the HONO so formed would photolyze rapidly to form both OH radicals and NO

$$HONO + h\nu \rightarrow OH + NO$$

Previously, the radical source and NO_x offgasing were represented as separate processes, as

$$Walls + h\nu \rightarrow OH \qquad (RS)$$

$$Walls + h\nu \rightarrow NO_2 \qquad (ENO_2)$$

with the rates of each being assigned independently based on appropriate characterization runs (n-butane - NO_x or CO - NO_x runs for the radical source, and pure air or acetaldehyde-air runs for NO_x offgasing) (Carter and Lurmann, 1990, 1991; Carter et al, 1995d, 1997a). However, in most cases the rates of these two reactions tended to be the same to within the uncertainty of the determination, suggesting that they may be due to the same process. For that reason, the revised representation, using Reactions (RN) and (RS), is used in this work. Note that the NO_2 dependence of the radical source, represented by Reaction (RS), appears to be significant only in the case of the EC, so that reaction is assigned a nonzero rate constant only for runs in that chamber. If there is an NO_2 dependence for the radical source in the other chambers, it is much less than the run-to-run variability of the radical source.

Table 47 gives the rate constants and other wall-dependent parameters that were assigned to the experiments used in this evaluation. Note that the "Set(s)" column on the table indicates the "characterization set" (Carter et al, 1995d), which refers to a group of runs that are all assumed to have the same characterization parameters. The characterization set assigned to each experiment is given with the run listing in Table B-1 in Appendix B. In most cases, this refers to runs in a given reaction bag, though sometimes the characterization set changes if the results of characterization runs indicate that the wall effects parameters have changed. For the CTC, characterization sets are also used to refer to runs that are assumed to have the same spectral distribution. Since the spectral distribution changes more rapidly then the reactor characteristics, for that chamber there are many characterization sets where the same wall effects parameters are assigned.

3. Other Reaction Conditions

The other reaction conditions that need to be represented in the simulations are the initial reactant concentrations, temperature, humidity and dilution. In most cases the initial reactant concentrations are determined from measurements made prior to the start of the irradiation, but in some reactivity experiments with missing data for a "base case" reactant the average concentration measured in similar experiments is used. The one exception to this is the initial HONO that may be introduced as a contaminant with the NO_x injections; this is represented by the parameter "HONO-F", whose value is derived based on results of radical source characterization runs as indicated on Table 47. The humidity used in the simulations is also indicated on Table 47.

Table 47. Chamber wall effect and background characterization parameters used in the environmental chamber model simulations for mechanism evaluation.

Cham.	Set(s)	Value	Discussion
RN-I (ppb)			Ratio of the rate of **wall + hn -> HONO** to the NO_2 photolysis rate.
ITC	All	0.045	Average of value of RS-I which gave best fits to n-butane - NOx chamber experiments carried out in this chamber. The initial HONO was optimized at the same time. Temperature does not vary significantly in the ITC runs used for evaluation.
ETC	2-3	9.00e+9 exp(-9712/T) 0.078 @ 300K	The few n-butane - NOx experiments in this chamber appear to be anomalous. The preexponential factor is derived to minimize biases in model simulations of the large number of mini-surrogate - NOx chamber experiments carried out in this chamber. The activation energy is based on the value that gives best fits to temperature dependences of RN-I values which fit n-butane - NOx and CO - NOx experiments in the OTC and other Teflon bag chambers.
DTC	1	0.058	Average of value of RS-I which gave best fits to n-butane - NOx chamber experiments carried out in this chamber. The initial HONO was optimized at the same time. If a temperature dependence is shown, it was derived from the temperature dependence of the RN-I values that best fit characterization data in outdoor chamber experiments, with the same activation energy used in all cases. If a temperature dependence is not shown, then the temperature variation for experiments in this set is small compared to the run-to-run variability in the best fit RN-I values. Note that the radical source in Sets 3, 12, 13, and 16 runs was anomalously high.
	3	2.16e+10 exp(-9712/T) 0.188 @ 300K	
	10	8.14e+9 exp(-9712/T) 0.071 @ 300K	
	11	0.080	
	12	0.277	
	13	0.146	
	14	0.082	
	15	0.057	
	16	0.212	
	17	0.073	
	18	0.066	
XTC	1	5.25e+9 exp(-9712/T) 0.0457 @ 300K	Same procedure as DTC
CTC	1-8	0.064	Same procedure as DTC
	9	0.097	
	10	0.064	
OTC		6.04e+9 exp(-9712/T) 0.053 @ 300K	Same procedure as DTC
EC	1	0.308	Based on the NO2 dependence radical source derived by Carter et al (1981), adjusted downward by 20% to reduce biases in simulations of n-butane - NOx experiments carried out in this chamber. The NO2-dependent radical source term, RS-S, was reduced by an equal factor.
RS-S (unitless)			Ratio of the rate of **NO2 + hv -> 0.5 HONO + 0.5 wall NOx** to the NO_2 photolysis rate.
EC	1	0.17%	Based on the NO2 dependence radical source derived by Carter et al (1981), adjusted downward by 20% to reduce biases in simulations of n-butane - NOx experiments carried out in this chamber. The NO2-independent radical source term, RN-I, was reduced by an equal factor.
All others		0	Any dependence of apparent radical source on initial NOx levels in Teflon bag chambers was found to be much less than the run-to-run variability.

Table 47 (continued)

Cham.	Set(s)	Value	Discussion
HONO-I (ppb)			Initial HONO in experiment, assumed to be independent of other reactants.
ITC	All	1.7	Average of initial HONO value which gave best fits to n-butane - NOx chamber experiments carried out in this chamber. The RN-I parameter was optimized at the same time. The best fit initial HONO values appear to be approximately independent of the initial NO2.
HONO-F (unitless)			Ratio of the initial HONO concentration to the measured initial NO2. [The initial NO2 in the experiment is reduced by a factor of 1 - (HONO-F)]. Unless the characterization data indicate otherwise, it is assumed that the initial HONO is introduced with the NO2 injection, so is it is assumed to be proportional to the initial NO2 concentration.
ETC	2-3	0	Initial HONO assumed to be small for these experiments, where special procedures were employed to minimize HONO contamination. See Carter et al (1993a).
DTC	1	0.1%	Average of value of initial HONO to initial NO2 which gave best fits to n-butane - NOx chamber experiments carried out in this chamber. The RN-I parameter was optimized at the same time.
	3	0.4%	
	10	0.8%	
	11	0.6%	
	12	0.5%	
	13	0.9%	
	14	0.6%	
	15	0.7%	
	16	0.5%	
	17	0.3%	
	18	0.8%	
XTC	1	1.2%	Same procedure as DTC
CTC	1-8,10	0.8%	Same procedure as DTC
	9	0.8%	
OTC	10-12	0	Apparently not significant compared to RN-I.
E-NO2/K1 (ppb)			Ratio of rate of NO2 offgasing from the walls to the NO2 photolysis rate.
EC	1	0.10	Adjusted to fit O3 formation in acetaldehyde/air run EC-253.
All Teflon Bag Chambers		0	The NOx offgasing caused by representing the radical source by HONO offgasing appears to be sufficient for accounting for NOx offgasing effects in most cases. RN-I parameters adjusted to fit experiments sensitive to the radical source are consistent with NOx offgasing rates adjusted to fit pure air or aldehyde - air runs, to within the uncertainty and variability.
k(NO2W) (min^{-1})			Rate of unimolecular loss (or hydrolysis) of NO2 to the walls.
All Teflon Bag Chambers		1.6e-4	Based on dark NO2 decay and HONO formation measured in the ETC by Pitts et al. (1984). Assumed to be the same in all Teflon bag chambers, regardless of volume.
EC	1	2.8e-4	Based on dark NO2 decay and HONO formation measured in the EC by Pitts et al. (1984).
YHONO			Yield of HONO in the unimolecular reaction (hydrolysis) of NO2 on the walls.

Table 47 (continued)

Cham.	Set(s)	Value	Discussion
All Teflon Bag Chambers		0.2	Based on dark NO2 decay and HONO formation measured in the ETC by Pitts et al. (1984). Assumed to be the same in all Teflon bag chambers, regardless of volume.
EC	1	0.5	Based on dark NO2 decay and HONO formation measured in the EC by Pitts et al. (1984).
k(O3W) (min^{-1})			Unimolecular loss rate of O3 to the walls.
ITC	All	1.5e-4	Based on results of O_3 decay in Teflon bag chambers experiments as discussed by Carter et al (1995d).
ETC	All	1.5e-4	Same as ITC
DTC	All	1.5e-4	Same as ITC
XTC	All	1.5e-4	Same as ITC
CTC	All	8.5e-5	Based on results of O_3 decay experiments in this chamber
OTC	All	1.7e-4	Based on results of O_3 decay experiments in this chamber
EC	All	1.1e-3	Based on results of O_3 decay in Teflon bag chambers experiments as discussed by Carter et al (1995d).
k(N26I) (min^{-1})			Rate constant for **N2O5 -> 2 Wall-NOx**. This represents the humidity-independent portion of the wall loss of N_2O_5, or the intercept of plots of rates of N_2O_5 loss against humidity.
All Teflon Bag Chambers		2.8e-3	Based on N_2O_5 decay rate measurements made by Tuazon et al (1983) for the ETC. Assumed to be independent of chamber size (Carter et al, 1995d).
EC	1	4.7e-3	Based on N_2O_5 decay rate measurements made by Tuazon et al (1983) for the EC. See also Carter et al (1995d).
k(N26S) (ppm^{-1} min^{-1})			Rate constant for **N2O5 + H2O -> 2 Wall-NOx.** This represents the humidity dependent portion of the wall loss of N_2O_5, or the slope of plots of rates of N_2O_5 loss against humidity.
All Teflon Bag Chambers		1.1e-6	Based on N_2O_5 decay rate measurements made by Tuazon et al (1983) for the ETC. Assumed to be independent of chamber size (Carter et al, 1995d).
EC	1	1.8e-6	Based on N_2O_5 decay rate measurements made by Tuazon et al (1983) for the EC. See also Carter et al (1995d).
k(XSHC) (min^{-1})			Rate constant for **OH -> HO2**. This represents the effects of reaction of OH with reactive VOCs in the background air or offgased from the chamber walls. This parameter does not significantly affect model simulations of experiments other than pure air runs.
All Teflon Bag Chambers		250	Estimated from modeling several pure air in the ITC (Carter et al, 1996d), and also consistent with simulations of pure air runs in the ETC (Carter et al, 1997a).
EC	1	0	Assumed to be negligible because the EC is generally evacuated overnight between experiments (Carter et al, 1995d).
H2O (ppm)			Default water vapor concentration for runs where no humidity data are available.
ITC	all	2.0e+4	This corresponds to ~50% RH at 303K, which is the condition for most experiments in this chamber.

Table 47 (continued)

Cham.	Set(s)	Value	Discussion
All Other Teflon Bag Chambers		1.0e+3	Experiments in these chambers were carried out using dried purified air. The limited humidity data for such runs indicate that the humidity was less than 5%, probably no more than ~2.5%, and possibly much less than that. The default value corresponds to ~2.5 - 3% RH for the conditions of most experiments.
EC	1	2.0e+4	This corresponds to ~50% RH at 303K, which is the condition for most experiments in this chamber. Humidity data are available for most EC runs, so the default is usually not used.

The temperature used in the simulations is derived from the measurements made during the experiments, as discussed by Carter et al (1995d). The dilution varies depending on the chamber, and is derived as also discussed by Carter et al (1995d). The dilution is relatively small for all experiments used for mechanism evaluation in this work, being about 2% per hour in the EC, and generally less than 1% per hour in the Teflon bag chambers, which can collapse as samples are withdrawn.

Most experiments used in this evaluation were 6-hour runs. A few multi-day runs were included in the evaluation set, but only the simulation results for the first day are shown. Except for the few outdoor runs, most of the experiments were carried out with constant light intensity and approximately constant temperature.

4. Incremental Reactivity Simulations

Most incremental reactivity experiments consisted of simultaneous irradiations of two mixtures in the two reactors (or "sides") of the chamber, one with and one without the added test compound. Those were simulated by separately simulating the experiment on each side, using the reactant concentrations and conditions measured for that side. The incremental reactivity data (i.e., change in measured quantities caused by adding the VOC, divided by the amount added) were then calculated from the results of these two simulations in exactly the same way the experimental reactivity data were calculated from the experimental measurements.

This procedure could not be used when simulating incremental reactivity experiments carried out in the ECT, where base case and added test VOC irradiations were carried out as separate experiments, and temperature and some other conditions tended to vary from run to run (Carter et al, 1993a). In those cases, the base case conditions used to derive the experimental incremental reactivity measurement was derived using correlations between experimental conditions and results of the separate base case experiments (Carter et al, 1993a). In the model simulations, the base case was simulated by simulating the test VOC experiment without the test compound added, and the incremental reactivities were calculated from the differences in the results of that simulation and the simulation of the actual experiment.

5. Chemical Mechanism Employed

The chemical mechanism employed in the chamber simulations consisted of the base mechanism with reactions added as needed to represent the VOCs present, together with the reactions used to represent the chamber effects. The base mechanism used is listed in Table A-2 in Appendix A. The

reactions used to represent the individual VOCs not in the base mechanism, which were derived as discussed in previous sections, are listed in Table A-6 in Appendix A[19]. No lumping of initially present VOCs was employed except when simulating the components of the mineral spirits samples (MS-A through MS-D), where lumped species with averaged parameters were used to represent the alkanes and (for MS-A) aromatics and alkenes present. The reactions and parameters added to represent chamber effects are as discussed above in Section V.A.2.

B. Chamber Simulation Results

The results of the simulation of the chamber experiments are summarized in Table B-1 and in the various figures in Appendix B. Table B-1 gives the experimental and calculated values of the quantity $\Delta(O_3\text{-}NO)$[20] for 2, 4, and 6-hours into the experiments for all experiments used in the evaluation except for the pure air and acetaldehyde-air runs. The quantity $\Delta (O_3\text{-}NO)$ is defined as

$$\Delta (O_3\text{-}NO)_t = [O_3]_t - [NO]_t - ([O_3]_0 - [NO]_0) \qquad \text{(XXX)}$$

where $[O_3]_0$, $[NO]_0$, $[O_3]_t$, and $[NO]_t$ are the initial and time=t concentrations of ozone, and NO, respectively. As discussed previously (e.g., Carter and Lurmann, 1990, 1991); Carter and Atkinson, 1984), this gives a measure of the ability of the model to simulate the chemical processes that cause ozone formation that gives a useful measure even where ozone is suppressed by the presence of excess NO. Table B-1 also shows the percentage error in the calculation for each experiment where $\Delta(O_3\text{-}NO)$ is greater than 1 pphm (0.01 ppm). This is defined as

$$\Delta\% = 100 \text{ x (Calculated value - Experimental value) / Calculated value} \qquad \text{(XXXI)}$$

This gives a measure of the performance of the model in simulating the rates of O_3 formation and NO oxidation at various times in the individual experiments.

Because of the large number of experiments, Table B-1 is not very useful for giving a sense of the overall model performance in simulating the various types of experiments. For that reason, most of Appendix B consists of various figures displaying the model performance in graphical form. Depending on the types and numbers of runs involved, these can consist of concentration - time plots of $\Delta(O_3\text{-}NO)$ or (in a few cases) of other species; distribution plots of percentage errors in model simulations of $\Delta(O_3\text{-}NO)$ (calculated using Equation XXXI), or plots of incremental reactivity data.

The incremental reactivity data plots include plots of experimental and calculated $\Delta(O_3\text{-}NO)$ for the base case and added VOC ("test") experiment, and plots of experimental and calculated incremental reactivities (IR)'s for $\Delta(O_3\text{-}NO)$ and IntOH. These quantities are defined as follows:

$$\text{IR } \Delta(O_3\text{-}NO)_t = \{\Delta(O_3\text{-}NO)_t^{\text{Added VOC Experiment}} - \Delta(O_3\text{-}NO)_t^{\text{Base Case Experiment}}\} / [\text{VOC added}]$$

$$\text{IR IntOH}_t = \{\text{IntOH}_t^{\text{Added VOC Experiment}} - \text{IntOH}_t^{\text{Base Case Experiment}}\} / [\text{VOC added}]$$

[19] The VOCs were actually represented in the software using generalized reactions with variable parameters, whose values were assigned depending on the particular VOC being represented. However, the effect is the same as explicitly incorporating the reactions as shown in Table A-6.

[20] Note that $\Delta(O_3\text{-}NO)$ is sometimes referred to as d(O3-NO) or D(O3-NO) on some of the tabulations of the results.

and IntOH is the integrated OH radical levels, calculated from the rates of consumption of the most reactive VOC in the base case mixture that reacts only with OH radicals (usually m-xylene) (Carter et al, 1993a). Note that there are no "base case" data shown for incremental reactivity experiments carried out in the ETC, since there is no single base case experiment associated with those runs (see above).

As observed in previous mechanism evaluation studies, although there were runs that were not particularly well simulated by the model, overall the model fit most of $\Delta(O_3\text{-NO})$ data to within ±30% or better. The overall performance of the model in simulating all the runs listed in Table B-1 is shown on Figure 12. The model simulated the 6-hour $\Delta(O_3\text{-NO})$ to within ±5% for ~1/3 of the experiments, to within ±15% for ~3/4 of the runs, and to within ±25% for almost 90% of the experiments. The model has a slight bias (average Δ% of 9%) towards overpredicting the t=1 hour $\Delta(O_3\text{-NO})$ data, but this bias decreases to ~4% for the later periods of the runs. This is a somewhat better model performance than the simulations of the previous versions of the SAPRC mechanism (e.g., Carter and Lurmann, 1991). However, this better overall performance may be more a result of eliminating poorly characterized experiments or more difficult to characterize outdoor runs from the evaluation set than to changes or improvements in the mechanism.

Table 48 gives a summary of the results of the evaluations of the mechanisms for the various types of experiments, and indicates the figures in Appendix B where the various evaluation results are shown. The table also gives codes indicating the overall mechanism performance. These include

1. Fits the data to within the experimental uncertainty or with biases that are not considered to be significant. For mixtures, this is used to indicate that there is no overall bias in the distribution of fits to $\Delta([O_3]\text{-}[NO])$.
2. Poor fits for some runs or non-negligible overall biases indicate possible problems with the mechanism for this compound, or there are insufficient data for satisfactory mechanism evaluation. For mixtures, this is used to indicate that there is a non-negligible bias in the distribution of fits to $\Delta([O_3]\text{-}[NO])$.
3. The mechanism either does not satisfactorily fit the data, or is considered to be too unrepresentative of the chemistry involved to give reliable atmospheric reactivity predictions. For mixtures, this is used to indicate that there is a large bias in the distribution of fits to $\Delta([O_3]\text{-}[NO])$.

The compounds where the evaluation results indicated possible adjustments to the mechanism may be appropriate or where there was insufficient data for satisfactory evaluation included the following: Cresols, naphthalene, dimethyl naphthalene, and tetralin are included because the data are considered insufficient for satisfactory mechanism development; 4-diethyl hexane, cyclohexanone, t-butyl alcohol, and dimethyl glutarate, because there are non-negligible biases in simulations of full surrogate experiments after adjusting the nitrate yields to fit the mini-surrogate runs; β-pinene is included because of poor fits to the data for some runs; and benzene is included because of poor fits to the data in some runs and for some measures of reactivity. Reactivity predictions for these compounds are therefore considered to be somewhat uncertain, though not as uncertain as those for compounds for which no data are available for mechanism evaluation.

The compounds where the mechanism does not satisfactorily fit the data or is considered to be too uncertain for reliable reactivity predictions are the alkyl bromides and trichloroethylene. As discussed in Section IV.B.5, halogen chemistry is not included in this version of the mechanism, and highly simplified “placeholder” mechanisms are used to make approximate estimates of likely reactivity ranges.

Figure 12. Distribution plots of model simulations of the hourly $\Delta(O_3\text{-NO})$ data for all the experiments used for mechanism evaluation.

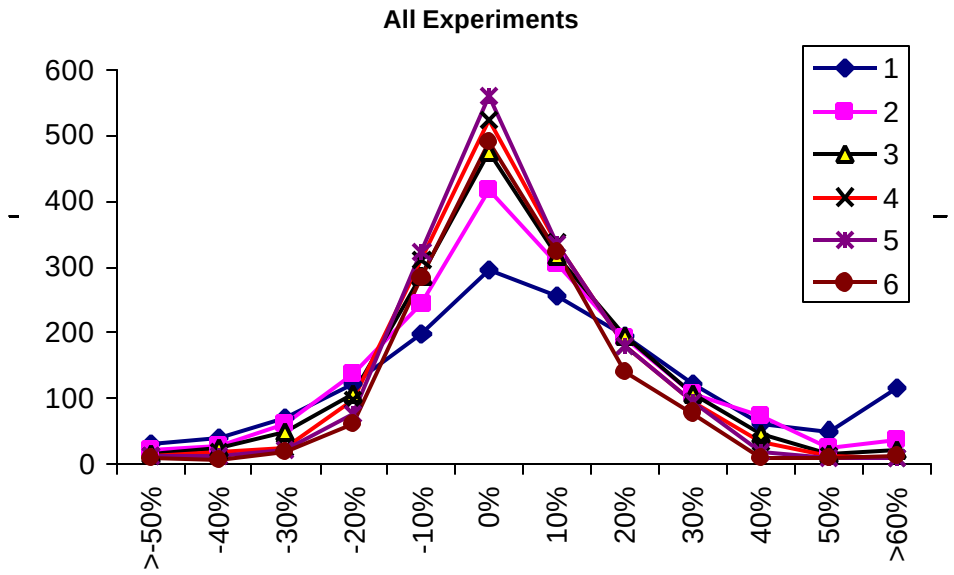

The reactivity predictions for these compounds should be considered to be almost as uncertain as those for compounds where no data are available.

However, as indicated on the table, the evaluation results for most VOCs are given code "1", indicating acceptable fits to the data. Of course, as also indicated on the table, this is often a result of adjusting uncertain aspects of the mechanism to fit the data. For the aromatics this consisted of the various adjustments to the parameterized mechanisms as discussed in Section IV.A, while in most other cases this consisted of adjusting the nitrate yield in the OH reaction (see Section III.I).

Table 48. Summary of results of mechanism evaluation for the various types of experiments, and figures in Appendix B where the evaluation results are shown.

Run Type	Figure no. [a] C	D	R	P	Fit [c]	Comments [d,e]
NOx Offgasing Characterization Runs.	1					NOx offgasing parameter adjusted to fit data for various characterization sets. Ozone fit in most runs, but overpredicted in some cases.
Radical Source Characterization Runs		2				Radical source parameter adjusted to fit data for each characterization set. Scatter indicates run-to-run variability, with most of the data being fit to within +/- 40%. No consistent biases.
Carbon Monoxide			3		1	Slight tendency to underpredict d(O3-NO) reactivity in some experiments, but generally good fits. No adjustments. (MRE, MR3, MR8, R8) (B)
Formaldehyde	4		8		1	Tendency to somewhat overpredict initial NO oxidation rates in most (but not all) blacklight chamber runs. Good fits to the xenon arc chamber runs. No adjustments. (S, MRE, MR3, MR8, R8) (B, X)
Acetaldehyde	5		9		1	Reasonably good fits with no consistent biases. No adjustments. (S, MR3, MR8, R8) (B, X)
Acetone	6		10		1	Reasonably good fits to most data. May be slightly biased towards overpredicting d(O3-NO). No adjustments for this evaluation. (S, MRE, MR3, MR8, R8) (B, X, O)
Methyl Ethyl Ketone	7		11	7	1	Necessary to increase the overall quantum yield to 0.15 to remove biases in simulations.. Good fits to d(O3-NO), and formaldehyde data. Underpredicts acetaldehyde in two runs, fits it in two others. (S, MR3, MRX, MR8) (B, X)
Benzaldehyde			12		1	Reasonably good fit for one experiment and fair fit to the other, where the model does not simulate the base case well. No adjustments. (MR4, R8) (B)
Cresols	13				2	Mechanism adjusted to fit d(O3-NO) data in o-cresol run. Reasonably good fit to d(O3-NO) in p-cresol run, but d(O3-NO) underpredicted in run with m-cresol. (S) (X)
Methacrolein	14				1	Overall quantum yield optimized to fit d(O3-NO) data. Quality of fits similar to that reported by Carter and Atkinson (1996). (S) (B, X, O)
Methylvinyl ketone	14				1	Overall quantum yield optimized to fit d(O3-NO) data. Quality of fits similar to that reported by Carter and Atkinson (1996). (S) (B, X)
Ethane			15		1	Fits most data to within experimental uncertainty. No adjustments. (MRE, MR3) (B)
Propane			16		1	Good fits to data in two MR3 runs; underpredicts d(O3-NO) reactivity in the third. No adjustments. (MR3) (B)

Table 48 (continued)

Run Type	Figure no. [a] C	D	R	P	Fit [c]	Comments [d,e]
n-Butane			17		1	Significantly underpredicts d(O3-NO) reactivity in MRE experiments, but base case is not particularly well simulated. Good fits to MR3, R3, MR8, and R8 reactivity data. No adjustments. (MRE, MR3, R3, MR8, R8) (B) [e]
n-Hexane			18		1	Significantly overpredicts d(O3-NO) inhibition in the MRE run, but good fits to MR3 reactivity data. No adjustments. (MR3) (B)
n-Octane			18		1	Good fits to data in most runs, but somewhat underpredicts d(O3-NO) reactivity in some runs. No adjustments. (MR3, MR8, R8) (B, X)
n-Dodecane			19		1	Slight bias towards overpredicting inhibition in MR3 runs, but reasonably good fits for full surrogate runs. No adjustments. MR3, MR8, R8) (B)
n-Tetradecane			20		1	Similar bias towards overpredicting d(O3-NO) reactivity as in n-dodecane runs, but slight bias towards underpredicting d(O3-NO) inhibition in some (but not all) MR8 runs. No adjustments. (MR3, MR8) (B)
n-Pentadecane			21		1	No consistent biases. Somewhat overpredicts inhibition in MR3 run, underpredicts in MR8 run. (MR3, MR8) (B).
n-Hexadecane			21		1	No consistent biases for MR3 runs. Fair fits for MR8 runs. (MR3, MR8) (B, X)
Isobutane			22		1	Rate of decomposition of t-butoxy radicals adjusted in part based on simulations of these experiments. No consistent biases after adjustment. Generally fits within experimental uncertainty and variability. (MR3) (B)
2,2,4-Trimethyl Pentane			22		1	Nitrate yields from C7 and C8 peroxy radicals adjusted to fit data. Good fits after adjustment. (MR3) (B)
2,6-Dimethyl Octane			22		1	Slight tendency to overpredict d(O3-NO) reactivities in MR4 and MR8 runs may indicate need to adjust nitrate yield slightly, but no adjustments made. Good fit to d(O3-NO) reactivity in R8 run. (MR4, MR8, R8) (B)
2-Methyl Nonane			23		1	Very slight tendency to overpredict d(O3-NO) reactivities in MR3 and MR8 runs may indicate a need to slightly adjust nitrate yield slightly, but no adjustments made. (MR3, MR8, R8) (B)
3,4-Diethyl Hexane			23		2	Non-negligible tendency to overpredict d(O3-NO) inhibition in MR4 experiments and to overpredict d(O3-NO) reactivity in low NOx (R8) runs indicate that adjustments need to be made to the mechanism, but no adjustments made. (MR3, MR8, R8) (B).
Cyclohexane			24		1	Slight bias towards underpredicting inhibition in MR3 runs but good fits for full surrogate runs. No adjustments (MR3, MR8, R8) (B)

Table 48 (continued)

Run Type	Figure no. [a] C	D	R	P	Fit [c]	Comments [d,e]
Hexyl Cyclohexane			24		1	Fits most data to within experimental uncertainty. No adjustments. (MR3, MR8, R8) (B)
Octyl Cyclohexane			25		1	Fits data to within uncertainty for all but one MR3 run, where d(O3-NO) inhibition is slightly overpredicted. No adjustments. (MR3, MR8, R8) (B)
Ethene	27	26	28		1	Variable fits to the large number of ethene - NOx experiments, but overall bias in d(O3-NO) predictions is small (may be slightly high). Tends to underpredict O3 in the outdoor chamber ethene - NOx runs. Good fits to reactivity experiments. No adjustments (S, MR3, MR8, R8) (B, O)
Propene	29	30	31		1	Radical yields in O3P reaction had to be assumed to be low and radical yields in O3 reaction had to be reduced in order to remove bias in simulations of the large number of propene - NOx runs. No bias in d(O3-NO) simulations of propene - NOx runs in blacklight chambers, negative bias for XTC, CTC, and OTC runs and positive bias for EC runs. Fits reactivity data to within experimental uncertainty and variability. (S, MRE, MR3, MR8, R8) (B, X, O)
1-Butene	32				1	Radical yields in both O3P and O3 reaction had to be assumed to be low to approximately fit data, even though assuming low OH yield in O3 reaction is inconsistent with laboratory data. Some variability in fits to data, but no consistent biases after adjustment. (S) (B,X)
1-Hexene	32					Radical yields in both O3P and O3 reaction had to be assumed to be low to approximately fit data, even though assuming low OH yield in O3 reaction is inconsistent with laboratory data. Reasonably good fits to the data after adjustment. (S) (B)
Isobutene	32		33		1	Nitrate yield in OH reaction adjusted upwards to fit data. Somewhat overpredicts maximum O3 in isobutene - NOx runs. Good fits to reactivity data. (S, MR3) (B)
trans-2-Butene	32		33		1	Good fits to data for most runs without adjustments. (S, MRE, MR3, MR8, R8, RE) (B, X)
Isoprene	34		35		1	Reasonably good fits to most (but not all) isoprene - NOx runs; similar to the fits reported by Carter and Atkinson (1996). Bias towards underpredicting O3 reactivity at end of MRE and RE runs, but good fits to MR3 reactivity data. (S, MRE, MR3, RE) (B, X, O)
2-Pentanone	36		37		1	Overall quantum yield for photodecomposition had to be reduced to 0.1 to fit data. Good fits to MPK - NOx and reactivity data after this adjustment. (S, MR3, MR8, R8) (X)

Table 48 (continued)

Run Type	Figure no. [a] C	D	R	P	Fit [c]	Comments [d,e]
Cyclohexanone	36		38		2	Branching ratio for reactions of OH radicals at different positions and overall nitrate yield in OH reaction had to be adjusted to improve model simulations to reactivity data. Photolysis is assumed not to form radicals, so overall quantum yield not adjusted. Fair fits to reactivity data after adjustment, but d(O3-NO) reactivity is still overpredicted in some full surrogate experiments. Model underpredicts d(O3-NO) in the cyclohexanone - NOx experiments in the DTC runs, but gives reasonably good fits to the d(O3-NO) data in the CTC runs. (S, MR3, MR8, R8) (B, X)
4-Methyl-2-Pentanone	39		40		1	Need to adjust quantum yield to 0.04 to fit reactivity data. Reasonably good fits for ketone - NOx, mini-surrogate and high NOx full surrogate runs. Also gives good fits to formaldehyde data in the ketone - NOx runs. Somewhat overpredicts reactivity at end of low NOx full surrogate runs. (S, MR3, MR8, R8) (B, X)
2-Heptanone	36		40		1	Overall quantum yield for photodecomposition had to be reduced to 0.02 to fit data. Good fits to MPK - NOx and reactivity data after this adjustment. (S, MR3, MR8, R8) (X)
Methanol			41		1	Fits data to within experimental uncertainty without adjustments. (MR3) (B)
Ethanol			41		1	Fits data to within experimental uncertainty without adjustments. (MR3) (B)
Isopropyl Alcohol			43		1	Variable fits. Good fits to some mini-surrogate runs, some where d(O3-NO) reactivity underpredicted. No consistent biases for full surrogate runs. No adjustments. (MR3, MR8, R8) (B)
t-Butyl Alcohol			42		2	Nitrate yields adjusted to fit data in the MR3 experiments. The resulting mechanism overpredicts d(O3-NO) reactivities by about 30-50%, but is more consistent with the data for the R8 experiments. Data are somewhat better fit if the rate constant is reduced by about a factor of 1.6 to the estimated value, but the rate constant was not adjusted in the mechanism used. (MR3, MR8, R8) (B)
1-Octanol			44		1	Good fits to two experiments and tendency to overpredict d(O3-NO) reactivity in two others. No adjustments (MR3, MR8, R8) (B)
2-Octanol			44		1	Fits data to within experimental uncertainty and variability. No adjustments (MR3, MR8, R8) (B)
3-Octanol			44		1	Slight bias towards overpredicting d(O3-NO) reactivity. No adjustments. (MR3, MR8, R8) (B)
Propylene Glycol			45		1	Mechanism fits data to within experimental uncertainty. No adjustments (MR3, MR8, R8) (B)

Table 48 (continued)

Run Type	Figure no. [a] C	D	R	P	Fit [c]	Comments [d,e]
Dimethyl Ether			47		1	Mechanism fits data to within experimental uncertainty. No adjustments (MR3) (B)
Diethyl Ether			47		1	Mechanism may be slightly biased towards overpredicting d(O3-NO) reactivity. No adjustments. (MR3, MR8, R8) (B)
Methyl t-Butyl Ether			46		1	Fits data to within experimental uncertainty after adjusting overall nitrate yield (MR3) (B)
1-Methoxy-2-Propanol			48		1	Fits data to within experimental uncertainty after adjusting overall nitrate yield (MR3, MR8, R8) (B)
2-Ethoxyethanol			49		1	Fits data to within experimental uncertainty after adjusting overall nitrate yield (MR3) (B)
2-(2-Ethoxy-ethoxy) Ethanol			49		1	Fits data to within experimental uncertainty after adjusting overall nitrate yield (MR3) (B)
2-Butoxyethanol			50		1	Fits most data to within experimental uncertainty after adjusting overall nitrate yield (MR3, MR8, R8) (B)
Methyl Acetate			51		1	Chamber data are somewhat better fit is it is assumed that reaction at the acetate group is assumed to be negligible. Also necessary to adjust overall nitrate yield somewhat. Adjusted mechanism fits data without consistent biases. (MR3, MR8, R8) (B)
Ethyl Acetate			52		1	Nitrate yield adjusted to improve fits to data. Model fits data for all but one MR8 experiment within experimental uncertainty. (MR3, MR8, R3, R8) (B, X)
Isopropyl Acetate			53	54	1	Reactivity data fit to within experimental uncertainty. Formaldehyde and acetone yields may be slightly underpredicted. No adjustments. (MR3, MR8) (B).
t-Butyl Acetate			53	54	1	Overall nitrate yield adjusted to fit data, but these is still a slight bias towards overpredicting d(O3-NO) reactivity. Model gives good fits to formaldehyde data but may slightly underpredict acetone yields. (MR3, MR8, R8) (X)
Methyl Pivalate			55	56	1	Overall nitrate yields adjusted upwards to fit data. Model gives reasonably good fits to reactivity, formaldehyde, and acetone data, though there may be a slight bias towards underpredicting formaldehyde and acetone yields. (MR3, MR8, R8) (B)
Methyl Isobutyrate			57	58	1	In order to even approximately fit the reactivity data for this compound, it is necessary to assume that radicals such as CH3-O-CO. react with NO2 to form a PAN analogue rather than decompose. Overall nitrate yields and initial OH reaction branching ratios adjusted to improve fits to chamber data. (MR3, MR8, R8) (B)

Table 48 (continued)

Run Type	Figure no. [a] C	D	R	P	Fit [c]	Comments [d,e]
n-Butyl Acetate			59		1	Nitrate yield adjusted to fit data. Fits most data to within experimental uncertainty, though may be slight bias towards overpredicting d(O3-NO) reactivity in the MR8 runs. (MR3, MR8, R8) (B)
Dimethyl Carbonate			60		1	Model gives good fits to data without adjustment. (MR3, MR8, R8) (B)
Methyl Isopropyl Carbonate			61	63	1	Nitrate yields had to be adjusted downwards slightly to fit data. Good fits to d(O3-NO) reactivity data and formaldehyde and acetone yields, though estimation method for reactions of carbonate-derived alkoxy radicals was derived in part based on fits to data for this compound. Model has a bias towards underpredicting IntOH reactivity. (MR3, MR8, R8) (B)
Propylene Carbonate			62		1	Nitrate yields reduced to by relatively large factor to fit mini-surrogate (MR3) runs, and branching ratio for initial OH reaction had to be adjusted also to reduce biases in simulations of full surrogate reactivity runs. Adjusted model still slightly overpredicted reactivity in full surrogate runs. Run DTC243 appears to be anomalous and wasn't used in judging fits. (MR3, MR8, R8) (B)
1-Methoxy-2-Propyl Acetate			64		1	Model gives reasonably good fits to the data without adjustments. May be slight bias towards overpredicting d(O3-NO) reactivity in the MR8 experiments. (MR3, MR8) (B)
Dimethyl Succinate			65		2	Mechanism needed a number of adjustments to yield acceptable fits to the data. Isomerization of the CH3-O-CO-C[O.]-R radical had to be assumed to dominate, which is within the uncertainty of the estimates. Adjusted model fits data to within experimental uncertainty except that it tends to underpredict the d(O3-NO) reactivity in the R8 experiments. (MR3, MR8, R8) (X)
Dimethyl Glutarate			65		2	Had to adjust branching ratio for initial OH reaction, overall nitrate yield, and an alkoxy intermediate branching ratio in order for model to be consistent with the chamber data and available product data. Adjusted model somewhat overpredicts d(O3-NO) reactivity in MR8 experiments, but gives good fits to the data for the MR3 and R8 runs. (MR3, MR8, R8) (X)
Acetylene	66		67		1	Quantum yields for radical formation from the photolysis of glyoxal had to be assumed to be much higher than estimated previously in order to even approximately fit reactivity data for acetylene (see documentation of base mechanism). Model gives reasonably good fits to data from acetylene - NOx runs and reactivity runs, but there may be a slight bias towards underpredicting d(O3-NO) reactivity in the MR3 runs. (S, MR3, MR8, R8) (B, X)

Table 48 (continued)

Run Type	Figure no. [a] C	D	R	P	Fit [c]	Comments [d,e]
Acrolein	68				2	Overall quantum yield adjusted to fit data for acrolein - NOx runs. Good fits for runs at lower acrolein / NOx ratios, but initial NO oxidation rate underpredicted in higher acrolein / NOx run ITC946. (S) (B)
a-Pinene	69		70		1	Overall nitrate yield and number of NO to NO2 conversions in OH reaction adjusted to fit chamber data. Very good fits to a-pinene - NOx runs, reactivity runs fit to within experimental variability and uncertainty. (S, MRE, R8, RE) (B, X, O)
b-Pinene	69		70		2	Overall nitrate yield and numbers of NO to NO2 conversions assumed to be the same as best fits a-pinene data since using significantly different values did not improve fits for this compound. Although initial NO oxidation rates reasonably well fit in the b-pinene - NOx runs, the maximum ozone yield is consistently overpredicted. Fair fits to the incremental reactivity data. (S, MRE, RE) (B, X, O)
3-Carene	69				1	Overall nitrate yield and numbers of NO to NO2 conversions assumed to be the same as best fits a-pinene data since using significantly different values did not improve fits for this compound. Although initial NO oxidation rates reasonably well fit, the maximum ozone yield was underpredicted in three of the four runs. (S) (B)
Sabinene	69				1	Overall nitrate yield and numbers of NO to NO2 conversions assumed to be the same as best fits a-pinene data since using significantly different values did not improve fits for this compound. Slight tendency to overpredict O3 formation rate in middle of run, but maximum O3 concentration reasonably well simulated in most cases. (S) (B)
d-Limonene	69				1	Overall nitrate yield and numbers of NO to NO2 conversions assumed to be the same as best fits a-pinene data since using significantly different values did not improve fits for this compound. Slight tendency to overpredict O3 formation rate in middle of run (though not as much as for sabinene) but maximum O3 concentration reasonably well simulated in most cases. (S) (B)
Benzene	71		79		2	Representation of reactive products adjusted to fit benzene - NOx experiments as discussed in the aromatic mechanism documentation section. Tendency of model to overpredict peak O3 yields in some benzene - NOx runs, and very poor fits to data for one run (ITC562). Reasonably good fits to d(O3-NO) reactivity in reactivity runs, but tendency to underpredict IntOH reactivity. (S, MR3, R8) (B)

Table 48 (continued)

Run Type	Figure no. [a] C	D	R	P	Fit [c]	Comments [d,e]
Toluene	72		79		1	Representation of reactive products adjusted to fit aromatic - NOx experiments as discussed with aromatic mechanism documentation. Reasonably good fits to most toluene - NOx runs. Fits d(O3-NO) reactivity in reactivity experiments within experimental uncertainty and variability, but tends to somewhat underpredict IntOH reactivity. (S, MR3, MR8, R8) (B, X)
Ethyl Benzene	73		79		1	Representation of reactive products adjusted to fit aromatic - NOx experiments as discussed with aromatic mechanism documentation. Reasonably good fits to most ethylbenzene - NOx runs. Fits reactivity runs to within the uncertainty of the data, but effect of added ethylbenzene too small for good mechanism evaluation. (S, MR3) (B, X)
m-Xylene	74		80		1	Representation of reactive products adjusted to fit aromatic - NOx experiments as discussed with aromatic mechanism documentation. Reasonably good fits to most m-xylene - NOx runs. Fits most reactivity runs to within the uncertainty of the data. (S, MR3, MR8, R8) (B, X)
o-Xylene	75				1	Representation of reactive products adjusted to fit aromatic - NOx experiments as discussed with aromatic mechanism documentation. Fair fits to most o-xylene - NOx runs. (S) (B, X)
p-Xylene	76		80		1	Representation of reactive products adjusted to fit aromatic - NOx experiments as discussed with aromatic mechanism documentation. Fair fits to most p-xylene - NOx runs, though some variability in simulations of some CTC runs. Fits the one reactivity run to within the uncertainty of the data, but effect of added p-xylene too small for good mechanism evaluation. No adjustments were made. (S, MR3) (B, X)
1,2,3-Trimethyl Benzene	77		81		1	Representation of reactive products adjusted to fit aromatic - NOx experiments as discussed with aromatic mechanism documentation. Good fits to most 123-TMB - NOx runs, but incremental reactivities somewhat underpredicted in MR3 experiments.. (S, MR3) (B, X)
1,2,4-Trimethyl Benzene	77		81		1	Representation of reactive products adjusted to fit aromatic - NOx experiments as discussed with aromatic mechanism documentation. Fair fits to most 124-TMB - NOx runs. (S) (B, X)
1,3,5-Trimethyl Benzene	78		81		1	Representation of reactive products adjusted to fit aromatic - NOx experiments as discussed with aromatic mechanism documentation. Good fits to most 135-TMB - NOx runs, but incremental reactivities somewhat overpredicted in the MR3 experiment. (S, MR3) (B, X)

Table 48 (continued)

Run Type	Figure no. [a] C	D	R	P	Fit [c]	Comments [d,e]
Naphthalene	82				2	Representation of reactive products adjusted to fit aromatic - NOx experiments as discussed with aromatic mechanism documentation. Unlike the alkylbenzenes, it is necessary to assume significant formation of products that react like PAN analogues in order to approximately fit the naphthalene - NOx runs. Fair fits to most runs, but peak O3 may be somewhat overpredicted in some low NOx experiments. (S) (B)
2,3-Dimethyl Naphthalene	82				1	Representation of reactive products adjusted to fit aromatic - NOx experiments as discussed with aromatic mechanism documentation. Unlike the alkylbenzenes, it is necessary to assume significant formation of products that react like PAN analogues in order to approximately fit the 2,3-dimethylnaphthalene - NOx runs. Good fits to most runs. (S) (B)
Tetralin	82				1	Representation of reactive products adjusted to fit aromatic - NOx experiments as discussed with aromatic mechanism documentation. Unlike the alkylbenzenes, it is necessary to assume significant formation of products that react like PAN analogues in order to approximately fit the tetralin - NOx runs. Fair fits to most runs, with some discrepancies but no consistent biases. (S) (B)
Styrene			83		1	Necessary to adjust the nitrate yield in the OH reaction and the radical yield in the O3 reaction to fit the chamber data. Reasonably good fits to most of the reactivity data. (MR3, MR8, R8) (X)
Toluene Diisocyanate			84		1	A highly simplified parameterized mechanism was adjusted to fit the chamber data. Reasonably good fits were obtained, with no consistent biases. (MR3, MR8, R8) (B).
Para Toluene Isocyanate			85		1	A highly simplified parameterized mechanism was adjusted to fit the chamber data. Reasonably good fits were obtained, with no consistent biases. (MR3, MR8, R8) (B).
N-Methyl-2-Pyrrolidone			86		1	The nitrate yield in the OH reaction was adjusted to fit the chamber data. Reasonably good fits to the reactivity data were obtained.
n-Propyl Bromide			87		3	Bromine chemistry is not represented in this version of the mechanism. The highly simplified "placeholder" mechanism used for all halocarbons (with the appropriate OH rate constant) somewhat overpredicted reactivity in the high NOx runs and incorrectly predicted positive reactivity in the low NOx runs, where the compound actually inhibited O3. (MR3, MR8, R8) (B)

Table 48 (continued)

Run Type	Figure no. [a] C	D	R	P	Fit [c]	Comments [d,e]
n-Butyl Bromide			87		3	Bromine chemistry is not represented in this version of the mechanism. The highly simplified "placeholder" mechanism used for all halocarbons (with the appropriate OH rate constant) approximately fit initial reactivity data in the MR3 experiments, overpredicted reactivity in the high MR8 runs by about a factor of 2, and incorrectly predicted positive reactivity in the low NOx runs, where the compound actually inhibited O3. No adjustments were made. (MR3, MR8, R8) (B)
Trichloroethylene			88		3	Chlorine chemistry is not represented in this version of the mechanism. The highly simplified "placeholder" mechanism used for all halocarbons (with the appropriate OH rate constant) gave surprisingly good fits to the reactivity data, considering the crudity of the mechanism and the fact that no adjustments were made. (MR3, MR8, R8) (B)
Mineral Spirits Samples			89		1	The compositions assumed when simulating experiments with these mixtures are given in Table C-5 in Appendix C. The Model fits the reactivity data to within the experimental uncertainties for samples "B", "C", and "D", but slightly underpredicted the reactivity of sample "A" under higher NOx conditions. Much better mechanism performance than observed previously (Carter et al, 1997f). No adjustments were made. (MR3, MR8, R8) (B)
Exxon D95® Fluid			90		1	The composition assumed when simulating experiments with this mixture is given in Table C-5 in Appendix C. The Model fits data to within the experimental uncertainty for most runs. See Carter et al (2000x) for details and a discussion of the derivation of the composition of this fluid. (MR3, MR8, R8) (B)
Exxon Isopar-M® Fluid			91		2	The composition assumed when simulating experiments with this mixture is given in Table C-5 in Appendix C. The model has a slight bias towards overpredicting d(O3-NO) inhibition in the MR8 runs, but fits data to within the experimental uncertainty for the other runs. See Carter et al (2000x) for details and a discussion of the derivation of the composition of this fluid. (MR3, MR8, R8) (B)
Exxon Exxate-1000® Fluid (Oxo-Decyl Acetate)			92		1	The composition assumed when simulating experiments with this mixture is given in Table C-5 in Appendix C. The model fits the data to within the experimental variability, with no consistent biases. See Carter et al (2000x) for details and a discussion of the derivation of the composition of this fluid. (MR3, MR8, R8) (B)
"MIX-A" Mix		93			1	Fits are variable, but the model does not have a significant bias for the group as a whole. D(O3-NO) is predicted to within +/- 40% for most runs.

Table 48 (continued)

Run Type	Figure no. [a] C	D	R	P	Fit [c]	Comments [d,e]
"SURG-4" Mix		94			3	Model has definite bias towards overpredicting O3 in these experiments, and even more towards overpredicting initial NO oxidation rate. Possible experimental problems with these low NOx runs; NOx zeros do not appear to be correct in some cases.
"SURG-7" Mix		95			2	Model has a tendency to overpredict d(O3-NO) by about 20% on the average.
"SURG-8S" Mix		96			2	Fits are highly variable for this group, with the model having a bias towards underprediction by about 20%.
"SURG-3M" Mix		97			1	Fits are variable, with overall biases being small but somewhat different in different chambers. D(O3-NO) is usually simulated to within +/- 30%.
"SURG-8M" Mix		98			1	Generally good fits with no or small overall bias. D(O3-NO) is usually simulated by +/- 20%.
"SURG-8" Mix		99			1	Generally good fits with no or small overall bias. D(O3-NO) is usually simulated by +/- 20%.
"SURG-X" Mix		100			2	Most runs are reasonably well simulated, but there are more cases where d(O3-NO) is overpredicted than underpredicted, especially in the first hour of the run.

[a] Figure types codes: C = concentration/time plots; D = distribution plots; R = reactivity data; P = product data plots.

[b] Types of experiments used to evaluate mechanisms for VOC or mixture is indicated in parentheses after comments. S = single VOC - NOx, MR3 = "MR3" reactivity, etc. (See Table 45 for reactivity experiment type codes.). Types of light source indicated in parentheses after experiment type codes. B = blacklight chambers, X = xenon arc chambers, O = outdoor chambers.

[c] Fit codes for evaluations of mechanisms of individual VOCs are as follows:

1 Model fits data to within experimental uncertainty, no consistent biases, or biases are considered not large enough to be significant. This code also used if data are not adequate to sufficiently evaluate mechanism. For mixtures, this code means no consistent biases in d(O3-NO) predictions.

2 Some poor fits or biases indicate possible mechanism problems or needs for improvement. For mixtures, this means that there are some biases in d(O3-NO) predictions.

3 The mechanism either does not satisfactorily fit the data, or is considered to be too unrepresentative of the chemistry involved to give reliable atmospheric reactivity predictions. For mixtures, this means that there are large biases in d(O3-NO) predictions.

[d] Model tends to consistently underpredict IntOH reactivities in all low NOx (e.g., R8) incremental reactivity experiment, possibly due to problems in representation of radical reactions under low NOx conditions. This is not noted in the comments for the individual VOCs.

[e] Although there are a large number of single VOC - NOx runs for n-butane and some for a few other alkanes, these are not useful for mechanism evaluation because of their large sensitivity to the chamber radical source (Carter and Lurmann, 1990).

VI. LUMPED MECHANISM FOR AIRSHED MODELS

Airshed model applications require simulations of highly complex mixtures of large numbers of VOCs, and in most cases it is not necessary or practical to represent each of them separately. For such applications, models with lumped model species that represent reactions of a large number of species with similar reaction rates and mechanisms, are generally employed. Even for VOC reactivity assessment it is only really necessary to separately represent the VOC whose reactivity is being assessed, the reactions of most of the other VOCs present in the ambient simulation can be represented using appropriate lumped model species. This was the approach that was employed in our previous reactivity studies (e.g., Carter and Atkinson, 1989a, Carter, 1994a), and continues to be the approach used in this work.

In this section, we describe the lumping approach we recommend for use when employing this mechanism in regional model simulations, which is also the approach used in the EKMA models when calculating the reactivity scales discussed in Section VII.A. Before discussing the specific approach, we briefly summarize the various types of lumping methods that can be employed, and the factors that need to be considered when determining the recommended method.

A. Summary of Lumping Approaches

As with the previous mechanism (Carter, 1988), two different approaches, referred to as lumped molecule and variable lumped parameter condensation, can be employed to represent VOCs in complex mixtures. A third approach, referred to here as fixed parameter condensation is used in condensed models such as the LCC (Lurmann et al, 1987), RADM-2 (Stockwell et al, 1990), and RACM (Stockwell et al, 1997) can also be employed, and may be appropriate or necessary in some applications. A fourth approach, referred to as lumped structure is employed in the widely-used Carbon Bond mechanism (Gery et al, 1988) and was used to represent hydroperoxides in the previous SAPRC mechanism (Carter, 1990), though it is not used in the current mechanism. These are discussed below.

1. Lumped Molecule Approach

The lumped molecule approach involves representing the VOC by a model species in the base mechanism, on a molecule-for-molecule basis. This is the same as the approach used to represent most of the product species in the various VOC reactions, as discussed above in Section II.C.1. For example, the lumped higher aldehyde species, RCHO, can be used to represent all aldehydes present in emissions or other complex mixtures, if it is not necessary to represent them explicitly for the purpose of estimating their reactivities. Although this is less accurate than the lumped or fixed parameter approaches discussed below, it is appropriate for classes of compounds that are believed to react very similarly, or are not sufficiently important in the emissions to justify more complex approaches.

2. Variable Lumped Parameter Approach

The variable lumped parameter approach representing a group of VOCs that react with similar rate constants with model species whose kinetic and product yield parameters are weighted averages of the mixture of VOCs they are being used to represent. This is potentially the most accurate lumping method, permitting lumping of species with quite different mechanisms, provided that they react with the same species with similar rate constants, or at least have similar kinetic reactivities (fractions reacted) in

the model scenarios (Carter, 1988). Two weighting methods can be used when deriving the parameter values given the mixture of emitted or ambient VOCs being represented.

In reactivity weighting, the contribution of a given VOC to the parameters derived for the lumped model species is proportional to the amount of the VOC that is estimated to react in the scenario, which, if the VOC reacts only with OH radicals, is given by

$$\text{Amount Reacted} = \text{Amount Emitted} \cdot \text{Fraction Reacted} \qquad \text{(XXXII)}$$

where

$$\text{Fraction Reacted} = \text{Kinetic Reactivity} \approx (1 - e^{-kOH \cdot IntOH}) \qquad \text{(XXXIII)}$$

and kOH is the OH radical rate constant and IntOH is an effective integrated OH radical rate constant that is characteristic of the type of model scenario (Carter, 1988; Middleton et al, 1990), which is estimated to be ~110 ppt-min for regional model applications (Middleton et al, 1990). This is most appropriate when lumping VOCs with widely varying kinetic reactivities, as is necessary when lumping slowly reacting VOCs into a single group. However, this has the disadvantage that the number of moles of model species is different from the number of moles of compounds being represented, which detracts from the chemical realism of the mechanism. In addition, the value of IntOH appropriate for a single day urban or EKMA simulation will not be appropriate for a multi-day regional simulation, and vise-versa.

In molar weighting, the contribution of a given VOC to the parameters of the lumped model species is simply proportional to the amount of VOC emitted or input into the scenario. This is appropriate if the VOCs being lumped have similar kinetic reactivities, as is generally the case for rapidly reacting VOCs[21]. This lumping is also more chemically realistic because it preserves moles, and does not depend on any aspect of the scenario other than the emissions.

Note that a variant of the lumped parameter approach is used when representing the individual VOCs for the purpose of evaluating the mechanism against chamber data or calculating its atmospheric reactivity. However, in this case there is no lumping involved, one model species, with parameters set equal to those of the compound being represented, is used for each VOC whose mechanism is being evaluated or whose reactivity is being calculated. The one exception is model simulations of experiments or reactivities of complex mixtures (such as mineral spirits or vehicle exhausts), where species in the mixtures are lumped in the same way as recommended for regional model simulations.

Although potentially the most accurate, the lumped parameter approach has the disadvantages that nature of the model species depends on the emissions, and requires special emissions processing procedures that involves software that is not available on most modeling systems. In addition, emissions speciation is often highly uncertain, and model simulations using scenario-specific parameters for the lumped species may not necessarily be significantly more accurate than those using parameters derived using a “typical” or “representative” ambient mixture or emissions profile.

3. Fixed Parameter Approach

The fixed parameter approach is a variant of the lumped parameter approach where the parameters for the lumped species are derived using a typical or representative ambient mixture or emissions profile, and then used in all subsequent model applications regardless of the actual emissions

[21] VOCs with OH rate constants $\geq 10^{-11}$ cm^3 $molec^{-1}$ s^{-1} have kinetic reactivities greater than 80% for IntOH = 110 ppt-min. Since kinetic reactivities can be no greater than 100%, this means that kinetic reactivities of VOCs with this or higher rate constants are all within ± 20%.

involved. This is the approach that was used in the RADM-2 mechanism (Stockwell et al, 1990), where the parameters for the lumped alkane, alkene, and aromatic species were derived based on the RADM-2 emissions inventory, and then held fixed for all model applications using that mechanism (Carter and Lurmann, 1990). This greatly simplifies mechanism implementation and emissions processing, and is potentially as accurate as the variable lumped parameter approach if the emissions composition is uncertain or reasonably well represented by the composition used when deriving the mechanism.

In this work we present a fixed parameter version of this mechanism that can be used to permit implementation of this mechanism in modeling systems that do not support the emissions processing needed for implementing the variable parameter approach. This is discussed in Section VI.B, below. It is based on the ambient mixture of VOCs obtained from analysis of air quality data (Jeffries et al, 1989; Carter, 1994a,b) which was used to represent the base case reactive organic gas (ROG) mixture in the previous (e.g., Carter, 1994a,b) and current (see Section VII) reactivity scale calculation.

However, it is recommended that the variable parameter approach be used in model applications where it is believed that the composition of the initial and/or emitted VOC species are known with reasonable accuracy. In particular, it should be used in applications where the composition of the emitted or ambient species is believed to be significantly different from that of the base ROG mixture used to derive the lumped parameters in the fixed parameter mechanism.

4. Lumped Structure Approach

The widely-used Carbon Bond IV mechanism uses the "lumped structure" approach, where different parts of the molecule are treated as if they react independently (Gery et al, 1988). This permits representation of a large number of compounds with a relatively small number of model species, and performs reasonably well in simulating experiments with complex mixtures that are representative of those used when the mechanism was developed (Gery et al, 1988). However, as seen from the detailed mechanistic discussion given above in Section III, different parts of molecules actually do not react independently. Examples of where the lumped structure approximation break down include the dependence of nitrate yields on the size of the peroxy radicals (Section III.I) the importance of internal isomerization and rearrangement reactions undergone by larger alkoxy radicals (Section III.J). For that reason, this approximation is not used in the current version of the mechanism.

B. Recommended Lumping for Regional Model Applications

1. Lumping Approach

The optimum lumping approach in terms of minimizing the number of model species without introducing nonnegligible approximations depends on the model application and type of scenario employed. The use of the variable parameter approach permits a high degree of lumping with very little approximation in single box or EKMA model scenarios, which involve only a single day simulation with all the VOCs being introduced together (Carter, 1988). However, the requirements of multi-cell and multi-day regional models are more demanding. This is because different compositions of VOCs can be emitted at different times and locations, so no single parameterization may represent the emissions profile in all locations at all times. In addition, representing slowly reacting VOCs with more rapidly reacting model species using reactivity weighting may not appropriately represent these VOCs in multi-day simulations, since they would persist longer than the model species used to represent them. More lumped classes are therefore needed to minimize the time and space variation of the reactivity characteristics of

the VOCs represented by any given lumped species, and to permit the slowly reacting species to be more appropriately represented in multi-day scenarios.

The approach adopted in this work is to recommend a lumping approach that addresses the requirements of regional, multi-cell, multi-day model applications. Since that is the most demanding requirement, this will then give a mechanism that should be appropriate for most applications, albeit with more species than may be necessary for some applications such as EKMA. This permits use of a consistent mechanism and degree of condensation, regardless of the application.

Table 49 gives a summary of the lumped classes recommended for use with regional models. The lumping for the more reactive classes of compounds are similar to that used in other mechanisms such as the RADM-2 (Stockwell et al. 1990) and RACM (Stockwell et al, 1997) mechanisms, and condensed versions of the SAPRC-90 mechanism (Lurmann et al, 1991; Kumar et al, 1995). However, there is a larger number of slowly reacting "alkane and others" classes, to allow for appropriate representations of compounds such as ethane and propane in regional model simulations. Separate classes are used for ethane and propane and compounds with similar reactivities, with non-methane organics that react slower than half that of ethane being treated as inert. The dividing lines in terms of OH rate constants are somewhat arbitrary in the case of the alkane classes, but are chosen in the recommended lumping to be consistent with those used in the RADM-2 emissions processing system, as discussed by Middleton et al (1990). This permits the mechanism to be used in models with emissions data processed for the RADM-2 mechanism, as discussed in the following section.

Biogenic compounds are represented in separate classes because their emissions can have significantly different spatial and temporal profiles than anthropogenic emissions, and their reactivity characteristics are quite different from those of the anthropogenic alkenes they otherwise would be lumped with. Isoprene, which is the dominant biogenic in many U.S. scenarios, is represented explicitly, and a separate lumped class is used is used for terpenes.

Note that the lumped molecule assignments takes advantage of the fact that this version of the mechanism uses a relatively large number of model species represent reactive products, compared to previous mechanisms. This permits, for example, unsaturated aldehydes and ketones to be represented using isoprene product species whose mechanisms are probably closer to the compounds being represented than the generic higher saturated aldehyde or ketone species used in most mechanisms. Although the saturated higher aldehydes and ketones could be represented using the lumped parameter approach since explicit mechanisms for such compounds can be generated, the lumped molecule approach is employed because they are not sufficiently important in emissions or ambient air masses to justify using separate model species for them.

Table 49 shows that that the lumping approach for representing most oxygenated species when present in mixtures is the same as used when representing them when formed as products in the oxidations of other VOCs, as discussed above in Sections II.C.1 and II.C.2. The major exceptions are oxygenated compounds that react only with OH radicals, such as esters, acids, etc. These are represented using the appropriate lumped alkane class (ALK1, … ALK5) depending on their OH rate constant when they are primary VOCs, but are represented by MEK, PROD2, or (for acids) RCO-OH if they are formed as reactive products of other VOCs. This is because in principle the use of lumped parameter species can permit a more accurate representation of the impacts of these compounds when present in complex mixtures, if the parameters are derived to take the contributions of these species into account. The MEK and PROD2 model species are only used to represent ketones, whose photolysis reactions cannot be represented using lumped alkane classes.

Table 49. Summary of lumped classes and lumped molecule representations recommended for representing complex mixtures in ambient model applications.

Model Species	Description
Emitted Compounds Represented Explicitly	
CH4	Methane
ETHENE	Ethene
ISOPRENE	Isoprene
HCHO	Formaldehyde
ACET	Acetone
MEOH	Methanol
PHEN	Phenol
Lumped Molecule Groups	
CCHO	Acetaldehyde and Glycolaldehyde
RCHO	Lumped C3+ Aldehydes
MEK	Ketones that react with OH radicals slower than 5×10^{-12} cm^3 $molec^{-2}$ sec^{-1}.
PROD2	Ketones that react with OH radicals faster than 5×10^{-12} cm^3 $molec^{-2}$ sec^{-1}.
CRES	Cresols
BALD	Aromatic aldehydes (e.g., benzaldehyde)
METHACRO	Methacrolein and acrolein
ISOPROD	Unsaturated aldehydes other than acrolein and methacrolein.
MVK	Unsaturated ketones
Unreactive Compounds	
INERT	Compounds other than CO or methane that do not react, or react only with OH with a rate constant less than approximately half that of ethane, or ~2×10^2 ppm-1 min-1.
Lumped Parameter Groups (Lumped using molar weighting except as indicated)	
ALK1	Alkanes and other non-aromatic compounds that are react only with OH, and have an OH rate constant (kOH) between 2×10^2 and 5×10^2 ppm-1 min-1. (Primarily ethane)
ALK2	Alkanes and other non-aromatic compounds that react only with OH, and have kOH between 5×10^2 and 2.5×10^3 ppm-1 min-1. (Primarily propane and acetylene)
ALK3	Alkanes and other non-aromatic compounds that react only with OH, and have kOH between 2.5×10^3 and 5×10^3 ppm-1 min-1.
ALK4	Alkanes and other non-aromatic compounds that react only with OH, and have kOH between 5×10^3 and 1×10^4 ppm-1 min-1.
ALK5	Alkanes and other non-aromatic compounds that react only with OH, and have kOH greater than 1×10^4 ppm-1 min-1.
ARO1	Aromatics with kOH < 2×10^4 ppm-1 min-1. (Primarily toluene and other monoalkyl benzenes.) Benzene and slower reacting aromatics such as halobenzens are lumped with reactivity weighting based on their OH rate constant relative to that of toluene, all others are lumped using molar weighting. Group given kOH of toluene.
ARO2	Aromatics with kOH > 2×10^4 ppm-1 min-1. (Primarily xylenes and polyalkyl benzenes)
OLE1	Alkenes (other than ethene) with kOH < 7×10^4 ppm-1 min-1. (Primarily terminal alkenes)
OLE2	Alkenes with kOH > 7×10^4 ppm-1 min-1. (Primarily internal or disubstituted alkenes)
TRP1	Biogenic alkenes other than isoprene (primarily terpenes)

The mechanisms for the model species ALK_n, ARO_n, OLE_n, and TRP1 are derived depending on the mixture of VOCs they are being used to represent, which depends on the emissions or initial VOCs in the model simulation. To conserve moles and for greater chemical realism, it is recommended that molar weighting rather than reactivity weighting be used in most cases. Note that for the lowest reactivity "alkane and others" class, ALK1, this means that compounds reacting much slower than the rate constant for the class should not be lumped with the class. For this reason, compounds with OH rate constants lower than about half that of ethane are treated as "inert", i.e., not lumped with ALK1. (The one exception is methane, which, because of the relatively large amount present, is represented explicitly.) Although these slowly reacting compounds, such as HCFC's, etc., may eventually react to some extent in multi-day regional episodes, the amounts emitted and therefore the amounts reacted are very small, and would have negligible effect. Of course, if the reactivities or persistence of these compounds are of interest, then separate model species should be used to represent them.

The one area where it is recommended that reactivity weighting be used concerns the representation of benzene and other slowly reacting aromatics. Because they are emitted in relatively small amounts and contribute relatively little to the overall reactivity of the mixture, it is not considered worthwhile to represent them separately, so they are represented using the ARO1 group, which is dominated by toluene and the alkylbenzenes. However, benzene has a kinetic reactivity which is less than 1/3 that of toluene, so representing it using a group that represents primarily monoalkylbenzenes would not be appropriate. For that reason, the recommended approach is to use reactivity weighting for benzene and other slowly reacting when being represented by the ARO1 group, but use molar weighting for toluene and the alkylbenzenes, and give the group the OH rate constant of toluene. If an IntOH of 110 ppt-min, as used for the RADM-2 mechanism (Middleton et al, 1990), this means that one mole of benzene would be represented by 0.295 moles of ARO1. Of course, if calculations of the persistence or role of benzene are of particular interest, then a separate model species should be used for this purpose.

The mechanisms for the model species ALK_n, ARO_n, OLE_n, and TRP1 can be derived from the emissions inventory as discussed by Carter (1988). This requires assigning all the emissions classes in the emissions inventory to detailed model species in the present mechanism, which is beyond the scope of this report. However, they can also be derived using the mixture of reactive organic measured in ambient air, as discussed in the following section.

2. Fixed Parameter Mechanism

Although state-of-the-art modeling systems should include the ability to derive the most appropriate parameters for the model species from the VOC emissions data, in practice very few modeling systems presently support this capability. In addition, use of variable parameter mechanism to represent ambient or emitted VOCs may not be necessary or appropriate in all cases. These include model applications where the compositions of the emissions input are uncertain or highly variable, or model applications that employ idealized scenarios representing a wide distribution of conditions are employed. The latter includes developing general reactivity scales such as the Carter (1994a) scales that are updated in this work. Therefore, a fixed parameter version of this mechanism is derived to address these needs, as discussed in this section.

The base case model scenarios used to derive the Carter (1994a) reactivity scales use a standard mixture of hydrocarbons and oxygenates to represent the reactive VOCs that are emitted or initially present in the scenarios. The composition of this mixture, which is given in Table 50, was derived from an analysis of hydrocarbons in urban atmospheres in the United States (Jeffries et al, 1998) and from

Table 50. Composition of the base ROG mixture used in the reactivity simulations and to derive the lumped parameters in the fixed parameter mechanism.

VOC Name	Moles VOC / Mole C Mix	Represented By	Lumped with
Ethane	0.01685	ETHANE	ALK1
Propane	0.01413	PROPANE	ALK2
n-Butane	0.01807	N-C4	ALK3
n-Pentane	0.00613	N-C5	ALK4
n-Hexane	0.00132	N-C6	ALK4
n-Heptane	0.00120	N-C7	ALK5
n-Octane	0.00074	N-C8	ALK5
n-Nonane	0.00074	N-C9	ALK5
n-Decane	0.00184	N-C10	ALK5
n-Undecane	0.00016	N-C11	ALK5
n-Dodecane	0.00033	N-C12	ALK5
n-Tridecane	0.00001	N-C13	ALK5
Isobutane	0.00788	2-ME-C3	ALK3
Iso-Pentane	0.01516	2-ME-C4	ALK4
2-Methyl Pentane	0.00355	2-ME-C5	ALK4
3-Methylpentane	0.00253	3-ME-C5	ALK4
2,2-Dimethyl Butane	0.00046	22-DM-C4	ALK3
2,3-Dimethyl Butane	0.00095	23-DM-C4	ALK4
2,4-Dimethyl Pentane	0.00060	24-DM-C5	ALK4
3-Methyl Hexane	0.00127	3-ME-C6	ALK5
2,3-Dimethyl Pentane	0.00112	23-DM-C5	ALK5
Cyclopentane	0.00071	CYCC5	ALK4
Methylcyclopentane	0.00161	ME-CYCC5	ALK4
Cyclohexane	0.00068	CYCC6	ALK5
Methylcyclohexane	0.00068	ME-CYCC6	ALK5
Ethylcyclohexane	0.00018	ET-CYCC6	ALK5
Branched C6 Alkanes	0.00024	0.5 23-DM-C4 + 0.25 3-ME-C5 + 0.25 2-ME-C5	ALK4
Branched C7 Alkanes	0.00209	0.5 24-DM-C5 + 0.25 3-ME-C6 + 0.25 2-ME-C6	0.5 ALK4 + 0.5 ALK5
Branched C8 Alkanes	0.00403	0.5 24-DM-C6 + 0.25 4-ME-C7 + 0.25 2-ME-C7	ALK5
Branched C9 Alkanes	0.00171	0.5 24-DM-C7 + 0.25 4-ME-C8 + 0.25 2-ME-C8	ALK5
Branched C10 Alkanes	0.00156	0.5 26DM-C8 + 0.25 4-ME-C9 + 0.25 2-ME-C9	ALK5
Branched C11 alkanes	0.00016	0.5 26DM-C9 + 0.25 4-ME-C10 + 0.25 3-ME-C10	ALK5
Branched C12 Alkanes	0.00033	0.5 36DM-C10 + 0.25 5-ME-C11 + 0.25 3-ME-C11	ALK5
Branched C13 Alkanes	0.00001	0.5 36DM-C11 + 0.25 5-ME-C12 + 0.25 3-ME-C12	ALK5
C7 Cycloalkanes	0.00012	ME-CYCC6	ALK5
Ethene	0.01346	ETHENE	ETHE
Propene	0.00318	PROPENE	OLE1
1-Butene	0.00115	1-BUTENE	OLE1
C4 Terminal Alkenes	0.00014	1-BUTENE	OLE1
3-Methyl-1-Butene	0.00032	3M-1-BUT	OLE1

Table 50 (continued)

VOC Name	Moles VOC / Mole C Mix	Represented By	Lumped with
1-Pentene	0.00080	1-PENTEN	OLE1
1-Hexene	0.00033	1-HEXENE	OLE1
Isobutene	0.00115	ISOBUTEN	OLE2
2-Methyl-1-Butene	0.00092	2M-1-BUT	OLE2
trans-2-Butene	0.00115	T-2-BUTE	OLE2
cis-2-Butene	0.00091	C-2-BUTE	OLE2
2-Methyl-2-Butene	0.00052	2M-2-BUT	OLE2
1,3-Butadiene	0.00062	13-BUTDE	OLE2
Isoprene	0.00130	ISOPRENE	ISOP
Cyclohexene	0.00018	CYC-HEXE	OLE2
C5 Terminal Alkenes	0.00044	1-PENTEN	OLE1
C6 Terminal Alkenes	0.00223	1-HEXENE	OLE1
C7 Terminal Alkenes	0.00119	1-HEPTEN	OLE1
C8 Terminal Alkenes	0.00024	1-OCTENE	OLE1
C9 Terminal Alkenes	0.00052	1-C9E	OLE1
C10 Terminal Alkenes	0.00010	1-C10E	OLE1
C11 Terminal Alkenes	0.00019	1-C11E	OLE1
C4 Internal Alkenes	0.00014	0.5 T-2-BUTE + 0.5 C-2-BUTE	OLE2
C5 Internal Alkenes	0.00317	0.5 C-2-PENT + 0.5 T-2-PENT	OLE2
C6 Internal Alkenes	0.00100	0.5 C-2-C6E + 0.5 T-2-C6E	OLE2
C7 Internal Alkenes	0.00044	T-3-C7E	OLE2
C8 Internal Alkenes	0.00021	T-4-C8E	OLE2
C9 Internal Alkenes	0.00024	T-4-C9E	OLE2
C10 Internal Alkenes	0.00010	T-4-C10E	OLE2
C11 Internal Alkenes	0.00019	T-5-C11E	OLE2
C7 Cyclic or di-olefins	0.00019	T-2-C7E	OLE2
a-Pinene	0.00051	A-PINENE	TRP1
3-Carene	0.00019	3-CARENE	TRP1
C9 Styrenes	0.00048	STYRENE	ARO2
C10 Styrenes	0.00036	STYRENE	ARO2
Benzene	0.00329	BENZENE	0.295 ARO1
Toluene	0.00923	TOLUENE	ARO1
Ethyl Benzene	0.00128	C2-BENZ	ARO1
n-Propyl Benzene	0.00036	N-C3-BEN	ARO1
Isopropyl Benzene (cumene)	0.00019	I-C3-BEN	ARO1
C9 Monosub. Benzenes	0.00016	N-C3-BEN	ARO1
s-Butyl Benzene	0.00023	S-C4-BEN	ARO1
C10 Monosub. Benzenes	0.00018	N-C3-BEN	ARO1
C11 Monosub. Benzenes	0.00065	N-C3-BEN	ARO1
C12 Monosub. Benzenes	0.00002	N-C3-BEN	ARO1
o-Xylene	0.00183	O-XYLENE	ARO2
p-Xylene	0.00218	P-XYLENE	ARO2
m-Xylene	0.00218	M-XYLENE	ARO2
C9 Disub. Benzenes	0.00247	0.34 M-XYLENE + 0.33 O-XYLENE + 0.33 P-XYLENE	ARO2
C10 Disub. Benzenes	0.00154	0.34 M-XYLENE + 0.33 O-XYLENE + 0.33 P-XYLENE	ARO2
C11 Disub. Benzenes	0.00010	0.34 M-XYLENE + 0.33 O-XYLENE + 0.33 P-XYLENE	ARO2

Table 50 (continued)

VOC Name	Moles VOC / Mole C Mix	Represented By	Lumped with
C12 Disub. Benzenes	0.00009	0.34 M-XYLENE + 0.33 O-XYLENE + 0.33 P-XYLENE	ARO2
1,3,5-Trimethyl Benzene	0.00072	135-TMB	ARO2
1,2,3-Trimethyl Benzene	0.00075	123-TMB	ARO2
C9 Trisub. Benzenes	0.00236	0.34 135-TMB + 0.33 123-TMB + 0.33 124-TMB	ARO2
C10 Trisub. Benzenes	0.00160	0.34 135-TMB + 0.33 123-TMB + 0.33 124-TMB	ARO2
C11 Trisub. Benzenes	0.00010	0.34 135-TMB + 0.33 123-TMB + 0.33 124-TMB	ARO2
C12 Trisub. Benzenes	0.00009	0.34 135-TMB + 0.33 123-TMB + 0.33 124-TMB	ARO2
C10 Tetrasub. Benzenes	0.00042	0.34 135-TMB + 0.33 123-TMB + 0.33 124-TMB	ARO2
Acetylene	0.00974	ACETYLEN	ALK2
Formaldehyde	0.00792	FORMALD	HCHO
Acetaldehyde	0.00477	ACETALD	CCHO
Propionaldehyde	0.00070	PROPALD	RCHO
C4 aldehydes	0.00031	1C4RCHO	RCHO
C5 Aldehydes	0.00107	1C5RCHO	RCHO
C6 Aldehydes	0.00073	1C6RCHO	RCHO
Benzaldehyde	0.00016	BENZALD	BALD
Acetone	0.00309	ACETONE	ACET
Methyl Ethyl Ketone	0.00110	MEK	MEK

oxygenate measurements in the California South Coast Air Basin (Carter, 1994a,b and references therein). Table 50 also shows the detailed model species used to represent each of measured components in the mixture, and groups used to represent them in the lumped mechanism. Since this mixture is based on VOC measurements in a variety of urban areas, it serves as an appropriate basis for deriving parameters for those lumped species that represent anthropogenic emissions.

This base ROG mixture cannot serve as a basis for deriving the parameters for the biogenic terpene (TRP1) group, since that mixture represents purely ambient VOCs. For this we use the estimated annual North American biogenic terpene emissions rates summarized by Guenther et al (2000), where the five most abundant terpenes are as follows:

Terpene	Tg C/year
α-Pinene	4.3
β-Pinene	3.1
Δ^3 O_3	1.9
Sabinene	1.1
d-Limonene	1.0

Although other terpenes listed by Guenther et al (2000) total more than 3 Tg C/year and other classes of compounds, such as alcohols and aldehydes, are also important in the biogenic inventory, this profile is used as the basis for deriving the recommended parameters for the TRP1 lumped group for the present

mechanism. Note that since the appropriate lumped group used for anthropogenic species can be used to represent the biogenic alcohols and aldehydes, the contributions of these compounds to the biogenic emissions do not affect the parameters derived for TRP1.

Table 51 gives a summary of the compounds used to derive the mechanism for each of the lumped model species in the fixed parameter mechanism. The relative contributions of the species to the parameters of each group are also shown. Except for benzene (see discussion above) the relative contributions were determined by the mole fractions of the compounds in the mixtures.

The rate constants and mechanisms for the reactions for these lumped species that are derived using this set of anthropogenic base ROG and biogenic terpene mixtures are given in Table A-3 in Appendix A. The reactions of ethene and isoprene that are used for these explicitly represented species are also shown on that table. These explicit and lumped primary VOC reactions are added to the base mechanism to constitute the full fixed parameter SAPRC-99 mechanism for use in ambient simulations. This mechanism is used in the base case simulations in the incremental reactivity calculations discussed in Section VII.

It should be emphasized, however, that for model applications where the emissions inventory is known, or where the effects of changing the composition of the inventory is being assessed, the parameters should be derived using the specific inventories used in the simulations. This is particularly true if the inventories indicate significant contributions of classes of compounds that are not in the base ROG mixture used to derive the current fixed parameter mechanism. In particular, the base ROG mixture consists primarily of the hydrocarbons of the type found in gasoline vehicle exhausts, and the parameters derived using this mixture may not be appropriate if sources involving emissions of other types of VOCs, such as glycols or alcohols, are important.

Table 51. Summary of compounds used to derive mechanisms for lumped parameter groups in the fixed parameter mechanism.

Compound	Cont'n	Compound	Cont'n	Compound	Cont'n
ALK1		ALK5		ARO1	
Ethane	100%	2,4-Dimethyl Hexane	11%	Toluene	70%
		n-Decane	10%	n-Propyl Benzene	10%
ALK2		3-Methyl Hexane	10%	Ethyl Benzene	10%
Propane	59%	n-Heptane	7%	Benzene [a]	7%
Acetylene	41%	2,3-Dimethyl Pentane	6%	s-Butyl Benzene	2%
		2-Methyl Heptane	6%	Isopropyl Benzene	1%
ALK3		4-Methyl Heptane	6%		
n-Butane	68%	2,4-Dimethyl Heptane	5%	ARO2	
Isobutane	30%	Methylcyclohexane	4%	m-Xylene	22%
2,2-Dimethyl Butane	2%	2,6-Dimethyl Octane	4%	p-Xylene	22%
		n-Nonane	4%	o-Xylene	20%
ALK4		n-Octane	4%	1,3,5-Trimethyl Benzene	14%
Iso-Pentane	45%	Cyclohexane	4%	1,2,3-Trimethyl Benzene	14%
n-Pentane	18%	2-Methyl Hexane	3%	1,2,4-Trimethyl Benzene	9%
2-Methyl Pentane	11%	4-Methyl Octane	2%		
3-Methylpentane	8%	2-Methyl Octane	2%		
2,4-Dimethyl Pentane	5%	4-Methyl Nonane	2%		
Methylcyclopentane	5%	2-Methyl Nonane	2%		
n-Hexane	4%	n-Dodecane	2%		
2,3-Dimethyl Butane	3%	Ethylcyclohexane	1%		
Cyclopentane	2%	n-Undecane	1%		
		3,6-Dimethyl Decane	1%		

[a] Reactivity weighting factor of 0.295 used for benzene. See text.

VII. ATMOSPHERIC REACTIVITY ESTIMATES

To estimate the effects of VOC emissions on ozone formation under conditions more representative of polluted urban atmospheres, incremental reactivities were calculated for all VOCs that are represented in the current mechanism. This includes not only the VOCs whose mechanisms were derived or estimated as discussed in the previous sections, but also VOCs, or mixtures of isomeric VOCs, that are represented by other VOCs using the "lumped molecule" approach. In addition to "best estimate" reactivity estimates that were derived using the mechanisms discussed above, upper limit reactivity estimates were made for the purpose of estimating maximum likely ozone impacts. The latter may be useful in some regulatory approaches as a means to take uncertainties into account. Qualitative uncertainty classifications are given for all VOCs to aid the use of uncertainty information in regulatory applications, and for determining where further studies are most needed.

Atmospheric reactivities are derived for the Maximum Incremental Reactivity (MIR) and other scales, with ozone impacts quantified in terms of both effects on peak O_3 concentration and 8-hour averages. However, the emphasis in this work is on the MIR scale because this is the scale used in the California vehicle emissions regulations (CARB, 1993), and being considered for use in consumer product regulations (CARB, 1999). Because of this, upper limit reactivity estimates are made only for the MIR scale, though an analogous approach could be applied for other scales.

A. Atmospheric Reactivity Modeling Methods

The modeling approach and scenarios used for estimating atmospheric reactivities of VOCs is generally the same as used by Carter (1994a) when developing the MIR and other scales with the SAPRC-90 mechanism. The only modification made in this work is that the MIR and other "adjusted NO_x" scales were derived by averaging the incremental reactivities of the individual adjusted NO_x scenarios (rather than by separately averaging the kinetic and mechanistic reactivities), and that reactivities are calculated for 8-hour averages rather than integrated ozone. Since the general methods and scenarios are the same as described in detail previously (Carter et al, 1994a,b), they are only briefly summarized here.

1. Scenarios Used for Reactivity Assessment

Base Case Scenarios. The scenarios employed were those used by Carter (1994a,b) to develop various reactivity scales to quantify impacts of VOCs on ozone formation in various environments. These were based on a series of single-day EKMA box model scenarios (EPA, 1984) derived by the EPA for assessing how various ROG and NO_x control strategies would affect ozone nonattainment in various areas of the country (Baugues, 1990). The characteristics of these scenarios and the methods used to derive their input data are described in more detail elsewhere (Baugues, 1990; Carter, 1994b). Briefly, 39 urban areas in the United States were selected based on geographical representativeness of ozone nonattainment areas and data availability, and a representative high ozone episode was selected for each. The initial non-methane organic carbon (NMOC) and NO_x concentrations, the aloft O_3 concentrations, and the mixing height inputs were based on measurement data for the various areas, the hourly emissions in the scenarios were obtained from the National Acid Precipitation Assessment Program emissions inventory (Baugues, 1990), and biogenic emissions were also included. Table 52 gives a summary of the urban areas represented and other selected characteristics of the scenarios.

Table 52. Summary of the conditions of the scenarios used for atmospheric reactivity assessment.

	Scenario	Max O_3 (ppb)	Max 8-Hr Avg O_3 (ppb)	ROG / NOx	NO_x / MOIR NO_x	Height (kM)	Init.and Emit. ROG (m.mol m^{-2})	O_3 aloft (ppb)	Integrated OH (ppt-min)
Avg.	Max React (MIR)	187	119	3.1	1.5	1.8	15	70	128
Cond.	Max O_3 (MOIR)	239	165	4.5	1.0	1.8	15	70	209
	Equal Benefit (EBIR)	227	172	6.4	0.7	1.8	15	70	210
Base	Atlanta, GA	179	132	7.3	0.7	2.1	12	63	200
Case	Austin, TX	175	144	9.3	0.5	2.1	11	85	179
	Baltimore, MD	334	215	5.2	1.1	1.2	17	84	186
	Baton Rouge, LA	241	173	6.8	0.9	1.0	11	62	186
	Birmingham, AL	244	202	6.9	0.5	1.8	13	81	208
	Boston, MA	197	167	6.5	0.6	2.6	14	105	262
	Charlotte, NC	143	126	7.8	0.3	3.0	7	92	212
	Chicago, IL	278	226	11.6	0.5	1.4	25	40	164
	Cincinnati, OH	205	153	6.4	0.7	2.8	17	70	220
	Cleveland, OH	252	179	6.6	0.9	1.7	16	89	187
	Dallas, TX	208	141	4.7	1.2	2.3	18	75	176
	Denver, CO	204	139	6.3	1.1	3.4	29	57	143
	Detroit, MI	246	177	6.8	0.7	1.8	17	68	235
	El Paso, TX	182	135	6.6	1.0	2.0	12	65	138
	Hartford, CT	172	144	8.4	0.5	2.3	11	78	220
	Houston, TX	312	217	6.1	0.9	1.7	25	65	225
	Indianapolis, IN	212	148	6.6	0.9	1.7	12	52	211
	Jacksonville, FL	155	115	7.6	0.6	1.5	8	40	206
	Kansas City, MO	159	126	7.1	0.6	2.2	9	65	233
	Lake Charles, LA	286	209	7.4	0.6	0.5	7	40	233
	Los Angeles, CA	568	406	7.6	1.0	0.5	23	100	134
	Louisville, KY	212	155	5.5	0.8	2.5	14	75	260
	Memphis, TN	229	180	6.8	0.6	1.8	15	58	249
	Miami, FL	132	111	9.6	0.4	2.7	9	57	181
	Nashville, TN	167	138	8.0	0.4	1.6	7	50	225
	New York, NY	365	294	8.1	0.7	1.5	39	103	159
	Philadelphia, PA	247	169	6.2	0.9	1.8	19	53	227
	Phoenix, AZ	277	193	7.6	1.0	3.3	40	60	153
	Portland, OR	166	126	6.5	0.7	1.6	6	66	233
	Richmond, VA	242	172	6.2	0.8	1.9	16	64	217
	Sacramento, CA	204	142	6.6	0.8	1.1	7	60	209
	St Louis, MO	324	209	6.1	1.1	1.6	26	82	176
	Salt Lake City, UT	186	150	8.5	0.6	2.2	11	85	182
	San Antonio, TX	133	98	3.9	1.0	2.3	6	60	192
	San Diego, CA	193	150	7.1	0.9	0.9	8	90	146
	San Francisco, CA	229	126	4.8	1.8	0.7	25	70	61
	Tampa, FL	230	153	4.4	1.0	1.0	8	68	211
	Tulsa, OK	231	160	5.3	0.9	1.8	15	70	264
	Washington, DC	283	209	5.3	0.8	1.4	13	99	239

Several changes to the scenario inputs were made based on discussions with the California ARB staff and others (Carter, 1994b). Two percent of the initial NOx and 0.1% of the emitted NO_x in all the scenarios was assumed to be in the form of HONO. The photolysis rates were calculated using solar light intensities and spectra calculated by Jeffries (1991) for 640 meters, the approximate mid-point of the mixed layer during daylight hours. The composition of the VOCs entrained from aloft was based on the analysis of Jeffries et al. (1989).

The composition of the initial and emitted reactive organics (referred to as the "base ROG" mixture) is given on Table 50, above. It is derived from the “all city average” mixture derived by Jeffries et al (1989) from analysis of air quality data, with minor modifications as discussed by Carter (1994a,b). Note that this same mixture is used to derive the parameters for the lumped parameter products (RNO3 and PROD2) in the base mechanism, and for the lumped species in the recommended fixed parameter condensed mechanism (see Sections II.C.2 and VI.B.2, respectively).

Complete listings of the input data for the scenarios are given elsewhere (Carter, 1994b).These are referred to as "base case" scenarios, to distinguish them from those where NOx inputs are adjusted as discussed below.

Adjusted NO_x Scenarios. In addition to these 39 base case scenarios, adjusted NO_x scenarios were developed to represent different conditions of NOx availability. NO_x levels were found to be the most important factor affecting differences in relative ozone impacts among most VOCs (Carter and Atkinson, 1989a; Carter, 1994a). Because of this, separate scales were derived to represent different conditions of NO_x availability, as follows:

- In the "Maximum Incremental Reactivity" (MIR) scenarios, the NO_x inputs for each of the 39 base case scenarios are adjusted such that the final O_3 level is most sensitive to changes in VOC emissions. This represents relatively high NO_x conditions where VOC control is the most effective means to reduce ozone formation. Note that the MIR NO_x levels vary from scenario to scenario, so it is not correct to say that there is a characteristic ROG/NO_x ratio that corresponds to MIR conditions.
- In the "Maximum Ozone Incremental Reactivity" (MOIR) scenarios the NOx inputs are adjusted to yield the highest maximum O_3 concentration. This represents conditions that are optimum for ozone formation. This represents moderate NO_x conditions where O_3 formation is just starting to become NO_x limited. Generally, NO_x levels of MOIR scenarios are about 70% of those of MIR conditions (Carter, 1994a). Although O_3 formation is also sensitive to VOC control under these conditions, it is less sensitive than in the higher NO_x MIR scenarios.
- In the "Equal Benefit Incremental Reactivity" (EBIR) scenarios, the NOx inputs are adjusted such that relative changes in VOC and NOx emissions had equal effect on ozone formation. This represents conditions where O_3 formation is NO_x limited to such an extent, but not to such a large extent that VOC controls are ineffective. Generally, NO_x levels in EBIR scenarios are about 70% those of MOIR scenarios, and about half those of MIR scenarios.

As discussed by Carter (1994a), there represent respectively the high, medium and low ranges of NO_x conditions that are of relevance when assessing VOC control strategies for reducing ozone. Although lower NO_x conditions than EBIR occur in many areas (especially non-urban areas), O_3 formation under such conditions is primarily sensitive to NO_x emissions, and VOC control is not as important as NO_x control under those conditions.

Averaged Conditions Scenarios. In addition to the above, "averaged conditions" MIR, MOIR, and EBIR scenarios were developed for use for screening or sensitivity calculations. This consists of developing a scenario whose inputs are based on averaging those representing the 39 urban areas, with NO_x inputs adjusted to yield MIR, MOIR, or EBIR conditions as discussed above (Carter, 1994a,b). These scenarios are also summarized on Table 52.

2. Quantification of Atmospheric Reactivity

The reactivity of a VOC in an airshed scenario is measured by its incremental reactivity. For ambient scenarios, this is defined as the change in ozone caused by adding the VOC to the emissions, divided by the amount of VOC added, calculated for sufficiently small amounts of added VOC that the incremental reactivity is independent of the amount added[22].

$$\mathrm{IR(VOC, Scenario)} = \lim_{VOC \to 0} \left[\frac{\mathrm{O_3(Scenario\ with\ VOC) - O_3(Base\ Scenario)}}{\mathrm{Amount\ of\ VOC\ Added}} \right] \qquad \text{(XXXIV)}$$

The specific calculation procedure is discussed in detail elsewhere (Carter, 1994a,b).

Incremental reactivities derived as given above tend to vary from scenario to scenario because they differ in their overall sensitivity of O_3 formation to VOCs. These differences can be factored out to some extent by using "relative reactivities", which are defined as ratios of incremental reactivities to the incremental reactivity of the base ROG mixture.

$$\mathrm{RR(VOC, Scenario)} = \frac{\mathrm{IR(VOC, Scenario)}}{\mathrm{IR\ (Base\ ROG, Scenario)}} \qquad \text{(XXXV)}$$

These relative reactivities can also be thought of as the relative effect on O3 of controlling emissions of the particular VOC by itself, compared to controlling emissions from all VOC sources equally. Thus, they are more meaningful in terms of control strategy assessment than absolute reactivities, which can vary greatly depending on the episode and local meteorology.

In addition to depending on the VOC and the scenario, the incremental and relative reactivities depend on how the amounts of VOC added and amounts of ozone formed are quantified. In this work, the amount of added VOC is quantified on a mass basis, since this is how VOCs are regulated, and generally approximates how VOC substitutions are made in practice. Note that relative reactivities will be different if they are quantified on a molar basis, with VOCs with higher molecular weight having higher reactivities on a mole basis than a gram basis.

Relative reactivities can also depend significantly on how ozone impacts are quantified (Carter, 1994a). Two different ozone quantification methods are used in this work, as follows:

- "Ozone Yield" incremental reactivities measure the effect of the VOC on the total amount of ozone formed in the scenario at the time of its maximum concentration. Incremental reactivities are quantified as grams O_3 formed per gram VOC added. Most previous recent studies of incremental reactivity (Dodge, 1984; Carter and Atkinson, 1987, 1989a, Chang and Rudy, 1990;

[22] Note that this differs from how the term "incremental reactivity" is used in the context of chamber experiments. In that case, the incremental reactivity refers to the relative change observed in the individual experiments, which in general depends on the amount added.

Jeffries and Crouse, 1991) have been based on this quantification method. The MIR, MOIR, and EBIR scales of Carter (1994a) also use this quantification.

- "Max 8 Hour Average" incremental measure the effect of the VOC on the average ozone concentration during the 8-hour period when the average ozone concentration was the greatest, which in these one-day scenarios was the last 8 hours of the simulation. This provides a measure of ozone impact that is more closely related to the new Federal ozone standard that is given in terms of an 8 hour average. This quantification is used for relative reactivities in this work.

In previous reports, we have reported reactivities in terms of integrated O_3 over a standard concentration of 0.09 or 0.12 ppm. This provides a measure of the effect of the VOC on exposure to unacceptable levels of ozone. This is replaced by the Max 8 Hour Average reactivities because it is more representative of the new Federal ozone standard and because reactivities relative to integrated O_3 over a standard tend to be between those relative to ozone yield and those relative to 8-hour averages. Therefore, presenting both ozone yield and maximum 8-hour average relative reactivities should be sufficient to provide information on how relative reactivities vary with ozone quantification method. Incremental reactivities are quantified as ppm O_3 per milligram VOC emitted per square meter.

If a reactivity scale is developed based on incremental reactivities in more than one scenario, then the method used to derive the scale from the reactivities in the individual scenarios will also affect the scale. Although as discussed by Carter (1994a) a number of aggregation methods can be used, in this work we use only simple averaging of incremental or relative reactivities, as discussed below. Note that this differs somewhat from the method used by Carter (1994a) to derive the MIR and other adjusted NO_x scales, where averages of kinetic and mechanistic reactivities were used.

Based on these considerations, reactivities in the following scales were derived in this work, as follows:

- The MIR scale consists of averages of the incremental reactivities in the 39 MIR scenarios (i.e., the 39 base case scenarios with NO_x adjusted to represent MIR conditions), with O_3 quantified by ozone yields, and VOCs quantified by mass. The units are grams O_3 formed per gram VOC added.
- The MOIR and EBIR scales are derived from averages of the ozone yield incremental reactivities in the 39 MOIR or EBIR scenarios, in a manner analogous to the derivation of the MIR scale.
- The Averaged Conditions MIR, MOIR, and EBIR scales are the ozone yield incremental reactivities in the corresponding averaged conditions scenario. For most VOCs, the averaged conditions reactivities are very close to those derived from the 39 adjusted NO_x scales as discussed above.
- The Base Case O_3 Yield Scales are O_3 yield incremental and relative reactivities in the 39 base case scenarios. Thus there are 39 such scales, one for each of the 39 urban areas. Averages and standard deviations of the relative reactivities are also presented.
- The Base Case Maximum 8-Hour Average Scales are relative reactivities based on effects of the VOCs on the maximum 8-hour average ozone in the 39 base case scenarios. Averages and standard deviations of the relative reactivities in these 39 scales are also presented.

Note that the MIR scale is the one recommended by Carter (1994a) for regulatory applications requiring use of a single scale, and is preferred by the California ARB for regulatory use (e.g., CARB, 1993, 1998). This is because MIR reactivities reflect conditions that are most sensitive to VOC controls,

and serve as an appropriate complement to NO_x controls in a comprehensive control strategy. Relative reactivities in the MIR scale also correspond reasonably well to integrated O_3 reactivities in lower NO_x scenarios, because both are strongly influenced by factors of a VOCs mechanism that affect O_3 formation rates (Carter, 1994a). However, relative reactivities can differ depending on the scenarios or quantification method used, and regulatory applications that do not require use of a single scale should be based on considerations of reactivities in multiple scales.

3. Chemical Mechanism Used

The chemical mechanism employed in the atmospheric reactivity simulations consisted of the lumped mechanism discussed in Section VI with reactions added as needed to represent the VOC or mixture whose reactivity is being assessed. The lumped mechanism, which consists of the base mechanism listed in Table A-1 and the mechanism for the lumped species listed in Table A-3 is used in the "base case" simulations without the added VOCs. No lumping was employed when representing an individual VOC for calculating its reactivity, and Table A-6 in Appendix A gives the reactions used for those VOCs that are not in the base mechanism[19]. When calculating reactivities of complex mixtures (e.g., MS-A or the base ROG mixture), the components were lumped using the approach recommended in Table 49, with the parameters for the lumped model species being derived based on the specific mixtures being represented. The compositions of the mixtures whose reactivities were calculated are given in Table C-5 in Appendix C. Note that separate model species were used to represent components whose reactivities were being assessed than used to represent VOCs in the base mixture in the reactivity calculations, except for components that are already represented explicitly in the mechanism.

B. VOC Classes and Uncertainty Classifications

Atmospheric reactivity estimates were made for all VOC classes that can be used to represent emitted VOCs in the current mechanism. These classes, which are also referred to as "detailed model species", can represent either a single compound or a mixture of isomers that are assumed to have similar mechanisms, or whose detailed compositions are unknown. The individual compounds include compounds whose reactions are represented explicitly, and compounds represented by other compounds using the lumped molecule approach. The mixtures of isomers are represented by one or more compounds that are assumed to be representative of the types of compounds in the mixtures.

Table C-1 in Appendix C lists all the detailed model species used in the current version of the mechanism (including some for which mechanistic and therefore reactivity estimates have not been made), and gives other summary information concerning these species. This includes the following:

- Name. Each detailed model species has a 2-8 character detailed model species name that is used to identify it in the modeling system. Note that this name is the primary means to identify these species in some of the tabulations in this report, so can be used to identify what the name represents if this is not obvious.
- Description. The name of the VOC or the group of the VOCs that are represented by this class.
- Molecular Weight (Mwt). Because each detailed model species refers to either a single compound or set of isomeric compounds, each has a unique molecular weight associated with it. The molecular weight is used when processing mass-based emissions data, or when computing impacts of compounds on a weight basis.
- The uncertainty code (Unc) assigned to the mechanism for this model species. These codes, which are defined in Table C-2, indicate the author's subjective opinion of the likelihood that the mechanism,

and the ozone impact predictions resulting from using the mechanism, will change significantly in the future as new data become available. Note a higher number means a higher uncertainty (with 6 being the highest), and it is recommended that any reactivity-based regulation use uncertainty adjustments for those VOCs whose uncertainty classifications are greater than 4.

- The experimental data availability code (Exp.). These codes, which are defined in Table C-3, indicate the extent to which the mechanism for the compound has been or can be experimentally evaluated. Reference is also made in some cases to the availability of data to test the mechanism under MIR conditions; this refers to experiments testing the effects of the compounds on O_3 formation in surrogates representing relatively high NO_x conditions. Note that a code of "-" means there are no data available to evaluate the mechanism. The evaluation of mechanism is discussed in Section V (see also Appendix B).
- Additional information and comments (Notes). These footnotes, which are defined in Table C-4, give additional information about the representation of the detailed model species and the status of its evaluation. For example, note "1" indicates the mechanism is considered to be reasonably well established, "2" means the evaluation of mechanism for this species is discussed in this report, "4" means that the mechanism was adjusted to improve fits to chamber data, "7" means that the appropriateness of the lumped molecule representation used is uncertain, etc.
- The method used to represent the chemical reactions of the compound in the model. This could be one of the following:
  - Explicit in the base mechanism (Expl). This means that reactions of this model species are part of the base mechanism because it is used, in part, to represent organic oxidation products. The mechanisms for the organic product species in the base mechanism are discussed in Section II.C
  - Mechanism Generated (Gen'd). This means that the mechanism was generated using the mechanism estimation and generation system that is discussed in Section III. The structure that was used when generating the mechanism (see Section III.B) is also shown.
  - Assigned Parameters (Asn'd). This means that the mechanism for this compound was derived or estimated as discussed in Section IV. This includes aromatics, terpenes, and other compounds for which the mechanism generation system cannot be used.
  - Lumped Molecule (L.Mol). This means that this detailed model species is represented in the model by another model species (or mixture thereof), on a mole for mole basis. The model species or mixture used to represent it is also shown. Note that mixtures are used for detailed model species that refer to an unspecified mixture of isomers that have different reactivity. Because of analytical limitations, such unspecified mixture classes tend to occur in many speciation profiles in emissions inventories.
  - Not in model (-). The current version of the mechanism does not have mechanistic assignments for this class of compounds. It is included in the list because it occurs in speciated emissions inventories. The molecular weight and carbon number information can be used when determining an approximate representation of the compound in model applications when mixtures containing these species are emitted.
  - Mixture (Mix). This is a complex mixture. This is not strictly a detailed model species, but is included in the tabulation of reactivity results for comparison purposes, or because their reactivities are of particular interest or have been studied for other projects. These include the mixture used to represent the Base ROG in the reactivity calculations, several mixtures used by the California Air Resources Board to represent exhausts from transitional low emissions vehicles

(TLEVs) or low emissions vehicles (LEVs), several mineral spirits commercial hydrocarbon mixtures studied for Safety-Kleen (Carter et al, 1997f) or Exxon corporation (Carter et al, 2000g), and commercial ortho-acetate solvents also studied for Exxon corporation (Carter et al, 2000g). The compositions of the mixtures whose reactivities have been tabulated are given in Table C-5.

- Lumped Group. This is the lumped or explicit model species that is used in the condensed mechanism when representing the representing the detailed model species when present in mixtures, or in lumped model simulations when its reactivity is not being assessed. The footnote indicates abbreviations that are used.

C. Reactivity Results

The results of the reactivity calculations in the different scales are given in various tables in Appendix C. The incremental reactivity in the MIR scale is given in Table C-1, along with the estimated upper limit MIR, derived as discussed in the following section. Table C-6 gives reactivity data in various scales, including MIR, MOIR, EBIR, and averages, standard deviations, minima, and maxima in the O_3 yield and maximum 8-hour average relative reactivities calculated for the various scales. The incremental reactivities calculated for all the individual scenarios are given in Table C-7 and Table C-8, where Table C-7 gives the data for the ozone yield reactivities, and Table C-8 gives the data for the maximum 8-hour average reactivities. Because of their size, the latter tables are not included with the printed version of this report, but are included with the electronic version, which can be downloaded from http://cert.ucr.edu/~carter/reactdat.htm[23].

It can be seen that there have been changes in the incremental and relative reactivities for a number of VOCs, relative to previous versions. The largest changes are for the VOCs whose mechanisms have been changed because of new data or revised estimates, but other changes have resulted from changes in the base mechanism and treatment of reactive products. For example, MIR's for some high molecular weight species whose mechanisms have not otherwise changed increased because of the use or PROD2 rather than the less reactive MEK to represent reactive ketone or other non-aldehyde oxygenated products. A complete analysis of the changes to the reactivity scale due to the mechanism updates has not been carried out, but may give useful insights concerning the effects of chemical mechanism uncertainties on incremental reactivity scales.

As indicated on Table C-6, the mechanisms for some VOCs are considered to be highly uncertain, and it is recommended that any regulations that use incremental reactivity data take these uncertainties into account. In particular, it is recommended that appropriate uncertainty adjustments be used for those VOCs that are given an uncertainty code of "4" or greater. A discussion of exactly what constitutes an appropriate uncertainty adjustment is beyond the scope of this work. However, at the request of the CARB, the author developed a means to estimate “upper limit” MIR’s for VOCs, given available information concerning the reaction rates and chemical type of the VOC, and the calculated MIRs for VOCs with known or estimated mechanisms (Carter, 1997). These upper limit estimates were updated for the current version of the mechanism, and the results are included on Table C-1. The methods and data used to derive these upper limit estimates are given in Appendix D to this report.

[23] This site may contain updated information when the mechanism and reactivity scale are updated in the future. However, it is expected that links and files will be retained so the version of the tables discussed in this report can still be downloaded.

VIII. REFERENCES

Alcock, W. G. and B. Mile (1975): "The Gas-Phase Reactions of Alkylperoxy Radicals Generated by a Photochemical Technique," Combust. Flame 24, 125.

Alvaro A., E. C. Tuazon, S. M. Aschmann, J. Arey and R. Atkinson (1999): "Products and mechanisms of the gas-phase reactions of OH radicals and O_3 with 2-methyl-3-buten-2-ol," Atmos. Environ. 33, 2893-2905.

Arey, J. , S. M. Aschmann, E. S. C. Kwok, and R. Atkinson (2000) Alkyl nitrate, hydroxyalkyl nitrate, and hydroxycarbonyl formation from the NO_x-air photooxidations of C_5-C_8 n-alkanes. J. Phys. Chem. A, to be submitted for publication.

Aschmann, S. M., A. A. Chew, J. Arey and R. Atkinson (1997): "Products of the Gas-Phase Reaction of OH Radicals with Cyclohexane: Reactions of the Cyclohexyl Radical," J. Phys. Chem. A, 101, 8042-8048.

Aschmann, S. M. and R. Atkinson (1998): "Kinetics of the Gas-Phase Reactions of the OH Radical with Selected Glycol Ehters, Glycols, and Alcohols," Int. J. Chem. Kinet, 30, 533-540.

Aschmann, S. M. and R. Atkinson (1999): "Products of the Gas-Phase Reactions of the OH Radical with Methyl n-Butyl Ether and 2-Isopropoxyethanol: Reactions of ROC(O·)< Radicals," Int. J. Chem. Kinet, 31, 501-513.

Atkinson, R. (1987): "A Structure-Activity Relationship for the Estimation of Rate Constants for the Gas-Phase Reactions of OH Radicals with Organic Compounds," Int. J. Chem. Kinet., 19, 799-828.

Atkinson, R. (1989): "Kinetics and Mechanisms of the Gas-Phase Reactions of the Hydroxyl Radical with Organic Compounds," J. Phys. Chem. Ref. Data, Monograph no 1.

Atkinson, R. (1990): "Gas-Phase Tropospheric Chemistry of Organic Compounds: A Review," Atmos. Environ., 24A, 1-24.

Atkinson, R. (1991): "Kinetics and Mechanisms of the Gas-Phase Reactions of the NO_3 Radical with Organic Compounds," J. Phys. Chem. Ref. Data, 20, 459-507.

Atkinson, R. (1994): "Gas-Phase Tropospheric Chemistry of Organic Compounds," J. Phys. Chem. Ref. Data, Monograph No. 2.

Atkinson, R. (1997a): "Gas Phase Tropospheric Chemistry of Volatile Organic Compounds: 1. Alkanes and Alkenes," J. Phys. Chem. Ref. Data, 26, 215-290.

Atkinson, R. (1997b): "Atmospheric Reactions of Alkoxy and Beta-Hydroxyalkoxy Radicals," Int. J. Chem. Kinet., 29, 99-111.

Atkinson, R. (2000): "Atmospheric Chemistry of VOCs and NO_x," Atmospheric Environment, 34, 2063-2101.

Atkinson, R., R.A. Perry, and J. N. Pitts, Jr. (1978): "Rate Constants for the reactions of the OH radical with $(CH_3)_2NH$, $(CH_3)_3N$, and $C_2H_5NH_2$ over the temperature range 298-426 °K," J. Chem. Phys. 68, 1850.

Atkinson, R., S. M. Aschmann, W. P. L. Carter and J. N. Pitts, Jr. (1982): "Rate constants for the Gas-Phase Reaction of OH Radicals with a Series of Ketones at 299±2 K," Int J. Chem. Kinet. 14, 839, 1982.

Atkinson, R., S. M. Aschmann, W. P. L. Carter, A. M. Winer and J. N. Pitts, Jr. (1982b): "Alkyl Nitrate Formation from the NO_x-Air Photooxidations of C_2-C_8 n-Alkanes," J. Phys. Chem. 86, 4562-4569.

Atkinson, R., S. M. Aschmann and J. N. Pitts, Jr. (1983): "Kinetics of the Gas-Phase Reactions of OH Radicals with a Series of α,β-Unsaturated Carbonyls at 299±2 K," Int. J. Chem. Kinet. 15, 75.

Atkinson, R., W. P. L. Carter, and A. M. Winer (1983b): "Effects of Temperature and Pressure on Alkyl Nitrate Yields in the NO_x Photooxidations of n-pentane and n-heptane" J. Phys. Chem. 87, 2012-2018.

Atkinson, R. and W. P. L. Carter (1984): "Kinetics and Mechanisms of the Gas-Phase Reactions of Ozone with Organic Compounds under Atmospheric Conditions," Chem. Rev. 84, 437-470.

Atkinson, R. and A. C. Lloyd (1984): "Evaluation of Kinetic and Mechanistic Data for Modeling of Photochemical Smog," J. Phys. Chem. Ref. Data 13, 315.

Atkinson, R., S. M. Aschmann, W. P. L. Carter, A. M. and Winer (1984): "Formation of Alkyl Nitrates from the Reaction of Branched and Cyclic Alkyl Peroxy Radicals with NO," Int. J. Chem. Kinet., 16, 1085-1101.

Atkinson, R., S. M. Aschmann, A. M. Winer and J. N. Pitts, Jr. (1985): "Atmospheric Gas Phase Loss Processes for Chlorobenzene, Benzotrifluoride, and 4-Chlorobenzotrifluoride, and Generalization of Predictive Techniques for Atmospheric Lifetimes of Aromatic Compounds," Arch Environ. Contamin. Toxicol. 14, 417.

Atkinson, R. and S. M. Aschmann (1986): "Kinetics of the Reactions of Naphthalene, 2-Methylnaphthalene, and 2,3-Dimethylnaphthalene with OH Radicals and with O_3 at 295±1 K," Int J. Chem. Kinet. 18, 569.

Atkinson, R. and S. M. Aschmann (1987): "Kinetics of the Gas-Phase Reactions of Alkylnaphthalenes with O_3, N_2O_5 and OH Radicals at 298±2 K," Atmos. Environ. 21, 2323.

Atkinson, R., S. M. Aschmann, and M. A. Goodman (1987): "Kinetics of the Gas-Phase Reactions NO_3 Radicals with a Series of Alkynes, Haloalkenes, and α,β-Unsaturated Aldehydes," Int. J. Chem. Kinet., 19, 299.

Atkinson, R. and S. M. Aschmann (1988a): "Kinetics of the Reactions of Acenaphthalene and Acenaphthylene and Structurally-Related Aromatic Compounds with OH and NO_3 Radicals, N_2O_5 and O_3 at 296±2 K," Int J. Chem. Kinet. 20, 513.

Atkinson, R., and S. M. Aschmann (1988b): "Rate Constant for the Reaction of OH Radicals with Isopropylcyclopropane at 298+/-2-k - Effects of Ring Strain on Substituted Cycloalkanes," Int. J. Chem. Kinet. 20, (4) 339-342.

Atkinson, R., S. M. Aschmann, J. Arey and W. P. L. Carter (1989): "Formation of Ring-Retaining Products from the OH Radical-Initiated Reactions of Benzene and Toluene," Int. J. Chem. Kinet. 21, 801.

Atkinson, R., S. M. Aschmann, and J. Arey (1991): "Formation of Ring-Retaining Products from the OH Radical-Initiated Reactions of o-, m-, and p-Xylene," Int. J. Chem. Kinet. 23, 77.

Atkinson, R., D. L. Baulch, R. A. Cox, R. F. Hampson, Jr., J. A. Kerr, and J. Troe (1992): "Evaluated Kinetic and Photochemical Data for Atmospheric Chemistry. Supplement IV (IUPAC)," J. Phys. Chem. Ref. Data 21, 1125-1568.

Atkinson, R., and W. P. L. Carter (1995): "Measurement of OH Radical Reaction Rate Constants for Purasolv ELS and Purasolv ML and Calculation of Ozone Formation Potentials," Final Report to Purac America, Inc., June.

Atkinson, R., E. S. C. Kwok, J. Arey and S. M. Aschmann (1995): "Reactions of Alkoxyl Radicals in the Atmosphere," Faraday Discuss. 100, 23.

Atkinson, R., D. L. Baulch, R. A. Cox, R. F. Hampson, Jr., J. A. Kerr, M. J. Rossi, and J. Troe (1997): "Evaluated Kinetic, Photochemical and Heterogeneous Data for Atmospheric Chemistry: Supplement V and VI, IUPAC Subcommittee on Gas Kinetic Data Evaluation for Atmospheric Chemistry," Phys. Chem. Ref. Data, 26, 521-1011 (Supplement V) and 1329-1499 (Supplement VI).

Atkinson, R., E. C. Tuazon, and S. M. Aschmann (1998): "Products of the Gas-Phase Reaction of the OH Radical with 3-Methyl-1-Butene in the Presence of NO," Int. J. Chem. Kinet., 30, 577-587.

Atkinson, R., D. L. Baulch, R. A. Cox, R. F. Hampson, Jr., J. A. Kerr, M. J. Rossi, and J. Troe (1999): "Evaluated Kinetic, Photochemical and Heterogeneous Data for Atmospheric Chemistry: Supplement VII, Organic Species (IUPAC)," J. Phys. Chem. Ref. Data, 28, 191-393.

Atkinson, R. et al. (2000a) Manuscript on OH rate constants for branched alkanes. In preparation.

Atkinson, R., E. C. Tuazon and S. M. Aschmann (2000b): "Atmospheric Chemistry of 2-pentanone and 2-heptanone," Environ. Sci. Technol., 34, 623-631.

Baldwin, A. C., J. R. Barker, D. M. Golden and G. G. Hendry (1977): "Photochemical Smog. Rate Parameter Estimates and Computer Simulations," J. Phys. Chem. 81, 2483.

Batt and Robinson (1987): "Decomposition of the t-Butoxy Radical – I. Studies over the Temperature Range 402-443 K," Int. J. Chem. Kinet. 19, 391.

Baugues, K. (1990): "Preliminary Planning Information for Updating the Ozone Regulatory Impact Analysis Version of EKMA," Draft Document, Source Receptor Analysis Branch, Technical Support Division, U. S. Environmental Protection Agency, Research Triangle Park, NC, January.

Baxley, J. S., M. V. Henley and J. R. Wells (1997). "The Hydroxyl Radical Reaction Rate Constant and Products of Ethyl 3-Ethoxypropionate," Int. J. Chem. Kinet., 29, 637-644.

Becker, K. H., V. Bastian, and Th. Klein (1988): "The Reactions of OH Radicals with Toluene Diisocyanate, Toluenediamine and Methylenedianiline Under Simulated Atmospheric Conditions," J. Photochem. Photobiol A., 45 195-205.

Bennett, P. J. and J. A. Kerr (1989): "Kinetics of the Reactions of Hydroxyl Radicals with Aliphatic Esters Studied Under Simulated Atmospheric Conditions," J. Atmos. Chem. 8, 87.

Benson, S. W. (1976): "Thermochemical Kinetics, 2nd Ed.", John Wiley and Sons, New York.

Bierbach A., Barnes I., Becker K.H. and Wiesen E. (1994) Atmospheric chemistry of unsaturated carbonyls: Butenedial, 4-oxo-2-pentenal, 3-hexene-2,5-dione, maleic anhydride, 3H-furan-2-one, and 5-methyl-3H-furan-2-one. Environ. Sci. Technol., 28, 715-729.

Baulch, D. L., I. M. Campbell, S. M. Saunders, and P. K. K. Louie (1989): "Rate Constants for the Reactions of the Hydroxyl Radical with Indane, Indene and Styrene," J. Chem. Soc. Faraday. Trans. 2, 85, 1819.

Bridier, I., H. Caralp, R. Loirat, B. Lesclaux and B. Veyret (1991): "Kinetic and Theoretical Studies of the Reactions of CH3C(O)O2 + NO2 + M <=> CH3C(O)O2NO2 + M between 248 and 393 K and between 30 and 760 Torr," J. Phys. Chem. 95, 3594-3600.

CARB (1993): "Proposed Regulations for Low-Emission Vehicles and Clean Fuels -- Staff Report and Technical Support Document," California Air Resources Board, Sacramento, CA, August 13, 1990. See also Appendix VIII of "California Exhaust Emission Standards and Test Procedures for 1988 and Subsequent Model Passenger Cars, Light Duty Trucks and Medium Duty Vehicles," as last amended September 22, 1993. Incorporated by reference in Section 1960.

CARB (1999) California Air Resources Board, Proposed Regulation for Title 17, California Code of Regulations, Division 3, Chapter 1, Subchapter 8.5, Article 3.1, sections 94560- 94539.

Calvert, J. G., and J. N. Pitts, Jr. (1966): "Photochemistry," John Wiley and Sons, New York.

Canosa-Mass et al (1996): "Is the reaction between $CH_3C(O)O_2$ and NO_3 important in the night-time troposphere?," J. Chem. Soc. Faraday Trans. 92, 2211.

Carter, W. P. L. (1987): "An Experimental and Modeling Study of the Photochemical Reactivity of Heatset Printing Oils," Report #2 on U. S. EPA Cooperative Agreement No. CR810214-01.

Carter, W. P. L. (1988): "Development and Implementation of an Up-To-Date Photochemical Mechanism for Use in Airshed Modeling," Final Report for California Air Resources Board Contract No. A5-122-32, October.

Carter, W. P. L. (1990): "A Detailed Mechanism for the Gas-Phase Atmospheric Reactions of Organic Compounds," Atmos. Environ., 24A, 481-518.

Carter, W. P. L. (1994a): "Development of Ozone Reactivity Scales for Volatile Organic Compounds," J. Air & Waste Manage. Assoc., 44, 881-899.

Carter, W. P. L. (1994b): "Calculation of Reactivity Scales Using an Updated Carbon Bond IV Mechanism," Report Prepared for Systems Applications International Under Funding from the Auto/Oil Air Quality Improvement Research Program, April 12.

Carter, W. P. L. (1995): "Computer Modeling of Environmental Chamber Measurements of Maximum Incremental Reactivities of Volatile Organic Compounds," Atmos. Environ., 29, 2513-2517.

Carter, W. P. L. (1996): "Condensed Atmospheric Photooxidation Mechanisms for Isoprene," Atmos. Environ., 30, 4275-4290.

Carter, W. P. L. (1997). "Estimation of Upper Limit Maximum Incremental Reactivities of VOCs," Prepared for California Air Resources Board Reactivity Research Advisory Committee, July 16. Available at http://www.cert.ucr.edu/~carter/absts.htm#maxmir.

Carter, W. P. L (1998):. "Estimation of Atmospheric Reactivity Ranges for Parachlorobenzotrifluoride and Benzotriflouride," Report to Occidental Chemical Corporation, March.

Carter, W. P. L., K. R. Darnall, A. C. Lloyd, A. M. Winer and J. N. Pitts, Jr. (1976): "Evidence for Alkoxy Radical Isomerizaiton in Photooxidations of C4-C6 Alkanes Under Simulated Atmospheric Conditions", Chem. Phys. Lett 42, 22-27.

Carter, W. P. L., A. C. Lloyd, J. L. Sprung, and J. N. Pitts, Jr. (1979): "Computer Modeling of Smog Chamber Data: Progress in Validation of a Detailed Mechanism for the Photooxidation of Propene and n-Butane in Photochemical Smog", Int. J. Chem. Kinet, 11, 45.

Carter, W. P. L., P. S. Ripley, C. G. Smith, and J. N. Pitts, Jr. (1981): "Atmospheric Chemistry of Hydrocarbon Fuels: Vol I, Experiments, Results and Discussion," Final report to the U. S. Air Force, ESL-TR-81-53, November.

Carter, W. P. L., and R. Atkinson (1985): "Atmospheric Chemistry of Alkanes", J. Atmos. Chem., 3, 377-405, 1985.

Carter, W. P. L. and R. Atkinson (1987): "An Experimental Study of Incremental Hydrocarbon Reactivity," Environ. Sci. Technol., 21, 670-679

Carter, W. P. L., A. M. Winer, R. Atkinson, S. E. Heffron, M. P. Poe, and M. A. Goodman (1987): "Atmospheric Photochemical Modeling of Turbine Engine Fuels. Phase II. Computer Model Development," Report on USAF Contract no. F08635-83-0278, Engineering and Services Laboratory, Air Force Engineering and Services Center, Tyndall Air Force Base, Florida, August.

Carter, W. P. L. and R. Atkinson (1996): "Development and Evaluation of a Detailed Mechanism for the Atmospheric Reactions of Isoprene and NOx," Int. J. Chem. Kinet., 28, 497-530.

Carter, W. P. L. and R. Atkinson (1989a): "A Computer Modeling Study of Incremental Hydrocarbon Reactivity", Environ. Sci. Technol., 23, 864.

Carter, W. P. L. and R. Atkinson (1989b): "Alkyl Nitrate Formation from the Atmospheric Photooxidation of Alkanes; a Revised Estimation Method," J. Atm. Chem. 8, 165-173.

Carter, W. P. L., and F. W. Lurmann (1990): "Evaluation of the RADM Gas-Phase Chemical Mechanism," Final Report, EPA-600/3-90-001.

Carter, W. P. L. and F. W. Lurmann (1991): "Evaluation of a Detailed Gas-Phase Atmospheric Reaction Mechanism using Environmental Chamber Data," Atm. Environ. 25A, 2771-2806.

Carter, W. P. L., F. W. Lurmann, R. Atkinson, and A. C. Lloyd (1986): "Development and Testing of a Surrogate Species Chemical Reaction Mechanism," EPA-600/3-86-031, August.

Carter, W. P. L., R. Atkinson, A. M. Winer, and J. N. Pitts, Jr. (1982): "Experimental Investigation of Chamber-Dependent Radical Sources," Int. J. Chem. Kinet., 14, 1071.

Carter, W. P. L., Winer, A. M., Atkinson, R., Dodd, M. C. and Aschmann, S. A. (1984a): Atmospheric Photochemical Modeling of Turbine Engine Fuels. Phase I. Experimental studies. Final Report to the USAF, ESL-TR-84-32, September.

Carter, W. P. L., Dodd, M. C., Long, W. D. and Atkinson, R. (1984b): Outdoor Chamber Study to Test Multi-Day Effects. Volume I: Results and Discussion. Final report, EPA-600/3-84-115.

Carter, W. P. L., A. M. Winer, R. Atkinson, S. E. Heffron, M. P. Poe, and M. A. Goodman (1987): "Atmospheric Photochemical Modeling of Turbine Engine Fuels. Phase II. Computer Model Development," Report on USAF Contract no. F08635-83-0278.

Carter, W. P. L., J. A. Pierce, I. L. Malkina, and D. Luo (1992): "Investigation of the Ozone Formation Potential of Selected Volatile Silicone Compounds," Final Report to Dow Corning Corporation, Midland, MI, November.

Carter, W. P. L., J. A. Pierce, I. L. Malkina, D. Luo and W. D. Long (1993a): "Environmental Chamber Studies of Maximum Incremental Reactivities of Volatile Organic Compounds," Report to Coordinating Research Council, Project No. ME-9, California Air Resources Board Contract No. A032-0692; South Coast Air Quality Management District Contract No. C91323, United States Environmental Protection Agency Cooperative Agreement No. CR-814396-01-0, University Corporation for Atmospheric Research Contract No. 59166, and Dow Corning Corporation. April 1.

Carter, W. P. L, D. Luo, I. L. Malkina, and J. A. Pierce (1993b): "An Experimental and Modeling Study of the Photochemical Ozone Reactivity of Acetone," Final Report to Chemical Manufacturers Association Contract No. KET-ACE-CRC-2.0. December 10.

Carter, W. P. L., D. Luo, I. L. Malkina, and J. A. Pierce (1994): "Environmental Chamber Studies of Atmospheric Ozone Formation from Selected Biogenic Compounds" Presented at the 207th ACS National Meeting, March 13-17, San Diego, CA.

Carter, W. P. L., J. A. Pierce, D. Luo, and I. L. Malkina (1995a): "Environmental Chamber Studies of Maximum Incremental Reactivities of Volatile Organic Compounds," Atmos. Environ. 29, 2499-2511.

Carter, W. P. L., D. Luo, I. L. Malkina, and J. A. Pierce (1995b): "Environmental Chamber Studies of Atmospheric Reactivities of Volatile Organic Compounds. Effects of Varying ROG Surrogate and NO_x," Final report to Coordinating Research Council, Inc., Project ME-9, California Air Resources Board, Contract A032-0692, and South Coast Air Quality Management District, Contract C91323. March 24.

Carter, W. P. L., D. Luo, I. L. Malkina, and J. A. Pierce (1995c): "Environmental Chamber Studies of Atmospheric Reactivities of Volatile Organic Compounds. Effects of Varying Chamber and Light Source," Final report to National Renewable Energy Laboratory, Contract XZ-2-12075, Coordinating Research Council, Inc., Project M-9, California Air Resources Board, Contract A032-0692, and South Coast Air Quality Management District, Contract C91323, March 26.

Carter, W. P. L., D. Luo, I. L. Malkina, and D. Fitz (1995d): "The University of California, Riverside Environmental Chamber Data Base for Evaluating Oxidant Mechanism. Indoor Chamber Experiments through 1993," Report submitted to the U. S. Environmental Protection Agency, EPA/AREAL, Research Triangle Park, NC., March 20..

Carter, W. P. L., D. Luo, and I. L. Malkina (1996a): "Investigation of Atmospheric Ozone Formation Potentials of C12 - C16 n-Alkanes," Report to the Aluminum Association, October 28.

Carter, W. P. L., D. Luo, and I. L. Malkina (1996b): "Investigation of the Atmospheric Ozone Impact of Methyl Acetate," Report to Eastman Chemical Company, July.

Carter, W. P. L., D. Luo, and I. L. Malkina (1996c): "Investigation of the Atmospheric Ozone Formation Potential of t-Butyl Alcohol, N-Methyl Pyrrolidinone and Propylene Carbonate," Report to ARCO Chemical Corporation, July 8.

Carter, W. P. L., D. Luo, and I. L. Malkina (1996d): "Investigation of the Atmospheric Ozone Formation Potential of Trichloroethylene," Report to the Halogenated Solvents Industry Alliance, August.

Carter, W. P. L., D. Luo, and I. L. Malkina (1997a): "Environmental Chamber Studies for Development of an Updated Photochemical Mechanism for VOC Reactivity Assessment," Final report to the California Air Resources Board, the Coordinating Research Council, and the National Renewable Energy Laboratory, November 26.

Carter, W. P. L., D. Luo, and I. L. Malkina (1997b): "Investigation of the Atmospheric Ozone Formation Potential of Propylene Glycol," Report to Philip Morris, USA, May 2.

Carter, W. P. L., D. Luo, and I. L. Malkina (1997c): "Investigation of the Atmospheric Ozone Formation Potential of Acetylene," Report to Carbind Graphite Corp., April 1.

Carter, W. P. L., D. Luo, and I. L. Malkina (1997d): "Investigation of the Atmospheric Ozone Formation Potential of Selected Alkyl Bromides," Report to Albemarle Corporation, November 10.

Carter, W. P. L., D. Luo, I. L. Malkina, S. M. Aschmann and R. Atkinson (1997e): "Investigation of the Atmospheric Ozone Formation Potentials of Selected Dibasic Esters," Report to the Dibasic Esters Group, SOCMA, August 29.

Carter, W. P. L., D. Luo, and I. L. Malkina (1997f): "Investigation of the Atmospheric Ozone Formation Potentials of Selected Mineral Spirits Mixtures," Report to Safety-Kleen Corporation, July 25.

Carter, W. P. L., D. Luo, and I. L. Malkina (1997g): "Investigation of the Atmospheric Ozone Formation Potential of t-Butyl Acetate," Report to ARCO Chemical Corporation, July 2.

Carter, W. P. L., D. Luo and I. L. Malkina (1997h): "Investigation of that Atmospheric Reactions of Chloropicrin," Atmos. Environ. 31, 1425-1439.; Report to the Chloropicrin Manufacturers Task Group, May 19.

Carter, W. P. L., D. Luo, and I. L. Malkina (1997i): "Investigation of the Atmospheric Ozone Formation Potential of Toluene Diisocyanate," Report to Society of the Plastics Industry, December.

Carter, W. P. L., D. Luo, and I. L. Malkina (1999a): "Investigation of the Atmospheric Ozone Formation Potential of Para Toluene Isocyanate and Methylene Diphenylene Diisocyanate," Report to the Chemical Manufacturers Association Diisocyanates Panel, March.

Carter, W. P. L., D. Luo, and I. L. Malkina (1999b): 'Investigation of the Atmospheric Impacts and Ozone Formation Potential of Styrene," Report to the Styrene Information and Research Center. March 10.

Carter, W. P. L., M. Smith, D. Luo, I. L. Malkina, T. J. Truex, and J. M. Norbeck (1999c): "Experimental Evaluation of Ozone Forming Potentials of Motor Vehicle Emissions", Final Report to California Air Resources Board Contract No. 95-903, and South Coast Air Quality Management District Contract No 95073/Project 4, Phase 2, May 14.

Carter. W. P. L. D. Luo, and I. L. Malkina (2000a): "Investigation of Atmospheric Reactivities of Selected Consumer Product VOCs," Draft Report to California Air Resources Board, Contract 95-308, April 29.

Carter, W. P. L., D. Luo, and I. L. Malkina (2000b): "Investigation of the Atmospheric Impacts and Ozone Formation Potentials of Selected Branched Alkanes," Report to the Safety-Kleen Corporation, in preparation.

Carter, W. P. L., et al. (2000c), "An Experimental and Modeling Study of the Photochemical Reactivity of Selected C12+ Cycloalkanes," Report to the Aluminum Association, in preparation.

Carter, W. P. L., D. Luo, and I. L. Malkina (2000d): "Investigation of the Atmospheric Ozone Formation Potentials of Selected Compounds," Report to Exxon Chemical Company, in preparation..

Carter, W. P. L. et. al (2000e): "Investigation of the Atmospheric Ozone Formation Potentials of Selected Solvents," report to Eastman Chemical Company, in preparation.

Carter, W. P. L., et. al. (2000f): "Investigation of the Atmospheric Ozone Formation Potentials of Selected Glycol Ethers," Report to the Chemical Manufacturers Association Glycol Ethers Panel, in preparation.

Carter, W. P. L., D. Luo, and I. L. Malkina (2000g): "Investigation of the Atmospheric Ozone Formation Potentials of Selected Commercial Mixtures," Report to Exxon Chemical Company, in preparation.

Chang, T. Y. and S. J. Rudy (1990): "Ozone-Forming Potential of Organic Emissions from Alternative-Fueled Vehicles," Atmos. Environ., 24A, 2421-2430.

Christensen, L. K., T. J. Wallington, A. Guschin, and M. D. Hurley (1999): "Atmospheric Degradation Mechanism of CF_3OCH_3," J. Phys. Chem A, 4202-4208.

Christensen, L. K., J. C. Ball and T. J. Wallington (2000): "Atmospheric Oxidation Mechanism of Methyl Acetate," J. Phys. Chem. A, 104, 345-351.

Cox, R. A., K. F. Patrick, and S. A. Chang (1981): "Mechanism of Atmospheric Photooxidation of Organic Compounds. Reactions of Alkoxy Radicals in Oxidation of n-Butane and Simple Ketones," Environ. Sci. Technol. 15, 587.

Croes, B., California Air Resources Board Research Division, personal communication.

Dagaut, P. T. J. Wallington, R. Liu and M. J. Kurylo (1988a): 22nd International Symposium on Combustion, Seattle, August 14-19.

Dagaut, P., T. J. Wallington, R. Liu and J. J. Kurylo (1988b): "A Kinetics Investigation of the Gas-Phase Reactions of OH Radicals with Cyclic Ketones and Diones: Mechanistic Insights," J. Phys. Chem. 92, 4375.

Dimitriades, B. (1999): "Scientific Basis of an Improved EPA Policy on Control of Organic Emissions for Ambient Ozone Reduction," J. Air & Waste Manage. Assoc. 49, 831-838

Dodge, M. C. (1984): "Combined effects of organic reactivity and NMHC/NOx ratio on photochemical oxidant formation -- a modeling study," Atmos. Environ., 18, 1657.

Donaghy, T., I. Shanahan, M. Hande and S. Fitzpatrick (1993): "Rate Constant and Atmospheric Lifetimes for the Reactions of OH Radicals and Cl Atoms with Haloalkanes," Int. J. Chem. Kinet, 25, (4) 273-284.

Donahue, N. M. M. K. Dubey, R. Mohrschaldt, K. L. Demerjian, and J. G. Anderson (1997): "High Pressure Flow Study of the Reactions $OH+NO_x$ -> $HONO_x$: Errors in the Falloff Region," J. Geophys. Res.-Atmos.102, (D5) 6159-6168.

Eberhard, J. C. Muller, D. W. Stocker, and J. A. Kerr (1993): "The Photo-Oxidation of Diethyl Ether in Smog Chamber Experiments Simulating Tropospheric Conditions: Product Studies and Proposed Mechanism," Int. J. Chem. Kinet. 25, 630-649.

Eberhard, J., C. Muller, D. W. Stocker and J. A. Kerr (1995): "Isomerization of Alkoxy Radicals under Atmospheric Conditions," Environ. Sci. Technol. 29, 232.

EPA (1984): "Guideline for Using the Carbon Bond Mechanism in City-Specific EKMA," EPA-450/4-84-005, February.

Fantechi G, NR Jensen, J Hjorth, and J Peeters (1998): "Determination of the Rate Constants for the Gas-Phase Reactions of Methyl Butenol with OH Radicals, Ozone, NO_3 radicals, and Cl Atoms," Int. J. Chem. Kinet. 30, (8) 589-594.

Forster, R., M. Frost, D. Fulle, H. F. Hamann, H. Hippler, A. Schlepegrell, and J. Troe (1995): "High-Pressure Range of the Addition of HO to HO, NO, NO_2, and CO .1. Saturated Laser-Induced Fluorescence Measurements at 298 K," J. Chem. Phys. 103, (8) 2949-2958.

Ferronato C, Orlando JJ, and Tyndall GS (1998): "Rate Mechanism of the Reaction of OH and Cl with 2-Methyl-3-Buten-2-ol," J. Geophys. Res.-Atoms. 103, (8) 25579-25586

Gardner, E. P., P. D. Sperry, and J. G. Calvert (1987): "Photodecomposition of Acrolein in O_2-N_2 Mixtures," J. Phys. Chem. 91, 1922.

Gery, M. W., D. L. Fox, R. M. Kamens, and L. Stockburger (1987): "Investigation of Hydroxyl Radical Reactions with o-Xylene and m-Xylene in a Continuous Stirred Tank Reactor," Environ. Sci. Technol. 21, 339.

Gery, M. W., G. Z. Whitten, and J. P. Killus (1988): "Development and Testing of the CBM-IV For Urban and Regional Modeling,", EPA-600/ 3-88-012, January.

Grosjean and Grosjean (1994): Int. J. Chem. Kinet. 26, 1185.

Guenther, A., C. Geron, T.Pierce, B. Lamb, P. Harley, and R.Fall (2000): "Natural emissions of non-methane volatile organic compounds, carbon monoxide, and oxides of nitrogen from North America" Atmospheric Environment, 34, 2205-2230.

Hartmann, D., A. Gedra, D. Rhasa, and R. Zellner (1986): Proceedings, 4th European Symposium on the Physico-Chemical Behavior of Atmospheric Pollutants, 1986; D. Riedel Publishing Co., Dordrecht, Holland, 1987, p. 225.

Hatakeyama, S., N. Washida, and H. Akimoto, (1986): "Rate Constants and Mechanisms for the Reaction of OH (OD) Radicals with Acetylene, Propyne, and 2-Butyne in Air at 297 +/- 2 K," J. Phys Chem. 90, 173-178.

Jeffries, H. E., K. G. Sexton, J. R. Arnold, and T. L. Kale (1989): "Validation Testing of New Mechanisms with Outdoor Chamber Data. Volume 2: Analysis of VOC Data for the CB4 and CAL Photochemical Mechanisms," Final Report, EPA-600/3-89-010b.

Jeffries, H. E. (1991): "UNC Solar Radiation Models," unpublished draft report for EPA Cooperative Agreements CR813107, CR813964 and CR815779".

Jeffries, H. E. and R. Crouse (1991): "Scientific and Technical Issues Related to the Application of Incremental Reactivity. Part II: Explaining Mechanism Differences," Report prepared for Western States Petroleum Association, Glendale, CA, October.

Jenkin, M. E., R. A. Cox, M. Emrich and G. K. Moortgat (1993): "Mechanisms for the Cl-atom-initiated Oxidation of Acetone and Hydroxyacetone in Air," J. Chem. Soc. Faraday Trans. 89, 2983-2991.

Kelly, N. and J. Heicken (1978): "Rate Coefficient for the Reaction of CH3O with CH3CHO at 25^o C," J. Photochem. 8, 83.

Kircher, C. C. and S. P. Sander (1984): "Kinetics and Mechanism of HO_2 and DO_2 Disproportionations" J. Phys. Chem. 88, (19) 2082-2091.

Kirchner, F. and W. R. Stockwell (1996): "Effect of Peroxy Radical Reactions on the Predicted Concentrations of Ozone, Nitrogenous Compounds, and Radicals," J. Geophys. Res. 101, 21,007-21,022.

Kirchner, F., F. Zabel and K. H. Becker (1992): "Kinetic Behavior of Benzoylperoxy Radicals in the Presence of NO and NO2," Chem. Phys. Lett. 191, 169-174.

Kirchner, F., L. P. Thüner, I. Barnes, K. H. Becker, B. Donner, and F. Zabel (1997): Environ. Sci. Technol. 31, 1801.

Kwok, E. S. C., and R. Atkinson (1995): "Estimation of Hydroxyl Radical Reaction Rate Constants for Gas-Phase Organic Compounds Using a Structure-Reactivity Relationship: An Update," Atmos. Environ 29, 1685-1695.

Kwok, E. S. C., R. Atkinson, and J. Arey (1995): "Observation of Hydrocarbonyls from the OH Radical-Initiated Reaction of Isoprene," Envrion. Sci. Technol. 29, 2467.

Kwok, E. S. C., S. Aschmann, and R. Atkinson (1996): "Rate Constants for the Gas-Phase Reactions of the OH Radical with Selected Carbamates and Lactates," Environ. Sci. Technol 30, 329-334.

Kumar, N., F. W. Lurmann, and W. P. L. Carter (1995), "Development of the Flexible Chemical Mechanism Version of the Urban Airshed Model," Report to California Air Resources Board, Agreement no. 93-716. Document No. STI-94470-1508-FR, Sonoma Technology, Inc. Santa Rosa, CA, August.

Langford, A. O, and C. B. Moore (1984): "Collision complex formation in the reactions of formyl radicals with nitric oxide and oxygen," J. Chem. Phys. 80, 4211.

Langer, S., E. Jjungstrom, I Wangberg, T. J. Wallington, M. D. Hurley and O. J. Nielsen (1995): "Atmospheric Chemistry of Di-tert-Butyl Ether: Rates and Products of the Reactions with Chlorine Atoms, Hydroxyl Radicals, and Nitrate Radicals, "Int. J. Chem. Kinet., 28, 299-306.

Lurmann, F. W., W. P. L. Carter, and R. A. Coyner (1987): "A Surrogate Species Chemical Reaction Mechanism for Urban-Scale Air Quality Simulation Models. Volume I - Adaptation of the Mechanism," EPA-600/3-87-014a.

Lurmann, F. W., M. Gery, and W. P. L. Carter (1991): "Implementation of the 1990 SAPRC Chemical Mechanism in the Urban Airshed Model," Final Report to the California South Coast Air Quality Management District, Sonoma Technology, Inc. Report STI-99290-1164-FR, Santa Rosa, CA.

Magnotta, F. and H. S. Johnston (1980): "Photo-Dissociation Quantum Yields for the NO_3 Free-Radical," Geophys. Res. Lett. 7, (10) 769-772.

Mellouki, A., R. K. Talukdar, A. M. R. P. Bopegedera, and C. J. Howard (1993): " Study of the Kinetics of the Reactions of NO_3 with HO_2 and OH," Int. J. Chem. Kinet. 25, (1) 25-39.

Majer, Naman, and Robb (1969): "Photolysis of Aromatic Aldehydes," Trans. Faraday Soc, 65 1846.

Mentel T.F., D. Bleilebens. and A. Wahner (1996): "A study of nighttime nitrogen oxide oxidation in a large reaction chamber - the fate of NO_2 , N_2O_5 , HNO_3 , and O_3 at different humidities." Atmos. Environ., 30, 4007-4020.

Middleton, P., W. R. Stockwell, and W. P. L. Carter (1990): "Aggregation and Analysis of Volatile Organic Compound Emissions for Regional Modeling," Atmos. Environ., 24A, 1107-1133.

Mineshos, G., and S. Glavas (1992): "Thermal Decomposition of Peroxypropionyl Nitrate –Kinetics of the Formation of Nitrogenous Products," React. Kinet. Catal. Lett. 45, (2) 305-312.

Muthuramu, K., P. B. Shepson and J. M. O'Brien (1993): "Preparation, Analysis, and Atmospheric Production of Multifunctional Nitrates," Environ. Sci. Technol. 27, 1117.

NASA (1994): "Chemical Kinetics and Photochemical Data for Use in Stratospheric Modeling, Evaluation Number 11," JPL Publication 94-26, Jet Propulsion Laboratory, Pasadena, California, December.

NASA (1997): "Chemical Kinetics and Photochemical Data for Use in Stratospheric Modeling, Evaluation Number 12," JPL Publication 97-4, Jet Propulsion Laboratory, Pasadena, California, January.

H. Niki, P. D. Maker, C. M. Savage, and L. P. Breitenback (1985): "An FTIR Study of the Cl-Atom-Initiated Reaction of Glyoxal," Int. J. Chem. Kinet. 17, 347.

NIST (1994): "NIST Standard Reference Database 25. Structures and Properties, Version 2.01," National Institute of Standards and Technology, Gaithersburg, MD 20899.

NIST (1998): "The NIST Chemical Kinetics Database, NIST Standard Reference Database 17 - 2Q98," National Institute of Standards and Technology, Gaithersburg, MD 20899.

Paulson, S. E., J. J. Orlando, G. S. Tyndall, and J. G. Calvert (1995): "Rate Coefficients for the Reactions of $O(^3P)$ with Selected Biogenic Hydrocarbons," Int. J. Chem. Kinet. 27, 997.

Pitts, J. N., Jr., K. Darnall, W. P. L. Carter, A. M. Winer, and R. Atkinson (1979): "Mechanisms of Photochemical Reactions in Urban Air," EPA-600/ 3-79-110, November.

Pitts, J. N., Jr., E. Sanhueza, R. Atkinson, W. P. L. Carter, A. M. Winer, G. W. Harris, and C. N. Plum (1984): "An Investigation of the Dark Formation of Nitrous Acid in Environmental Chambers," Int. J. Chem. Kinet., 16, 919-939.

Plum, C. N., Sanhuesa, E., Atkinson, R., Carter W. P. L. and Pitts, J. N., Jr. (1983): "OH Radical Rate Constants and Photolysis Rates of alpha-Dicarbonyls," Environ. Sci. Technol. 17, 479-484.

Porter, E., G. Locke, J. Platz, J. Treacy, H. Sidebottom, W. Mellouki, S. Teton, and G. LeBras. (1995): "Kinetics and Mechanisms for the OH Radical Initiated Oxidation of Oxygenated Organic Compounds," Workshop on Chemical Mechanisms Describing Oxidation Processes in the Troposphere, Valencia, Spain, April 25-28.

Roberts, J. M. and S. B. Bertman (1992): "The Thermal Decomposition of PeroxyAcetic Nitric Anhydride (PAN) and Peroxymethacrylic Nitric Anhydride (MPAN)," Int J. Chem. Kinet. 24, 297.

Rudich Y, R Talukdar, JB Burkholder, and AR Ravishankara (1995): "Reactions of Methylbutenol with Hydroxyl Radical – Mechanism and Atmospheric Implications," J. Phys. Chem. 99, (32) 12188-12194.

Rudich Y, RK Talukdar, RW Fox, and AR Ravishankara (1996): "Rate Coefficients for Reactions of NO_3 with a few Olefins and Oxygenated Olefins," J. Phys. Chem. 100, (13) 5374-5381.

Saunders, S. M., D. L. Baulch, K. M. Cooke, M. J. Pilling, and P. I. Smurthwaite (1994): "Kinetics and mechanisms of the reactions of OH with some oxygenated compounds of importance in tropospheric chemistry," Int. J. Chem. Kinet., 26, 113-130.

Schurath, U. and V. Wipprecht (1980): "Reactions of peroxiacycl radicals." Proc. 1st European Symp. On the Physico-Chemical Behavior of Atmospheric Pollutants, pp. 157-166. Commiss. European Commun.

Seefeld, S. and J. A. Kerr (1997): "Kinetics of the Reactions of Propionylperoxy Radicals with NO and NO_2: Peroxypropionyl Nitrate Formation under Laboratory Conditions Related to the Troposphere," Environ. Sci. Technol. 31, (10) 2949-2953

Shepson, P. B., E. O. Edney, and E. W. Corse (1984): "Ring Fragmentation Reactions on the Photooxidations of Toluene and o-Xylene," J. Phys. Chem. 88, 4122.

Shepson, P. B., E. O. Edney, T. E. Kleindienst, G. R. Namie and L. T. Cupitt (1985): "The Production of Organic Nitrates from Hydroxyl and Nitrate Radical Reaction with Propylene," Environ Sci. Technol., 19, 849.

Sidebottom, H. W., G. LeBras, K. H. Becker, J. Wegner, E. Porter, S. O'Donnell, J. Morarity, E. Collins, A. Mellouki, S. Le Calve, I. Barnes, C. Sauer, K. Wirtz, M. Martin-Revejo, L. Theuner and J. Bea (1997): "Kinetics and Mechanisms for the Reaction of Hydroxyl Radicals with $CH_3OCH_2OCH_3$ and Related Compounds," Final Report to Lambiotte & Cie, S.A., September.

Slagle, I. R., J.-Y. Park, and D. Gutman (1984): "Kinetics of polyatomic free radicals produced by laser photolysis. 3. Reactions of vinyl radicals with molecular oxygen," J. Mm. Chem. Soc. 106, 4356-4361.

Smith, D. F, T. E. Kleindienst, E. E. Hudgens, C. D. McIver and J. J. Bufalini (1991): "The Photooxidation of Methyl Tertiary Butyl Ether," Int. J. Chem. Kinet. 23, 907-924.

Smith, D. F, T. E. Kleindienst, E. E. Hudgens, C. D. McIver and J. J. Bufalini (1992): "Kinetics and Mechanism of the Atmospheric Oxidation of Ethyl Tertiary Butyl Ether," Int. J. Chem. Kinet. 24, 199-215.

Stemmler, K. D. J. Kinnison and J. A. Kerr (1996): "Room Temperature Coefficients for the Reactions of OH Radicals with Some Monoethylene Glycol Monoalkyl Ethers," J. Phys. Chem, 100, 2114.

Stemmler, K., W. Mengon and J. A. Kerr (1996): "OH Radical Initiated Photooxidation of 2-Ethoxyethanol under Laboratory Conditions Related to the Troposphere: Product Studies and Proposed Mechanism," Environ. Sci. Technol. 30, 3385-3391.

Stemmler, K. , Mengon, W. and J. A. Kerr (1997a): "Hydroxyl-Radical-Initiated Oxidation of Isobutyl Isopropyl Ether Under Laboratory Conditions Related to the Troposphere: Product Studies and Proposed Mechanism," J. Chem. Soc., Faraday Trans. 93, 2865-2875.

Stemmler, K. W. Mengon, D. A. Kinnison, and J. A. Kerr (1997b): "OH Radical Initiated Photooxidation of 2-Butoxyethanol under Laboratory Conditions Related to the Troposphere: Product Studies and Proposed Mechanism," Environ. Sci. Technol. 31, 1496-1504.

Stockwell, W.R. and J.G. Calvert (1983): "The Mechanism of the HO-SO_2 Reaction," Atmos. Envir., 17, 2231 - 2235.

Stockwell, W. R., P. Middleton, J. S. Chang, and X. Tang (1990): "The Second Generation Regional Acid Deposition Model Chemical Mechanism for Regional Air Quality Modeling," J. Geophys. Res. 95, 16343- 16376.

Stockwell, W.R., F. Kirchner, M. Kuhn, and S. Seefeld (1997): "A new mechanism for regional atmospheric chemistry modeling," J. Geophys. Res., 102, 25847-25880.

Takagi, H., N. Washida, H. Akimoto, K. Nagasawa, Y. Usui, and M. Okuda (1980): "Photooxidation of o-Xylene in the NO-H_2O-Air System," J. Phys. Chem. 84, 478.

Tsang, W.; and R. F. Hampson (1986): "Chemical kinetic data base for combustion chemistry. Part I. Methane and related compounds," J. Phys. Chem. Ref. Data 15, 1087.

Tsang, W (1987): "Chemical kinetic data base for combustion chemistry. Part 2. Methanol," J. Phys. Chem. Ref. Data 16, 471.

Tsang, W (1988): "Chemical kinetic data base for combustion chemistry. Part 3. Propane," J. Phys. Chem. Ref. Data 17, 887.

Tuazon, E. C., R. Atkinson, C. N. Plum, A. M. Winer, and J. N. Pitts, Jr. (1983): "The Reaction of Gas-Phase N_2O_5 with Water Vapor," Geophys. Res. Lett. 10, 953-956.

Tuazon E.C., R. Atkinson R. and W. P. L. Carter W.P.L. (1985): "Atmospheric Chemistry of cis- and trans-3-Hexene-2,5-dione,". Environ. Sci. Technol., 19, 265-269.

Tuazon, E. C., H. MacLeod, R. Atkinson, and W. P. L. Carter (1986): "Alpha-Dicarbonyl yields from the NO_x-air photooxidations of a series of aromatic-hydrocarbons in air," Environ. Sci. Technol. 20, (4) 383-387

Tuazon, E. C. and R. Atkinson (1989): "A Product Study of the Gas-Phase Reaction of Methacrolein with the OH Radical in the Presence of NO_x," Int. J. Chem. Kinet. 22, 591-602.

Tuazon, E. C., and R. Atkinson (1990): "Formation of 3-Methylfuran from the Gas-Phase Reaction of OH Radicals with Isoprene and the Rate Constant for its Reaction with the OH Radical," Int. J. Chem. Kinet., 22, 591.

Tuazon, E. C., W. P. L. Carter and R. Atkinson (1991a): "Thermal Decomposition of Peroxyacetyl Nitrate and Reactions of Acetyl Peroxy Radicals with NO and NO_2 Over the Temperature Range 283-313 K," J. Phys. Chem., in 95, 2434.

Tuazon, E. C., W. P. L. Carter, S. M. Aschmann, and R. Atkinson (1991b): "Products of the Gas-Phase Reaction of Methyl tert-Butyl Ether with the OH Radical in the Presence of NO_x," Int. J. Chem. Kinet., 23, 1003-1015.

Tuazon, E. C., S. M. Aschmann and R. Atkinson (1998a): "Products of the Gas-Phase Reactions of the OH radical with 1-Methoxy-2-Propanol and 2-Butoxyethanol," Environ. Sci. Technol., 32, 3336-3345.

Tuazon, E. C., S. M. Aschmann, R. Atkinson, and W. P. L. Carter (1998b): "The reactions of Selected Acetates with the OH radical in the Presence of NO: Novel Rearrangement of Alkoxy Radicals of Structure RC(O)OCH(O.)R'", J. Phys. Chem A 102, 2316-2321.

Tuazon, E., C., S. M. Aschmann, and R. Atkinson (1999): "Products of the Gas-Phase Reaction of the OH Radical with the Dibasic Ester $CH_3OC(O)CH_2CH_2CH_2C(O)OCH_3$," Environ. Sci. Technol., 33, 2885-2890.

Veillerot, M., P. Foster, R. Guillermo, and J. C. Galloo (1995): "Gas-Phase Reaction of n-Butyl Acetate with the Hydroxyl Radical under Simulated Tropospheric Conditions: Relative Rate Constant and Product Study," Int. J. Chem. Kinet. 28, 233-243.

Wallington, T. J. and M. J. Kurylo (1987): "Flash Photolysis Resonance Fluorescence Investigation of the Gas-Phase Reactions of OH Radicals with a Series of Aliphatic Ketones over the Temperature Range 240-440 K," J. Phys. Chem 91, 5050.

Wallington, T. J., P. Dagaut, R. Liu and M. J. Kurylo (1988a): "Rate Constants for the Gas Phase Reactions of OH with C_5 through C_7 Aliphatic Alcohols and Ethers: Predicted and Experimental Values," Int. J. Chem. Kinet. 20, 541.

Wallington, T. J., R. Liu, P. Dagaut, and M. J. Kurylo (1988b): "The Gas-Phase Reactions of Hydroxyl Radicals with a Series of Aliphatic Ethers over the Temperature Range 240-440 K," Int. J. Chem. Kinet. 20, 41.

Wallington, T. J., P. Dagaut and M. J. Kurylo (1988c): "Correlation between Gas-Phase and Solution-Phase Reactivities of Hydroxyl Radicals toward Saturated Organic Compounds," J. Phys. Chem. 92, 5024.

Wallington, T. J., P. Dagaut, R. Liu, and M. J. Kurylo (1988d): "The Gas Phase Reactions of Hydroxyl Radicals with a Series of Esters Over the Temperature Range 240-440 K," Int. J. Chem. Kinet. 20, 177.

Wallington, T., J., W. O. Siegl, R. Liu, Z. Zhang, R. E. Huie, and M. J. Kurylo (1990): "The Atmospheric Reactivity of à-Methyltetrahydrofuran," Env. Sci. Technol. 24, 1568-1599.

Wallington, T. J. and S. M. Japar (1991): "Atmospheric Chemistry of Diethyl Ether and Ethyl tert-Butyl Ether," Environ. Sci. Technol. 25, 410-415.

Wallington, T. J., J. M. Andino, A. R. Potts, S. J. Rudy, W. O. Siegl, Z. Zhang, M. J. Kurylo and R. H. Huie (1993): "Atmospheric Chemistry of Automotive Fuel Additives: Diisopropyl Ether," Environ. Sci. Technol. 27, 98.

Wallington, T. J., M. D. Hurley, J. C. Ball, A. M. Straccia, J. Platz, L. K. Christensen, J. Schested, and O. J. Nielsen (1997): "Atmospheric Chemistry of Dimethoxymethane ($CH_3OCH_2OCH_3$): Kinetics and Mechanism of Its Reaction with OH Radicals and Fate of the Alkoxy Radicals $CH_3CHO(\cdot)OCH_3$ and $CH_3OCH_2OCH_2O(\cdot)$," J. Phys. Chem. A, 101, 5302-5308.

Weaver, J.; J. Meagher, R. Shortridge, and J. Heicklen (1975): "The Oxidation of Acetyl Radicals," J. Photochem. 4, 341.

Wells, J. R., F. L. Wiseman, D. C. Williams, J. S. Baxley, and D. F. Smith (1996): "The Products of the Reaction of the Hydroxyl Radical with 2-Ethoxyethyl Acetate," Int. J. Chem. Kinet., 28, 475-480.

Wyatt, S. E., J. S. Baxley and J. R. Wells (1999), "The Hydroxyl Radical Reaction Rate Constant and Products of Methyl Isobutyrate," Int. J. Chem. Kinet. 31, 551-557.

DOCUMENTATION OF THE SAPRC-99 CHEMICAL MECHANISM FOR VOC REACTIVITY ASSESSMENT

VOLUME 1 OF 2
DOCUMENTATION TEXT

REVISED DRAFT

Report to California Air Resources Board
Contract 92-329
Contract 95-308

By

William P. L. Carter

May 8, 2000

Air Pollution Research Center and
College of Engineering
Center for Environmental Research and Technology
University of California
Riverside, California 92521

00-AP-RT17-001-FR

DOCUMENTATION OF THE SAPRC-99 CHEMICAL MECHANISM FOR VOC REACTIVITY ASSESSMENT

VOLUME 2 OF 2 APPENDICES

REVISED DRAFT

Report to California Air Resources Board
Contract 92-329
Contract 95-308

By

William P. L. Carter

May 8, 2000

Air Pollution Research Center and
College of Engineering
Center for Environmental Research and Technology
University of California
Riverside, California 92521

00-AP-RT17-001-FR